

DEVELOPMENT OF NOVEL ADSORBENTS FOR REMOVAL OF NOXIOUS IMPURITIES FROM WASTEWATER

Ph.D. THESIS

by

INDERJEET TYAGI



**DEPARTMENT OF CHEMISTRY
INDIAN INSTITUTE OF TECHNOLOGY ROORKEE
ROORKEE - 247 667 (INDIA)
APRIL, 2016**

DEVELOPMENT OF NOVEL ADSORBENTS FOR REMOVAL OF NOXIOUS IMPURITIES FROM WASTEWATER

A THESIS

*Submitted in partial fulfilment of the
requirements for the award of the degree*

of

DOCTOR OF PHILOSOPHY

in

CHEMISTRY

by

INDERJEET TYAGI



**DEPARTMENT OF CHEMISTRY
INDIAN INSTITUTE OF TECHNOLOGY ROORKEE
ROORKEE-247 667 (INDIA)
APRIL, 2016**

**©INDIAN INSTITUTE OF TECHNOLOGY ROORKEE, ROORKEE-2016
ALL RIGHTS RESERVED**



INDIAN INSTITUTE OF TECHNOLOGY ROORKEE ROORKEE

CANDIDATE'S DECLARATION

I hereby certify that the work which is being presented in this thesis entitled **“DEVELOPMENT OF NOXIOUS ADSORBENTS FOR REMOVAL OF NOXIOUS IMPURITIES FROM WASTEWATER”** in partial fulfillment of the requirements for the award of the Degree of Doctor of Philosophy and submitted in the Department of Chemistry of the Indian Institute of Technology Roorkee is an authentic record of my own work carried out during a period from January, 2014 to April, 2016 under the supervision of **Dr. V. K. Gupta**, Professor, Department of Chemistry, Indian Institute of Technology Roorkee, Roorkee.

The matter presented in this thesis has not been submitted by me for the award of any other degree of this or any other Institute.

(Inderjeet Tyagi)

This is to certify that the above statement made by the candidate is correct to the best of our knowledge.

(Prof. V.K. Gupta)
Supervisor

Dated: 29.06.2016

The Ph.D. Viva-Voce Examination of **Mr. Inderjeet Tyagi**, Research Scholar, has been held on

Chairman, SRC

Signature of External Examiner

This is to certify that the student has made all the corrections in the thesis.

Signature of Supervisor

Head of the Department

Dedicated
To
My Grandmother and
Parents

ACKNOWLEDGEMENT

∞-----It would never have been possible without them-----∞

The accomplishment of the present research is a blessing of many. It has received precious guidance, incessant encouragement, unconditional support & painstaking efforts of many personalities; I would like owe my thanks to all of them -----∞

A single flower cannot make a garland or a single star can not make the beautiful shiny sky, in the same way a research work can never be an outcome of a single individual's talent or efforts. During my journey from objective to goal, I have experienced showers of blessings; guidance and inspiration from my teacher, parents and friends which give me a seafaring right direction and made me to achieve the goal. Although it is not possible for me to name and thank them all individually, but it is great pleasure for me to pen down some of the special personalities who have made it possible for me to put this research work in present form.

*At First, I bow my head before **Almighty God**, the omnipotent, the omnipresent, the merciful, the most gracious, the compassionate, the beneficent, who is the entire and only source of every knowledge and wisdom endowed to mankind and who blessed me with the ability to do this work. It is his blessings which enabled me to achieve the goal.*

*With my profound pleasure, I take this opportunity to express my deepest gratitude to my esteemed supervisor **Dr. Vinod Kumar Gupta**, Professor, Department of Chemistry, Indian Institute of Technology, Roorkee, whose flawless guidance, boundless enthusiasm, enlightening discussions, provision of fearless work environment and valuable suggestions have enabled me to complete this work. I consider myself fortunate to have the opportunity to work under his guidance. Beside of being an excellent supervisor, he was as close as a guardian to me.*

*I shall extend my gratitude and sincere thanks to **Dr. M.R. Maurya**, Professor and Head, Indian Institute of Technology, Roorkee, for providing me all specific amenities required during the entire course of my research work. I shall pay special thanks to him for permitting me to work in lab even before and after departmental timings.*

*I am thankful to the members of my doctoral student research committee (SRC), **Dr U.P. Singh (Chairman)**, **Dr. P. Jeevanandam (Internal member)** and **Dr. Shashi (External member)** for their useful suggestions and critical evaluation of the progress of my thesis.*

ACKNOWLEDGEMENT

*I am indebted to **Dr. Suhas**, Assistant Professor, Department of Chemistry, Gurukula Kangri Vishwavidyalaya for incessant encouragement, fruitful valuable suggestions, and encouragement. His inspirational words, unconditional support and moral boosting at the time of crisis during the entire course of work would be remembered lifelong.*

I gratefully acknowledge the funding source that made my Ph.D. work possible. I highly thankful to Department of Science and Technology for providing financial assistance (Nov. 2013-Aug 2015) and Ministry of Human Resource Development (MHRD) for providing financial assistance (Sept. 2015-till date) that made my research work smooth and prompt. I would not have imagined the situation without their help and assistantship.

*My gratitude is also extended to my seniors who taught me research skills such as synthetic and analytical techniques, and their selfless help and moral support all through my research work and guided me as a guardian in many difficult moments: **Dr. Shilpi Agarwal**, **Dr. Arvind Kumar Bharti**, **Dr. Lokesh Kumavat**, **Dr. Naveen Mergu**, **Dr. Sudhir Kumar Shoor**a and **Mr. Monu Verma** who went through hard times together, cheered me on, and celebrated each accomplishment. Thank you for their support and help for completing my thesis.*

On a personal note I must say thank you to my dearest family, for their support and endless love, particularly during those periods of intense research and writing when they had to endure much neglect.

*I am, as the saying goes, saving the best for last and that is to convey heartfelt appreciation and gratitude to my family, specially My Granny **Late Mrs. Padma Tyagi** and my dearest uncle, **Dr Saras Tyagi**.*

*I would like to bow my head with utter respect and convey my pleasant regards to most adorable my beloved parents **Mr Umesh Tyagi** and **Mrs Mamta Tyagi** for their blessings, constant support, courage and enthusiasm; that they have shown throughout my work without which the thesis would not have appeared in the present form and my always supporting uncle **Mr. Sitaram Tyagi** and **Mr. Anuj Tyagi** for their encouragement throughout the process.*

ACKNOWLEDGEMENT

*Special thanks to my lovely sisters- **Keerti** and **Julie** and sister-in-laws-**Rakhi Tyagi** and **Anu Tyagi**, my brothers-**Ishu**, **Varun**, **Subo** and brother in laws **Rajat ji** and **Shekhar ji**, I seriously doubt that could have completed my thesis without their continuous guidance and direction. Special thanks to my grandfather **Mr N.K. Tyagi** and my Tai ji, **Mrs. Vandana Tyagi**, You both continue to inspire me in the journey with your optimism. My special thanks my lucky charm's; dearest nieces-**Prisha** and **Poorvi** many thanks to you both.*

*Friends in need are friends indeed; Words are inadequate to thank my most beloved friends and colleagues **Ashish Kumar Dhara**, **Dilshad Ali**, **Harendra Tyagi**, **Vishvajeet Shandilaya**, **Ravikant**, **Vibhrant Tyagi** and **Nitish kumar**, who were always with me in all situations. They were true sentinels in extending their support, inspiration and affection to me in all these years. I also owe thanks to my friends **Paras Bhardwaj**, **Ankit Sharma**, **Shaili Surya**, and **Pratibha Singh** for their support, kind concern, valuable suggestions and the best wishes they have done for me. I am very much thankful to God for giving me such nice friends.*

My heartfelt thanks to everybody who have helped me for successful realization of this thesis and my sincere apologies, if I have missed someone; but I am grateful for their keen support. Finally, I would also like to thank all the readers of this work, since any piece of academia is useful if it is read and understood by other so that it can become a bridge for further research.

Inderjeet Tyagi

ACKNOWLEDGEMENT

Abstract

Over the past few years, the quality of water is of very important concern for living beings as well prevailing flora and fauna since it has direct connection with the human welfare and ecosystem. Numerous unwanted and noxious impurities are discharged in to the aquatic ecosystem, which directly affects the aquatic food chain. The major sources of water pollution are domestic waste from urban, rural areas and industries wastes which discharged directly into the nearby aquatic streams. The large number of water pollutants includes organic and inorganic pollutants, sediments, radioactive materials and thermal pollutants. Once they come into our body, they perturb our biochemical processes leading to deadly consequences. Several techniques like electrochemical oxidation and sensors, sorption, chemical coagulation, solvent extraction, bioremediation, photo catalytic degradation and adsorption were reported for the removal of noxious impurities from polluted aquatic source, but among all the adsorption was proved to be the most economical and efficient method for the removal of noxious inorganic and organic impurities from aqueous solution, it has been extensively applied because it is a simple and cost effective technique and low cost adsorbents, these adsorbents are particularly attractive to current researchers due to its potential applications in the wastewater treatment, wastewater management and environmental research areas. The research and development (R&D) in the field of wastewater treatment and wastewater management has expanded exponentially in terms of financial investment, numbers of paper published, and the number of active researchers worldwide. Hence for the remediation of aquatic sources we designed efficient and excellent adsorbents, which lead to rapid removal and fast adsorption of these noxious inorganic and organic impurities.

The main objective of the present work is to convert waste products, nanoparticles and surface hydrogels in to novel adsorbents for the removal of noxious inorganic contaminants i.e. Ni^{2+} , As(III) and As(V) and organic contaminants i.e. Phenols and its derivatives and noxious dyes like Acid Blue 129 (AB 129), Congo Red (CR) and Malachite green (MG) from the solvent phase. The results of these investigations are incorporated in the present thesis; a chapter wise summary of the thesis content is discussed below:

In Chapter 1, a general introduction and a survey of novel, low cost and potential adsorbents reported in the literature, various types of water pollutants i.e. heavy metals, dyes, pesticides, biological agents and dissolved and non-dissolved solids are well investigated and

reported in this chapter. This chapter also summarised the different sources of the adsorbents i.e. Silica gel, Zeolites and ion exchange resins and activated carbon prepared from various sources i.e. rubber tire, lignin, fly ash, bagasse ash etc are well elucidated and presented. The chapter finally concludes with the scope and objective of the research work undertaken.

In **Chapter 2**, the theory which involve during the adsorption phenomenon of various noxious impurities is described. Details related to the adsorption isotherms and kinetics will be discussed in the different subsections. Several adsorption isotherm models i.e. Langmuir and its types such as Type 1, 2, 3, and 4, Freundlich, Temkin and Dubinin-Raduskevich etc, additionally various kinetics model such as Pseudo-first-order, Pseudo-second order and Intraparticle-diffusion etc are well investigated and discussed in this chapter. Various analytical characterization techniques and adsorbent preparation methods have also been discussed in this chapter.

In **Chapter 3**, the potential of scrap tire as adsorbent for the rapid removal of Ni^{2+} from the aqueous source is presented. The developed adsorbent is well characterized using SEM, EDAX and FT-IR. The activated carbon prepared showed porous morphology and favorable surface chemistry for binding to Ni^{2+} . Batch adsorption method is used for the optimization of influential parameters such as adsorbent dose, pH, contact time and temperature, the obtained optimized data reveals that a 0.5 g/L adsorbent dose was found to be optimum at a pH of 7, contact time of 50 min and temperature of 55 °C for achieving $\geq 95\%$ Ni^{2+} removal from synthetic solution containing 0.1 ppm Ni^{2+} concentration. Thermodynamic studies revealed the feasibility and endothermic nature of the system. The results of the present study suggest that scrap tire can be used beneficially for Ni^{2+} removal from aqueous solution.

In **Chapter 4**, waste tire rubber derived activated carbon-alumina composites (ACALs) and Tire rubber alumina composite (TRAL) were used as efficient adsorbent for the rapid removal of As (III) and As (V). The developed adsorbents i.e. activated carbon-alumina composites were synthesized through two-steps pyrolytic technique at 700°C in the presence of N_2 gas along with steam and characterized using FE-SEM, EDX and FT-IR. Ratio metric preparation of the activated carbon-alumina composites was carried out using activated carbon and aluminium hydroxide in 1:1 ratio by weight i.e. activated carbon-alumina composites (ACAL) 11, and 1:2 ratio by weight i.e. activated carbon-alumina composites (ACAL) 12 and

2:1 ratio by weight i.e. activated carbon-alumina composites (ACAL) 21. Though TRAL has greater BET surface area, its adsorptive capacity towards arsenic in aqueous solution is lower than that of ACAL11. Further, TRAL contains sulphur derived from tire rubber but ACAL11 is free of sulphur as it is prepared from AC-HCl which is free from sulphur as well as other acid soluble impurities. Adsorption of As(III) as well as As(V) on ACAL11 and TRAL are best fitted to Langmuir adsorption isotherm with pseudo-second order kinetics.

In **Chapter 5**, the Rubber tire activated carbon modification (RTACMC) and rubber tire activated carbon (RTAC) were prepared from waste rubber tire by microwave assisted chemical treatment and physical heating respectively. A greater improvement in porosity and total pore volume was achieved in RTACMC as compared to that of RTAC. But both have a predominantly mesoporous structure. Under identical operating conditions, an irradiation time of 10 min, chemical impregnation ratio of 1.50 and a microwave power of 600W resulted in maximizing the efficiency of RTACMC for p-cresol (250 mg/g) at a contact time of 90 min while RTAC showed a 71.43 mg/g adsorption capacity at 150 min. Phenol, due to its higher solubility was adsorbed to a lesser extent by both adsorbents. Physical nature of interactions, pore diffusion mechanism and exothermic nature of the adsorption process was operative in both adsorbents. The outcomes support the feasibility of preparing high quality activated carbon from waste rubber tire by microwave assisted chemical activation.

In **Chapter 6**, a novel adsorbent, copper oxide nanoparticle loaded on activated carbon (CuO-NP-AC) was synthesized by a simple, low cost and efficient procedure. Subsequently, this novel sorbent was characterized and identified using different techniques such as scanning electron microscopy (SEM), X-ray diffraction (XRD), and laser light scattering (LLS). The effects of some variables including pH, adsorbent dosage, initial dye concentration, contact time and temperature were examined and optimized. The adsorption kinetic data were modelled using the pseudo-first-order, pseudo-second order, intraparticle diffusion and Elovich models, respectively.

In **Chapter 7**, applications of compounds like 2-Hydroxyethylmethacrylate (HEMA), 2-Hydroxyethyl methacrylate-ethoxy ethyl methacrylate-methacrylic acid (HEMA-EEMA-MA), and Polyvinyl alcohol (PVA) as an adsorbent for the removal of two hazardous toxic azo dyes i.e. Malachite green (MG) and Congo red (CR) from aqueous solutions were well

explained and elucidated. The adsorbents under consideration were synthesized and characterized by using SEM, and ATR-FTIR. The dye removal depends on the pH of the solution, the optimum pH for this experimentation was found to be 9. The adsorption affinity of MG onto HEMA–EEMA–MA was increased from 245 to 330 mg/g > CR onto PVA 169–236 mg/g > MG onto HEMA 130–205 mg/g > CR onto HEMA–EEMA–MA 90–155mg/g > MG onto PVA 35–140mg/g > CR onto HEMA 17–57 mg/g, respectively.

CONTENTS

Chapter 1:	Introduction	Page No.
1.1	General introduction	1
1.2	Pollution and pollutants	3
	1.2.1 Pollution	3
	1.2.2 Pollutants	3
	1.2.2.1 In vivo biological agents	4
	1.2.2.2 Heat	5
	1.2.2.3 Heavy metals	5
	1.2.2.3.1 Chromium [Cr (VI)]	7
	1.2.2.3.2 Arsenic [As (III) and (V)]	7
	1.2.2.3.3 Lead [Pb (II)]	7
	1.2.2.3.4 Nickel [Ni (II)]	8
	1.2.2.4 Dissolved and Non-Dissolved Chemicals	8
	1.2.2.5 Colored Synthetic compounds	9
	1.2.2.6 Biocides agents	9
	1.2.2.7 Phenol and its derivatives	10
	1.2.2.8 Detergents	10
	1.2.2.9 Polychlorinated biphenyls and Polybrominateddiphenyl ether	11
	1.2.2.10 Polycyclic aromatic nuclear hydrocarbons	11
	1.2.2.11 Hormone mimicking substances	12
	1.2.2.12 Radioactive substances	12
	1.2.2.13 Artificial chemicals as pollutants	12
1.3	Wastewater Treatment Technologies	12
	1.3.1 Primary Water Treatment Technologies	13
	1.3.2 Secondary Water Treatment Technologies	14
	1.3.3 Tertiary Water Treatment Technologies	14
1.4	Adsorption technology	14

1.5	Adsorbents	15
	1.5.1 Conventional adsorbents	18
	1.5.1.1 Amorphous substances as adsorbents	18
	1.5.1.2 Alumina as adsorbent	18
	1.5.1.3 Zeolites and Ion exchange Resins	19
	1.5.1.4 Activated carbon	19
	1.5.1.5 Modified activated carbon	21
	1.5.2 Alternative low cost adsorbents	21
	1.5.2.1 Rural wastes as low-cost adsorbents	22
	1.5.2.2 Industrial and municipal wastes as low-cost adsorbents	22
	1.5.2.3 Bio sorbents as low-cost adsorbents	22
1.6	Problem statement	23
	1.6.1 Waste tire and disposal problem	23
	1.6.2 Nanoparticles as adsorbents	23
	1.6.3 Surface hydrogel as adsorbent	24
1.7	Objective of study	24
1.8	Scope of the study	25
	References	27
Chapter 2:	Experimental Methods and Materials	43
2.1	Reagents and Materials	43
2.2	Instrumentation	46

2.3	Methodology	47
	2.3.1 Preparation of adsorbents	47
	2.3.1.1 Preparation of activated carbon from scrap tire	48
	2.3.1.2 Preparation rubber tire derived activated carbon modified with alumina composite	48
	2.3.1.3 Preparation of RTAC and RTACMC	49
	2.3.1.4 Preparation of CuO-NP-AC	49
	2.3.1.5 Preparation and synthesis of HEMA and HEMA-EEMA-MA	51
	2.3.2 Methods of adsorbent characterization	51
	2.3.2.1 Fourier Transform Infrared Spectroscopy (FT- IR)	51
	2.3.2.2 X-ray Diffraction Analysis	52
	2.3.2.3 Scanning Electron Microscopy (SEM) Studies	53
	2.3.2.4 Energy-Dispersive X-ray Spectroscopy (EDX)	54
	2.3.2.5 Thermal Gravimetric Analysis	54
	2.3.2.6 Determination of Surface Area	55
	2.3.2.7 Elemental Analysis	55
	2.3.2.8 Determination of Point of Zero Charge (PHpzc)	56
	2.3.3 Adsorption Experimental Method	57
	2.3.3.1 Batch Adsorption Method	57
	2.3.3.1.1 Adsorption Isotherms	59
	2.3.3.1.2 Classification of isotherms	59
	2.3.3.1.2.1 Langmuir Isotherm	62
	2.3.3.1.2.2 Freundlich Isotherm	63
	2.3.3.1.2.3 Dubinin-Radushkevich (D-R) isotherm	64
	2.3.3.1.2.4 Temkin isotherm	64
	2.3.3.1.3 Thermodynamic Study	65
	2.3.3.1.4 Adsorption Kinetic Models	65
	2.3.3.1.4.1 Reaction based models	65
	2.3.3.1.4.1.1 Pseudo-First-Order Model	65

2.3.3.1.4.1.2 Pseudo-Second-Order Model	66
2.3.3.1.4.2 Diffusion-based models	67
2.3.3.1.4.2.1 Boyd model	67
2.3.3.1.4.2.2 Bangham's Equation	68
2.3.3.1.4.2.3 Intraparticle Diffusion	68
2.3.3.2 Column Adsorption Method	69
2.3.3.2.1 Breakthrough Curve	70
2.3.4 Desorption and Regeneration Experiments	73
2.3.5 Test with Simulated and Real Industrial Effluents	73
2.3.6 Quality assurance/Quality control	73
References	75
Chapter 3 Rubber Tire activated carbon for the removal of Ni²⁺	79
3.1 Introduction	79
3.2 Results and discussion	80
3.2.1 Characterization of activated carbon prepared from scrap tire	80
3.2.2 Prefatory experimental adsorption studies	82
3.2.2.1 Effect of pH and the adsorption mechanism	82
3.2.2.2 Effect of initial concentration	84
3.2.2.3 Effect of contact time	84
3.2.2.4 Effect of Adsorbent Dose	85
3.2.2.5 Adsorption isotherm modelling	87
3.2.2.6 Thermodynamic study and the effect of temperature	89
3.2.2.7 Adsorption Kinetics	89
3.2.2.8 Mechanism of the adsorption process	90
3.2.2.9 Testing under industry effluent simulation condition	92
3.2.2.10 Comparison with other reported adsorbents	94

3.3	Conclusion	94
	References	96
Chapter 4	Alumina composite modified rubber tire for removal of Arsenic	99
4.1	Introduction	99
4.2	Results and Discussion	100
	4.2.1 Characterization of adsorbents	100
	4.2.2 Preliminary batch experiment	104
	4.2.2.1 Effect of initial pH	104
	4.2.2.2 Effect of adsorbent dose	106
	4.2.2.3 Adsorption Kinetic Study	107
	4.2.2.4 Modeling of Adsorption isotherms	110
	4.2.2.5 Effect of competitive ions	112
	4.2.2.6 Regeneration of adsorbent	112
	4.2.2.7 Comparison with other adsorbents	113
4.3	Conclusion	115
	References	115
Chapter 5	RTACMC and RTAC for phenols and p-Cresol removal	121
5.1	Introduction	121
5.2	Results and discussion	122
	5.2.1 Effect of pretreatment conditions of microwave on the performance of activated carbons	122
	5.2.2 Characterization of adsorbent material	124
	5.2.3 Effect of pH	126
	5.2.4 Effect of contact time	127
	5.2.5 Adsorption isotherm modelling	129
	5.2.6 Thermodynamic study and effect of temperature	131
	5.2.7 Adsorption kinetics	132

	5.2.8 Adsorption mechanism	134
	5.2.9 Comparison with other reported adsorbents	136
5.3	Conclusion	137
	References	138
Chapter 6	CuO-NP-AC for removal of noxious Acid Blue 129	141
6.1	Introduction	141
6.2	Results and discussion	141
	6.2.1 Characterization of CuO nanoparticles	141
	6.2.2 Effect of initial solution pH	142
	6.2.3 Effect of contact time	143
	6.2.4 Effect of the amount of adsorbent	144
	6.2.5 Effect of initial dye concentration on adsorption of AB 129	145
	6.2.6 Effect of temperature	146
	6.2.7 Adsorption isotherm modelling	147
	6.2.8 Thermodynamic study	149
	6.2.9 Adsorption Kinetics	150
	6.2.10 Adsorption mechanism	152
	6.2.11 Comparison with other previously developed adsorbents	153
6.3	Conclusions	154
	References	155
Chapter 7	Surfaces of hydrogel polymers as adsorbent for removal of dyes	159
7.1	Introduction	159
7.2	Results and discussion	159
	7.2.1 Spectral analysis	159
	7.2.2 Effect of contact time	163

	7.2.3 Effect of pH	164
	7.2.4 Effect of initial concentration	165
	7.2.5 Effect of agitation speed	166
	7.2.6 Adsorption kinetics	166
	7.2.7 Mechanism of the adsorption process	168
7.3	Conclusion	169
	References	171

List of Figures

Figure 1.1	Pictorial presentation of water distribution on earth	2
Figure 1.2	Pictographic appearances of noxious pollutants on the basis of chemical nature	4
Figure 1.3	Schematic presentations of the water treatment technologies	13
Figure 1.4	Activated carbon sub divided in the basis of porous nature	14
Figure 1.5	Classification of adsorbents	17
Figure 1.6	Classification of industrial and agricultural wastes as adsorbents	18
Figure 2.1	Schematic diagram of FT-IR	51
Figure 2.2	Bragg's diffraction at lattice planes	52
Figure 2.3	Principle of SEM.	53
Figure 2.4	Schematic working principle presentation of TGA	54
Figure 2.5	A pictorial presentation of the Quantachrome Nova 2200E (Spain)	55
Figure 2.6	Typical adsorption isotherm from batch experiment.	57
Figure 2.7	The IUPAC classification of adsorption isotherm	60
Figure 2.8	Giles classification of isotherm shapes.	61
Figure 2.9	Schematic presentation of the column used for the adsorption experiment.	69
Figure 2.10	Breakthrough Curve (C_0 : Concentration of influent; C : Concentration of effluent).	70
Figure 2.11	Representation of the movement of the adsorption zone and the resulting breakthrough curve	71
Figure 3.1	(a) SEM image of activated carbon (before adsorption) (b) SEM image of activated carbon after Ni^{2+} adsorption	80
Figure 3.2	(a) EDAX of activated carbon from scrap tire (before Ni^{2+} adsorption) (b) EDAX of activated carbon from scrap tire (after Ni^{2+} adsorption)	81
Figure 3.3	FTIR spectrum of activated carbon from scrap tire	81
Figure 3.4	Effect of solution pH on the adsorption capacity of activated carbon for Ni^{2+} (adsorbent dose of 0.1 g/L, Ni^{2+} concentration of 20 ppm, temperature of 55°C)	82
Figure 3.5	Effect of initial Ni^{2+} concentration on the adsorption capacity of	83

	activated carbon for Ni ²⁺ (fixed contact time of 50 mins, adsorbent dose of 0.1 g/L, pH of 7, temperature of 55°C)	
Figure 3.6	Effect of contact time and initial Ni ²⁺ concentration on the adsorption capacity of activated carbon for Ni ²⁺ (adsorbent dose of 0.1 g/L, pH 7, temperature 55°C)	85
Figure 3.7	(a) Effect of adsorbent dose on the adsorption capacity of activated carbon for Ni ²⁺ (Ni ²⁺ concentration of 20 ppm, pH 7, temperature 55°C)	86
	(b) Effect of adsorbent dose on the adsorption capacity of activated carbon (Ni ²⁺ concentration of 0.1 ppm, pH 7, temperature 55°C); (c) Effect of adsorbent dose on % removal of Ni ²⁺ (Ni ²⁺ concentration of 0.1 ppm, pH 7, temperature 55°C).	87
Figure 3.8	(a) Adsorption isotherms at three different temperatures (b) Langmuir model isotherms	88
Figure 3.9	Pseudo-second order plots for the adsorption of Ni ²⁺ onto the activated carbon at various concentrations ranging from 10 ppm to 40 ppm	91
Figure 3.10	Pseudo-second order plots for the adsorption of Ni ²⁺ onto the activated carbon at various concentrations ranging from 0.1 ppm to 2.0 ppm	91
Figure 3.11	Weber Morris plots at varying initial Ni ²⁺ concentration	93
Figure 4.1	Nitrogen adsorption desorption isotherms of (a) ACAL11 and (b) TRAL	101
Figure 4.2	X-ray diffraction patterns of (a) ACAL11 and (b) TRAL	101
Figure 4.3	FE-SEM images of (a) ACAL11, (b) ACAL11 after As(III) adsorption, (c) ACAL11 after As(V) adsorption and (d, e, f) corresponding EDX spectra.	102
Figure 4.4	FESEM images of (a) TRAL, (b) TRAL after As(III) adsorption, (c) TRAL after As(V) adsorption and (d, e, f) corresponding EDX spectra.	103
Figure 4.5	FTIR spectra of (a) AC-HCl, (b) ACAL11 and (c) TRAL	105
Figure 4.6	Determination of pH _{pzc} of (a) ACAL11 and (b) TRAL.	106
Figure 4.7	Effect of initial pH on arsenic removal at concentration 20mg/L, adsorbent dose 2.0g/L and contact time 8 h	107

Figure 4.8	Effect of adsorbent dose at initial concentration 20mg/L, pH 9 for As(III) solution, pH 3 for As(V) and contact time 8 h.	108
Figure 4.9	Effect of contact time on arsenic removal by ACAL11 at initial concentration 20mg/L, pH 9 for As(III) solution, pH 3 for As(V), adsorbent dose 4g/L for As(III) and 2g/L for As(V).	109
Figure 4.10	Effect of contact time on arsenic removal by TRAL at initial concentration 20mg/L, pH 9 for As(III), pH 3 for As(V), adsorbent dose 4g/L for As(III) and 2g/L for As(V).	109
Figure 4.11	Arsenic adsorption model of ACAL11 at pH 9 and adsorbent dose 4 g/L for As(III), and pH 3 and adsorbent dose 2 g/L for As(V), contact time 1 h.	111
Figure 4.12	Arsenic adsorption model of TRAL at pH 9 and adsorbent dose 4 g/L for As(III), and pH 3 and adsorbent dose 2 g/L for As(V), contact time 1 h.	112
Figure 5.1	Effect of (a) microwave power (at constant impregnation ratio of 1.5 and irradiation time of 10 min) (b) impregnation ratio (at constant microwave power of 600W and irradiation time of 10 min), (c) irradiation time (at constant microwave power of 600W and impregnation ratio of 1.5) on the adsorption capacity of RTACMC and removal% of p-cresol [adsorbate conc. 150 ppm; temperature 45 C, adsorbent dose: 0.6 g/L, pH-7; contact time-90 min]	123
Figure 5.2	SEM micrograph and EDAX of (a) RTACMC (b) RTAC before adsorption	125
Figure 5.3	FTIR spectra of the RTACMC and RTAC.	126
Figure 5.4	Effect of pH on the adsorption of p-cresol on the two adsorbents RTACMC and RTAC [adsorbate conc. 150 ppm; temperature 45 C, adsorbent dose: 0.6 g/L, pH-7; contact time-90 min for RTACMC and 150 min for RTAC].	127
Figure 5.5	Effect of contact time on the adsorption of p-cresol and phenol onto RTACMC and RTAC [adsorbate conc. 12 ppm and 150 ppm; temperature 45 C; adsorbent dose 0.6 g/L, pH 7]	128
Figure 5.6	Langmuir adsorption isotherms of adsorption of p-cresol and phenol	131

	onto RTACMC and RTAC at three different temperatures	
Figure 5.7	Lagergren pseudo-second order plots at two different adsorbate concentrations for adsorbents RTACMC and RTAC.	134
Figure 5.8	Weber Morris plot of adsorption of p-cresol and phenol onto RTACMC at two different concentrations of 12 ppm and 150 ppm	135
Figure 6.1	(a) X-ray diffraction (XRD) pattern (b) FE-SEM images and (c) Histogram of size distribution of the CuO nanoparticles.	142
Figure 6.2	Effect of pH on the removal of AB 129 by CuO-NP-AC at room temperature, adsorbent dosage of 0.045g in 50 mL, contact time of 20 and 25 min for dye concentrations of 10 and 20 mg L ⁻¹ , respectively.	143
Figure 6.3	Effect of contact time on the removal of AB 129 at 0.045 g of CuO-NP-AC in 50 mL at pH 2, at room temperature and AB 129 concentration of 10 and 20 mg L ⁻¹ .	144
Figure 6.4	Effect of adsorbent dosage on the removal of AB 129 at pH 2, at room temperature and AB 129 concentration of 10 and 20 mg L ⁻¹ .	145
Figure 6.5	Effect of initial dye concentration on the removal of AB 129 at 0.045 g of CuO-NP-AC in 50 mL at pH 2, at room temperature.	146
Figure 6.6	Effect of temperature on the removal of AB 129 at 0.045 g of CuO-NP-AC in 50 mL at pH 2, and AB 129 concentration of 10 and 20 mg L ⁻¹ .	146
Figure 6.7	Langmuir isotherm for adsorption of AB 129 onto 0.045 g of CuO-NP-AC in 50 mL of different initial dye concentration, room temperature, pH 2.	147
Figure 6.8	Vant's Hoff plots of AB 129 dye onto CuO-NP-AC for evaluating thermodynamics parameters.	149
Figure 6.9	Pseudo-second-order plots at two different adsorbate concentrations i.e. 10 and 20 mg/L for adsorbent CuO-NP-AC	152
Figure 6.10	Plots of Intraparticle diffusion model for dye concentration of 10 and 20 mg/L.	153
Figure 7.1	ATR-FTIR of (a) HEMA, (b) HEMA-EEMA-MA and (c) PVA before and after adsorption	160
Figure 7.2	SEM images of HEMA, HEMA-EEMA and PVA before and after	162

	adsorption	
Figure 7.3	The effect of contact time on the amount of dyes adsorbed on different adsorbents	163
Figure 7.4	The effect of pH on the amount of dye adsorbed on the adsorbent	164
Figure 7.5	The effect of initial concentration on the amount of dye adsorbed on the adsorbent	165
Figure 7.6	The effect of agitation speed on the amount of dye adsorbed on the adsorbent.	166
Figure 7.7	Pseudo-second order adsorption kinetics of MG and CR onto HEMA, HEMA-EEMA-MA and PVA surfaces.	167
Figure 7.8	Intraparticle diffusion model of MG and CR onto HEMA, HEMA-EEMA-MA and PVA surfaces.	168

List of Tables

Table 1.1	Origin sources and toxic effects of some major noxious metals ion on human health.	6
Table 1.2	Health hazards and origin sources of some organic pollutants	10
Table 2.1	Physico chemical properties of Ni (II), As (III) and As (V)	43
Table 2.2	Physico chemical properties of Phenol and p-Cresol	44
Table 2.3	Physico chemical properties of Acid blue 129, Congo red and Malachite green	45
Table 3.1	EDAX quantitative microanalysis of the activated carbon from scrap tire	81
Table 3.2	Langmuir and Freundlich isotherm parameters for adsorption of Ni ²⁺ at different temperature on activated carbon prepared from scrap tire	88
Table 3.3	Thermodynamic parameters for adsorption of Ni ²⁺ at different temperature on activated carbon prepared from scrap tire	89
Table 3.4	Kinetic Parameters for the adsorption of Ni ²⁺ onto activated carbon from scrap tire	90
Table 3.5	Intraparticle diffusion model parameters for the adsorption of Ni ²⁺ onto activated carbon from scrap tire	92
Table 3.6	Testing of activated carbon from scrap tyre under metal fabricating industrial waste effluent condition	93
Table 3.7	Comparison of maximum adsorption capacity for the removal of noxious Ni ²⁺ by different previously developed adsorbents.	94
Table 4.1	The physical properties of adsorbents.	100
Table 4.2	Result of preliminary batch experiment	105
Table 4.3	Kinetic parameters of As (III) and As (V) adsorption on ACAL11 and TRAL	110
Table 4.4	Langmuir and Freundlich parameters for adsorption of As(III) and As(V) on ACAL11 and TRAL	113
Table 4.5	Effect of co-ions in removal of As (V) on ACAL11.	114
Table 4.6	Comparison of maximum adsorption capacity for the removal of noxious As (III) and As (V) by different previously developed adsorbents	115
Table 5.1	Octanol-water partition coefficient values (log Kow) and experimental	129

adsorption equilibrium (q_e) at different concentration for both RTACMC and RTAC

Table 5.2	Adsorption isotherm parameters for adsorption of p-Cresol and phenols at different temperature on to different adsorbents i.e. RTACMC and RTAC	130
Table 5.3	Thermodynamic parameters for adsorption of p-Cresol and phenol at different temperature on to developed adsorbents i.e. RTACMC and RTAC	132
Table 5.4	Kinetic parameters for the adsorption of p-Cresol and phenol onto RTACMC and RTAC	133
Table 5.5	Intraparticle diffusion model parameters for the adsorption of p-Cresol and phenol onto developed adsorbent RTACMC and RTAC	135
Table 5.6	Comparison of maximum adsorption capacity for the removal of noxious p-Cresol and phenol by different previously developed adsorbents.	136
Table 6.1	Isotherm parameters correlation coefficients calculated by various adsorption models onto 0.045 g of CuO-NC-AC in 50 mL, pH 2, and room temperature. Thermodynamic parameters for adsorption of AB 129 onto	148
Table 6.2	0.045 g of CuO-NP-AC at pH 2 at initial dye Concentration of 10 and 20 mg/L	150
Table 6.3	Adsorption kinetic parameters at different initial AB 129 onto 0.045 g of CuO-NC-AC in 50 mL at pH 2, room temperature and AB 129 concentration of 10 and 20 mg/L.	151
Table 6.4	Comparison of performance of proposed method with some previously reported acid blue dyes adsorption systems.	153
Table 7.1	Kinetic Parameters for the adsorption of CR and MG onto surface hydrogel polymer i.e. HEMA, HEMA-EEMA-MA, and PVA.	167
Table 7.2	Intraparticle diffusion model parameters for the adsorption of CR and MG onto surface hydrogel polymer i.e. HEMA, HEMA-EEMA-MA, and PVA.	169

List of Schemes

Scheme 2.1	Solvothermal method for preparation of CuO nanoparticles	44
-------------------	--	----

List of Publications

1. Gupta, V. K., Nayak, A., Agarwal, S., **Tyagi, I.** (2014). Potential of activated carbon from Waste Rubber Tire for the adsorption of phenolics: Effect of pretreatment conditions, *J Colloids Surface Sci.*, 417, 420-430.
2. Karmacharya, M.S., Gupta, V.K., **Tyagi, I.**, Agarwal, S., Jha, V.K., (2016). Removal of As (III) and As (V) using rubber tire derived activated carbon modified with alumina composite, *Journal of Molecular Liquids* 216, 836-844.
3. Gupta, V. K., Suhas, Nayak, A., Agarwal, S., Chaudhary, M., **Tyagi, I.**, (2014), Removal of Ni (II) ions from water using porous carbon derived from scrap tyre, *J Molecular Liquids*, 190, 215-222.
4. Nekouei, F., Nekouei, S., **Tyagi, I.**, Gupta, V. K. (2015). Kinetic, Thermodynamic and Isotherm studies for acid blue 129 removals from Liquids using Copper Oxide nanoparticle-modified activated carbon as a novel adsorbent, *J. of Molecular Liquids*, 201, 124-133.
5. Gupta, V.K., **Tyagi, I.**, Agarwal, S., Sadegh, H., Shahryari-ghoshekandi, R., Yari, M., Yousefi-nejat, O., (2015). Experimental study of surfaces of hydrogel polymers HEMA, HEMA–EEMA–MA, and PVA as adsorbent for removal of azo dyes from liquid phase, *Journal of Molecular Liquids* 206, 129-136
6. Gupta, V.K., Chandra, R., **Tyagi, I.**, Verma, M., (2016). Removal of hexavalent chromium ions using CuO nanoparticles for water purification applications, *J Colloids Surface Sci.*, 478, 54-62.
7. Agarwal, S., **Tyagi, I.**, Gupta, V.K., Fakhri, A., Sadeghi, N. (2016). Adsorption of toxic carbamate pesticide oxamyl from liquid phase by newly synthesized and characterized graphene quantum dots nanomaterials, *J. Colloids Surface Sci.*, (Accepted).
8. Verma, M., **Tyagi, I.**, Chandra, R., Gupta, V.K., Adsorptive removal of Pb (II) ions from aqueous solutions using CuO nanoparticles synthesized by sputtering method, *J. of Molecular Liquids* (Accepted).



CHAPTER 1

Introduction



“A healthy environment makes a healthy man” is well known quote in the English literature; hence a hygienic environment is vital for the appropriate development, fitness, and the survival of the living organisms as well as prevailing flora and fauna. The conservation and the protection of the environment are essential in the present industrialized and developing world. The exponential growth in the population of some countries including India is one the most prevailing problems of our age, due to this one of the most important natural resource i.e. water, which is a vital requirement of life and used for various household as well as industrial activities unfortunately exploited the most due the day to day activities of the house hold and industries. Today the whole world is facing water crisis because of unrestricted and excessive exploitation of water, due to this exploitation, we can quote that “Waste water today, live in desert tomorrow”. Rapid urbanization of natural resources like, increase in industries, especially textile industries is posing a threat to the water bodies as these discharge effluents with various harmful and toxic components. This deteriorates the quality as well a quantity of water and makes it unsafe for further use.

1.1. General introduction

Water resources are the valuable environmental asset which requires keen attention. It is defined as the sources which produce the water for our different types of uses and also those source that provide the huge benefit to the life of the living beings. Life on earth is not possible without water, which was present long before the origin of life. It is well established that water is major constituent of the prevailing flora and fauna including human beings. The water available on earth is distributed in an uneven manner. Of the total water content present on the earth, approximately 97% is present in the form of oceans and cannot be used without any purification. The remaining 3% water is generally available as fresh water, but 68.7% of this 3% fresh water is locked in the form of ice caps and glaciers, 30.1% of this 3% is available in the form of ground water, 0.9% of this 3% is present in other form and rest 0.3% of this 3% is present in the form of surface water. A pictorial presentation of this water distribution is shown in Figure 1.1. The river, lakes and streams contain only 0.3% of the total [1], which is immediately available for use. The quality of water is of very important concern for the prevailing flora and fauna including living organisms. A few decades back, when there is no industrialization, the water available from lakes, rivers and underground reservoirs was pure and suitable for drinking and other daily purposes. However rapid urbanization and industrialization leads to numerous unwanted and toxic materials discharged into air, water and soil, due to this urbanization, industrialization, modern methods of agricultural and domestic activities, the demand for water has increased tremendously which resulted in the generation of

large amount wastewater [2, 3] containing a number of chemicals called ‘pollutants’, which are harmful to both aquatic flora and fauna including human beings. This wastewater in the beginning was generally mixed up with natural water resources, which resulted in the contamination and depletion of the potable nature of water.

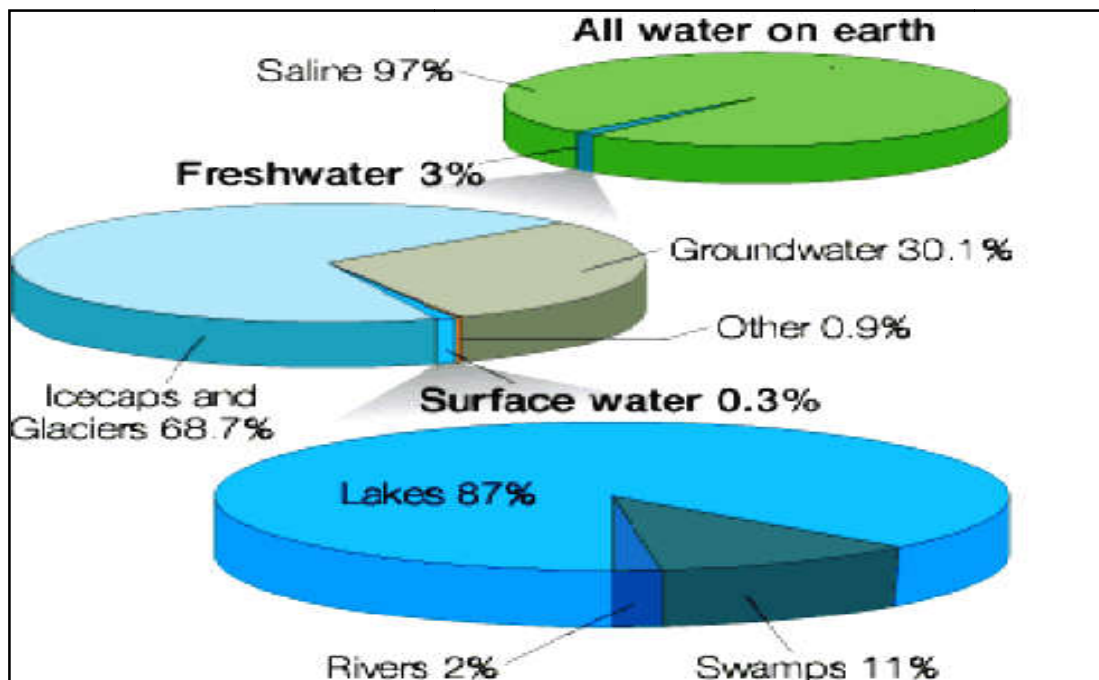


Figure 1.1 Pictorial presentation of water distribution on earth

According to FAO-UNICEF, India is the largest consumer of groundwater in the world with an estimated usage of 230 km³ per year [4]. Out of the total ground water about 60% is required for the agriculture purpose and rest is required for the other useful activities. According to the Department of Drinking Water and Sanitation (DDWS) nearly 90% of the rural water supply is from the groundwater sources. The Water and health of prevailing flora and fauna including human beings are closely related with each other. Unsafe water and poor sanitation contributed 7.5% of total deaths and 9.4% of total disability in India in 2002 [5]. About 1/3rd of the total deaths of the children’s of age group 0-5 years in India are due to diarrhoea and pneumonia [6]. Due to unsafe drinking water, the children’s suffer from several diseases which results in the weakening of the immune system, and in addition to this they become malnourished and underweight, which alters their learning ability throughout the life. According to the Statistical data, inappropriate dispose off of toxic waste, leads to water contamination in to the nearby aquatic streams. As per the CPCB, 2009 reports [7] there is about 38,000 million litres of the toxic waste is generated per day, and out of which only 12000

million litres per day of toxic waste is treated with the prevailing treatment techniques and procedures. Around 39% of the toxic waste treatment plants in India do not meet the general standards prescribed under the Environment Protection Rules. This work deals with the rapid removal and fast adsorption of noxious impurities from the wastewater. A few decades ago, there was a general feeling among many people that nature could effectively handle hazardous substances. Although, nowadays human beings are more concerned of their sensitive natural environment, pollution is still a problem.

1.2. Pollution and pollutants

1.2.1 Pollution

The word pollution derived from the Latin word “pollutionem” (defilement or to contaminate). It is defined as “The addition of any foreign material like inorganic, organic, biological or any radiological or any physical change occurring in nature which may harm or affect the living organisms directly or indirectly immediately or after a long time.”

1.2.2. Pollutants

According to Environment protection act (EPA) [8-10]; the term pollutant is defined as “A harmful solid, liquid or gaseous substance present in such concentration in the environment which tends to be injurious to environment.” In broad sense it refers to a substance/material that changes the nature quality of the environment by physical, chemical, or biological means. Pollutants can be classified in a number of ways:

1. On the basis of their forms they exist in the environment after their discharge:
 - Primary pollutants (NO_x, SO_x, CO)
 - Secondary pollutants (i.e. substance derived from primary pollutants like Peroxy Acetyl Nitrate (PAN)).
2. On the basis of ecosystem point of view:
 - Biodegradable pollutants are the substances which can be decomposed, removed or consumed and thus reduced to acceptable levels e.g. domestic wastes, heat etc.
 - Non biodegradable pollutants are those which either do not degrade or degrade slowly or partially and hence pollute the environment.

Thus we can conclude that when the waste products produced by human activities are not efficiently assimilated, decomposed or otherwise removed by natural biological or physical process, then they affect the prevailing ecosystem and food chain of the aqueous sources. The three main activities that mankind indulges in are domestic, agricultural and industrial, due all

these activities, large percentage of water fresh water is used, which is later on discharged in to the nearby aquatic streams in the form of wastewater containing different pollutants. On the type of human activity, pollutants are further categorised in to inorganic and organic pollutants [11-13], and biological agents as well as heat and radiations. A pictographic appearance of noxious pollutants on the basis of chemical nature is presented in Figure 1.2. Some of the major pollutants are discussed as under.

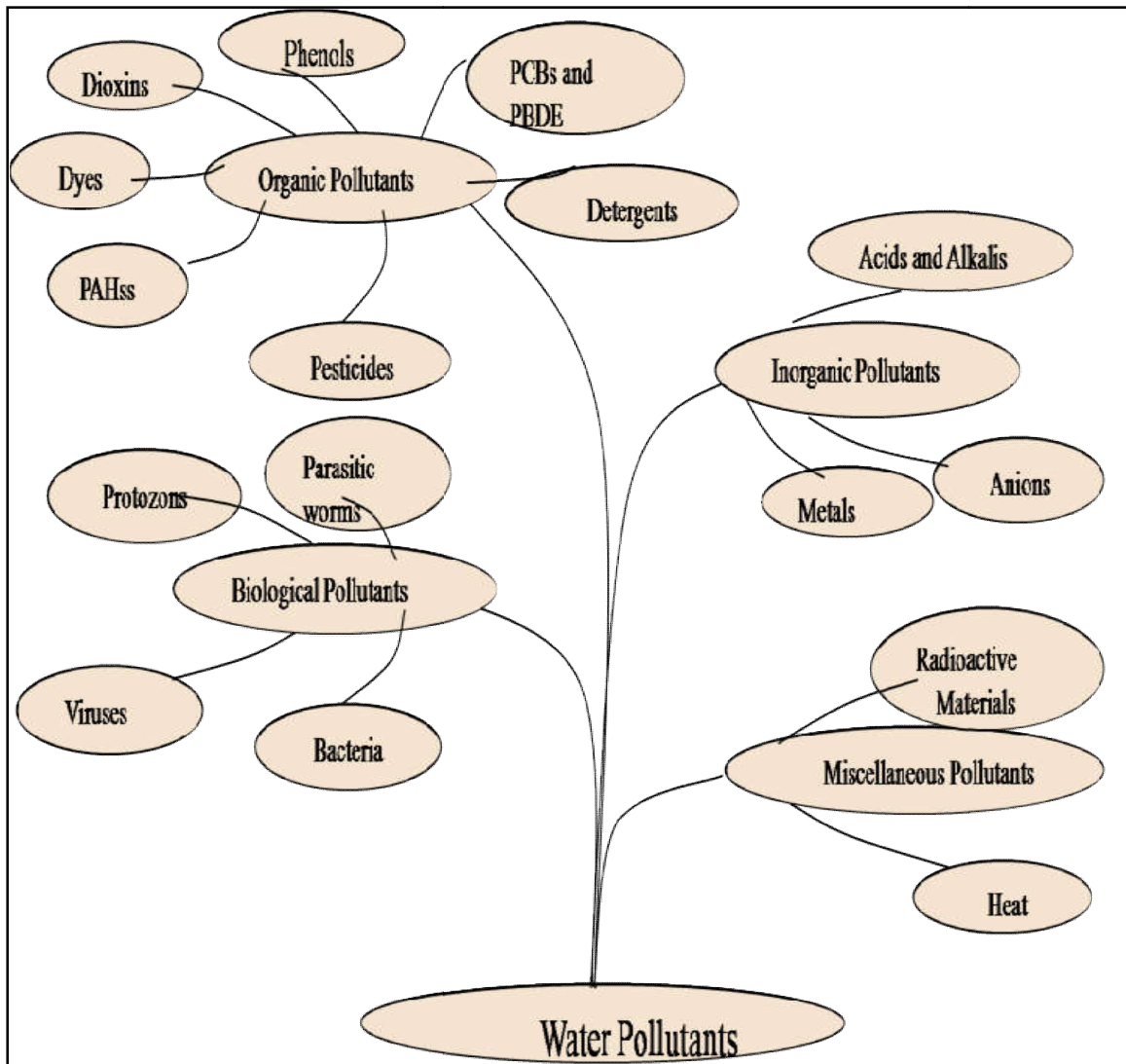


Figure 1.2 Pictographic appearances of noxious pollutants on the basis of chemical nature

1.2.2.1. In vivo biological agents

It may also be termed as biological threat agent or biological warfare agent. A biological agent is microorganism, which may be a protozoan, parasite, bacterium or fungus. These biological warfare agents may be present in the domestic effluent and sewage water. A

number of biological warfare agents [13], such as *Bacillus anthracis*, *Brucella abortus*, *Vibrio cholera*, *Corynebacterium diphtheriae*, and *Yersinia pestis* causes severe waterborne detrimental diseases such as anthrax, brucellosis, cholera, diphtheria and plague respectively. For prevention against such severe detrimental diseases, biological warfare agents are needed not to be removed from the aqueous source.

1.2.2.2. Heat

The term thermal pollution is defined as “The dilapidation in the quality of the aquatic sources due to the high temperature waste discharged in the aquatic sources”. The high temperature of this wastewater not only affects the aquatic ecosystem but it also causes many chemical and bacteriological reactions, such as formation of trihalomethane (THM) and higher corrosion activity [14]. These thermal pollutants when discharged in to the aquatic sources then it affect the biological oxygen demand, chemical oxygen demand and aquatic food chain of that aquatic ecosystem. This aquatic ecosystem deployment due to these thermal pollutants is also known as “thermal shock”.

1.2.2.3. Heavy metals

Noxious heavy metals in air, soil, and water are global problems that are a growing threat to the environment. The wastewater generated from many industries may contain a number of heavy metals which have significant toxic effects [15, 16], and thus considered as pollutants [17, 18]. There are several sources of heavy metal pollution, out of them the main sources are the coal, natural gas, paper, tanning, glassware, ceramics, electroplating industries etc. The wastewater of these industries contain heavy metal ions such as Cr(III), Cr(VI), Pb(II), Cd(II), As(III), As(V), Cu(I), Cu(II), Fe(II), Fe(III), Mn(II), V(III) and V(V), Ni (II), and Hg (II) etc. These heavy metals enter into the ecosystem mainly as: a) deposition of atmospheric particulates, b) discarding of metal enriched sewage sludge and other effluents and c) industrial wastes. The calculation of metal contribution in the ecosystem from the two later sources i.e. (b) and (c) is relatively easy to access. However, atmospheric contribution is difficult to calculate accurately because of atmospheric mixing of metal-bearing particulates and different metal-discharging sources which contribute to the metal content. These noxious metal ions possess severe detrimental effect on the human health and prevailing flora and fauna [19]. Table 1 reveals the origin sources and toxic effects of some major noxious metals ion on human health.

Novel adsorbent for noxious impurities removal

Table 1.1 Origin sources and toxic effects of some major noxious metals ion on human health.

Inorganic pollutants affecting the aqueous environment		
Pollutant	Usage sources	Health hazards and detrimental effects
Aluminum	Drainage of mining industries and weathering of rock	Changes water odour and responsible for water discoloration, increases water turbidity.
Antimony	Municipal wastes, glass, retardants, fireworks and natural weathering process.	Changes blood glucose and cholesterol levels on long term exposure, decreases longevity.
Barium	Enters environment through sandstones, soils and limestone industry	Cardiovascular disorder, gastrointestinal disorder and neurotoxic effect
Beryllium	Mining industries, from rocks also in low concentration, nuclear plants, petroleum industries	Carcinogenic agent, leads to acute and chronic toxicity, pleural disorders, osteoporosis
Cadmium	Form rocks, petroleum, paints and pigment industries, plastic plasticizers and stabilizers	Hypertension, renal damage, pleural damage, damages testicular cells and sometimes anaemia
Chromium	Leaching and mining process, combustion of fossil fuels. Cements plants.	Cr (VI) ion is toxic and leads to pleurisy and renal damage, lead to haemorrhaging, dermatitis and stomach ulcers
Copper	Domestic wastes, industrial outlets and leaching of minerals	Abdominal and intestinal ulcer, anaemia, and nephron damage
Iron	Through Sedimentation process of rocks, metal industries and mining industries	Changes water odour and taste made it astringent
Lead	Mining, plumbing industries in addition to this from coal and gasoline products	Affects RBC, mental retardation, causes deafening and hypertension in adults, sometimes it acts as carcinogenic agent also
Mercury	Used in many electrical industries and mining as well as pesticide manufacturing units	Causes Minimata disease, renal failure and respiratory disorder, nuero toxic agent
Zinc	Used in metal plating industries, plumbing and industrial waste	Changes water odour and color, changes water taste, causes health hazard in very high doses only

A detailed study on the adsorption properties of the some of the toxic metal ions such as Cr (VI), As (V), Pb (II), and Ni (II) were presented below:

1.2.2.3.1 Chromium [Cr (VI)]

Chromium is a highly toxic metal, which is extensively used industries and it enters the aqueous systems from various industries like electroplating, metal finishing, leather tanning, wood preserving and manufacturing of dyes and paints. It occurs in both the trivalent and hexavalent forms. Cr(III) is the most stable form, but is very insoluble and hence aqueous concentrations are well below water quality standards [20]. The Cr(VI) has high solubility in water and is more dangerous to living bodies since even low concentrations proved to be carcinogenic to the human beings. It exists in several stable forms in aqueous solution including $\text{Cr}_2\text{O}_7^{2-}$, HCr_2O_7^- , HCrO_4^- and CrO_4^{2-} depending on the Cr (VI) concentration and pH [21]. Chromate and dichromate ions can affect digestive organs adversely. The maximum allowable limit of hexavalent chromium for the discharge into public sewers, marine coastal areas, in land surface water [22] is 2, 1, 0.1 and 0.05 mg/L respectively.

1.2.2.3.2 Arsenic [As(III) and As(V)]

Arsenic is one of the main pollutants in waste discharges, it occurs in the environment in several oxidation states such as -3, 0, +3 and +5. Inorganic arsenic is generally found as trivalent arsenite or pentavalent arsenate form in the aqueous solution. It is introduced into the surroundings and aqueous system through geochemical reactions, industrial waste discharges and pesticides. In surface water under oxidizing conditions, arsenate predominates while arsenite becomes stable in anaerobic water under reducing conditions [23]. Arsenic toxicity is dependent on its chemical form, solubility and mobility. The As(V) is less hazardous than As (III) [24]. The presence of arsenic in the aquatic source leads to severe detrimental and harmful affect on prevailing flora and fauna. Chronic arsenic poisoning can occur from the ingestion of drinking water containing high levels of arsenic. Acute arsenic poisoning results in the muscle disorder, abdominal pain, headache and diarrhoea. Long term exposure of arsenic pollutant leads to severe detrimental effect on the vital organs i.e. cardiac diseases [25], bronchial disorder [26], diabetes [27] and sometimes it proved to be carcinogenic [28, 29] for living beings. According to the US Environmental protection agency, the acceptable value of arsenic in drinking water is limited to $10\mu\text{g/L}$ [30]

1.2.2.3.3. Lead [Pb (II)]

Among the heavy metal pollutants, lead is considered as a main environmental pollutant. It is commonly used in a wide variety of industrial processes such as textile dying, ceramic and glass industries, petroleum refining, battery manufacture and mining operations [31]. It has widespread use in electrical industries, fungicides, anti-fouling paints etc. Lead

Novel adsorbent for noxious impurities removal

contamination of drinking water occurs as a result of corrosion and leaching from lead pipes and Pb/Sn soldered joints associated with the copper used in house-hold plumbing [32]. It comes into the environment through effluents from lead smelters, battery manufacturers, paper and pulp industries and ammunition industries [33]. Major lead pollution is due to the manufacture of storage batteries, painting pigments, solder, plumbing fixtures, automobiles, cable coverings, radioactivity shields, caulking and bearings [34, 35]. The removal of lead in wastewater is major issue for many years due to their environmental harm and threat to life [36]. Lead is a general metabolic poison and enzyme inhibitor. It can cause mental retardation and semi-permanent brain damage in young children [37]. All lead compounds are considered as cumulative poisons. Acute lead poisoning can affect the nervous system and gastrointestinal track [38]. Lead accumulates mainly in bones, brain, kidney and muscles. In addition to this it may lead to severe disorders like anaemia, kidney diseases, nervous disorders, sickness and even death [39]. Lead ions concentrations approach 200-500 mg/L in the industrial wastewaters. This value is very high compared to the water quality standards and it should be reduced to 10µg/L [40].

1.2.2.3.4. Nickel [Ni (II)]

Wastewater contaminated by high doses of toxic metal ions has been a serious after effect of the rapid industrialization. There has been thus a rapid depletion in the availability of fresh water and consequent increase in water borne diseases to humans and aquatic life. Several industrial activities like mineral processing, electroplating, production of paints and batteries, manufacturing of sulphate and porcelain enamel industries etc. have generated wastewater containing nickel ions in doses higher than the limits [41-43]. The U.S. Environmental Protection Agency (EPA) requires nickel not to exceed 0.015 mg/L in drinking water [30] and the same prescribed by WHO is 0.02 mg/L [44]. Human exposure to nickel ions at higher doses is associated with serious health effects like dermatitis, nausea, coughing, chronic bronchitis, gastrointestinal distress, and reduced lung function and lung cancer [45, 46]. Because of its toxicity, persistency and bioaccumulation in the food chain [47], the nickel ion pollutant is a potential threat to the environment and there is a need for its effective removal in order to ensure adequately treated effluent quality for various uses.

1.2.2.4. Dissolved and Non-Dissolved Chemicals

During the course of domestic, industrial, and agricultural operations, a number of chemicals are used or produced and often get mixed up with fresh water, which is then

discharged as wastewater. The chemicals present in wastewater may be in a dissolved or non-dissolved state.

Non-dissolved substances are generally present as suspended solids in a dispersed form. The suspended solids make the water turbid and sometimes they may also slowly settle down with the formation of slit. The presence of suspended solids clogs waterways, fills up dams, and is harmful to aquatic life in many ways [48]. The most common chemicals [13] found in wastewater in a dissolved state and considered as potential pollutants are heavy metals, dyes, phenols, detergents, pesticides, polychlorinated biphenyls (PCBs), and a host of other inorganic and organic substances.

1.2.2.5. Colored synthetic compounds

Dyes are important materials that are currently in use both for domestic and industrial purposes. Since the invention of synthetic dyes [49] in 1856, several forms of dyes are now available, and more than 8000 dyes are being manufactured and consequently used for specific purposes. The dyes in use are both water soluble and insoluble. The big consumers of dyes are textile, dyeing, paper and pulp, tannery, and paint industries. Hence, the effluents of these industries as well as those from plants manufacturing dyes tend to contain dyes in sufficient quantities for them to be considered an objectionable type pollutant for two reasons: they impart colour to water, which is not acceptable on aesthetic grounds, and they are toxic and adversely affect life [50-53]. Table 2 reveals the health hazards and origin sources of some organic pollutants.

1.2.2.6. Biocides agents

Whereas many other pollutants are only important in the urban setting, pesticides are pre eminently a problem arising from rural activities. Depending on their function, pesticides [54] are sub classified as herbicides, algicides, slimicides, bactericides, fungicides, and insecticides. Among these, insecticides and fungicide are important pesticides with respect to human exposure in food because they are applied shortly before or even after harvesting. Herbicides production has increased significantly, as chemicals are being increasingly used during the cultivation of land for controlling weeds and now accounts for the majority of agricultural pesticides. Although DDT has been banned, various substitutes such as toxaphene, lindane, parathion, malathion, heptachlor and endrin can also cause environmental pollution (Table 2). The problem of pesticides pollution arises not only due to agricultural operations but also from pesticides manufacturing plants.

Table 2 Health hazards and origin sources of some organic pollutants.

Organic contaminants in aqueous environment		
Contaminant	Usage sources	Health hazards and detrimental effects
Volatile organic compounds	Enters in the ecosystem during the manufacturing of plastics, rubbers, Pesticides and insecticides, paints and pharmaceutical companies	Carcinogenic, pleural disorders, anaemia, dermatitis and blurred vision, respiratory infections.
Pesticides	Enters ecosystem through pesticides manufacturing units	Leads to frontal lobe disorder, results in intense headache, abdominal disorders, teratogenic, affects reproductive system
Plasticizers, chlorinated solvents, benzo[a]pyrene, and dioxin	Used as sealants, linings, solvents, pesticides, plasticizers, components of gasoline, disinfectant, and wood preservative.	Carcinogenic, respiratory disorder, dizziness, headache and teratogenic

1.2.2.7. Phenol and its derivatives

Like dies and metals, phenols are also considered priority pollutants [55, 56] as they impart bad test and odour to water and are also toxic, [57, 58] even at low concentrations. The determination and removal of phenols from water is therefore important. These are present in wastewater generated from pulp and paper, chemicals, paint, resin, pesticides, gas and coke manufacturing, tanning, textile, plastics, rubber, pharmaceutical and petroleum industries.

1.2.2.8. Detergents

Most detergents are phosphate based, which are major water pollutants, responsible, for 42% of human and animal diseases. According to literature “the main problem is that of phosphate-based detergents promoting eutrophication of aquatic environments”. Eutrophication or nutrient pollution is a process by which water bodies gradually age and become more productive. Sewage perhaps is a particular source of phosphorus when detergents containing large amounts of phosphates are drained during washing. Now a days sewage contains appreciable quantities of synthetic detergents too [59]. The persistent surfactants like alkyl benzene sulphonate (ABS) interfere with waste treatment process by stabilizing the small particles as colloidal suspensions and thereby decreasing the activity of biological filter beds and activated sludge.

1.2.2.9. Polychlorinated biphenyls and Polybrominated diphenyl ether

The term polychlorinated biphenyls (PCBs) refer to a group of 209 different chemical compounds. PCBs were used primarily for lubrication and insulation in electrical equipment and are generated in a variety of manufacturing processes which include manufacture of brake linings, glass ceramics, grinding wheels, various types of coatings, flame proof paints, varnishes, sealants, electrical equipments, plastic coating etc. they so high chemical, thermal and biological stability low vapour pressure and high dielectric constants. They do not cause biochemical oxygen demand problem in aquatic ecosystem but are extremely toxic [53]. PCBs are considered among the most dangerous of life threatening substances created by humans. They pollute the food chain and are present as contaminants in wildlife and humans at levels thousands of times higher than the surrounding air, water and soil. Many studies have shown that PCBs are capable of disrupting the endocrine system and are associated with reproductive failure, immune system disorders, behavior and learning disorders and cancers.

Polybrominated diphenyl ether (PBDE) is a flame-retardant sub-family of the brominated flame-retardant group. They have been used in a wide array of household products, including fabrics, furniture and electronics. These pollutants are of three main types according to the bromine atoms in the molecule i.e. penta, octa and deca. The family of PBDEs consists of 209 different substances, which are called congeners. There are two sub group viz. lower brominated and higher brominated. Lower brominated PBDEs have 1-5 bromine atoms and are regarded as the most dangerous ones, because of the smaller size which can be absorbed by living organisms easily. These PBDEs has been known to affect hormone levels in thyroid gland [54]. Whereas, higher brominated PBDEs have more than 5 bromine atoms and were formerly regarded as environmentally harmless chemical compounds.

1.2.2.10 Polycyclic aromatic nuclear hydrocarbons

Polycyclic aromatic nuclear hydrocarbons (PAHs) are chemical compounds that consists of fused aromatic rings and do not contain hetero atoms or other substituent. Some of them are known as suspected carcinogens. They are formed by incomplete combustion of carbon-containing fuels such as wood, coal, diesel, fat or tobacco [55]. PAHs toxicity is very structurally dependent, with isomer (PAHs with the same formula and no. of rings) varying from being nontoxic to being extremely toxic. Thus, highly carcinogenic PAHs may be small or large. One PAH compound, benzoic [a] pyrene, is regarded as first chemical carcinogenic agent.

1.2.2.11. Hormone mimicking substances

Dioxins are possibly the most cancer causing chemicals known because their chemical structure mimics that of hormones. They are toxic mainly because they are persistent organic pollutants [56]. Dioxins can exist in our body for up to seven years before they kill. The only known way to destroy dioxins is by burning the contaminated material, by heating it to almost 1000°C. The reason why dioxins are some of the most toxic chemicals in existence is because they do not dissipate naturally.

1.2.2.12. Radioactive substances

The radioactive substances [59] are handled with all precautions in view of harmful nature of radiations emitted by them. In spite of this, radioactive materials are often found in effluents coming from various industries and hospital outlets. Nowadays, many nuclear weapons are tested underground which is contaminating ground water radioactively.

1.2.2.13. Artificial chemicals as pollutants

A host of other organic chemicals may also be present in effluents generated from different industries. These include: trihalomethanes such as chloroform and bromoform, trichloroethylene, tetrachloroethylene, aromatic hydrocarbons such as benzene, toluene, xylene and biphenyls, halogenated aromatics, such as chlorobenzene, dichlorobenzene, chlorotoluene and chloroxylene, halogenated aliphatic compounds, including bromochloromethane, dibromomethane and tetrachloromethane, halogenated ethers, polycyclic aromatic hydrocarbons, such as naphthalene, acenaphthene, fluorine and phenanthrene, aldehydes, esters, alicyclic hydrocarbons and ketones.

The majority of the chemicals present in wastewater is toxic above certain concentration level and is, therefore, considered as pollutants. The lethal effects of the pollutants are well documented in literature [51, 60-61]. In view of general awareness created by modern methods of communication and information, it has become imperative on the part of government, industries and municipal authorities to work out methods for pollution control. A number of methods are of course available but sometimes cost factors override the importance of pollution control. The search for cost effective technology for safe and effective treatment of wastewater is always on.

1.3. Wastewater Treatment Technologies

Wastewater treatment and reuse is an important issue and scientists are looking for inexpensive and suitable technologies. Water treatment technologies are used for three

purposes i.e. water source reduction, wastewater treatment and recycling. At present, unit operations and processes are combined together to provide what is called as primary, secondary and tertiary treatment. In a complete water treatment plant, all these three processes are combined together for producing good and safe quality of water. The complete scheme of wastewater treatment is shown in Figure 1.3

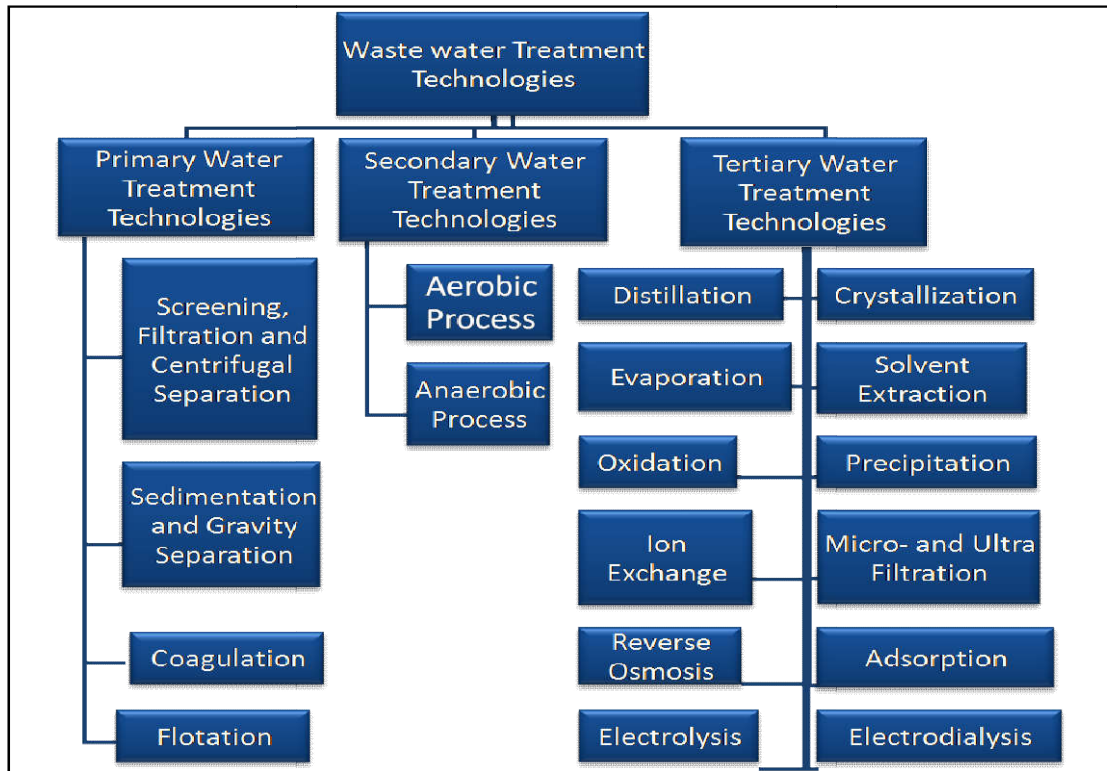


Figure 1.3 Schematic presentations of the water treatment technologies

Water treatment and recycling technologies have been classified on the following headings:

1.3.1. Primary Water Treatment Technologies

1.3.2. Secondary Water Treatment Technologies

1.3.3. Tertiary Water Treatment Technologies

1.3.1. Primary Water Treatment Technologies

In this category, water is treated at the primary level using screening, filtration, centrifugation [57, 62], sedimentation [58, 63], coagulation [64], and flotation [65, 66] methods. Normally, these methods are used when water is highly polluted.

1.3.2. Secondary Water Treatment Technologies

Secondary water treatment includes natural routes for the exclusion of soluble and inexplicable impurities by biological organisms [67, 68]. Water is circulated in a reactor that maintains a high concentration of microbes. The microbe usually bacterial and fungal strains convert the organic matters into water, carbon dioxide and ammonia gases [69-73]. The biological treatment includes aerobic [74, 75] and anaerobic digestion [76-81] of wastewater. Depending on the materials use, the cost of biological treatment varies between 20 and 200 UUS/ million litres. The disadvantage of the method is the production of a large quantity of bio solids, which require further costly management. The aerobic process is carried out by trickling filters or activated sludge processes or oxidation ponds.

1.3.3. Tertiary Water Treatment Technologies

Tertiary water treatment technologies includes processes like distillation [82], crystallization [83], evaporation [84], solvent extraction [85, 86], chemical oxidation carried out by potassium permanganate, chlorine, ozone, H_2O_2 , Fenton's reagent (H_2O_2 and Fe catalyst) and chlorine dioxides [87-95], advanced oxidation method using ozone [96-99], combined ozone and peroxide [100], ultra violet enhanced oxidation such as UV/fenton or photo-Fenton [101, 102], UV/hydrogen peroxide, UV/ozone [103], UV/air wet air oxidation and catalytic wet air oxidation (where air is used as the oxidant), photocatalysis using oxides such as TiO_2 , ZnO , ZrO_2 , CeO_2 , etc or sulphides such as CdS , ZnS etc. [104-112], sonolysis [113], precipitation [114], ion exchange [115-119], micro and ultrafiltration [120-122], reverse osmosis [123-129], and adsorption [130], electrolysis [131-136] and electrodialysis [137-140].

A particular treatment process may not be useful in removing numerous noxious impurities, in order to eradicate the noxious impurities rapidly from wastewater new techniques such as adsorption must be used because it has a capability of removing noxious impurities from wastewater.

In the present thesis we deal with the rapid removal and fast adsorption of various types of pollutants, hence it is desirable to survey literature on adsorption methodology. This is being discussed in following sections.

1.4. Adsorption technology

The ingenuity of adsorption in pollution control has been recognized and the importance of adsorption [141-146] in chemical, food, petroleum and pharmaceutical industries is also well established.

The term adsorption refers to a process wherein a material is concentrated at a solid surface from its liquid or gaseous surroundings. It is now customary to differentiate between two types of adsorption. If the attraction between the solid surface and the adsorbed molecules is physical in nature, the adsorption is referred to as physical adsorption. Generally, in physical adsorption, the attractive forces are van der Waals forces, and they are weak, the resulting adsorption is reversible in nature. On the other hand, if the attraction forces between adsorbed molecules and the solid surface arise due to chemical bonding, the adsorption process is called chemisorptions. In view of the higher strength of the bonding in chemisorptions, it is difficult to remove chemisorbed species from the solid surface. The strength of bonding in physical adsorption and chemisorptions is manifested in the values of enthalpy of adsorption which are much lower ($\leq 25\text{kJmol}^{-1}$) for the former as compared to later (of the order 200 kJmol^{-1}). The solids adsorbing the material are called adsorbents whereas the substances that are adsorbed are called adsorbates.

Adsorption has been found to be superior compared to the other techniques for water re-use in terms of initial cost, flexibility and simplicity of design, ease of operation and insensitivity to toxic pollutants. Adsorption also does not result in the formation of harmful substances and is regarded as one of the most effective and attractive processes with several advantages associated with no chemical sludge and high removal efficiency. Liquid-solid adsorption operations concern the ability of certain solids to preferentially concentrate specific substances from solution onto their surfaces, such as the removal of moisture dissolved in gasoline, the decolourisation of petroleum products and the removal of pollutants from aqueous effluents.

1.5. Adsorbents

Adsorbents are conveniently divided into three classes: inorganic materials, synthetic polymers, and carbons. Inorganic materials vary widely like activated alumina, silica gel, clays, fuller's earth and zeolites. Adsorbents based on synthetic polymers, like ion exchange or acrylic ester polymers are commonly used in wastewater treatment. Most interesting in this connection are carbons. The carbons have non-polar surfaces that are used to adsorb non-polar molecules. While activated carbon is especially known for its effectiveness in removing organic chemicals from wastewater, it is also surprisingly effective in removing a variety of inorganic pollutants. Adsorption plays a significant role in pollution control, where adsorbent can adsorb mere traces of solute, making this method especially useful for dilute solutions.

Novel adsorbent for noxious impurities removal

Molecules adsorb on virtually all surfaces, the amount they adsorb is roughly proportional to the amount of surface.

To examine the practical ability of a solid sorbent, the following characteristics must be considered: porosity, structural stability, reversible uptake and release and capability of surface modification for creating molecule-specific adsorption sites [147]. Most of the solid adsorbents possess a complex porous structure that consists of pores of different sizes and shapes. In terms of the science of adsorption, the total porosity is usually classified into three groups: micropores (smaller than 2nm), mesopores (in the range of 2 to 50nm) and macropores (larger than 50nm) [148]. The adsorption in micropores is a pore-filling process, because sizes of micropores are comparable to those of adsorbate molecules. All atoms or molecules of the adsorbent can interact with the adsorbate species. This is the fundamental difference between adsorption in micropores and meso- and macropores. The pore size distribution of micropores is another important property for characterizing adsorption capacity of adsorbents [149-151]. Mono and multilayer adsorption takes place successively on the surface of mesopores and their final fill proceeds according to the mechanism of capillary adsorbate condensation [152]. The basic parameters characterising mesopores are specific surface area, pore volume, pore size and pore volume distribution. Since the specific surface area of macropores solids is very small, adsorption on this surface is usually neglected. Hence the important characteristics of good adsorbents [153, 154] are their high porosity and consequently larger surface area with specific adsorption sites (Figure 1.4).



Figure 1.4 Activated carbon sub divided in the basis of porous nature

Most adsorbents which have been used in pollution control tend to have porous structure. The porous structure not only increases surface area and consequently adsorption but also affects the kinetics of the adsorption. A better adsorbent is considered one which has high surface area with less time for adsorption equilibrium. Thus, for removal of pollutants, one generally looks to adsorbents with high surface area and faster kinetics. There are numerous types of adsorbents, which have been used for wastewater treatment. The removal of heavy metals ions, phenols and noxious dyes from wastewater has been explored with the use of different types of adsorbents. Searching for low-cost and easily available adsorbents to remove heavy metal ions, phenols and noxious dyes have become a main research focus. Till date, several studies on the use of low-cost adsorbents have been published. Agricultural wastes, rubber tire wastes, nanoparticles, industrial by products and surface hydrogels and natural substances have been studied as low cost adsorbents for the heavy metal ions, phenols and noxious dyes wastewater treatment. A pictorial presentation of classification of adsorbents is shown in Figure 1.5. Among the classified adsorbents, the industrial and agricultural wastes were further sub-classified Figure 1.6.

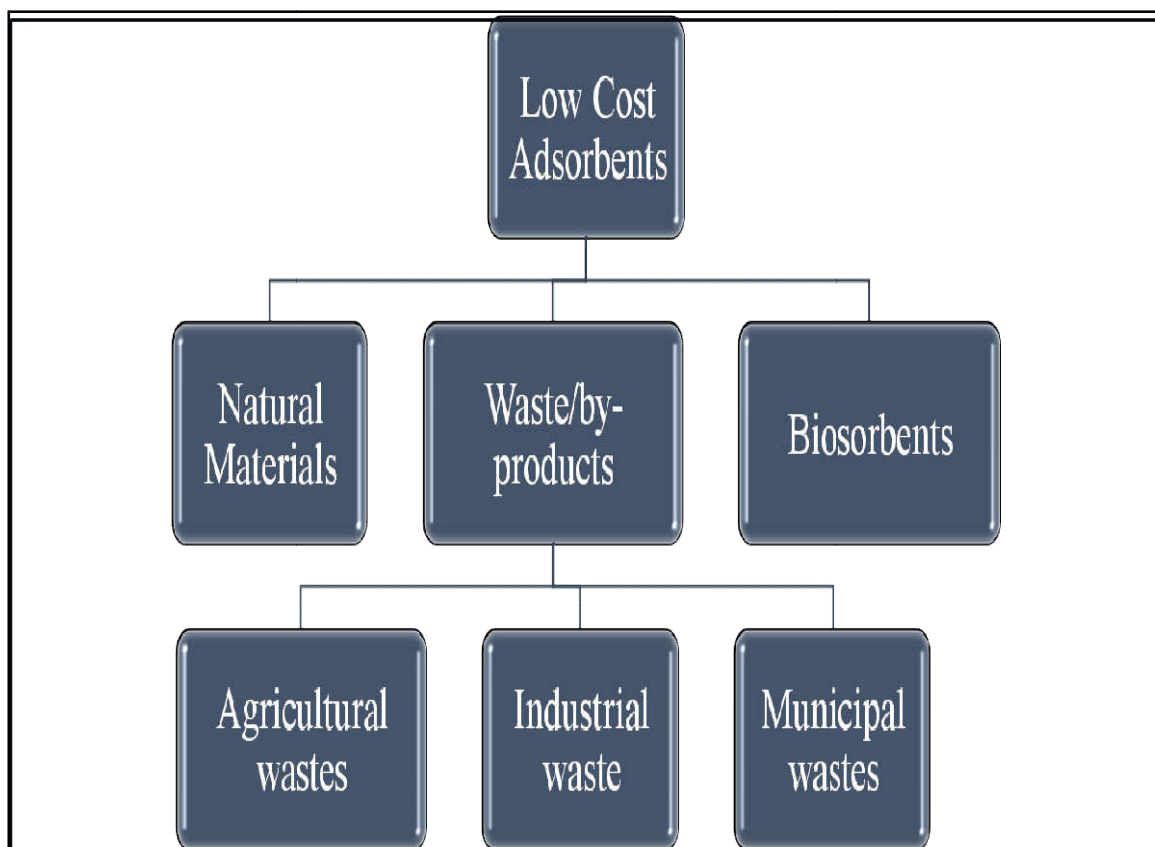


Figure 1.5 Classification of adsorbents

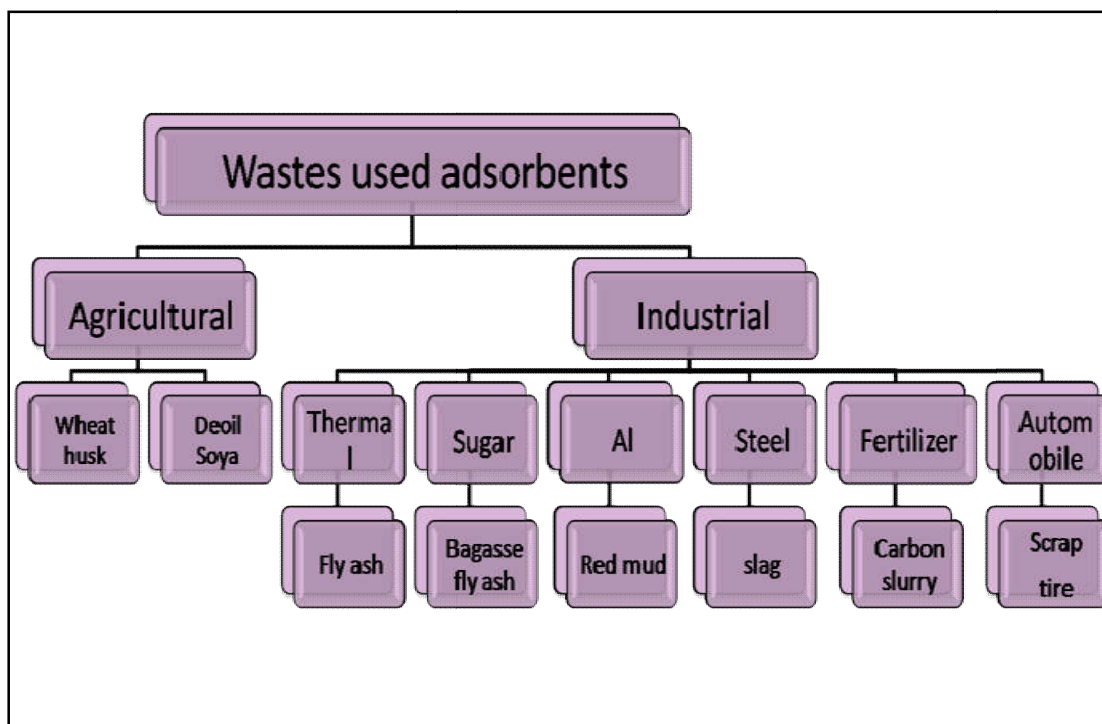


Figure 1.6 Classification of industrial and agricultural wastes as adsorbents

1.5.1. Conventional adsorbents

This class of adsorbent consists of costly adsorbents, which are in use for many years. High cost of these adsorbents is due to their manufacture by private companies and sale as per their high profit. As already discussed their use is often restricted due to their high cost and necessity of regeneration. Few of them are given below:

1.5.1.1. Amorphous substances as adsorbents

Silica gel is an amorphous adsorptive substance with stable chemical properties and has a highly complicated porous structure. It is used in various fields of our daily life as high adsorbent of high safety. Both siloxane, $-\text{Si-O-Si}-$, and silanol $-\text{Si-O-H}$, bonds are present in the gel structure. The gel is considered good adsorbent and is used in various industries for the treatment of noxious wastes and chemicals etc. [155-156]. Its cost varies with its particle size and purity, an ideal sample of silica gel with 99% purity, costs about US\$ 180 per kg.

1.5.1.2. Alumina as adsorbent

The activated alumina comprises a series of non equilibrium forms of partially hydroxylated alumina, Al_2O_3 . They are porous solids made by thermal treatment of aluminium hydroxide precursors and find applications mainly as adsorbents, catalyst and catalyst support. In general, as a hydrous alumina precursor is heated, hydroxyl groups are driven off leaving a

porous solid structure of activated alumina. One of the earliest uses for activated alumina was removal of water vapors from gases and this remains an important application. Activated alumina having surface area ranging from 200-300 m²/g [157], is also used to remove water from organic liquids including gasoline, kerosene, oils, aromatic hydrocarbons and many chlorinated hydrocarbons. Activated alumina is receiving renewed attention as an adsorbent and a wealth of information has been published [158-160] on its adsorption characteristics. The cost of alumina used for water purification is about US\$ 58 per kg.

1.5.1.3. Zeolites and Ion exchange Resins

Zeolites are basically hydrated alumina-silicate minerals with an “open” structure that can accommodate a wide variety of positive ions such as Na⁺, K⁺, Ca²⁺, Mg²⁺ and others. There are 40 natural and over 100 synthetic zeolites, among them the more common mineral zeolites are: analcime, chabazite, heulandites, natrolite, phillipsite, and stilbite. The zeolite channels (or pores) are microscopically small, and in fact, have molecular size dimensions such that they are often termed “molecular sieves.” The size and shape of the channels have extraordinary effects on the properties of these materials for adsorption processes, and this property leads to their use in separation processes. Molecules can be separated via shape and size effects related to their possible orientation in the pore, or by differences in strength of adsorption. They are also considered as selective adsorbents. Zeolites generally show a surface area in the range 1-20m²/g [157]. Zeolites-based materials are extremely versatile. Various zeolites have been employed for the removal of pollutants [161-162]. A number of ion-exchange resins have also been used widely in household and industrial water purifications to produce soft water. This is accomplished by exchanging calcium Ca²⁺ and magnesium Mg²⁺ cations against sodium Na⁺ or hydrogen H⁺ cations for the removal of specific compounds e.g. the removal of ammonia-nitrogen in ammonium chloride wastewater from rare earth smelters by Wang et al. [163], the removal of geosmin and methylisoborneol from drinking water by Ellis and Korth [164] and the removal of phenols and chlorophenols by Okolo et al. [165]. These adsorbents also have widespread applications in petroleum industry. The cost of zeolites, which are usually used for water treatment purpose, is about US\$ 210 per kg.

1.5.1.4. Activated carbon

Activated carbon is the most widely used adsorbent. The graphite structure gives carbon its very large surface area which allows the carbon to adsorb a wide range of compounds. It has the strongest physical adsorption forces or the highest volume of adsorbing porosity of any material known to mankind. Activated carbon can have surface area greater than 1000 m²/g.

Novel adsorbent for noxious impurities removal

The use of carbon extends so far back in to history that its origin is impossible to document. Charcoal was used for drinking water filtration by ancient Hindus in India since 2000 B.C. [153, 166], and carbonized wood was used as a medical adsorbent and purifying agent by the Egyptians as early as 1500 B.C. Modern development and use has been documented more precisely.

The activated carbon generally exists in two forms (i) powdered activated carbon (PAC) and (ii) granular activated carbon (GAC). Since granular form is more adaptable and there is no need to separate the carbon from the bulk fluid, most of the work on the removal of pollutants from water has been on GAC. On the other hand the use of PAC offers some practical problems like requirement of separation of the adsorbent from the fluid. However, in spite of these problems, PAC is also used for wastewater treatment due to low capital cost and lesser contact time requirements [164]. Two more specific forms viz. Activated carbon fibrous (ACF) and activated carbon clothe (ACC) are also in use [165, 167]. The cost of activated carbon varies from US\$ 2.5-55 per kg depending upon the purity and particle size.

Activated carbon was first generated industrially in the first part of twentieth century, when activated carbon from vegetable material was produced for use in sugar refining [168]. The first documented use of activated carbon in a large scale water treatment application was in 19th century in England, where it was used to remove undesirable odours and tastes from drinking water [169]. This carbon was found effective in decolorizing liquids. Activated carbon has since been used extensively for this purpose in many industries. In particular, it has been commonly used for the removal of organic dyes from textile wastewaters. In recent years, the use of activated carbon for the removal of priority organic pollutants has become very common. Today, hundreds of brands of activated carbon are manufactured for a large variety of purposes [170]. The credit of developing commercial activated carbon goes to Raphael von Ostrejko [171] whose inventions were patented in 1900 and 1901. Hassler [172] has summarized in his book the successful application of activated carbon in providing potable water. In USA, for the first time in 1928, activated carbon was used for the water supplies and within ten years the figure of water treatment plants with activated carbon increased to a thousand marks. The applicability of activated carbon for water treatment has been demonstrated by Weber et al., [173] and Green et al., [174] who talked about the potentiality of activated carbon for water and air purification. Stenzel [175] in his article describes the adsorption with granular activated carbon to be a proven technology for water purification.

It is thus seen wide variety of raw materials have been used to prepare activated carbon. However, the activated carbon used in wastewater treatment is generally prepared from coconut shells, peat, sawdust, wood char, lignin, petroleum coke, bone char, anthracite coal etc. [176]. Hence activated carbon has become the standard adsorbent for the reclamation of municipal and industrial wastewaters to a water potable quality.

1.5.1.5. Modified activated carbon

The adsorption efficiency of activated carbons is strongly dependent on their surface chemical features. Therefore, the surface chemical modification of carbon is of great interest in order to produce materials for specific applications. It has been observed by various workers that chemical treatment at the time of activation during the manufacture of activated carbons often enhances the adsorption properties [177-178]. This modification has been mainly carried out by oxidative methods, producing a more hydrophilic structure with a large number of oxygen containing groups. Various reagents have been used as oxidants: concentrated nitric or sulphuric acid, sodium hypochlorite, permanganate, bichromate, hydrogen peroxide, transition metals and ozone based gas mixtures. It was found that the type of surface structures and the extent of their formation depend on the oxidizing agent, the concentration and the pH of the oxidizing solution.

1.5.2. Alternative low cost adsorbents

As already stated, the activated carbon is the most popular adsorbent for the removal of pollutants from wastewater, but it has certain limitations. Activated carbon presents disadvantages [179] as it is costly and cannot be afforded at an economical level. The regeneration of saturated carbon is also expensive, not straightforward, and results in loss of the adsorbent. The use of carbons based on relatively expensive starting materials is also unjustified for most pollution control applications [180]. This has led research interest towards various natural solid supports, which are able to remove pollutants from contaminated water at low cost. Cost is actually an important parameter for comparing the adsorbent materials. According to Bailley et al. [181], a sorbent can be considered as low cost if it requires little processing, is abundant in nature or is a by-product or waste material from another industry. Certain waste products from industrial and agricultural operations, natural materials and bio sorbents represent potentially economical alternative adsorbents. Many of them have been tested and proposed for pollutants removal.

1.5.2.1. Rural wastes as low-cost adsorbents

Rural waste materials can also be used as low cost adsorbents due to its rich cellulose content. The basic components of the agricultural waste materials include hemicelluloses, lignin, lipids, proteins, simple sugars, water, hydrocarbons, and starch, containing variety of functional groups. Agricultural waste materials being economic and eco-friendly due to their unique chemical composition, availability in abundance, renewable nature and low cost are viable option for water and wastewater remediation. Agricultural waste is rich source for activated carbon production due to its low ash content and reasonable hardness [182], therefore, conversion of agricultural wastes into low cost adsorbents is a promising alternative to solve environmental problems and also to reduce the preparation costs. These agricultural waste materials have been used in their natural form or after some physical or chemical modification (Figure 1.6).

1.5.2.2. Industrial and municipal wastes as low-cost adsorbents

Widespread industrial activities generate huge amount of solid waste materials as by-products. Some of this material is being put to use while others find no proper utilization and are dumped elsewhere. The industrial waste material is available almost free of cost and causes major disposal problems. If the solid wastes could be used as low-cost adsorbents, it will provide a two-fold advantage to environmental pollution. Firstly, the volume of waste materials could be partly reduced and secondly the low cost adsorbent if developed can reduce the pollution of wastewaters at a reasonable cost. In view of the low cost of such adsorbents, it would not be necessary to regenerate the spent materials. Thus, a number of industrial wastes have been investigated with or without treatment as adsorbents for the removal of pollutants from wastewater (Figure 1.6). Some of them are fly ash or thermal power plant waste [183-185], steel industry wastes [186-188], red mud, or aluminium industry wastes [189-191], carbon slurry, or fertilizer industry wastes [192-193], leather industry wastes [194-195] etc.

1.5.2.3. Bio sorbents as low-cost adsorbents

The bio sorbents and their derivatives contain a variety of functional groups which can complex dyes. The bio sorbents are often much more selective than traditional ion-exchange resins and commercial activated carbons, and can reduce dye concentration to ppb levels. Bio sorption is a novel approach, competitive, effective and cheap. Several bio sorbents [196-198] can be efficiently used as adsorbents for the removal of noxious impurities from the solvent phase.

1.6. Problem statement

Water pollution is a serious threat to mankind in the present scenario and, hence many techniques are in use for water treatment. Out of them adsorption is a commonly used methods as it is simple, fast and universal in nature. Normally, activated carbon is used as an ideal adsorbent for wastewater treatment but it is costly and requires regeneration. The regenerated carbon exhibits lower adsorption capacity with further management problem of the effluent obtained from its regeneration. These facts have grown interest in many workers towards the search for low cost alternatives of activated carbon. Literature indicates some papers on adsorption using naturally occurring materials and industrial wastes as substitute adsorbents for the removal of water pollutants.

After the critical evaluation of the reported papers/reports, it was observed that most adsorbents show poor adsorption capacities, longer equilibration times, and maximum adsorption at extreme pH values. Moreover, the management of the exhausted adsorbent is of serious concern which has not been considered in the previously reported papers. Besides, the developed adsorbents have not been tested for different pollutants especially under column studies. In addition to this, many waste by-products have not been used for the preparation of adsorbents. Briefly, a lot of work is required in order to develop the more low cost alternatives of activated carbon. In view of the above discussed facts, it has been realized that development of low cost alternatives exhibiting good adsorption potential is still required.

1.6.1. Waste tire and disposal problem

It is worth mentioning that discarded tires comprise the biggest share amongst waste polymers in world. Waste rubber tire does not decompose easily owing to its cross linked structure and presence of stabilizers and other additives and hence, traditionally they are being disposed by incineration or land filling. Literature study reveals that carbon black obtained by untreated rubber tire pyrolysis may be treated physically and/or chemically to develop its physic-chemical properties and hence to improve its adsorption behaviour. In this research, as a means of reuse, we have developed various forms of novel activated carbon from waste tires for potential use in wastewater treatment for adsorption of various types of toxic pollutants.

1.6.2. Nanoparticles as adsorbents

Novel adsorbents combining nanotechnology have not only demonstrated high adsorption efficiency due to their large surface to volume ratio, but have shown additional benefits like ease of synthesis, easy usage, easy recovery, and manipulation via subsequent coating and funtionalization, absence of secondary pollutants, cost effectiveness and their eco

Novel adsorbent for noxious impurities removal

friendly nature. Materials with the particle size between 1 and 100 nm are defined as nanoparticles. With novel size- and shape-dependent properties, nanoparticles have been extensively used for the removal of noxious impurities. Nanoparticles should satisfy the following criteria:

- (I) The nano sorbents themselves should be non-toxic.
- (II) The sorbents present relatively high sorption capacities and selectivity to the low concentration of pollutants.
- (III) The adsorbed pollutant could be removed from the surface of the nano adsorbent easily.
- (IV) The sorbents could be infinitely recycled.

In the present work, a novel nano-adsorbent i.e. copper oxide nanoparticle was synthesized which was further loaded on activated carbon with the aim of exploring its feasibility as adsorbent for the removal of Acid blue 129 from the solvent phase.

1.6.3. Surface hydrogel as adsorbent

The surface active polymer adsorbent due to its high surface area and pore structure was proved to be a promising material for the removal of several noxious impurities. Hence in the present study, the surface active agents i.e. polymer modified adsorbents are those which can selectively adsorb noxious impurities and should consist of monomer groups such as such as 2-Hydroxy ethyl methacrylate (HEMA), 2-Hydroxyethyl methacrylate-ethoxy ethyl methacrylate-methacrylic acid (HEMA-EEMA-MA), and Polyvinyl alcohol (PVA), each having a different prominent role in this relevant process were synthesized and used for the rapid removal and fast adsorption of azo dyes i.e., CR and MG. The developed surface active polymer adsorbent consists of two groups i.e., one group, which forms a complex with the target impurities (removal part) and the other, which allows the polymers to stretch and shrink reversibly in response to ecological changes occurring during the removal and adsorption processes so that the developed adsorbent adapt accordingly (the responsive part).

1.7. Objective of study

- I. To develop novel adsorbents
 - a) Low cost novel adsorbent i.e., activated carbon-alumina composites (ACALs), Tire rubber alumina composite (TRAL), Modified rubber tire activated carbon modification (RTACMC) and rubber tire activated carbon (RTAC) from waste rubber tire granules by various physical and chemical activation methods for the removal of noxious impurities i.e. Ni^{2+} , As (III) and As (V) and phenolic compounds from the solvent phase.

- b) Copper oxide nanoparticles loaded on activated carbon was synthesized through solvothermal methods for the removal of noxious dye Acid blue 129 from the solvent phase.
 - c) 2-Hydroxy ethyl methacrylate (HEMA), 2-Hydroxyethyl methacrylate-ethoxy ethyl methacrylate-methacrylic acid (HEMA-EEMA-MA), and Polyvinyl alcohol (PVA), were synthesized and used for the rapid removal and fast adsorption of azo dyes i.e., CR and MG.
- II. Characterization of activated carbon produced with respect to surface texture, morphology, porosity, surface area, surface functional groups and elemental composition.
 - III. To carry out batch adsorption experiments in order to determine the optimum parameters of the adsorption process.
 - IV. Modelling of sorption data using various models in order to determine the best fit model applicable to the process and to determine mechanism with respect to thermodynamics and equilibrium.
 - V. To carry out kinetic studies using various kinetic models in order to determine the kinetics of the adsorption process and the rate process.
 - VI. To carry out column adsorption study to determine the various parameters necessary for the development of the fixed bed contractors on to pilot scale and for practical application of the technique to real wastewater treatment situations.
 - VII. To carry out the sorption and desorption studies of the adsorbent-adsorbate system for recycling and regeneration of adsorbents as well as the pollutants which is essential for the adsorption technology to have economic significance.

1.8. Scope of the study

The research work has focussed on the development of activated carbon from waste materials which are available in abundance and have no economic value for the removal of various types of pollutants. The wastes studied are waste rubber tires, nanoparticles and surface hydrogel polymer i.e. 2-Hydroxy ethyl methacrylate (HEMA), 2-Hydroxyethyl methacrylate-ethoxy ethyl methacrylate-methacrylic acid (HEMA-EEMA-MA), and Polyvinyl alcohol (PVA). These wastes have been processed, converted into surface adsorbents and used for the removal of noxious metal ions and dyes by using batch processes. These adsorbents were also tried for the removal of the noxious pollutants by using column operations at laboratory scale. The results of these investigations are presented in this thesis, which indicate efficiency, effectiveness and universal nature of the developed adsorbents. Therefore, the developed

Novel adsorbent for noxious impurities removal

adsorbents can be considered and used as low cost alternatives to activated carbon for the removal of a wide range of water pollutants from real water samples.

References

- [1] Snoeyink, V.L. and Jenkins, D., “Water Chemistry”, *John Wiley & Sons, New York* (2010).
- [2] Lehr, J.H., Gass, T.E., Pettyjohn and DeMarre, J., “Domestic Water Treatment”, McGraw-Hill Book Company, *New York* (1980).
- [3] Nemerow, N.L., “Industrial Water Pollution: Origine, Characteristics, and Treatment”, Addition –Wesley Publishing Company, Massachusetts (1978).
- [4] The World Bank, (2010). *Economics of Adaptation to Climate Change: Synthesis Report*. Washington, DC,
- [5] Prüss-Üstün, A, R. Bos, F. Gore and J. Bartram. “ Safer water, better health costs, benefits and sustainability of intervention to protect and promote health, 2008 60.
- [6] “World water council. Home WWC/Water cricis. Available at <http://www.worldwatercouncil.org/>.”
- [7] “United Nations world water development report UNRSCO. Water for people for life (2015).Availableat http://www.unesco.org/new/en/natural_sciences/environment/water/wwap/wwdr/2015-water-for-a-sustainable-world/.”
- [8] R. J. Bigda, “Consider Fenton’s Chemistry for Wastewater Treatment,” *Chem. Eng. Prog.*, 89, (1995), 62 – 66,
- [9] Zuane J. D., “Handbook of drinking water quality. New York Van Nostrand Reinhold (1997).” .
- [10] Kozirowski B. and Kucharski J., “Industrial waste disposal. Oxford pergamon Press (1972).”
- [11] C. A. Kozlowski and W. Walkowiak, “Removal of chromium(VI) from aqueous solutions by polymer inclusion membranes,” *Water Res.*, 36, (2002), 4870–4876,..
- [12] Bautista P., Mohedano A. F., Casas J. A., . Zazo J. A, and Rodriguez J. J., “An overview of the application of Fenton oxidation to industrial wastewaters treatment,” *J. Chem. Technol. Biotechnol.*, 83, (2008), 1323–1338,.
- [13] H. Ellision, “Handbook of chemical and biological warfare agents (CRCpress LLC, USA) 1991, 21-361.”
- [14] Conway R.A., and Ross, R.D., “Handbook of Industrial Waste Disposal”, Van Nostrand Reinhold, New strand Reinhold, New York (1980).
- [15] Okamura, H. and Aoyama, I., “Interactive Toxic Effect and Distribution of Heavy Metals in Phytoplankton”, *Environ. Toxicol. Water Qual.*, 9, (1994), 7-14.
- [16] Martin, T.R. and Holdich, D.M., “The Acute Lethal Toxicity of Heavy Metals to

- percarid Crustaceans(with particular References to Fresh-Water Asellids and Gammarids),” *Water Res.*, 20, (1986), 1137-1142.
- [17] Moore, J.W., “Inorganic contaminants of Surface Water Research and Monitoring Priorities”,*Springer-verlag*, New York (1991).
- [18] Murti, C.R.K. and Viswanathan, P., “Toxic Metals in the Indian Environment”,*Tata McGraw-Hill Publishing Company Limited*, New Delhi (1991).
- [19] Mesquita, J.P., Martelli, P.B. and Gorgulho, H.F., “Characterization of Copper adsorption on oxidized activated carbon,” *J. Braz. Chem. Soc*, 17, 2006 , 1133-1143.
- [20] Anderson, L.D., Kent, D.B. and Davis, J.A., “Batch experiments characterizing the reduction of Cr(VI) using suboxic material from a mildly reducing sand and gravel aquifer,” *Environ. Sci. Technol.*, 28, (1994), 178-185.
- [21] Ward A.J. , Hobbs P. J. , Holliman P. J. , Jones D. L., “Optimisation of the anaerobic digestion of agricultural resources,” *Bioresource technology* 99, (2008), 7928–7940.
- [22] IS: 2490, Part1, and drinking water (Bureau of Indian Standard, Environment Protection and Waste Management Sectional Committee, CHD 32, IS 3025 (Part 52) : 2003)
- [23] Payne K.B., Abdel-Fattah T.M., “Adsorption of Divalent Lead Ions by Zeolites and Activated Carbon: Effects of pH, Temperature, and Ionic Strength,” *J. Environ. Sci. Health*, 40, (2005), 723–749.
- [24] Tuna A.O.A., Ozdemir E., Simsek E.B., Beker U., Removal of As(V) from aqueous solution by activated carbon-based hybrid adsorbents: Impact of experimental conditions,” *Chem. Eng. J.* 223, (2013), 116–128.
- [25] Tseng C.H., Chong C.K., Tseng C.P.; "Long-term arsenic exposure and ischemic heart disease in arseniasis-hyperendemic villages in Taiwan". *Toxicol. Lett.* **137** (1–2) (2003) 15–21.
- [26] Hendryx M., "Mortality from heart, respiratory, and kidney disease in coal mining areas of Appalachia". *Int Arch Occup Environ Health* **82** (2) (2009) 243–249.
- [27] Smith AH, Hoppenhayn-Rich C, Bates MN; "Cancer risks from arsenic in drinking water". *Environ.HealthPerspect.* **97**, (1992),259–267. .
- [28] Navas-Acien A., Silbergeld E.K., Pastor-Barriuso R., Guallar E., "Arsenic exposure and prevalence of type 2 diabetes in US adults". *JAMA* **300** (7), (2008), 814–22.
- [29] Kile M.L., Christiani D.C. "Environmental arsenic exposure and diabetes". *JAMA* **300** (7)(2008), 845–846.
- [30] US E..P.A. “Environmental pollution control Alternatives. EPA/625/5-

- 90/025,PA/625/4-89/023, Cincinnati US.
- [31] Freitas, O. M., Martins, R.J., Delerue-Matos, C.M. and Boaventura, R.A. Removal of Cd(II), Zn(II), and Pb(II) from aqueous solution by brown marine macro algae: Kinetic modelling. *J. Hazard. Mater.* 153, (2008), 493-501.
- [32] Subramaniam, K.S. and Coonor, J.W., "Lead contamination of drinking water," *J. Environ. Sci. Health, Part A* 54, (1991), 29-33.
- [33] Sekar. M., Sakthi, V., Rengaraj, S., " Kinetics and equilibrium adsorption study of lead (II) on activated carbon prepared from coconut shell," *J. Colloid Interface Sci.* 79, 2004, 307-313.
- [34] Ake. C.L., Mayura, K., Huebner, H., Bratton, G.R. and Phillips, T. D., " Development of Porous clay- based composites for the sorption of lead of lead from water," *J. Toxicology Environ. Health Part A* 63 (6), (2001), 459-475.
- [35] Tunali, S., Akar, T., Ozcan, A.S., Kiran, I. and Ozcan, "A. Equilibrium and kinetics of biosorption of lead (II) from aqueous solutions by *Cephaosporium aphidicola*," *Sep. purif. Technol.* 47(3), 2006, 105-112.
- [36] Xiao. W., Yong, S. C., Won, S.L. and Byung, G.M., "Preparation and properties of chitosan/poly(vinylalcohol) Blend foams for copper adsorption," *Polym. Int.* , 55, (2006), 1230-1235.
- [37] Al-Khatib, M, and Al-Najar, H., "Hydro-geochemical characterisation of groundwater beneath the Gaza Strip," *J. Sci. Ind. Res.* 51, (1997), 523-532.
- [38] Zhang, F.S. Nriagu, J.O. and Itoh, H., "Mercury removal from water using activated carbon derived from organic sewage sludge," *Water Res.* 39, (2005), 389-395.
- [39] Chua, L. W. H., Lam, K. H. and Bi, S. P. "A comparative investigation on the biosorption of lead by filamentous fungal biomass," *Chemosphere* 39, (1999), 2723-2736.
- [40] Hussain, M. A., Salleh, A. and Milow, P. Characterization of the adsorption of the lead(II) by the nonliving biomass *spirogyra neglecta* (Hasall) Kutzing," *Am. J. Biochem. Biotechnol.* 5(2), (2009), 131-136.
- [41] Akhtar N., Iqbal J., Iqbal M., "Removal and recovery of nickel (II) from aqueous solution by loofa sponge-immobilized biomass of *Chlorella sorokiniana*: characterization studies", *J. Hazard. Mater. B*, 108, (2004), 85-94.
- [42] Beliles R.P., "The lesser metals, in: F.W. Oehme (Ed.), "Toxicity of Heavy Metals in the Environment", Part 2, Marcel Dekker, New York, (1978), 547-616.
- [43] Farooq U., Kozinski J.A., Khan M.A., Athar M., "Biosorption of heavy metal ions

- using wheat based biosorbents – a review of the recent literature”, *Bioresour. Technol.*, 101, (2010), 5043–5053.
- [44] WHO, “Guidelines for Drinking Water Quality”, Health Criteria and Other Supporting Information, *WHO, Geneva*, (1996), 973.
- [45] Arief V.O., Trilestari K., Sunarso J., Indraswati N., Ismadji S., “Recent progress on biosorption of heavy metals from liquids using low cost biosorbents: characterization, biosorption parameters and mechanism studies”, *Clean Soil Air Water*, 36, (2008), 937–962.
- [46] Kurniawan T.A., Chan G.Y.S., Lo W.H., Babel S., “Comparisons of low-cost adsorbents for treating wastewaters laden with heavy metals”, *Sci. Total Environ.*, 366, (2006), 409–426.
- [47] Ceribasi H.I., Yetis U., “Biosorption of Ni (II) and Pb (II) by *Phanaerochate Chrysosporium* from a binary metal system-kinetics”, *Water SA*, 27, (2001), 15-20.
- [48] Kupchella C.E., Hyland M.C., “Environmental science living within the system of nature,” *Allyn and Bacon* (1989).
- [49] Venkataraman K., *The chemistry of synthetic dyes*,” New York: *Academic press Inc.*(1965)
- [50] Newerow N.L., Doby T.A., “Colour removal in waste-water treatment plants,” *Sew.Ind. Wastes*, 30, (1958), 1160-
- [51] Walsh G.E., Bahner L.H., Horning W.B., “Toxicity of textile mill effluents to freshwater and estuarine algae, crustaceans and fishes,” *Environ. Pollut. Series A*, 21, (1980), 21
- [52] Anthony A.J., “Characteristics of impact of colored wastewater on free-flowing streams,” Proc.32nd industrial waste conference, Purdue University, *West Lafayette, indiana, USA* (1977).
- [53] Caturla F., Martin-Martinez J. M., Molina-Sabio M., Rodriguez-Reinoso F., Torregrosa R., “Adsorption of substituted phenols on activated carbon,” *J. Colloid Interface Sci.*, vol. 124, (1984), 528–534,.
- [54] Fingas M., Penner M., Silasi G., Colbourne F., “Treatment of intracerebral hemorrhage in rats with 12 h, 3 days and 6 days of selective brain hypothermia,” *Exp. Neurol.*, vol. 219, (2009), 156–162.
- [55] Wang Z., Fingas M., Blenkinsopp S., Sergy G., Landriault M., Sigouin L., Fought J., Weestlake D.W.S., “Comparison of oil composition changes due to biodegradation and physical weathering in different oils,” *J. Chromat. A*, 809, (1998), 89-107.

- [56] Catillo M., Barcelo D., "Identification of polar toxicants in industrial wastewater using toxicity-based fractionation with liquid chromatography/mass spectrometry," *Anal. Chem.*, 71, (1999), 3769-3775
- [57] Nemerow N., Gupta A.D., "Industrial and Hazardous Wastes Treatment. *Van Nostrand Reinhold*, New York (1991)."
- [58] Cheremisinoff N.P., "Handbook of water and wastewater Treatment Technologies," *Butterworth-Heinemann, Boston* 2002.
- [59] Okamura H., Aoyama I., "Interactive toxic effect and distribution of heavy metals in phytoplankton," *Environ. Toxicol. Water Qual.*, 9, (1994), 7-
- [60] Martin T.R., Holdich D.M., "The acute lethal toxicity of heavy metals to percarid crustaceans (with particular reference to fresh water asellids and gammarids)" *Water Res.*, 20, (1986), 1137-1145.
- [61] Moore J.W., "Inorganic contaminants of surface water res. And monitoring priorities," *New York Springer-Verlag*, (1991).
- [62] Franklin L.B., "wastewater engineering: treatment, disposal and reuse," *Mc Graw-Hill, Inc. New York* (1991).
- [63] Marmagne O., Coste C., "Colour removal from textile plant effluents" *Am. Dyestuff Rep.*, 85, (1996), 15-20.
- [64] Latifosoglu A.A., Surucu G., Evirgen M., "Improvement of the dewaterability of Ferric sludge produced from chemical treatment of wastewaters," *Water Pollut. IV Model. Meas., Predict.*, 4, (1997), 733 – 742.
- [65] Sinev I.O., Sinev O.P., Linevich S.N., "Apparatus of flotation treatment of natural water and wastewater," *Izobreteniya*, 26, (1997), 369-370.
- [66] Clark T., Stephenson T., "Effects of Chemical Addition on Aerobic Biological Treatment of Municipal Wastewater," *Environ. Technol.*, 19, (1998), 579–590.
- [67] Kato M.T., Field J.A., Lettinga G., "The anaerobic treatment of low strength wastewater in UASB and EGSB Reactors," *Water Sci., Tech.*, 36, (1997), 375-382.
- [68] Zinkus A. G., Byers W. D., Doerr W. W., "Identify Appropriate Water Reclamation Technologies," *Water reuse*, 20, (1998), 19–32.
- [69] Pearce C.I., Lloyd J.R., Guthrie J.T., "The removal of the colour from textile wastewater using whole bacterial cells: A Review," *Dye. pigm.*, 58, (2003), 179-196.
- [70] Fu Y., Viraraghavan T., "Removal of Congo Red from an aqueous solution by Fungus *Aspergillus niger*," *Adv. Environ. Res.*, 7, (2002), 239–247,

- [71] Pendashteh A. Fakhru R., 'l-Razi A., Chuah T. G., Radiah A. D., Madaeni S. S., Zurina Z. A., "Biological treatment of produced water in a sequencing batch reactor by a consortium of isolated halophilic microorganisms.," *Environ. Technol.*, 31, (2010), 1229–1239
- [72] Joss A., Keller E., Alder A.C., Globel A., Mc Ardell C.S., Ternes T., Siegrist H., "Removal of pharmaceuticals and fragrances in biological wastewater treatment," *Water Res.*, 39, (2005), 3139-3152.
- [73] Joss A., Zabczynski S., Gobel A., Hoffmann B., Löffler D., Mc Ardell C.S., Ternes T.A., Siegrist H., " Biological degradation of pharmaceuticals in municipal wastewater treatment: Proposing a classification scheme" *Water Res.*, 40, (2006), 1686-1696.
- [74] Barragan B.E., Costa C., Carmen Marquez M., "Biodegradation of azo dyes by bacteria inoculated on solid media," *Dyes Pigm.*, 75, (2007), 73-81.
- [75] Tian Q., Chen J., "Advanced treatment of waste water and slightly deteriorated raw water by biological activated carbon method under rich oxygen condition" *J. Dong Hua Univ.*, 17, (2000), 61-63.
- [76] Fux C., Boehler M., Huber P., Siegrist H., "Biological treatment of ammonium-rich wastewater by partial nitrification and subsequent anaerobic ammonium Oxidation (anammox) in a pilot Plant" *J. Biotechnol.*, 99, (2002), 295-306.
- [77] Van Der Zee F.P., Villaverde S., "Combined anaerobic-aerobic treatment of azo dyes-A short review of bioreactors studies," *Water Res.*, 39, (2005), 1425-1440.
- [78] Barnard O., Hadj-Sadok Z., Dochain D., Genovesi A., Steyer J.P., "Dynamical model development and parameter identification for anaerobic wastewater treatment process," *Biotechnol. Bioeng.*, 75,(2001), 424-438.
- [79] Bernet N., Delgenes N., Akunna J.C., Delgenes J.P., Moletta R., "Combined anaerobic-aerobic SBR for the treatment of piggery wastewater," *Water Res.*, 35, (2001), 425-432.
- [80] Talarposhti A.M., Donnelly T., Anderson G.K., "Color Removal from a simulated dye wastewater using a two phase anaerobic packed bed reactor," *Water Res.*, 35, (2001), 425-432.
- [81] Vankata M.S., Lalit B.V., Sarma P.N., "Anaerobic biohydrogen production from dairy wastewater treatment in sequencing batch reactor (AnSBR): Effect of organic loading rate," *Enz. Micro. Technol.*, 41, (2007), 506-515.
- [82] Bom P.R., "Method for Desalination containing water, single effective or multiple – Effective Distillation Apparatus" PCT Int.Appl. WO 9825679 (Cl.B01D1/26) (1998).

- [83] Vander Ham F., Witkamp G.J., deGrauw J., Van Rosmalen G.M., Eutectic freez, “Crystallization application to process streams and wastewater purification” *Chem. Eng. Process*, 37, (1998), 207-213.
- [84] Zinkus A. G., Byers W. D., Doerr W. W., “Identify Appropriate Water Reclamat ’ ion Technologies,” *Water reuse*, 20, (1998), 19–32.
- [85] Ahn J.W., Ahn J.G., “Solvent Extraction for the treatment of industrial wastes,” *Chawn Risaikring*, 6, (1997), 48-54.
- [86] Hall D.W., Joseph A.S., Rhonda E.M., “ An Overview of solvent extraction technologies,” *Env. Progress*, 9, (1990), 98-105.
- [87] Bigda R.J., “Consider Fenton’s Chemistry for Wastewater Treatment,” *Chem. Eng. Prog.*, 89, (1995), 62–66.
- [88] Gogate P. R. and Pandit A. B., “A review of imperative technologies for wastewater treatment I: Oxidation technologies at ambient conditions,” *Adv. Environ. Res.*, 8, (2004), 501–551.
- [89] Ternes T.A., Stuber J., Herrmann, N., McDowell D., Ried A., Kampmann M., Teiser B., “Ozonation: A tool for removal of pharmaceuticals, contrast media and musk fragrances from wastewater,” *Water Res.*, 37, (2003), 1976-182.
- [90] Huber M.M. Gobel A., Joss A., Hermann N., Loffler D., McArdell C.S., Ried A., Von Gunten U., “Oxidation of pharmaceuticals during ozonation of municipal wastewater effluents: A pilot Study,” *Environ. Sci. Technol.*, 39, (2005), 4290-4299.
- [91] Perez M., Torrades F., Domenech X., Peral J., “ Fenton and photo-fenton oxidation of textile effluents,” *Water Res.*, 36, (2002), 2703-2710.
- [92] Ali I., Aboul-Enein H.Y., Gaitonde V.D., Singh P., Rawat M.S.M., Sharma B., “Chiral separation of imidazole antifungle drugs on MyCoat RP column in HPLC,” *Chromatographia*, 70, (2009) 223-227.
- [93] Kavitha V., palanivelu K., “ The role of ferrous ion in fenton and photo-fenton processes for the degradation of phenol” *Chemosphere*, 55, (2004), 1235-1243.
- [94] Zazo J.A., Casas J.A., Mohedana A.F., Gilarranz M.A., Rodriguez J.J., “Chemical pathway and kinetics of phenol oxidation by Fenton’s reagent,” *Environ. Sci. Technol.*, 39, (2005), 9295-9302.
- [95] Bautista P., Mohedano A. F., Casas J. A., Zazo J. A., and Rodriguez J. J., “An overview of the application of Fenton oxidation to industrial wastewaters treatment,” *J. Chem. Technol. Biotechnol.*, 83, (2008), 1323–1338.

- [96] Yoon J., Lee Y., Kim S., “Investigation of the reaction pathway of OH radicals produced by Fenton oxidation in the conditions of wastewater treatment,” *Water Sci. Technol.*, 44, (2001), 15-21.
- [97] Comninellis C., Kapalka A., Malato S., Parsons S. A., Poulios I., Mantzavinos D., “Advanced oxidation processes for water treatment: advances and trends for R&D,” *J. Chem. Technol. Biotechnol.*, 83, (2008), 769–776
- [98] Chong M.N., Jin B., Chow C.W.K., Saint C., “Recent development in photocatalytic water treatment technology: A review,” *Water Res.*, 44, (2010), 2997-3027.
- [99] Wu J.J., Wu C.C., Ma H.W., Chang C.C., “Treatment of landfill leachate by ozone based advanced oxidation processes” *Chemosphere*, 54, (2004), 997-1003.
- [100] Balçioğlu I. A., Ötöker M., “Treatment of pharmaceutical wastewater containing antibiotics by O₃ and O₃/H₂O₂ processes,” *Chemosphere*, vol. 50, (2003), 85–95.
- [101] Ghaly M.Y., Hartel G., Mayer R., Haseneder R., “Photochemical oxidation of p-chlorophenol by UV/H₂O₂ and O₃/H₂O₂ and photo-fenton process. A comparative study” *Waste Management.*, 21, (2001), 41-47.
- [102] Gernjak W., Krutzler T., Glaser A., Malato S., Caceres J., Bauer R., Fernandez-Alba, A.R., “Photo-fenton treatment of water containing natural phenolic pollutants” *Chemosphere* 50, (2003), 71-78.
- [103] Esplugas S., Bila D. M., Krause L. G. T, and Dezotti M., “Ozonation and advanced oxidation technologies to remove endocrine disrupting chemicals (EDCs) and pharmaceuticals and personal care products (PPCPs) in water effluents,” *J. Hazard. Mater.*, 149, (2007), 631–642.
- [104] Herrera Melian J.A., Dona Rodriguez J.M., Viera Suarez A., Tello Rend E., Valdes Do Campo C., Arana J., and Perez Pena J., “The photocatalytic disinfection of urban waste waters,” *Chemosphere*, 41, (2000), 323–327.
- [105] Naik B., Parida K.M., Gopinath C.J., “Facile synthesis of N and S-incorporated nanocrystalline TiO₂ and direct solar light driven photocatalytic activity,” *Phys. Chem. C* 114, (2010), 19473-19482.
- [106] Parida K. M., Reddy K. H., Martha S., Das D. P., and Biswal N., “Fabrication of nanocrystalline LaFeO₃: An efficient sol-gel auto-combustion assisted visible light responsive photocatalyst for water decomposition,” *Int. J. Hydrogen Energy*, 35, (2010), 12161–12168.
- [107] Prieto-Rodriguez L., Miralles-Cuevas S., Oller I., Aguera A., Puma G.L., Malato S., “Treatment of emerging contaminants in wastewater treatment plants (WWTP) effluents

- by solar photo catalytic using low TiO₂ concentration ,” *J. Hazard. Mater.*, 211-212, (2012), 131-137.
- [108] Lachheb H., Puzenat E., Houas A., Kasibi M., Eloloui E., Guillard C., Hermann J.M., “Photocatalytic degradation of various types of dyes (Alizarin S, Crocein Orange G, Methyl Red, Congo Red, Methylene Blue) in water by UV-irradiated titania,” *Appl. Catal. B: Environ.*, 39, (2002), 75-90.
- [109] Li W., Huang H., Li H., Zhang W., and Liu H, “Stopped-flow studies of the mechanisms of ozone-alkene reactions in the gas phase: tetramethylethylene,” *Langmuir*, vol. 24, (2008), 8353–8366.
- [110] Neppolian B., Choi H.C., Sakthivel S., Arabindoo B., Murugesan V.,” Solar/UV induced photocatalytic degradation of three commercial textile dyes,” *J. Hazard. Mater.*, 89, (2002), 303-317.
- [111] Buncel E., Park K.T., Dust J.M., Manderville R.A., “Concerning the denticity of the dimethylsulfinyl anion in Meisenheimer complexation,” *J. Am. Chem. Soc.*, 125, (2003), 5388-5392.
- [112] Li Y., Schlup J.R., and Klabunde K.J., “Fourier Transform Infrared Photoacoustic Spectroscopy Study of the Adsorption of Organophosphorus Compounds,” *Langmuir*, 7, (1991), 1394–1399,.
- [113] Naffrechoux E., Chanoux S., Petrier, C. and Suptil, J., “Sonochemical and photochemical oxidation of organic matter,” *Ultrason. Sonochemistry*, 7, (2000), 255–259,
- [114] Nagasaki Y., “Treatment of organic wastewater, by Coagulation and precipitation,” JPN.Kokai Tokyo jp.1057967[9857967] (CI.C02F1/52) (1998).
- [115] McNulti J.T., “Anion exchange resin kinetics in mixed bed condensate polishing. In Ion Exchange Technology, (Edt. Naden D., Street, M.,) *Ellis Norwood Ltd., London* (1984).
- [116] Dabrowski A., “Adsorption: from theory to practice,” *Adv. colloid interface Sci.*, 93, (2001), 135–224.
- [117] Xu T., “Ion exchange membranes: state of their development and perspective,” *J. Memb. Sci.*, 263, (2005), 1-29.
- [118] Banerjee R., Gohil S., Bose S., and Ayyub P., “Influence of synthesis conditions on the nanostructure of immiscible copper-silver alloy thin films,” *Scr. Mater.*, 58, (2008), 842–845.
- [119] Rengaraj S., Yeon K., and Moon S., “Removal of chromium from water and wastewater by ion exchange resins,” *J. Hazard. Mater.*, 87, (2001), 273–287.
- [120] Lorch W., *Hand Book of water purification*, 2nd Ed. Ellis Hardwood Ltd, London (1981).

- [121] Koros W.J., "Membranes: Learning lesson from Nature," *Chem.Eng.Progress*, 91, (1995), 68-81.
- [122] Bick A., Oron G., Gilierman L., Manor Y., "Data envelopment analysis for assessing optimal operation of ultra-filtration systems for effluent polishing," *Water Sci. Technol.*, : Water supply, 3, (2003), 379-384.
- [123] Gupta V.K., Jain A.K., and Maheshwari G., "Aluminum(III) selective potentiometric sensor based on morin in poly(vinyl chloride) matrix.," *Talanta*, 72, (2007), 1469–1473.
- [124] Tewari Y.B., Kishore N., Lang B.E., Goldberg R.N., "Thermodynamics of reaction catalyzed by D-hydantoinase and N-carbamoyl-D-amino acid hydrolase," *J. Chem. Thermodyn.*, 39, (2007), 689-697.
- [125] Greenlee L.F., Lawler D.F., Freeman B.D., Marrot B., and Moulin P., "Reverse osmosis desalination: Water sources, technology, and today's challenges," *Water Res.*, 43, (2009), 2317–2348.
- [126] Packheiser T., Lang H., "Mixed Transition-Metal Complexes Based on Multitopic 1,3,5-triethynyl and 1-Diphenyl-phosphino-3,5-Diethynyl –Benzene Linking units," *Inorg. Chim Acta*, 366, (2011), 177-183.
- [127] Tang H., Cheng Z., Zhu H., Zuo G., and Zhang M., "Effect of acid and base sites on the degradation of sulfur mustard over several typical oxides," *Appl. Catal. B Environ.*, 79, (2008), 323–333.
- [128] Chandra R., Taneja P., John J., Ayyub P., Dey G., and Kulshreshtha S. K., "Synthesis and TEM study of nanoparticles and nanocrystalline thin films of silver by high pressure sputtering," *NanoStructured Mater.*, 11, (1999), 1171–1179.
- [129] Chandra S., Lokesh K.S., Lang H., "Iodide Recognition by the N,N-BisSuccinamide-Based Dendritic Molecule $[\text{CH}_2\text{C}(\text{O})\text{NHC}(\text{O})\text{CH}_2\text{-CH}_2\text{C}(\text{O})\text{OtBu}]_3$," *Sens.Autuator B137*, (2009), 350-356.
- [130] Gupta, V.K., Ali, I. "Adsorbents for water treatment: Low cost alternatives to carbon" *Encyclopaedia of surface and colloid science*, (edited by Hubbard A.), *Marcel Dekker, Inc., New York*, 1, (2002), 136-166.
- [131] Juttner, K., Galla, U., Schmieder, H. "Electrochemical approaches to environmental problems in the process industry" *Electrochimica Acta* 45, (2000), 2575-2594
- [132] Coin, R.J., Niksa, M.J. Elyanow D.I., "Wastewater Treatment by Electrochemistry" *Environ. Progress* 15, (1996), 122-127.
- [133] Lin, S.H., Chen, M.L., "Treatment of Textile Wastewater by Chemical methods for Reuse" *Water Res.* 31, (1997), 868-876

- [134] Zor, S., Yazici, B., Erbil, M., Galip, H., “The Electrochemical Degradation of Linear alkylbenzenesulphonate (LAS) on Platinum Electrode” *Water Res.* 32, (1998), 579-586.
- [135] Mollah M.Y.A., Morkovsky P., Gomes J.A.G., Kesmez M., Parga, J. and Cocke D.L., “Fundamentals, present and future perspectives of electrocoagulation,” *J. Hazard. Mater.*, B, 114, (2004),199–210,
- [136] Kobya, M., Can, O.T., Bayramoglu, M. “Treatment of textile wastewater by electrocoagulation using iron and aluminium electrodes” *J. Hazard. Mater.*, 100, (2003) 163-178
- [137] Gottberg, V., Antonia, J.M., Siwak L.R. “Electrodialysis Reversal process” *Int. Desalin. Water Reuse*, 7, (1998), 33-37.
- [138] X. Tongwen, “Electrodialysis processes with bipolar membranes (EDBM) in environmental protection - A review,” *Resour. Conserv. Recycl.*, 37,(2002), 1–22.
- [139] Afkhami A., Saber-Tehrani M., and Bagheri H., “Simultaneous removal of heavy-metal ions in wastewater samples using nano-alumina modified with 2,4-dinitrophenylhydrazine,” *J. Hazard. Mater.*, 181, (2010), 836–844.
- [140] Cruz A. Martinez-de la, Martinez D.S., and Cuellar E.L., “Synthesis and characterization of WO₃ nanoparticles prepared by the precipitation method: Evaluation of photocatalytic activity under vis-irradiation,” *Solid State Sci.*, 12, 2010) 88-94.
- [141] Cao J., Luo B., Lin H., Xu B., and Chen S., “Thermodecomposition synthesis of WO₃/H₂WO₄ heterostructures with enhanced visible light photocatalytic properties,” *Appl. Catal., B*, 111–112, (2012), 288–296.
- [142] Supothina S., Seeharaj, P., Yoriya, S., and Sriyudthsak, M., “Synthesis of tungsten oxide nanoparticles by acid precipitation method,” *Ceram. Int.*, 33, (2007), 931–936.
- [143] Rajagopalan S., Koper O., Decker S., and Klabunde K.J., “Nanocrystalline metal oxide as destructive adsorbents for organophosphorus compound at room temperature,” *Chem. Eur. J.*, 8, (2002), 2602 – 2607.
- [144] Rengaraj S., Yeon K., and Moon S., “Removal of chromium from water and wastewater by ion exchange resins,” *J. Hazard. Mater.*, 87, (2001), 273–287.
- [145] Carrott P.J.M., Ribeiro Carrott, M.M., Cansado L.I.P.P., and Nabais J.M.V, “Reference data for the adsorption of benzene on carbon materials,” *Carbon*, 38, (2000),465–474.
- [146] Zeng H., Du X.W., Singh S.C., Kulinich S.A., Yang S., He J., and Cai W., “Nanomaterials via laser ablation/irradiation in liquid: A review,” *Adv. Funct. Mater.*, 22, (2012), 1333–1353.

- [147] Miu, B., Watson, K.S., “Adsorption equilibrium of methane and carbon dioxide on porous metal-organic frame work Zn-BTB,” *Adsorption*, 17, (2011), 777-782.
- [148] Fuertes A.B., Nevskaja, D.M., Control of mesoporous structure of carbons synthesized using a mesostructured silica as template, *Micropor. Mesopore. Mater.*, 62, 2003, 177-190.
- [149] Duran, C., Ozdes, D., Gundogdu, A., Imamoglu, M., Senturk. H.B., Tea- industry waste activated carbon, as a novel adsorbent, for separation, preconcentration and speciation of chromium, *Analytica Chimica Acta*, 688, (2011), 75-83.
- [150] Slejko, F.L., “Adsorption Technology”, Marcel Dekker, New York, 1985.
- [151] Susuki, M., “Adsorption Engineering”, Elsevier, Amsterdam,
- [152] Ocik, J., Adsorption, Ellis Horwood, Chichester, PWN, Warsaw, 1982
- [153] Tien, C., “Adsorption Calculations and Modeling”, Butterworth-Heinemann, Boston (1994).
- [154] Linsen, B.G., “Physical and Chemical Aspect of Absorbent and Catalysts”, Academic press, London (1970).
- [155] Allingham, M.M., Cullen, J.M., Giles, C.H., Jain, S.K., Woods, J.S., “Adsorption at inorganic surface. II. Adsorption of dye and related compounds by silica”, *J. Appl. Chem.*, 8, 108 (1958).
- [156] Backhaus, W.K., Klumpp, E., Narres, H., Schwuger, M.J., “Adsorption of 2,4-dichlorophenol on montmorillonite and Silica: Influence of nonionic surfactants”, *J. Colloid Interface Sci.*, 242, (2001), 6-12.
- [157] Do, D.D., “Adsorption Analysis: Equilibria and Kinetics”, Imperial College Press, London (1998).
- [158] Revathi, M., Kavitha, B., Vasudevan, T., “Removal of nickel ions from industrial plating effluents using activated alumina as adsorbent”, *J. Environ. Sci. Eng.*, 47, (2005), 1-7.
- [159] Chen, A.S.C., Snoeyink, V.L., Mallevalle, J., Fiessinger, F., “Activated alumina for removing dissolved organic compound”, *J. Am. Water Work Assoc.*, 81, (1989), 53-58
- [160] Ishiguro, Y., Toba, M., Kondo, H., Matsumoto, N., Inoue T., Horinouchi, K., Ashitani, T., “Removal of arsenic from drinking groundwater by activated alumina adsorption method”, *Shigen Kankyo Taikyo*, 37, (2001), 1451-1456.
- [161] Ellis, J., Korth, W., “Removal of geosmin and methylisoborneol from drinking water by adsorption on ultrastable zeolite- Y”, *Water Res.*, 27, (1993), 535-540.

- [162] Okolo, B., Park, C., Keane, M.A., "Intrraction of phenol and chlorophenols with activated carbon and synthetic zeolite in aqous media", *J. Colloid Interface Sci.*, 226, (2000), 308-315.
- [163] Wang H., Liu Y. G., Zeng G. M., Hu X. J., Hu X., Li T. T., Li H. Y, Wang Y. Q., and Jiang L. H., "Grafting of β -cyclodextrin to magnetic graphene oxide via ethylenediamine and application for Cr(VI) removal," *Carbohydr. Polym.*, 113, (2014),166–173
- [164] Najm I.N., Snoeyink V.L., Lykins B.W. Jr., Adam J.Q., "Using powdered activated carbon: A critical review," *J.Am. Water Work Assoc.*, 83, (1991), 65-70
- [165] Gerçel Ö. and Gerçel. H. F., "Adsorption of lead(II) ions from aqueous solutions by activated carbon prepared from biomass plant material of *Euphorbia rigida*," *Chem. Eng. J.*, 132, (2007), 289–297.
- [166] Kieber R. J. and Helz G. R., "Indirect photoreduction of aqueous chromium (VI)," *Environ. Sci. Technol.*, 26, (1992), 307–312.
- [167] Gupta V.K., Jain A.K., and Maheshwari G., "Aluminum(III) selective potentiometric sensor based on morin in poly(vinyl chloride) matrix.," *Talanta*, 72, (2007), 1469–1473.
- [168] Bansal M., Singh D., and Garg V. K., "A comparative study for the removal of hexavalent chromium from aqueous solution by agriculture wastes' carbons," *J. Hazard. Mater.*, 171, 2009, 83–92.
- [169] Cheremisinoff P.N., Angelo C.M., "Carbon adsorption application," Ann Arbor science publishers, *Inc. Ann Arbor Michigan* 1980.
- [170] Smisek M., Cerney S., "Active carbon manufacture properties and application," *Elseveir Publishing Company*, Amsterdam (1970).
- [171] Ostrejko R., "Method for the production and regeneration of carbon with steam for decolouring," German patent number, 136, (1901), 792-800.
- [172] Hessler J.W., "Activated Carbon" Chemical publishing company, Inc., New York (1963).
- [173] Weber W. J. and Morris J. C., "Kinetics of Adsorption on carbon from Solution," *J. sanit. eng. div.*, 89, 31–60, 1963.
- [174] Green D.W., Hardy R.G., Beri P., Vickburg C.D., "Make activated carbon from Coke," *Hydrocarbon Process.*, 50, (1971), 105-112.
- [175] Xiong C., Yao C., Wang L., and Ke J., "Adsorption behavior of Cd(II) from aqueous solutions onto gel-type weak acid resin," *Hydrometallurgy*, 98, (2009), 318–324.
- [176] Zeng L., "Arsenic adsorption from aqueous solutions on an Fe (III)-Si binary oxide adsorbent," *Water Qual. Res. J. Canada*, 39, (2004), 267–275.

- [177] Eren E., Afsin B., and Onal Y., "Removal of lead ions by acid activated and manganese oxide-coated bentonite," *J. Hazard. Mater.*, 161, (2009), 677–685.
- [178] Mckay G., Blair H. S., and Gardener J. R., "Adsorption of dyes on chitin. I. Equilibrium studies," *J. Appl. Polym. Sci.*, 27, (1982), 3043–3057.
- [179] Bée A., Talbot D., Abramson S., and Dupuis V., "Magnetic alginate beads for Pb(II) ions removal from wastewater," *J. Colloid Interface Sci.*, 362, (2011), 486–492.
- [180] Moradi O., Aghaie M., Zare K., Monajjemi M., and Aghaie H., "The study of adsorption characteristics Cu²⁺ and Pb²⁺ ions onto PHEMA and P(MMA-HEMA) surfaces from aqueous single solution," *J. Hazard. Mater.*, 170, (2009), 673–679.
- [181] Venkata Ramana D.K., Yu J.S., and Seshaiiah K., "Silver nanoparticles deposited multiwalled carbon nanotubes for removal of Cu(II) and Cd(II) from water: Surface, kinetic, equilibrium, and thermal adsorption properties," *Chem. Eng. J.*, 223, (2013), 806–815.
- [182] Wang X., Wang Y., Liu M., Wu Z., Yang L., Xia S. and Zhao J., "Adsorption of Pb(II) from aqueous solution to Ni-doped bamboo charcoal," *J. Ind. Eng. Chem.*, 19, (2013), 353–359.
- [183] Conrad K., and Bruun Hansen H.C., "Sorption of zinc and lead on coir," *Bioresour. Technol.*, 98, (2007), 89–97.
- [184] Cho H., Oh D., and Kim K., "A study on removal characteristics of heavy metals from aqueous solution by fly ash," *J. Hazard. Mater.*, B127, (2005), 187 – 195.
- [185] Zulkali M.M.D., Ahmad A.L., and Norulakmal N.H., "L. husk as heavy metal adsorbent: Optimization with lead as model solution," *Bioresour. Technol.*, 97, (2006), 21–25.
- [186] Yu B., Zhang Y., Shukla A., Shukla S. S., and Dorris K. L., "The removal of heavy metals from aqueous solutions by sawdust adsorption--removal of lead and comparison of its adsorption with copper," *J. Hazard. Mater.*, B84, (2001), 83–94.
- [187] Raul P. K., Senapati S., Sahoo, Umlong A. K. I. M., . Devi R. R, Thakur A. J., and Veer V., "CuO nanorods: a potential and efficient adsorbent in water purification," *RSC Adv.*, 4, (2014), 40580–40587.
- [188] Kanan S. M. and Tripp C. P., "An infrared study of adsorbed organophosphonates on silica: A prefiltering strategy for the detection of nerve agents on metal oxide sensors," *Langmuir*, 17, (2001), 2213–2218.
- [189] Medine G. M., Zaikovskii V., and Klabunde K. J., "Synthesis and adsorption properties of intimately intermingled mixed metal oxide nanoparticles," *J. Mater. Chem.*, 14, (2004), 757-762.

- [190] Gupta V. K., Gupta M., Sharma S., Process development for the removal of lead and chromium from aqueous solutions using red mud}an aluminium industry waste,” PII: S0043-1354(00)00389-4
- [191] Altundoğan H.S. , Altundoğan S. , Tümen F. , Bildik M. “Arsenic adsorption from aqueous solutions by activated red mud,” *Waste Manag.*, 22, (3), (2002), 357–363.
- [192] Reddy K.J., “Method for removing arsenic from water, 2007, US Patent, 7, 235,179.” .
- [193] Goswami A., Raul P.K., and Purkait M.K., “Arsenic adsorption using copper (II) oxide nanoparticles,” *Chem. Eng. Res. Des.*, 90, (2012), 1387–1396.
- [194] Benguella B. and Benaissa H., “Cadmium removal from aqueous solutions by chitin : kinetic and equilibrium studies,” *Water Res.*, 36, (2002), 2463–2474.
- [195] Sun Q. and Yang L., “The adsorption of basic dyes from aqueous solution on modified peat – resin particle,” *Water Res.*, 37, (2003), 1535–1544.



CHAPTER 2
Experimental Methods and
Materials



Experimental Methods and Materials

This chapter deals with the detailed study of various reagents, adsorbents and experimental methods followed during experimental work of this thesis. Besides, mathematical background of experimental calculations is also equally important to mention, which have been presented. A section-wise description of individual component of experimental work is documented.

2.1. Reagents and Materials

Anhydrous nickel chloride (NiCl_2) for Ni^{2+} , Analytical reagent solid arsenic trioxide (As_2O_3) for As (III) and sodium arsenate ($\text{Na}_2\text{HAs}_2\text{O}_7 \cdot 7\text{H}_2\text{O}$) for As (V) was procured from M/s Merck, India and were worn as under observed noxious pollutant in different experimental procedures. Physico-chemical properties and ill effects of these noxious metals are shown in Table 2.1.

Table 2.1 Physico chemical properties of Ni (II), As (III) and As (V)

Phsico chemical Properties	Contaminant Ni (II)	Contaminant As (III) and As (V)
Atomic number	28	33
Atomic mass	58.71 g/mol	74.9216 g/mol
Density	8.9 g/cm ³ at 20 C	5.7 g/cm ³ at 14 C
Boiling Point	2913 C	615 C
Melting point	1453 C	814 C
Solubility in water	553 g/L at 20 C and 880 g/L at 99.9 C	As (III) hydride 700 mg/L, Arsenic (III) oxide 20 g/L
Sources to groundwater	Power plants, waste incinerators electroplating, stainless steel and alloy products, mining, and refining.	Enters environment from natural processes, industrial activities, pesticides, and industrial waste, smelting of copper, lead, and zinc ore.
Health Hazards	Sickness, Chronic bronchitis, lung embolism, pulmonary disorder, Birth defects, Asthma, Cardio vascular disorder, Skin ulceration, dermatitis.	Causes abdomen aches, RBC and WBC lethargy, liver and Renal damage; blood haemoglobin decrement, Oncogenic nature

Novel adsorbent for noxious impurities removal

Technical grade p-cresol and phenol of 98% purity were obtained from M/s Merck, India. Physico-chemical properties of p-cresol and phenol are given in Table 2.2.

Table 2.2 Physico chemical properties of Phenol and p-Cresol

Phsico chemical Properties	Contaminant Phenol	Contaminant p-Cresol
Chemical formula	C ₆ H ₆ O	C ₇ H ₈ O
Molar mass	94.11 g/mol	108.14 g/mol
Odour and appearance	Sweet and tarry, transparent crystalline solid	Greasy-looking solid
Density	1.07 g/cm ³	1.02 g/cm ³ , Liquid
Boiling Point	181.7 C	35.5 C
Melting point	40.5 C	201.9 C
Solubility in water	NiCl ₂ 8.3 g/100mL at 20 C	1.9g/100mL
Dipole moment	1.224D	1.58 D
UV-Vis (λ _{max})	269.9	277
Sources to groundwater	Paper pulp, aluminium, rubber, leather, plastics, resins, and steel industry	Coal gasification and liquefaction industries, poultry processing, refineries, shape oil,
Health Hazards	Dermatitis, lung edema, dysrhythmia, liver and renal failure, Seizures, Carcinogenic in nature	Causes abdomen pain, anaemia, liver and Renal damage; Facial paralysis, Nervous disorder,

A technical grade Acid Blue 129 (AB 129) (IUPAC name: 2-anthracenesulfonic acid, 1-amino-9, 10-dihydro-9, 10-dioxo-4-[(2, 4, 6 trimethylphenyl)amino]- sodium salt (1:1); Molecular formula: C₂₃H₁₉N₂NaO₅S and Molecular weight:458.46) was obtained from Sigma-Aldrich, India. Additionally the noxious dyes i.e. Malachite green (MG), which is a green

crystalline powder (IUPAC name: 4-{{4-(dimethylamino)phenyl}}(phenyl)methylidene}-N,N-dimethylcyclohexa-2,5-dien-1iminium chloride; Molecular formula: $[C_6H_5C(C_6H_4N(CH_3)_2)_2]Cl$ and molecular weight: 364.911) and Congo red (CR), which is a red crystalline powder (IUPAC name: disodium 4-amino-3-[4-[4-(1-amino-4-sulfonato-naphthalen-2-yl)diazenylphenyl]]phenyl]diazenyl naphthalene-1-sulfonate; Molecular formula: $C_{32}H_{22}N_6Na_2O_6S_2$; and Molecular weight: 696.665 g/mol) and were purchased from LABCHEM and used without any further purification. Physico-chemical properties of the dye Acid Blue 129, Congo red (CR), and Malachite Green (MG) are given in Table 2.3.

Table 2.3 Physico chemical properties of Acid blue 129, Congo red and Malachite green

Phsico chemical Properties	Contaminant Acid Blue 129	Contaminant Congo Red	Contaminant Malachite Green
Molecular formula	$C_{23}H_{19}N_2NaO_5S$	$C_{32}H_{22}N_6Na_2O_6S_2$	$[C_6H_5C(C_6H_4N(CH_3)_2)_2]Cl$
Molecular weight	458.46g/mol	696.665g/mol	364.911 g/mol
Color	Blue crystalline	Red crystalline	Green crystalline powdert
Melting point	>300 C	>360 C	158-160 C
Solubility in water	Partly miscible	Soluble in water to 5 mM	Partly miscible
UV-Vis (λ_{max})	629nm	498nm	618nm
Sources to water	dyeing of cotton, wool, silk, nylon, paper and leather	Majorly Textile industries	Leather, jute, wool, and silk industries
Health Hazards	Skin irritation, dermatitis, irritation of respiratory tract, emphysema, chronic bronchitis	Neurotoxic, Teratogenic, Anaphylactic shock and a carcinogenic agent, Thrombocytopenia, arthritis	Plueral adenomas, carcinogenic in nature, respiratory disorders and renal failures, moderately toxic and extreme irritant

Chemicals and reagents used in the experiments such as EEMA, MA and HEMA were purchased from Sigma Aldrich, India. These were used as monomers to prepare the polymers in the presence of ammonium peroxy disulfate (APS), and sodium disulfite (SDS) as initiator, ethylene glycol dimethacrylate (EGDMA) as cross-link agent (all from M/s Merck, India) and PVA was also purchased from Sigma Aldrich, India. All reagents (copper iodide (I), DMSO, oleic acid, ethylene-diamine) were purchased from M/s Merck, India. Besides the above mentioned chemicals, other reagents, like HCl, HNO₃, H₂O₂ and NaOH were also procured from Wishwani chemicals and were of analytical grade.

2.2. Instrumentation

The noxious metal Ni²⁺ concentration was determined using the atomic absorption spectrophotometer (model Z-7000, Hitachi, Japan) at a wavelength of 232 nm for Ni²⁺. While on the other hand As (V) concentration in aqueous solution was determined spectrophotometrically by standard Molybdenum blue method using Shimadzu UV-Visible spectrophotometer (Model UV-2450, Japan). As (III) was analyzed by oxidizing to As (V) by adding KMnO₄ and then following the same As (V) procedure, in addition to this the concentration of organic compounds i.e. phenols (λ_{\max} =269.9), p-cresol (λ_{\max} =277), Acid blue 129 (AB 129, λ_{\max} =629nm), Congo red (CR, λ_{\max} = 498nm) and Malachite green (MG, λ_{\max} =618nm) was determined spectrophotometrically using Shimadzu UV-Visible spectrophotometer (Model UV-2450, Japan). The pH measurements were made using a pH meter (Model Cyberscan 510, Singapore) and Metrohm pH-meter (Model 691, Switzerland). A high precision electronic balance (Sartorius GMBH) with an accuracy of 0.00001g was used for taking the weight of the adsorbates and adsorbents. The surface textural and morphological property of the adsorbent surface was analysed using the LEO 435 VP (Leo Elektronenmikroskopie GmbH, Germany). The elemental composition analysis i.e. Carbon, hydrogen, and nitrogen of the adsorbent and adsorbate were carried out using an Elementar Vario ELHI CHNS analyzer. The functional groups present on the surface of the developed adsorbent were analyzed in KBr discs on a Perkin Elmer Fourier transform infrared spectrophotometer (Model Perkin Elmer-1600 Series). The specific surface area of the adsorbents was measured by Nitrogen adsorption-desorption isotherm using multipoint Brunauer-Emmet-Teller (BET) and Barret-Joyner-Halenda (BJH) methods, respectively using surface area analyzer ASAP 2010 (UK) and Quantachrome Nova 2200E (Spain). The surface porosity and density of the developed adsorbents was determined using the mercury porosimeter (Pascal 440; M/s Spektron Instrument Inc., India) and by specific gravity bottles respectively. X-ray measurements were performed using a D8 advance (Bruker AXS

company, Germany) having Cu K α radiation ($\lambda = 1.541\text{\AA}$) and INEL X-ray diffractometer (model Equinox 3000, France). TEM images of the adsorbents were recorded by Transmission Electron Microscope (FEI TECNAI G2 microscope operating at 200 kV). Deionized water was prepared using a Millipore Milli-Q (Bedford, MA) water purification system.

2.3. Methodology

As stated earlier, the experimental work involves the adsorption studies of noxious Ni²⁺ on to the activated carbon prepared from scrap tire, As (III) and As (V) on to the alumina composite modified rubber tire, p-cresol and phenol on to the microwave modified rubber tire activated carbon, Acid Blue 129 on to the copper oxide nanoparticle modified activated carbon and finally the noxious dye i.e. Congo Red and Malachite Green on to the surface hydrogel polymers such as HEMA, HEMA-EEMA-MA, and PVA as efficient and excellent adsorbent. During each study, a set of methodology was followed, which involves a particular sequence of experimental steps which enabled us to understand the adsorption behaviour of the adsorbent, kinetics and thermodynamics of adsorption. Stepwise explanation of these certain experiments and methods used are given in succeeding sub-headings

2.3.1. Preparation of adsorbents

In the present experimental work, three different materials viz waste rubber tire, copper oxide nanoparticles and surface hydrogel polymers have been converted into low-priced adsorbents. These materials have been processed in the following manner so that they can be used as adsorbents. During the last decade many elementary studies were reported on the production of activated carbon prepared from pyrolysis of waste tires using two famous conventional methods i.e. physical and chemical activation. The potential of these products as possible adsorbents for various pollutants has been assessed and from the results obtained it is clear that they can be used efficiently as excellent adsorbent in the field of wastewater treatment. The most up-to-date approach in activated carbon production technology is physiochemical activation. This method is derived from a variety of combination of the both physical and chemical activation method. From the literatures, it was found that this method could present a very high quality activated carbon in terms of surface area, pore volume, porosity and favourable chemistry [1]. The main purpose of this work is to prepare highly mesoporous activated carbon from waste tires and to develop efficient adsorbents which are capable of rapid removal and fast adsorption of the noxious impurities from the aquatic ecosystem and food chain.

2.3.1.1. Preparation of activated carbon from scrap tire

Approximately 20 g of scrap tire pyrolytic carbon after initial cleaning i.e. thorough washing with deionized water and then dried in an oven at 100°C for 2h. The dried material was then heated to 500°C for 5h for carbonization. This was followed by treatment with Hydrogen peroxide (10%) for 24h at 60°C to oxidize the adhering organic impurities. The material was washed with deionized water three times to remove hydrogen peroxide and dried at 110°C for 2h in a vacuum oven. The dried material was now heated in a muffle furnace to a preset temperature of 900°C held isothermally for 5h in a covered silica crucible. The crucible was now removed from the furnace and cooled in desiccators to the final temperature of 110°C. The material were then treated with 1M HCl solution to remove the ash content and then washed with deionized water. The obtained product was now chemically activated using 1M nitric acid, stirred and refluxed to increase the porosity and surface active sites. This was followed by drying the materials for 24h at 100°C. The resultant dried product is our physiochemical activated carbon which is used for the rapid removal and fast adsorption of noxious Ni²⁺ from the aqueous ecosystem

2.3.1.2. Preparation rubber tire derived activated carbon modified with alumina composite

In this method, waste rubber tire is used as precursor material for the preparation of adsorbents. Finely grinded granules of waste rubber tire were washed thoroughly and dried in natural light. The obtained dried granules were then pyrolysed at 700°C in a tube furnace under the inert atmosphere of N₂ combined with steam. The obtained yield of pyrolysed tire rubber was 31.86%. Thereafter, the prepared pyrolysed raw carbon was then further grinded and treated with 5M hydrochloric acid for 24 h to remove all acid soluble impurities, which was thoroughly washed with deionised water until it was free from chloride and the obtained product was named as AC-HCl, which was kept in oven at 100°C for 24 h.

Two-step and single-step procedures were applied to obtain activated carbon-alumina composite. In two-step procedure, the AC-HCl and aluminium hydroxide were mixed in 1:1, 1:2 and 2:1 ratios by weight, grinded in mortar for thorough mixing and activated at 700°C in presence of N₂ gas along with steam. The heating rate was fixed at 10°C/min and flow rate of N₂ gas was 50 ml/sec. The composite was heated in isothermal condition at 700°C for 1 h and then cooled to room temperature. The percentage losses in weight were 8.57, 7.92 and 9.15 respectively. These three activated carbon-alumina composites were named as ACAL11, ACAL12 and ACAL21, respectively.

On the other hand, tire rubber-alumina composite (TRAL) was prepared in single step, by pyrolysis of mixture of fine pieces of waste tire rubber and aluminium hydroxide powder in 1:1 ratio by weight in at 700°C in tube furnace in inert atmosphere of N₂ gas along with steam as mentioned above. The percentage yield was 45.35%. All the adsorbents were sieved through BSS 200 mesh size sieve and stored in air tight plastic containers.

2.3.1.3. Preparation of RTAC and RTACMC

The ground tire granules were cleaned, thoroughly washed with deionized water, and then dried in an oven at 100°C for 2 h. The dried material was heated to 500°C for 5 h for carbonization [2]. This was followed by treatment with hydrogen peroxide solution for 24 h at 60°C to oxidize adhering organic impurities. The material was washed with deionized water for three times to remove hydrogen peroxide and dried at 110 °C for 2 h in vacuum oven. The dried material was activated to 900°C for 2 h in a covered silica crucible by heating in a muffle furnace. The crucibles were removed from the furnace and cooled in desiccators. The material was then treated with 1 M HCl solution to remove the ash content and was further washed with deionized water. This was followed by drying of the material at 100°C for 24 h. The dried product of particle size 150–200 µm is referred to as RTAC throughout the study and stored in separate vacuum desiccators until required.

The char obtained after carbonization was mixed with potassium hydroxide (KOH) pellets with varied KOH/char impregnation ratio of 0.5, 1, 1.5 and 2.

$$\text{The impregnation ratio} = \frac{\text{weight of KOH (g)}}{\text{weight of char (g)}} \quad (1)$$

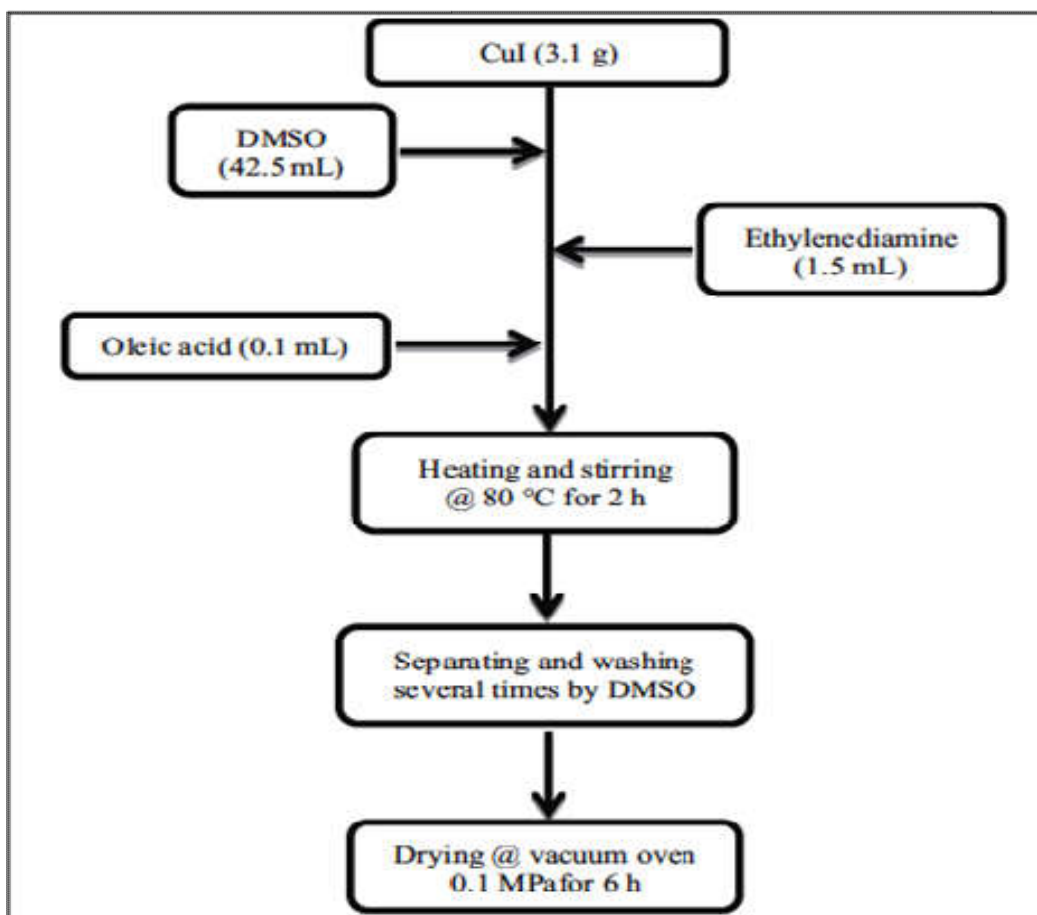
The activation step was performed in a glass reactor placed inside a microwave oven of input power set at 200, 400, 600 and 800W and an irradiation time of 5, 10, 15 min. After several trials, the process conditions of microwave cum chemical impregnation activation were optimized. A maximum 94% p-cresol removal was demonstrated by the resultant AC viz. RTACMC which was achieved under optimum conditions of chemical impregnation ratio of KOH/char of 1.50, microwave power of 600W and an irradiation time of 10 min. This sample was washed with deionized water until the pH of the solution was neutral and stored for further characterization and adsorption tests.

2.3.1.4. Preparation of CuO-NP-AC

Among the various chemical approaches for the synthesis of nanoparticles, the solvothermal method was chosen to synthesize CuO nanoparticles. In fact, solvothermal synthesis is a method for preparing a variety of materials such as metals, semiconductors, ceramics, polymers and nanocrystals. One of the most important characteristics of solvothermal

Novel adsorbent for noxious impurities removal

method is to allow for the precise control over the size, shape distribution, and crystalline nature of metal oxide nanoparticles or nanostructures. These characteristics can be altered by changing certain experimental parameters, including reaction temperature, reaction time, solvent type, surfactant type, and precursor type. CuO nanoparticles in DMSO were synthesized by the following method (Scheme 1): After dissolving 3.1 g of CuI in 42.5 mL DMSO, the solution was heated to 80 °C under a constant stirring rate. Then, 1.5 and 0.1 mL of ethylenediamine and oleic acid were added to the solution, respectively. The gray solution turned black and after a few minutes copper oxide particles were precipitated at the bottom of the experiment dish. The mixture was maintained at 80°C for 2 h and the color of the reaction solution became black completely. The resultant black products were separated from the reaction mixture and washed thoroughly with DMSO to remove CuI crystals if remained and dried at ambient condition (in a vacuum oven, 0.1 MPa) for 6 h prior to being characterized. Then, 1.2 g AC was added to mixture and stirred for 48 h and subsequently stand for 24 h. Finally, the CuO-NP-AC was precipitated and washed with distilled water and dried in an oven at 100°C.



Scheme 2.1 Solvothermal method for preparation of CuO nanoparticles

2.3.1.5. Preparation and synthesis of HEMA and HEMA-EEMA-MA

For synthesis of poly 2-Hydroxyethylmethacrylate (HEMA), 99.5% percent weight HEMA monomer, 0.5% percent weight EGDMA as cross-link agent, APS and SDS are used as initiators. Also for synthesis of poly 2-Hydroxyethyl methacrylate-ethoxy ethyl methacrylate-methacrylic acid (HEMA-EEMA-MA), weight percentage of EEMA-MA and HEMA monomers was changed. The amount of EGDMA was fixed at 0.5%, than APS and SDS are used as initiator for surface. All surfaces were dried at 105°C for 24h, then washed with distilled water several times to remove dust and other water-soluble impurities. The prepared surfaces were similar to other cited references [3-5]. HEMA and HEMA-EEMA-MA was cut in 1 cm of diameter and 0.5 mm thick pieces. It is notable that, HEMA has neutral surface charge, but HEMA-EEMA-MA has negative charge, because MA is a polar monomer.

2.3.2. Methods of adsorbent characterization

2.3.2.1. Fourier Transform Infrared Spectroscopy (FT-IR)

The technique of Infrared spectroscopy is well-known for identification and characterization of inorganic and organic compounds. It is the adsorption measurement of different IR frequencies by a sample positioned in the path of an IR beam. The principle of FT-IR spectroscopy exploits the fact that molecules or groups have specific frequencies at which these vibrate corresponding to the discrete energy levels. The schematic diagram of the FT-IR is shown in Figure 2.1

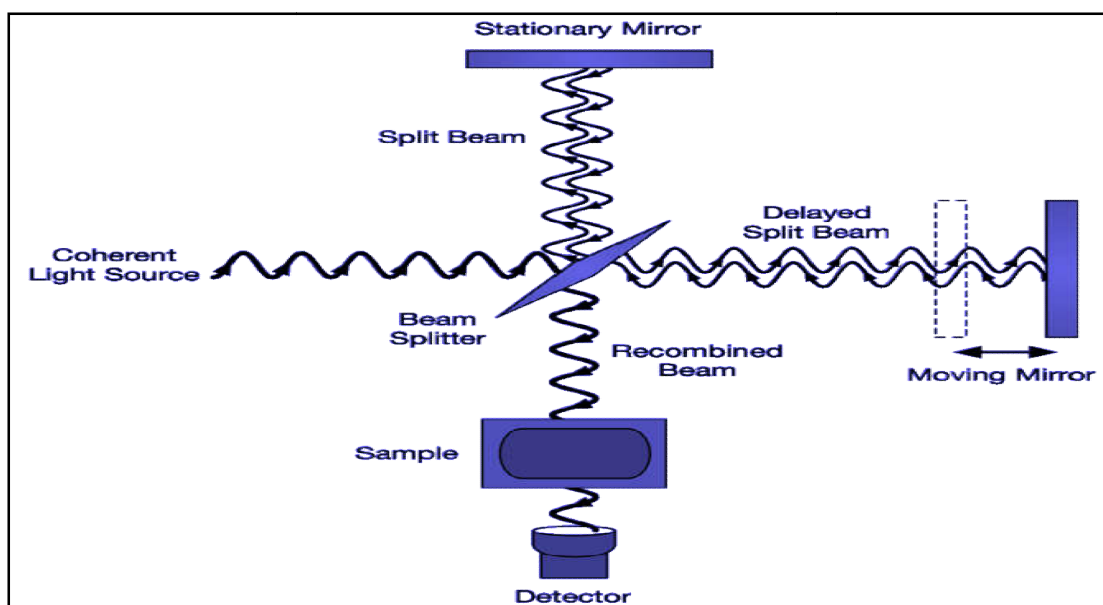


Figure 2.1 Schematic diagram of FT-IR

The frequencies are determined by the shape of the molecular potential energy surfaces, the masses of the atoms and by the associated vibrating coupling [6]. Thus, the frequency of the vibrations can be associated to a particular bond type. Complex molecules have many bonds with vibrational conjugations; leading to FT-IR absorptions at characteristic frequencies, which are related to functional groups. The presence of particular functional group on the surface of an adsorbent is identified in functional region while, complete structure is determined in exploiting finger print region.

2.3.2.2. X-ray Diffraction Analysis

X-ray diffraction is now a widespread practice for the study of crystal structures and atomic spacing. The basis of X-ray diffraction is the constructive interference of monochromatic X-rays and a sample which is crystalline. A cathode ray tube produces X-rays, filtered to make monochromatic radiation, collimated to focus and directed toward the sample. The interaction of the incident rays with the sample results constructive interference when conditions are favourable to satisfy Bragg's equation given below by equation 2:

$$n\lambda = 2d_{hkl} \sin\theta \quad (2)$$

where, λ is wavelength of incident radiation, d_{hkl} is the distance between lattice planes (hkl), θ is the diffraction angle and hkl are Miller indices.

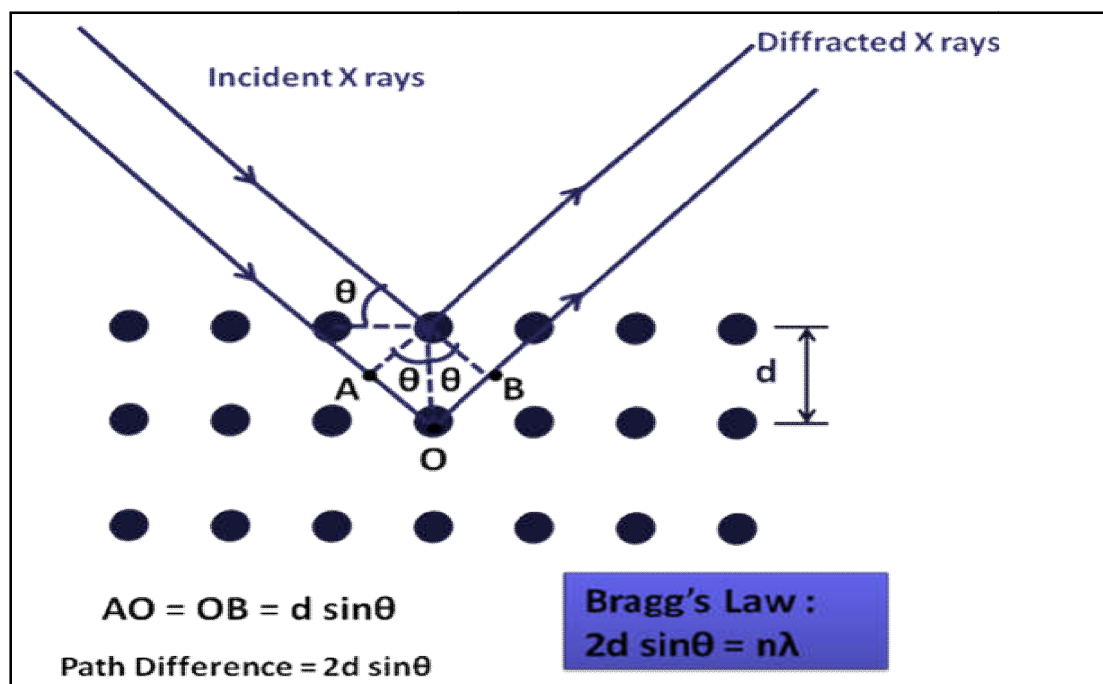


Figure 2.2 Bragg's diffraction at lattice planes

Hence this law gives relationship between the wavelength of electromagnetic radiation, the diffraction angle and the d-spacing in a crystalline sample (Figure 2.2). These diffracted X-rays are then examined, processed and counted. Because of the random orientation of the powdered material, all possible diffractions of the lattice should be obtained by scanning the sample material through a range of 2θ angles. The diffraction peaks are then converted into d-spacing which in turn helps in identifying the sample mineral because each mineral has got a set of distinct d-spacing values. In general, the d-spacing of the given sample are compared with standard reference patterns and the material is confirmed.

2.3.2.3. Scanning Electron Microscopy (SEM) Studies

Scanning electron microscopy (SEM) is used to ascertain the topography, morphology, composition and crystallographic information of the adsorbent material. SEM authorizes the observation of materials in macro and submicron ranges. SEM uses a beam of highly energetic electrons to examine objects [7]. SEM generates high energy electron beam of these fast moving electrons is focussed on a sample. These electrons are absorbed or scattered by the specimen and electronically processed into an image. The instrument is capable of generating three dimensional images for analysis of topographic features. Most electron microscopes use to study materials with image generation up to 10 Å. The working principle of SEM is presented in Figure 2.3

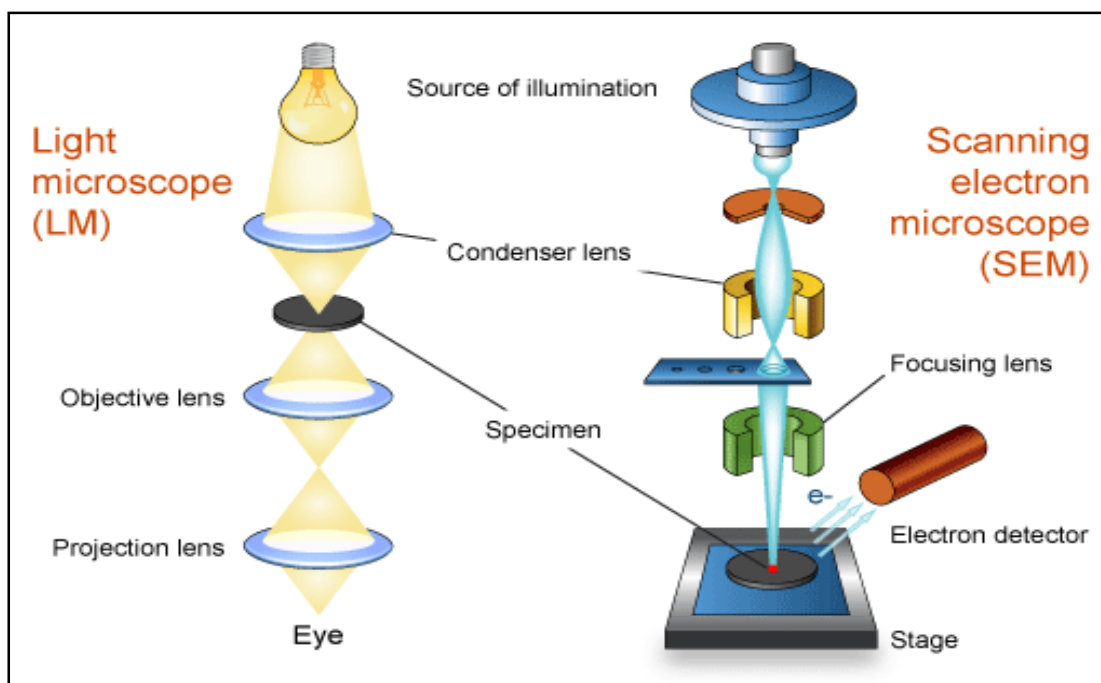


Figure 2.3 Principle of SEM

2.3.3.4. Energy-Dispersive X-ray Spectroscopy (EDX)

Energy-dispersive X-ray spectroscopy (EDX) is a widely used technique to analyze the chemical components in a material. EDX is frequently used in the analysis of adsorbents [8, 9]. This method relies on the investigation of X-rays produced as a result of electron interactions with the sample. The elemental analysis is based on the fundamental principle that each element has a unique atomic structure which generates unique set of peaks on its X-ray spectrum [10]. For stimulating the emission of X-rays, a high energy electrons or a beam of X-rays, is focused to the sample under investigation. The incident beam may eject an electron from inner shell, creating a hole. An electron from a higher and the lower energy shell is released in the form of an X-ray. The energy of the X-rays emitted is characteristic of the element and data is processed to obtain the percentage of each measured element present in the given sample particles.

2.3.3.5. Thermal Gravimetric Analysis

Thermal Gravimetric Analysis (TGA) determines the amount and rate of change in the mass of a material as a function of temperature or time in a controlled atmosphere. These measurements are used mainly to determine the composition of materials and to calculate their thermal stability at temperatures up to 1000°C. This method can explain materials that showing mass loss or gain due to chemical changes such as decomposition, oxidation, or dehydration. Figure 2.4 describes the schematic working of TGA.

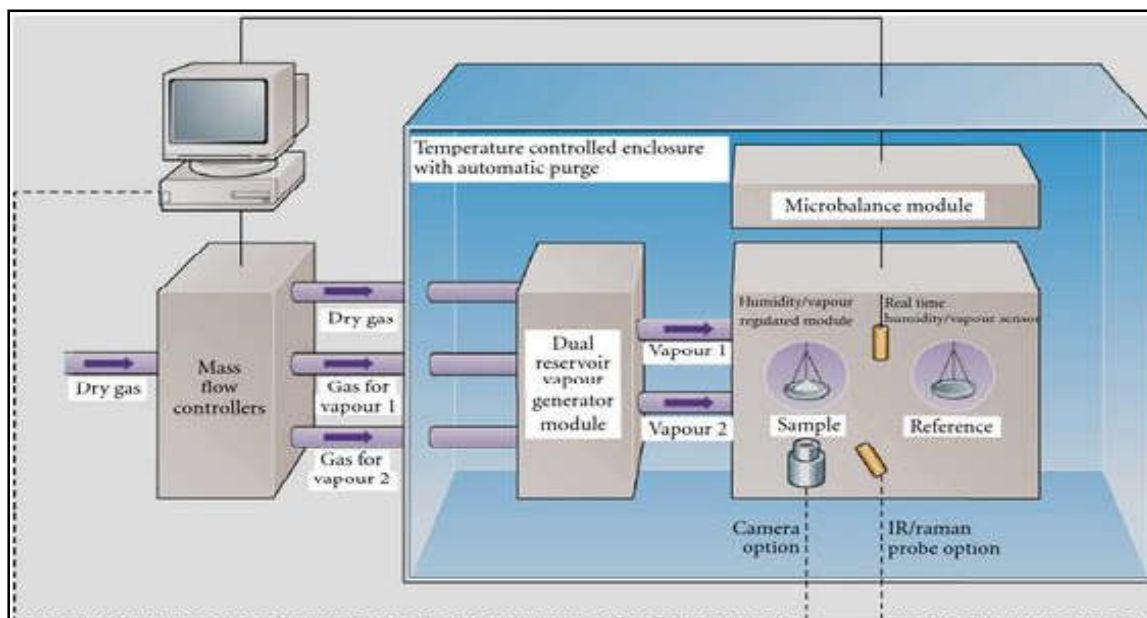


Figure 2.4 Schematic presentation of TGA working

2.3.3.6. Determination of Surface Area

The Brunauer-Emmett-Teller (BET) and Barret-Joyner-Halenda (BJH) surface area was measured by N₂ adsorption-desorption technique using Surface area analyzer ASAP 2010 (UK) and Quantachrome Nova 2200E (Spain). A pictorial presentation of the Quantachrome Nova 2200E (Spain) is shown in Figure 2.5. The cross-sectional area of nitrogen molecule was taken as $16.2 \times 10^{-20} \text{ m}^2$. Before adsorption, the sample was out gassed overnight at 140°C. The BET method is widely used in surface science for the calculation of surface areas of solid catalysts and adsorbents and the values obtained are seemed to be perfectly satisfactory.



Figure 2.5A pictorial presentation of the Quantachrome Nova 2200E (Spain)

2.3.3.7. Elemental Analysis

CHNS analysis of the adsorbent samples was carried out using an Elementar Vario ELHI CHNS analyzer at Indian Institute of Technology, Roorkee. The analyzer operates on the basis of the combustion dynamics of the sample. The sample is weighed on a tin capsule and is introduced along with a quantity of oxygen, through an automatic sampler, in a reactor of combustion. After combustion, the gases produced, N₂, CO₂, H₂O and SO₂ are transported by a stream of Helium through a layer of copper, contents of the reactor, and then separated by a column of GC and finally detected by a thermal conductivity detector (TCD). The time needed

for the total analysis is 12 min. The equipment is completely controlled by computer, through software and at the end of the analysis a full report showing the percentage of CHNS values is issued.

2.3.3.8. Determination of Point of Zero Charge (PH_{pzc})

Surface and interface properties of metal oxides play an important role in the overall behaviour and their surface get changed when exposed to the external environment. In aqueous media hydroxide groups develop on the surface of metal oxides create electrical charges. The formation of surface charge is proton balance between the oxide surface and the suspension which is determined by their acid-base behaviour. The nature and magnitude of surface charge on metal oxides depend upon the concentration and pH of the aqueous media [11]. The pH dependent surface charging of mineral oxide in aqueous media is very important, therefore, it become necessary to find an important parameter called point of zero charge (PZC) for such systems. The point of zero charge (pH_{pzc}) is related to adsorption, which is pH of the mineral surface in the aqueous medium at which that surface has a net neutral charge. At the point of zero charge, protonated positive surface sites are balanced by an equal number of deprotonated negative surface sites [12, 13]. PZC is a tool for the determination of chemical properties of mineral oxides and hydroxides [14]. The study of PZC plays an important role in the process of adsorption of colloidal particles on the surface [13].

The surface charges of adsorbent may be positive or negative or neutral, which depends on pH of the medium. PZC is one of the most important parameters used to describe variable-charge surfaces [15]. At higher pH of a medium than PZC, the surface will acquire negative charge and exhibits an ability to exchange cations, while the solid will attract anions electrostatically if its pH is below PZC. Several methods have been proposed for the determination of the point of zero charge on the solids. In the present study, pH of point of zero charge (pH_{pzc}) was determined by salt addition method reported in the literature [16, 17]. 50.0 mL of 0.1 M KNO₃ solution was taken in a series of 100 mL Erlenmeyer's flask. A range of initial pH value of the adsorbate solution was adjusted at 2, 4, 6, 8, 10 and 12 by adding 0.1 M HNO₃ or NaOH. 0.2 g of adsorbent was added to each flask. The suspension was shaken on magnetic stirrer for 30 min and allowed to equilibrate for 48 h. The suspension was centrifuged at 5000 rpm for 5 min and final pH values of the supernatant liquid were recorded. The pH_{pzc} is the point where the curve of the final pH versus initial pH crosses each other [18].

2.3.4. Adsorption Experimental Method

Several experimental techniques have been investigated by many researchers in order to make an intimate contact between adsorbate and adsorbent for the maximum uptake of pollutants from water. Both batch and column techniques were used for investigations. Adsorption isotherms were determined by batch method which is simple and easy to perform. Further, it permits convenient evaluation of parameters that influence the adsorption process. Column studies were also carried out to know the feasibility of the process in practice. These batch and column experimental technologies are discussed below.

2.3.4.1. Batch Adsorption Method

The development of batch adsorption process involves the plotting of isotherm; a typical isotherm plot is shown in Figure 2.6. This an equilibrium graph plotted between adsorbate concentrations on per gram of adsorbent (q_e) and in aqueous phase respectively at equilibrium (C_e). Basically, maximum adsorption of the adsorbate on a particular adsorbent can be achieved by optimizing various parameters of adsorption. The parameters affecting the adsorption process and considered for study were pH, adsorbent dose, and particle size, initial concentration of adsorbate, contact time and temperature.

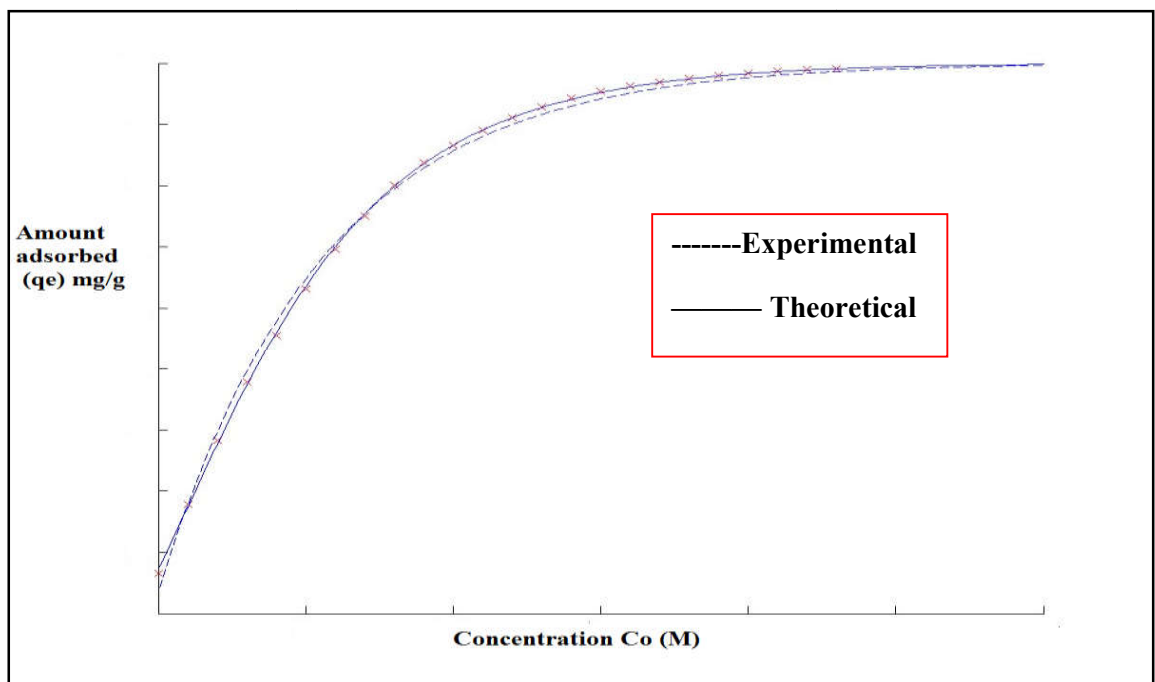


Figure 2.6 Typical adsorption isotherm from batch experiment

For the optimization purpose, the first experimental was indented to determine the effect of contact time and minimum time to reach equilibrium condition by adsorbate-adsorbent

Novel adsorbent for noxious impurities removal

system. A fixed amount of the adsorbent was added to 100 ml of adsorbate (Metal ions/dyes/phenols) solution of a fixed concentration in a number of 250 mL stoppered Erlenmeyer flask, which were placed in thermostat shaking assembly. The solutions were agitated at constant temperature on an orbital shaker at 100rpm and Erlenmeyer flasks were taken out from shaker after a regular period of time. The solution was filtered with 0.2 μm rated nylon membrane. The filtrate was analyzed to determine the remaining concentration of the adsorbate in solution. Remaining Erlenmeyer flasks were analyzed similarly until two successive Erlenmeyer flasks showed nearly equal adsorption and results so obtained were enabled to draw a progressive extent of adsorbent with the passage of time. The contact time after which adsorbent showed no noticeable adsorption is termed as equilibrium contact time. This optimized time period is generally employed in the succeeding experiments to study the effect of other factors.

To study the effect of the particle size of adsorbent on the extent of adsorption, three particle sizes i.e. 100-150, 150-200 and 200-250 BSS were used in three different series of Erlenmeyer flasks; each series contains a range of adsorbate solution. The experiments were carried out upto the optimum contact time and at fixed temperature. The samples were analyzed and results were plotted in terms of isotherms, which showed comparative performance of various particle size. The finest particle size (200-250 BSS) shows maximum adsorption capacity among them, due to larger surface area.

Likewise, similar sets, containing a range of adsorbate concentration, with different adsorbent dose were analyzed. The isotherms obtained from results were helpful to determine the optimized dose for maximum removal.

The pH of solution can alter the surface properties of adsorbent and adsorbate and therefore, affect the adsorption behaviour and extent of adsorption. In view of this phenomenon adsorption experiments were carried out at various pH values. For this purpose a series of Erlenmeyer flasks containing fixed adsorbate solution at different pH, depending on the physiochemical stability on the physiochemical stability of adsorbent or adsorbate at certain pH; were used. pH of solution was adjusted with the use of 0.1 M HNO_3 and 0.1 M NaOH as per requirement. These experiments are useful especially to explore the adsorption mechanism. The results were plotted as the extent of adsorption against pH of solution.

Similarly, temperature is also an important factor which influences the adsorption process. To observe the effect of solution temperature on the extent of adsorption, three sets of

experiments are conducted at different solution temperatures. The results showed the adsorption process as endothermic (increases with increase in temperature) or exothermic (decrease with increase in temperature). The resulting data were plotted as isotherms which were very useful in predicting the adsorption characteristics of adsorbent.

The adsorbate uptake q_e (mg/g) was determined as follows by equation 3:

$$q_e = \frac{(C_0 - C_e)V}{m} \quad (3)$$

Where C_0 and C_e (mg/L) are the liquid-phase concentration of dyes at initial and equilibrium, respectively. V is the volume of the solution (L) and m is the mass of adsorbent (g).

The data analysis was carried out using correlation analysis employing least-square method and the average relative error (ARE) [19, 20] is calculated using the following equation 4:

$$ARE(\%) = \frac{100}{n} \sum_i^n \left| \frac{q_{i,cal} - q_{i,exp}}{q_{i,exp}} \right| \quad (4)$$

Where n is the number of data points, $q_{i,exp}$ and $q_{i,cal}$ are experimental and calculated amount of adsorbed MG per unit weight of adsorbents (mg/g), respectively.

2.3.4.1.1. Adsorption Isotherms

The equilibrium isotherm is a significant criterion for the design of the adsorption system. It essentially expresses the relation between the concentrations of the solute in solution at equilibrium with the concentration of the solute adsorbed at constant temperature. To analyze the validity of the adsorption data Langmuir, Freundlich, Temkin and Dubinin-Radushkevich isotherm adsorption models were used. Besides, linear regression analyses of the adsorption data were carried out to select the suitable adsorption model. The shape of the adsorption isotherm gives quantitative information about the adsorption process and the extent of surface coverage by the adsorbate.

2.3.4.1.2. Classification of isotherms

A general systematic classification of isotherm was first proposed by Brunauer, Deming, Deming and Teller (BDDT) in 1940 containing five types of isotherms, I to V. Later Sing et al [21] included one additional type giving six types by IUPAC classification of isotherms as illustrated in Figure 2.7. Type I isotherm are characteristic of microporous

adsorbents. The detailed interpretation of such isotherms is controversial, but it is possible to obtain an estimate of the micropore volume from Type I isotherm. Type II isotherm indicates that the solid is non-porous while the Type IV isotherm is characteristic of a mesoporous solid. From both types of isotherm it is possible to calculate the surface area of the solid. From the Type IV isotherm the pore size distribution may also be evaluated. Isotherms of Type III and Type V seem to be characteristic of systems where the adsorbent-adsorbate interaction is unusually weak, and are much less common than those of the other three types. The stepped isotherm, appropriately designated Type VI, though relatively rare, is of particular theoretical interest. Finally Type VI represents stepwise multilayer adsorption on a uniform non-porous surface.

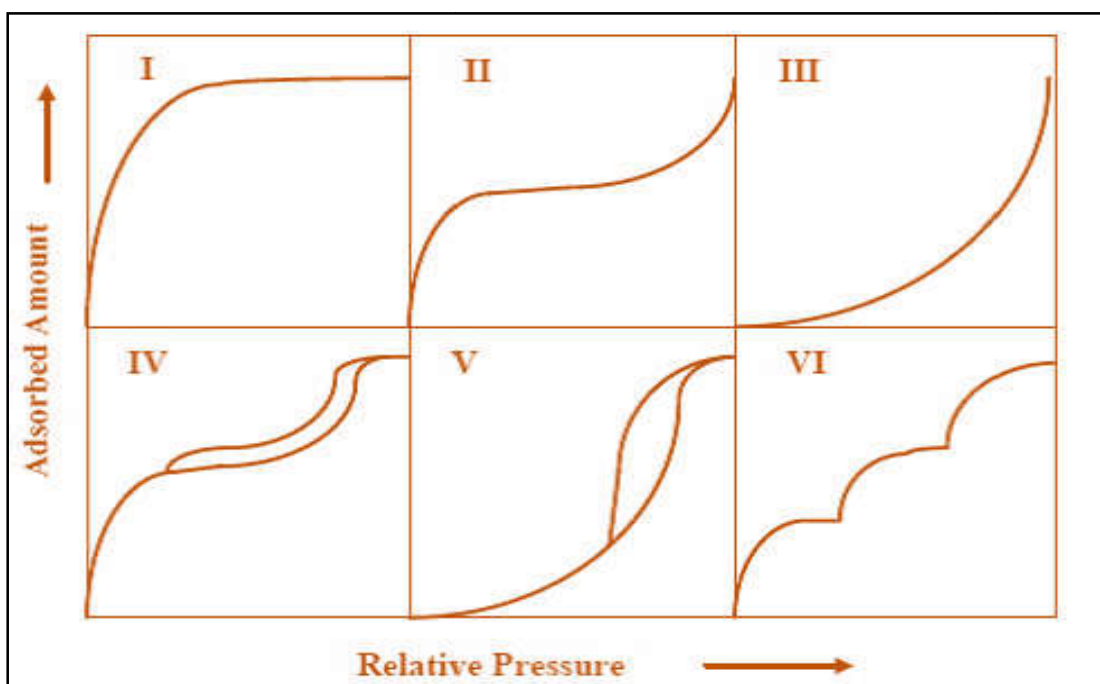


Figure 2.7 The IUPAC classification of adsorption isotherm

In 1960 Giles et al. [22] divided all isotherms into four main classes according to the initial slope. They are (i) S type (Sigmoid); (ii) L type (Langmuir); (iii) H type (high affinity) and (iv) C type (constant partition) and are shown in Figure 2.8. The S type isotherm is characterized by a small slope at low surface coverage that increases with adsorbate concentration. S curve suggests that affinity of the adsorbent for the adsorbate is less than that of aqueous solution when the solution concentration of the adsorbate is low. S curved isotherm occurs when (a) solute molecule is mono functional (b) has moderate intermolecular attraction

and (c) meets strong competition for substrate sites, from the solvent molecules or of another adsorbed species.

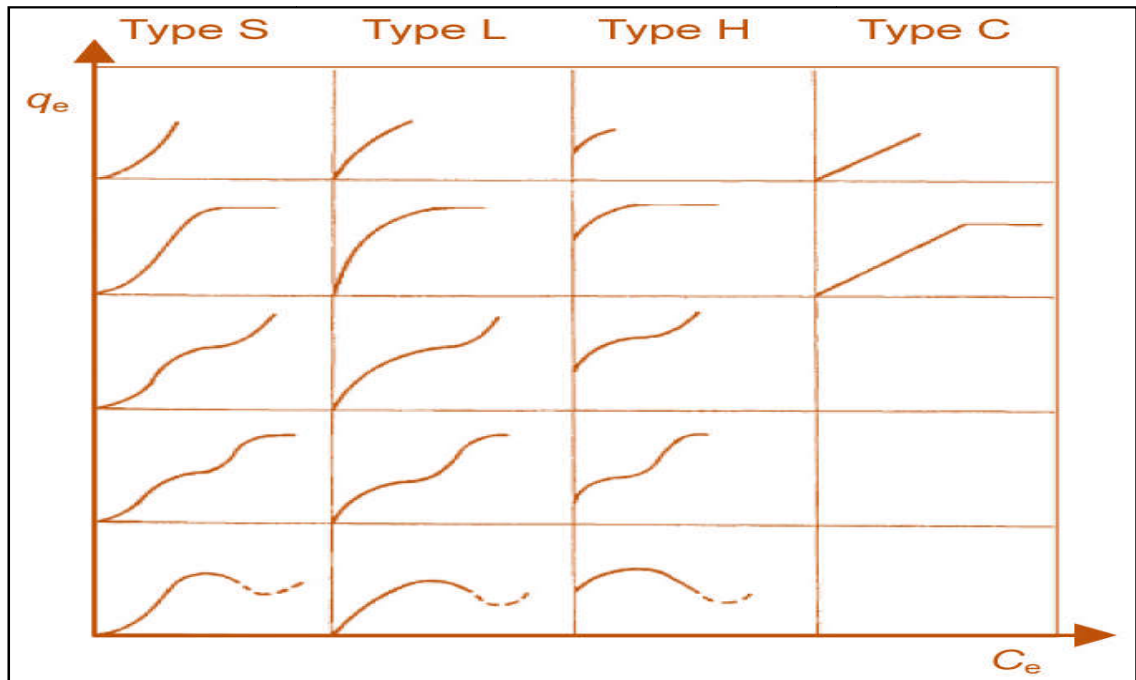


Figure 2.8 Giles classification of isotherm shapes

The L type is the most commonly encountered type of adsorption isotherm in wastewater treatment. L type isotherm indicates that the adsorbate has a relatively high affinity for the adsorbent surface a low surface coverage; it reveals that as the coverage increases, the affinity of the adsorbate for the adsorbent surface decreases. The L curve implies that either the adsorbed solute molecule is not vertically oriented or there is no strong competition from the solvent. The H type isotherm is an extreme version of the L type isotherm in which the solute has high affinity that in dilute solutions it gets completely adsorbed or there is no measurable amount remaining in solution. The initial part of the isotherm is therefore vertical. The C type isotherms are defined by a constant sorption affinity. This characterised by constant partition of solute between solution and substrate, right up to the maximum possible adsorption. The adsorption of non-ionic and hydrophobic organic compounds is usually described by C type isotherm.

The adsorption isotherms are mathematical models that describe the distribution of the adsorbate species among solid and liquid phases, and are important data to understand the mechanism of the adsorption. Several models have been described in literature to explain the

experimental data of the adsorption isotherms. Langmuir, Freundlich, Temkin and Dubinin-Radushkevich isotherm adsorption models are the most frequently employed models.

2.3.4.1.2.1. Langmuir Isotherm

The Langmuir isotherm is a theoretical isotherm model and is based on few assumptions [23]. All sites are identical and energetically equivalent. Thermodynamically this implies that each site can hold one adsorbate molecule, adsorption cannot proceed beyond monolayer. The ability of a molecule to be adsorbed at a given site is independent of the occupation of neighbouring sites, which mean, there will be no interactions between adjacent molecules on the surface and immobile adsorption, i.e. trans-migration of the adsorbate in the plane of the surface is precluded. The heat or energy of adsorption is constant over the entire surface. The volume of monolayer and the energy of adsorption are independent of temperature. Hence according to the Langmuir model during the uptake of metal ions on a homogenous surface all sites are identical and energetically equivalent, the adsorbent is structurally homogeneous without interaction between molecules adsorbed on neighbouring sites [24-26]. Langmuir adsorption isotherm is given by the equation 5:

$$q_e = \frac{q_m K_L C_e}{(1 + K_L C_e)} \quad (5)$$

This equation can be remodelled and rearranged into four different linear types by the following equations 6-8:

$$\text{Type 1} \quad \frac{C_e}{q_e} = \frac{1}{q_m K_L} + \frac{C_e}{q_m} \quad (6)$$

$$\text{Type 2} \quad \frac{1}{q_e} = \left(\frac{1}{q_m K_L} \right) \frac{1}{C_e} + \frac{1}{q_m} \quad (7)$$

$$\text{Type 3} \quad q_e = q_m - \left(\frac{1}{K_L} \right) \frac{q_e}{C_e} \quad (8)$$

$$\text{Type 4} \quad \frac{q_e}{C_e} = K_L q_m - K_L q_e \quad (9)$$

Where, q_e is the adsorption capacity at equilibrium (mg/g); q_m is the maximum adsorption capacity (mg/g); C_e is the equilibrium concentration of metal ions in solution (mg/L) and K_L is the Langmuir constant (L/mg). The values of isotherm constants (q_m and K_L) are defined from the slope and intercept of the linear plot of C_e/q_e versus C_e , respectively. The

linear forms of the isotherms at all temperature and the correlation coefficients were used to predict if the adsorption data closely follow the Langmuir model of sorption.

Hereby, a dimensionless constant, commonly known as separation factor (R_L) defined Webber and Chakkravorti [27] can be represented by equation 10:

$$R_L = \frac{1}{1 + K_L C_0} \quad (10)$$

where K_L (L/mg) is the Langmuir constant related to rate of adsorption and C_0 is denoted to the adsorbate initial concentration (mg/L). In this context, lower R_L value reflects that adsorption is more favourable. In a deeper explanation, R_L value indicates the adsorption nature to be either unfavourable ($R_L > 1$), linear ($R_L = 1$), favourable ($0 < R_L < 1$) or irreversible ($R_L = 0$).

2.3.4.1.2.2. Freundlich Isotherm

Freundlich (1906) proposed an empirical equation, which can be applied for solutions in the low to intermediate concentration range. This model assumes a heterogeneous adsorption surface with sites that have different energies of adsorption and are not equally available. The Freundlich isotherm is derived by assuming an exponential decay energy distribution function inserted into the Langmuir equation [28]. It describes reversible adsorption and is not restricted to the formation of the monolayer. The Freundlich equation is an empirical equation employed to describe heterogeneous systems, in which it is characterized by the heterogeneity factor $1/n$. When $n=1$, the Freundlich equation reduces to Henry's law. Hence, the empirical equation can be written as equation 11:

$$q_e = K_f C_e^{\frac{1}{n}} \quad (11)$$

Where K_f is the Freundlich constant ($L(mg^{1-1/n}g)^{-1}$) which is an indicative of relative adsorption capacity of the adsorbent, and $1/n$ is the heterogeneity factor. A linear form of the Freundlich expression can be obtained by taking logarithms of equation 12:

$$\log q_e = \log K_f + \frac{1}{n} \log C_e \quad (12)$$

Therefore, the plots of $\log q_e$ versus $\log C_e$ were drawn to calculate the values of K_f and $1/n$ from the intercept and slope respectively. The linear forms of the isotherms at all temperature and the correlation coefficients were used to predict if the adsorption data closely follow the Freundlich model of sorption.

2.3.4.1.2.3. Dubinin-Radushkevich (D-R) isotherm

Dubinin-Radushkevich (D-R) isotherm [29] is an empirical model initially conceived for the adsorption of subcritical vapors onto micropore solids following a pore filling mechanism. It is generally applied to express the adsorption [2 13] with a Gaussian energy distribution onto a heterogeneous surface. The model has often successfully fitted high solute activities and the intermediate range of concentration data well.

A linear expression of the D-R equation is:

$$\ln q_e = \ln q_m - K_D \varepsilon^2 \quad (13)$$

Where K_D is a constant related to the adsorption energy and ε is the Polanyi potential which is related to equilibrium concentration through the expression:

$$\varepsilon = RT \ln \left(1 + \frac{1}{C_e} \right) \quad (14)$$

When $\ln q_e$ is plotted against ε^2 , the mean adsorption energy (E) is:

$$E = \frac{1}{\sqrt{2K_D}} \quad (15)$$

The magnitude of E may characterize the type of the adsorption as chemical ion exchange ($E= 8-16$ kJ/mol) describes the chemical ion exchange or physical adsorption ($E < 8$ kJ/mol).

2.3.4.1.2.4. Temkin isotherm

The dependence of temperature on equilibrium capacity can be identified based on the heat of adsorption value using the Temkin equation. The Temkin isotherm contains a factor that explicitly takes into account adsorbate/adsorbate interactions. The heat of adsorption of all the molecules in the layer would decrease linearly with coverage because of adsorbate/adsorbate interactions. The Temkin isotherm can be used to describe binding site [30]. The Temkin equation is expressed as

$$q_e = \frac{RT \ln (AC_e)}{b} \quad (16)$$

Where $\frac{RT}{b} = B$ is the Temkin constant related to heat of sorption (Jmol^{-1}), A the Temkin isotherm constant (Lg^{-1}) corresponding to the maximum binding energy, R the gas constant ($8.314 \text{Jmol}^{-1} \text{K}^{-1}$) and T the absolute temperature (K).

2.3.4.1.3. Thermodynamic Study

In order to study the feasibility of adsorption, three thermodynamic equations 17-19 were applied to equilibrium adsorption isotherms to calculate the related parameters (Free energy (ΔG°), enthalpy (ΔH), and entropy (ΔS)) for the adsorption systems.

$$\Delta G^\circ = - RT \ln b \quad (17)$$

$$H^\circ = \frac{RT_2T_1}{T_2-T_1} \ln \frac{b_2}{b_1} \quad (18)$$

$$S^\circ = \frac{H^\circ - G^\circ}{T} \quad (19)$$

Where b , b_1 and b_2 are Langmuir constants at different temperatures and other terms have their usual meanings. The negative value of free energy (ΔG°) reflects feasibility of adsorption system and vice versa. The positive and negative values of enthalpy (H°) show endothermic or exothermic nature of adsorption respectively. Similarly, positive or negative values of entropy (S°) change give an idea about increase or decrease in randomness in adsorption process.

2.3.4.1.4. Adsorption Kinetic Models

Adsorption process is significant since the sorption process reach the equilibrium rapidly with the increase in adsorption capacity with time. Hence adsorption is a time dependent process. Measurement of sorption rate constants and order of the reaction are important physic-chemical parameters to evaluate the basic qualities of a good sorbent. Prediction of kinetics is necessary for the design of sorption systems. More than 25 models have been put forward to describe or predict the adsorption kinetics. Each of these models has its own limitations and strengths and is derived according to certain initial conditions based on specific experimental and theoretical assumptions. Normally adsorption kinetic models can be divided into two main types: reaction based models and diffusion based models [31].

2.3.4.1.4.1. Reaction based models

2.3.4.1.4.1.1. Pseudo-First-Order Model

The pseudo-first-order equation suggested by Lagergren [32] is considered as the first rate equation for the adsorption of solid/liquid systems. A pseudo-first-order Lagergren model is based on the assumption that the rate of adsorbate seizing the adsorption sites is proportional to the amount of untaken adsorption sites. It can be expressed as

$$\log(q_e - q_t) = \log q_e - \frac{k_1 t}{2.303} \quad (20)$$

Where q_e is the adsorption capacity at equilibrium (mg/g); q_t is the adsorption capacity at the time of t (mg/g); and k_1 is the first order rate constant (1/min). The values of kinetic constants (q_e and k_1) are defined experimentally from the slope and intercept of the linear plot of $\log(q_e - q_t)$ versus t , respectively. In many cases, pseudo-first-order does not fit well over the range of contact times under investigation. It fits the experimental data for an initial period of the first reaction step only.

2.3.4.1.4.1.2. Pseudo-Second-Order Model

For the pseudo-second-order model reaction the rate limiting step may be chemisorptions or chemisorptions involving sharing or exchange of electrons between the adsorbent and adsorbate. The rate of the reaction may be dependent on the amount of metals ions on the surface of the adsorbent and the amount of metal ions sorbed at equilibrium. It means that the rate of reaction is directly proportional to the number of active sites on the surface of the adsorbent. The pseudo-second-order rate equation developed by Ho and Mckay [33], can be expressed as

$$\frac{dq_t}{dt} = k_2(q_e - q_t)^2 \quad (21)$$

Equation (21) can be linearized into four different linear types by the following equations 22-25:

$$\text{Type 1} \quad \frac{t}{q_t} = \frac{1}{k_2 q_e^2} + \frac{1}{q_e} t \quad (22)$$

$$\text{Type 2} \quad \frac{1}{q_t} = \left(\frac{1}{k_2 q_e^2} \right) \left(\frac{1}{t} \right) + \frac{1}{q_e} \quad (23)$$

$$\text{Type 3} \quad q_t = q_e - \left(\frac{1}{k_2 q_e} \right) \frac{q_t}{t} \quad (24)$$

$$\text{Type 4} \quad \frac{q_t}{t} = k_2 q_e^2 - k_2 q_e q_t \quad (25)$$

Where q_t and q_e are the amount adsorbed at any time t and at equilibrium and k_2 is the second order rate constant (g/mg min). The values of kinetic constants (q_e and k_2) are defined

experimentally from the slope and intercept of the linear plot of t/q_t versus t , respectively. Pseudo-second-order model predict the behaviour over the whole concentration range and is in agreement with chemical sorption being rate-controlling step.

2.3.4.1.4.2. Diffusion-based models

The adsorption process involves particle diffusion or film diffusion. Three consecutive steps, which occur in the adsorption of an adsorbate by a porous adsorbent, are:

1. Transport of the adsorbate to the external surface of the adsorbent (film diffusion);
2. Transport of the adsorbate within the pores of the adsorbent (particle diffusion);
3. Adsorption of the adsorbate on the interior surface of the adsorbent.

Step 3 is considered to be very rapid and does not represent the rate-determining step in the uptake of adsorbate. The following three distinct possibilities exist for the remaining two steps in the overall transport process:

Case I: External transport > Internal transport.

Case II: External transport < Internal transport.

Case III: External transport \approx Internal transport.

In cases I and II, the rate is governed by the particle and film diffusion, respectively, but in case III, the transport of ions to the boundary may not be possible at a significant rate, thereby, leading to the formation of a liquid film with the formation of a concentration gradient at the adsorbate particle.

To investigate the actual process involved in the adsorption process, the mathematical treatment recommended by Boyd, Bangham and the intra particle diffusion model were employed.

2.3.4.1.4.2.1. Boyd model

The mathematical treatment recommended by Boyd et al. [34] was employed to explore whether the adsorption process involves particle diffusion or film diffusion. A quantitative treatment of the sorption dynamics was employed with the help of the following expressions 26-28:

$$F = 1 - \frac{6}{\pi^2} \sum_1 \left(\frac{1}{n^2} \right) \exp(-n^2 B_t) \quad (26)$$

$$F = \frac{Q_t}{Q} \quad (27)$$

$$B = \frac{\pi^2 D_i}{r_o^2} = \text{Time Constant} \quad (28)$$

Where, F is the fractional attainment of equilibrium at time t , n is the Freundlich constant of the adsorbate and B_t is the time constant; Q_t and Q_∞ are the amounts adsorbed (mgg^{-1}) after time t and after infinite time, respectively; B is the time constant after time t , D_i is the effective diffusion coefficient of the adsorbate and r_0 is the radius of spherical adsorbent particle.

Based on the values of Fractional attainment, B_t values are derived from Reichenberg's table [35]. The linearity of the B_t vs time plots with straight lines passing through the origin will suggest that the rate determining process is particle diffusion where external transport of the adsorbate ions is much favoured than the internal transport.

2.3.4.1.4.2.2. Bangham's Equation

The applicability of the following Bangham's equation [36] to kinetic study was tested to learn about the slow step occurring in the adsorption process:

$$\text{Log log} \left(\frac{C'_o}{C'_o - q'm'} \right) = \text{log} \left(\frac{k_o m'}{2.303V} \right) + \alpha \text{ log } t \quad (29)$$

Where C'_o is initial concentration of the adsorbate in solution (mgL^{-1}), V the volume of solution (mL), m' the weight of adsorbent used per litre of solution (gL^{-1}), q' (mgg^{-1}) the amount of adsorbate retained at time t and α (<1) and k_o are constants. $\text{Log log} \left(\frac{C'_o}{C'_o - q'm'} \right)$ values were plotted against $\text{log } t$ in Bangham's plot. The linearity of these plots confirms the applicability of Bangham's equation and indicates that diffusion of adsorbate molecules into pores of the adsorbent mainly controls the adsorption process rather a film diffusion controlled process.

2.3.4.1.4.2.3. Intraparticle Diffusion

In a well-agitated batch adsorption system, there can also be a possibility of intraparticle pore diffusion [37] of adsorbate ions, which can be the rate limiting step.

$$q_t = k_i t^{0.5} + I \quad (30)$$

Where q_t is the adsorption capacity at the time of t (mg/g); k_i is the second order rate constant (mg/g min) and I indicates the thickness of the boundary layer (mg/g). The values of kinetic constants (k_i and I) are defined from the slope and intercept of the linear plot of q_t versus $t^{0.5}$, respectively.

The linearity of the plots of q_t versus $t^{0.5}$ with straight lines passing through the origin will imply that although intraparticle diffusion is involved in the adsorption process, it is not the sole rate controlling step and that some other mechanisms may play an important role.

2.3.4.2. Column Adsorption Method

Column-type continuous flow operations have many distinct advantages over batch studies. The main objective of flow through column experiments is to provide a more sensible simulation of how the adsorbent material adsorbs the noxious contaminant. Although adsorption studies provide parameters which are useful for the application of adsorbents for the removal of noxious contaminants yet column experiments are also necessary to provide operational information with respect to the adsorption a particular adsorbent-adsorbate system [38]. Additionally column experiments also provide a much closer approximation of the physical conditions and chemical processes rather than the batch experiments. Hence, the practical applicability of the product for column operations has also been studied to obtain some parameters necessary for a factual design model. In this method, a column of adsorbent is loaded, saturated and effluent is allowed to pass through it at a definite rate. The adsorbent has to be granular with sufficient particle size; otherwise the column becomes choked in no time. The effluent from the column is taken and analyzed for the concentration of the adsorbate and breakthrough curves are obtained. These investigations provide information regarding the optimum mass, height and area of the column and the rate of the effluent flow which will permit best treatment of the wastewater.

In the present work, a glass column (30 x 2.5cm) is fully loaded with adsorbent on a glass wool support. A schematic diagram of column, used in the experiments, is given as Figure 2.9.

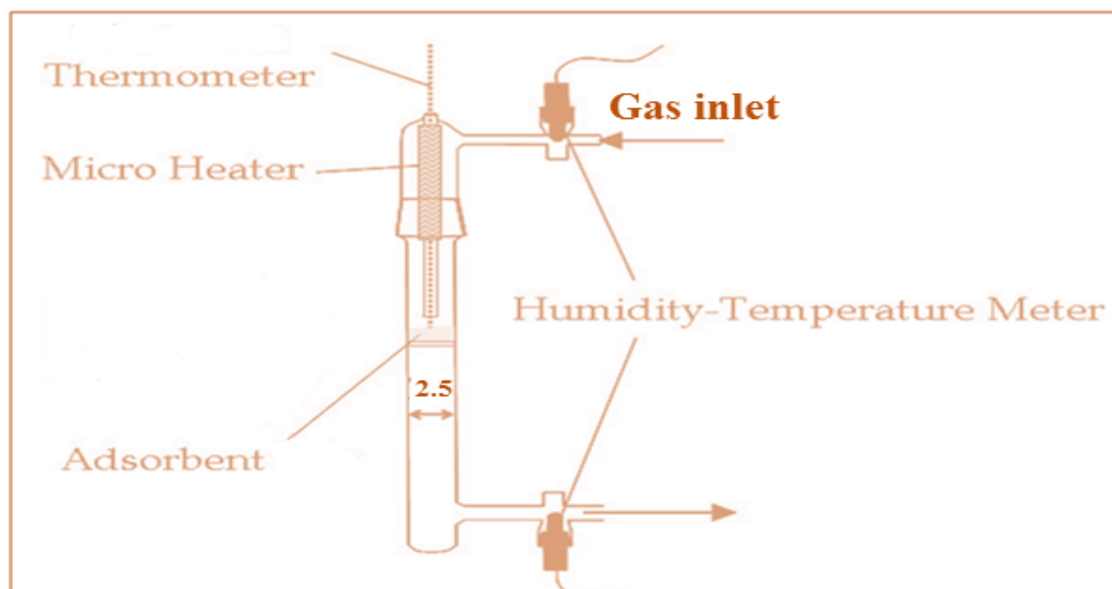


Figure 2.9 Schematic presentation of the column used for the adsorption experiment

Double distilled water was used to rinse the adsorbent and to remove any bubbles present. A dye/phenols/metal ions was poured into the column and the column effluent was taken and the concentration of the solute (Noxious impurities under investigation) determined from time to time by spectrophotometric/AAS method is required. This process is continued till the concentration in the column effluent becomes constant. The plots of the concentration of the adsorbate in the column effluent and volume of the effluent provide breakthrough curves.

2.3.4.2.1. Breakthrough Curve

The efficiency of column operations is understood in terms of breakthrough curve. A breakthrough curve is obtained by plotting column effluent concentration versus volume treated or the time of treatment or the number of bed volumes (BV) treated. A typical breakthrough curve is shown in Figure 2.10.

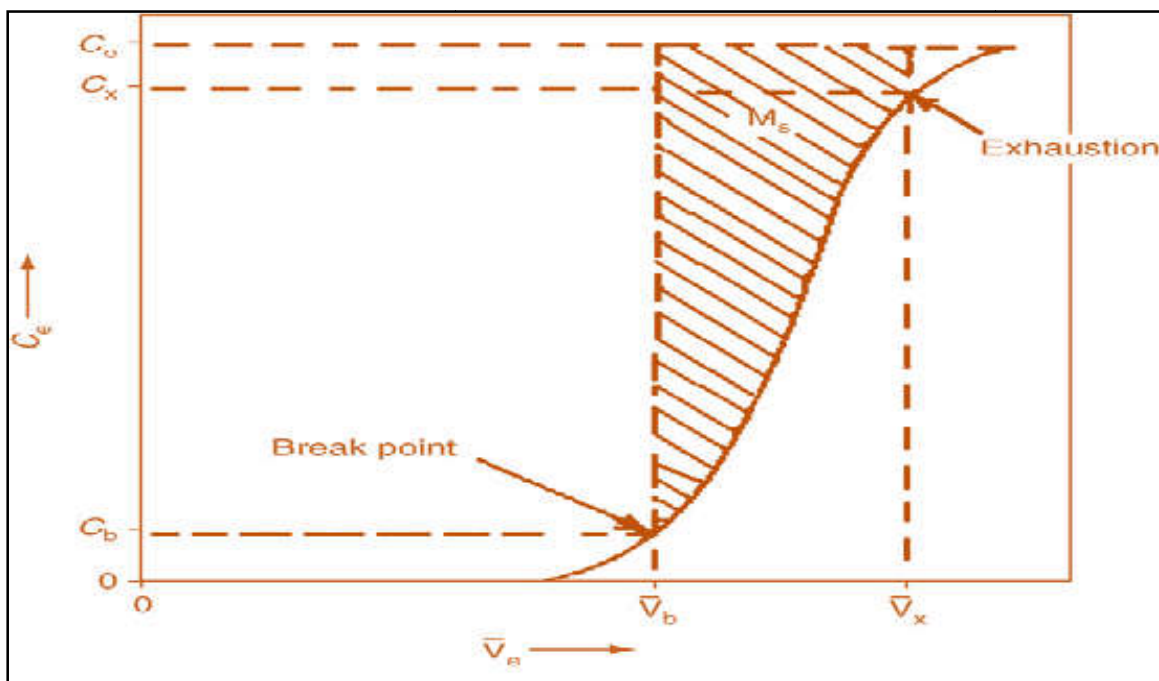


Figure 2.10 Breakthrough Curve (C_o : Concentration of influent; C : Concentration of effluent).

A breakthrough curve is a plot of the column effluent concentration as a function of either volume treated or the time of treatment or the number of bed volumes (BV) treated. The important features of a breakthrough curve [39] are breakthrough capacity (BC), exhaustion capacity (EC) and degree of column utilization (DOC). The definition of breakthrough capacity is the mass of adsorbate eliminated by the adsorbent at breakthrough concentration, which in turn is defined as utmost acceptable (desired) concentration. When the effluent concentration touches this value, at that time the developed adsorbent may be replaced. The DOC utilization

may be defined as the ratio of mass adsorbed at breakthrough to the mass adsorbed at complete saturation i.e. when effluent concentration becomes equal to or nearly equal to influent concentration. The EC is defined as the mass of the adsorbate removed by one unit weight of the adsorbent at the point of saturation. Various factors [39, 40] effects the breakthrough curves like adsorbate nature and adsorbent nature, pH, concentration of solute, adsorption mechanism (Rate limiting step), equilibrium conditions, size of particle, column geometry and operating condition. At extremely high adsorption rate and favorable adsorption isotherm the point of breakthrough and the point of exhaustion coincide practically and the breakthrough curve becomes sharp [41]. Mass transfer rate effect the sharpness of the breakthrough curves, as the transfer of mass are finite breakthrough curve, which are diffuse and S shaped. For most adsorption operations in water and wastewater treatment, breakthrough curves exhibit a characteristic S shape but with varying degree of steepness [40] (Figure 2.11).

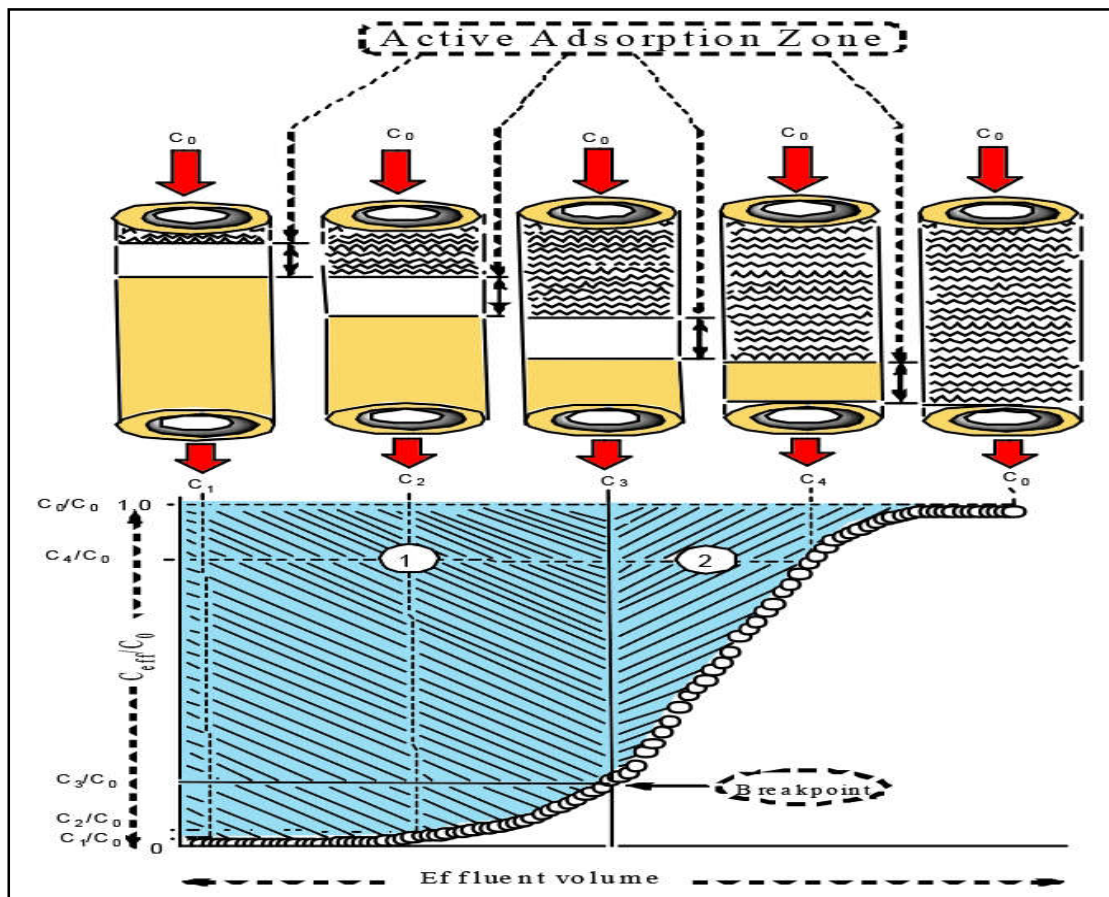


Figure 2.11 Representation of the movement of the adsorption zone and the resulting breakthrough curve

Weber [40] explained the relationship between the nature of breakthrough curves and the fixed bed absorber as shown in Figure 2.11. When the feed water is introduced through the inlet of the column, the solute is adsorbed most rapidly and effectively by the upper few layers of the fresh adsorbent during the initial stages of operations. These upper layers are: of course; in contact with the solution at its highest concentration level, C_o (Concentration of the influent). The small amounts of solute which escape adsorption in the first few layers of the adsorbent are then removed from the solution in the lower strata of the bed, and essentially no solute escape from the adsorbent initially (effluent concentration, $C=0$). The primary adsorption zone is concentrated near the top or influent end of the column. As the polluted feed water continues to flow in to the column, the top layers of the adsorbent become practically saturated with the solute and become less effective for further adsorption. Thus, the primary adsorption zone now moves downward to regions of fresher adsorbent. The wave like movement of this zone, accompanied by a movement of the C_o concentration front, occurs at a rate which is generally much slower than the linear velocity of the feed water. As the primary adsorption zone moves downwards, more and more solute tends to escape in the effluent, as indicated in Figure 2.11. The plots of C/C_o versus time or volume, for a constant flow rate, depict the increase in the ratio of effluent to influent concentration as the zone moves through the column.

The breakpoint on the curve has been adopted by various workers differently to determine the breakthrough capacity of the column [42, 43]. The calculation [44] of the BC, EC and DOC utilization have been evaluated from the breakthrough curves as per equation 31-37 and Figure 2.11 using a Excel worksheet, developed to calculate curve area.

$$\text{Breakthrough capacity} = \text{area 1} \times C_o \quad (31)$$

$$\text{Exhaustion capacity} = (\text{area 1} + \text{area 2}) \times C_o \quad (32)$$

$$\text{Degree of column utilization (\%)} = [\text{area1}/(\text{area 1} + \text{area 2}) \times 100 \quad (33)$$

Another method of calculating the various experimental parameters was as follows:

$$q_{tot} = t_s \times F \times \frac{C_o - C_s}{1000} \quad (34)$$

$$q_b(mg) = t_b \times F \times \frac{C_o - C_b}{1000} \quad (35)$$

$$M_{tot}(mg) = t_s \times F \times \frac{C_o}{1000} \quad (36)$$

$$\%RM = \frac{q_{tot}}{M_{tot}} \times 100 \quad (37)$$

Where q_{tot} and q_b are the adsorbate adsorbed by the column at saturation and breakpoint respectively, t_s and t_b are time at saturation and breakpoint respectively, F is flow rate (mL/min), C_o and C_s are the concentration of the metal ion (mg/L) at saturation and breakpoint

respectively. M_{tot} is the total adsorbate supplied to the column and RM is the adsorbate removal rate by the column.

2.3.5. Desorption and Regeneration Experiments

Desorption studies help to elucidate the mechanism of adsorption as to recover the pollutants from the spent adsorbent apart from protecting the environment from solid waste disposal problem. After the column is exhausted by the studied adsorbate, acidic or basic solution or buffers or organic solvents were used for desorbing the adsorbate depending on the type of pollutants adsorbed on the adsorbent. The desorbing medium is passed through the column at a constant flow rate 1.5 ml/min. Once complete elution of the adsorbate from the column had taken place the columns were washed properly with distilled water. The amount of pollutant desorbed from the adsorbate is thereby calculated.

Regeneration of the adsorbent for repeated use is of crucial importance in industrial practice for pollutant removal from wastewater. This fulfils an important criterion for advanced adsorbents. Reusability study of adsorbent was carried out by following the adsorption-desorption study for 5 cycles. The adsorption efficiency in each cycle was analyzed. Both the adsorption and desorption experiments were followed as described above.

2.3.6. Test with Simulated and Real Industrial Effluents

Since the ultimate objective of the adsorption technology is the removal of pollutants from the industrial or real wastewaters that often contain varied types of pollutants simultaneously, column adsorption experiments were conducted with actual industrial wastewater. Urban wastewater from IIT Roorkee campus was collected and was spiked with the studied dyes, pesticides and metal ions to obtain wastewater which is simulated an actual textile, pesticides metal plating and electroplating industry effluent. The noxious pollutant removal was carried out in the laboratory column set up filled with the standard adsorbent having bed depth of 15 cm and flow rate of 1.5 mL/min.

2.3.7. Quality assurance/Quality control

In order to establish the accuracy, reliability and reproducibility of the collected data, all the batch isotherm tests are replicated thrice and the experimental blanks are run in parallel. Check standards and blanks are run. Multiple sources of National Institute of Standard and Technology (NIST) traceable standards are used for the instrument calibration and standard verification. All jars, conical flasks, and containers used in the study are prepared by soaking in 5% HNO_3 solution for a period of 3 days before being doubly rinsed with distilled, deionized

Novel adsorbent for noxious impurities removal

water and oven dried. In different experiments, blanks are run and corrections made wherever necessary. All observations are recorded in triplicate and average values are reported.

References

- [1] Hu, Z., Guo, H., Srinivasan, P.M., Yaming, N., “A simple method for developing mesoporosity in activated carbon” *Sep. Purif. Technol.*, 31, (2003), 47-52.
- [2] Gupta V.K., Gupta B., Rastogi A., Agarwal S., Nayak A., “A comparative investigation on adsorption performances of mesoporous activated carbon prepared from waste rubber tire and activated carbon for a hazardous azo dye—Acid Blue 113,” *J. Hazard. Mater.*, 186, (2011), 891–901.
- [3] Garrett Q., Laycock B., Garrett R. W., “Hydrogel lens monomer constituents modulate protein sorption,” *Investigative ophthalmol. vis. sci.*, 41, (2000), 1687-1695.
- [4] Domínguez J.M., Palacios J., Espinosa G., Schifter I., Surface microstructure MMA HEMA polymer membranes,” *J. appl. Polym. sci.*, 48(11), (1993), 1897-1904.
- [5] Chekina N. A., Pavlyuchenko V. N., Danilichev V. F., Ushakov N. A., Novikov S. A., Ivanchev S. S., “A New polymeric silicone hydrogel for medical applications: synthesis and properties,” *Polym. Adv. Technol.*, 17, (2006), 872-877.
- [6] Murthy N.S., “Recent developments in polymer characterization using X-ray diffraction,” *Rigaku J.*, 21, (2004), 15-24.
- [7] Biskupek J., Kaiser U., Falk F., “Heat and electron-beam-induced transport of gold particles into silicon oxide and silicon studied by in situ high-resolution transmission electron microscopy,” *J. Electron Microsc (TOKYO)*, 57, (3)(2008), 83-89.
- [8] Iqbal M. Saeda A., Saeed I. Z., “ FTIR spectro-photometry, kinetics and adsorption isotherms modelling, ion exchange, and EDX analysis for understanding the mechanism of Cd⁺² and Pb⁺² removal by mango peel waste,” *J. Hazard. Mater.*, 164(1)(2009), 161-171.
- [9] Boparai H.K., Joseph M., O’Carroll D.M., “Kinetics and thermodynamics of cadmium ion removal by adsorption onto nano zerovalent iron particles, *J. Hazard. Mater.*, 186, (1)(2011), 458-465.
- [10] Goldstein J., “Scanning electron microscopy and X-ray micro analysis,” *Springer, ISBN 978-0-306-47292-3* (2003), retrieved on 26 may 2012.
- [11] Mustafa S., Shahida P., Naeem A., Dilara B., “Sorption studies of divalent metal ions on ZnO,” *Langmuir.*, 18(6),(2002),2255-2259
- [12] Yukselen Y., Kaya A., “Zeta potential of kaolinite in the presence of alkali, alkaline earth and hydrolyzable metal ions,” *Water Air Soil Poll.*, 145, (2003), 155-168.
- [13] Kosmulski M., “pH- depended surface charging and points of zero charge. IV. Update and new approach,” *J. Colloid interf. Sci.*, 337, (2009), 439-448.

- [14] Jodin M.C., Gaboriaud F., Humbert B., "Limitation of potentiometric studies to determine the surface charge of gibbsite γ -Al(OH)₃ particles," *J. Colloid Interf. Sci.*, 287, (2005), 581-591.
- [15] Parks G. A., De Bruyn P.L., "The zero point of charge of Oxides," *J. Phys. Chem.*, 66,(1961) 967-973.
- [16] Tripathy S.S., Kanungo S.B., "Adsorption of Co²⁺, Ni²⁺, Cu²⁺ and Zn²⁺ from 0.5M NaCl and major ion sea water on a mixture of δ -MnO₂ and amorphous FeOOH," *J. Colloid Interf. Sci.*, 284(1), (2005), 30-38.
- [17] Zhu Zhi-liang, Hong-mei M.A., Zhang Rong-hua, Yuan-xin G.E., Zhao Jiang-fu, "Removal of cadmium using MnO₂ loaded D301 resin," *J. Environ. Sci.*, 19, (2007), 652-656.
- [18] Foil N., Villaescusa I., "Determination of sorbent zero charge usefulness in sorption studies," *Environ. Chem. Lett.*, 7, (2009), 79-84.
- [19] Rahmat A.R., Rahman W.A.W.A., Sin L.T., Yussuf A.A., "Approaches to improve compatibility of starch filled polymer system: A review," *Mater. Sci. Eng., C*, 29, (2009), 2370-2377.
- [20] Jishi R.A., Venkataraman L., Dresselhaus M.S., Dresselhaus G., "Phonon modes in carbon nanotubes," *Chem. Phys. Lett.* 209, (1993), 77-82.
- [21] Singh K.S.W., Everett D.H., Haul R.A.W., Moscou L., Pierotti R.A., Rouquerol J., Siemieniowska T., "Reporting physisorption data for gas/solid systems with special reference to determination of surface area and porosity (Recommendations 1984)," *Pure Appl. Chem.*, 57, (1985), 603-919.
- [22] Giles C.H., McEwan H., Nakhwa S.N., Smith D., "Studies in adsorption . Part III.A system of classification of solution and adsorption isotherm and its use in diagnosis of adsorption mechanisms and in measurement of specific surface area in solution," *J. Chem.Soc.*, 786, (1960), 3973-3993.
- [23] Langmuir I., "The constitution and fundamental properties of solids and liquids" *J. Am. Chem. Soc.*, 38, (1916), 2221-2295.
- [24] Allen S.J., McKay G., Porter J.F., "Adsorption isotherm models for basis dye adsorption by peat in single and binary component systems," *J. Colloid Interf. Sci.*, 280, (2004), 322-333.
- [25] Vijayaraghavan K., Padmesh T.V.N., Palanivelu K., Velan M., "Biosorption of nikel(II) ions onto Sargassum Wightii: application of two-parameter and three parameter isotherm models," *J. Hazard. Mater. B*, 133, (2006), 304-308.

- [26] Perez-Marin A.B., Zapata V.M., Ortuno J.F., Aguilar M., Saez J., Llorens M., "Removal of cadmium from aqueous solutions by adsorption onto orange waste," *J. Hazard. Mater. B*, 139, (2007), 122-131.
- [27] Webber T.W., Chakkravorti R.K., "Pore and solid diffusion models for fixed-bed adsorbers," *AIChE J.*, 20, (1974), 228-238.
- [28] Freundlich H.M.F., "Over the adsorption in solution," *J. Phys. Chem.*, 57, (1996), 385-471.
- [29] Dubinin M.M., Radushkevich L.V., "The equation of the characteristic curve of the activated charcoal," *Proc. Acad. Sci. USSR Phys. Chem. Sect.*, 55, (1947), 331-337.
- [30] Stumm W., Morgan J.J., "Aquatic chemistry," *Wiley*, New York, 1981
- [31] Degs Y.S.A., Barghouthi M.I.E., Issa A.A., Kgraisheh M.A., Walker G.M., "Sorption of Zn(II), Pb(II) and Co(II) using a natural sorbent: equilibrium and kinetics studies," *Water Res.*, 40, (2006), 2645-2658.
- [32] Lagergren S., "About the theory of so-called adsorption of soluble substance," *K. Sven. Vetenskapsakad. Hand.*, 40, (1918), 1361-1403.
- [33] Ho Y.S., McKay G., "The kinetics of sorption of divalent metal ions onto sphagnum moss peat," *Water Res.*, 34(3), (2000), 735-742.
- [34] Boyd E., Adamson A.W., Meyers L.S., "The exchange adsorption of ions from aqueous solution by organic zeolites. II. Kinetics," *J. Am. Chem. Soc.*, 69, (1947), 2836-2848.
- [35] Reichenberg D., "Properties of ion exchangers, resin in relations to their structure. III. Kinetics of exchange," *J. Am. Chem. Soc.*, 75, (1953), 589-597.
- [36] Aharoni C., Sideman S., Hoffer E., "Adsorption of phosphate ions by colloid ion-coated alumina," *J. Chem. Technol. Biotechnol.*, 29, (1979), 404-412.
- [37] Zhu C.S., Wang L.P., Chen W., "Removal of Cu(II) from aqueous solution by agricultural by-product: Peanut hull," *J. Hazard. Mater.*, 168, (2009), 739-746.
- [38] Eckenfelder W.W., "Industrial water pollution control; McGraw-Hill Series in water resources and environmental engineering ; 3rd ed.; McGraw-Hill Higher Education, (2000), 584.
- [39] Snoeyink V. L., Summers R.S., "Adsorption of organic compounds. Water quality and treatment: a handbook of community water supplies. R. D. Letterman and A. W. W. Association, McGraw-Hill 1999.
- [40] Weber W.J., "Physicochemical processes for water quality control, *Wiley-Interscience*. 1972.

- [41] Shang G., Shen G., Wang T., Chen Q., "Effectiveness and mechanisms of hydrogen sulfide adsorption by camphor-derived biochar." *J. Air Waste Manage. Assoc.* 62(8), (2012), 873-879.
- [42] Cloutier J-N., Leduy A., Ramalho R.S., "Peat adsorption of herbicide 2,4-D from wastewaters," *Can. J. Chem. Eng.*, 63, (1985), 250-257.
- [43] Mollah A.H., Robinson C.W., "Pentachlorophenol Adsorption and desorption characteristics of granular activated carbon-II.Kinetics," *Water Res.*, 30, (1996), 2907-2913.
- [44] Pontius F.W., "Water Quality and Treatment," 4th ed., *McGraw-Hill Inc.*, New York (1990).



CHAPTER 3

Rubber Tire Activated Carbon For the Removal of Ni^{2+}



3.1. Introduction

Wastewater contaminated by high doses of toxic metal ions leads to the rapid depletion of aquatic sources and likewise it causes exponential increase in the severe detrimental water borne diseases, which act as life threatening agent for humans and prevailing aquatic flora and fauna. Large number of industries viz., mineral processing, electroplating, alkali and paints production units, manufacturing of sulphate etc have generated wastewater containing Ni²⁺ in doses higher than the limits prescribed by WHO and EPA [1-3]. The maximum permissible limit for noxious metal nickel in the aqueous solution according to U.S. Environmental Protection Agency (EPA) and WHO is 0.015 and 0.02 mg/L respectively [4, 5]. High amount of Ni²⁺ consumption causes serious health hazards like dermatitis, nausea, coughing, chronic bronchitis, gastrointestinal distress, and bronchospasmic carcinoma [6, 7]. Due to its toxic impact, persistency and its ability to bio accumulate in tropic levels [8], the Ni²⁺ as pollutant is a potential threat to the ecosystem and it is necessitate requirement of the living beings to remove this noxious metal rapidly and effectively for the aqueous sources. Several previously developed techniques processes have been employed for the removal of nickel ions from water and wastewater and these include chemical precipitation, ion exchange, flotation, membrane filtration, electrochemical treatment and coagulation–flocculation [9]. However, these methods were either inefficient or expensive when heavy metal exists in lower concentrations [10]. Among all the developed techniques adsorption technology in wastewater treatment for the removal of diverse metal pollutants from the water bodies especially at trace concentration is fast gaining momentum due to its environmental friendliness, enhanced efficiency and cost effectiveness as compared to other treatment technologies. Various effective adsorbents for large scale use in water decontamination have been developed from industrial and agricultural wastes and used for the removal of various micro pollutants [11].

The present study thus focuses on the synthesis of activated carbon from scrap tire as low cost novel adsorbent for the rapid removal and fast adsorption of noxious Ni²⁺ from the solvent phase. This study provides a systematic investigation of the adsorption characteristics exhibited by activated carbons produced from the scrap tire. The results can be used to determine the potential use of these carbons in industrial applications that require the removal of a range of toxic metal ions. Activated carbon derived from scrap tire was characterized on the basis of porosity, surface textural and morphological properties and chemistry. The developed scrap tire derived activated carbon was later investigated for its adsorption characteristics using the Ni²⁺. The influential parameters such as pH, contact time, temperature, adsorbent dose and initial concentration was optimized using batch adsorption method. The

experimental data were modelled to the various adsorption isotherms and kinetic models to determine the adsorption capacities and reaction kinetics of the adsorption phenomenon. The surface properties of the activated carbon were assessed by various analytical methods in order to understand the nickel ion removal mechanism. Finally, the developed adsorbent was assessed for its practical role in the rapid removal of Ni^{2+} from a real metal fabrication industrial wastewater.

3.2. Results and discussion

3.2.1. Characterization of activated carbon prepared from scrap tire

The SEM image of the activated carbon as shown in Figure 3.1a reveals the morphological and microstructure characteristics favourable for metal adsorption. The particles represent the presence of varied mixture of mesopores and micropores. Adsorption of metal ions onto the activated carbon shows a changed morphology as evident from Figure 3.1b.

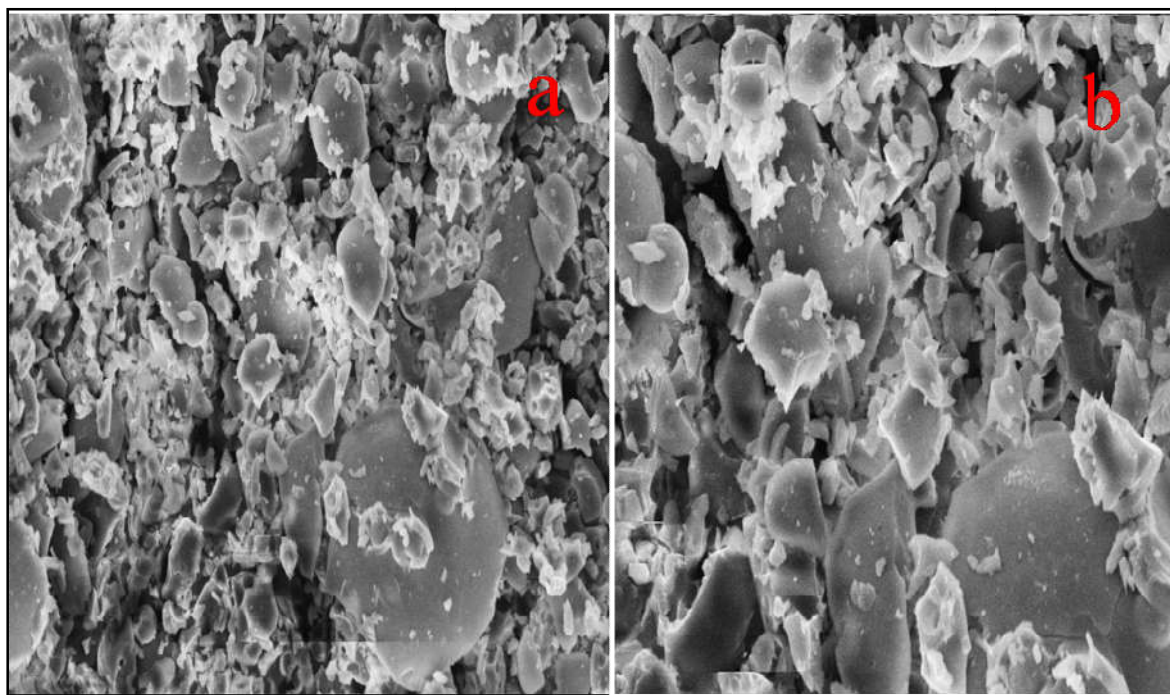


Figure 3.1 (a) SEM image of activated carbon (before adsorption) (b) SEM image of activated carbon after Ni^{2+} adsorption

The EDAX spectrum as evident from Figure 3.1a confirms the presence of only carbon and oxygen elements in the activated carbon particles; thereby revealing its carbonaceous nature. This is further evident from the EDAX quantitative microanalysis of the activated carbon as summarized in Table 3.1.

The quantitative analysis calculated from the peak areas of the EDAX spectrum. The occurrence of adsorption of Ni²⁺ on the surface of activated carbon is evident from the presence of Ni²⁺ in the EDAX spectrum (Figure 3.2b) and from the quantitative analysis (Table 3.1b)

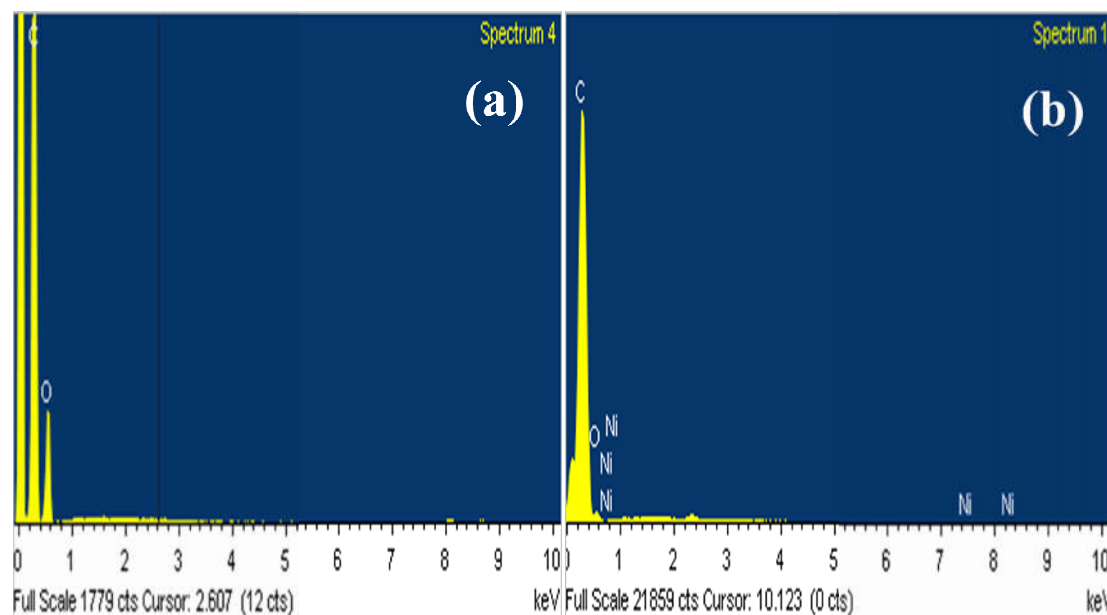


Figure 3.2 (a) EDAX of activated carbon from scrap tire (before Ni²⁺ adsorption) (b) EDAX of activated carbon from scrap tire (after Ni²⁺ adsorption)

Table 3.1 EDAX quantitative microanalysis of the activated carbon from scrap tire

Activated Carbon			Activated Carbon after Ni ²⁺ adsorption		
Element	Weight%	Atomic%	Element	Weight%	Atomic%
C K	95.75	93.84	C K	94.14	96.20
O K	4.25	6.16	O K	4.70	3.50
Ni K			Ni K	1.16	0.30
Total	100.00		Total	100.00	

The FTIR spectrum of the activated carbon sample (Figure 3.3) reveals the presence of prominent bands at 3428.74 cm⁻¹, 1736.21 cm⁻¹, 1591 cm⁻¹ and 1103.28 cm⁻¹ which can be inferred to the presence of a OH group of phenols and C=O group of esters. The 1736 and 1591 cm⁻¹ bands are ascribable to the C=O stretching vibrations of the carboxyl and carbonyl groups

in acidic oxygen surface groups. Such acidic oxygen surface groups are usually taken in account for the removal of metal ions from aqueous solution.

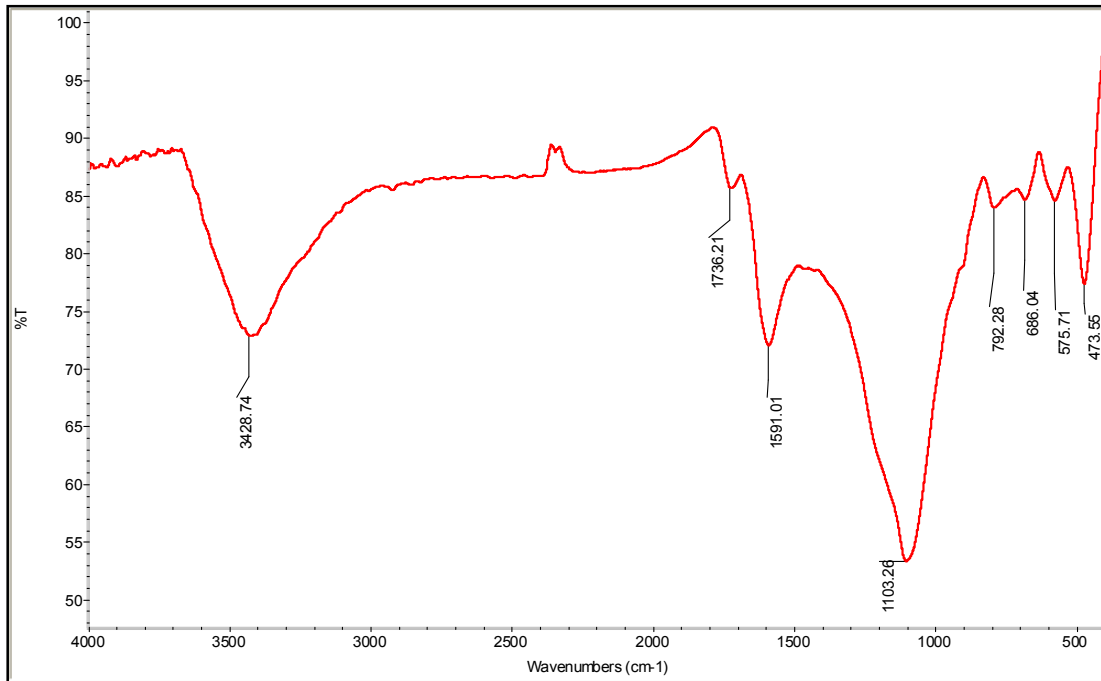


Figure 3.3 FTIR spectrum of activated carbon from scrap tire

3.2.2. Prefatory experimental adsorption studies

Contact time, metal ion concentration, pH, temperature etc are important parameters that controls the characteristics of the adsorbent surface and the metal binding capacity of the adsorbent are mainly controlled by the contact time, metal ion concentration, pH, temperature etc [12]. So batch adsorption studies were carried out on the developed adsorbent to observe the effects of these above said parameters.

3.2.2.1. Effect of pH and the adsorption mechanism

pH of the aqueous medium plays an important role in the adsorption of the metal ions, as speciation of the metal ions is generally observed. This is related to the pH as it affects the chemical speciation and behaviour of the metal adsorbates. The pH of the solution also affects the mechanism of adsorption and it is related to the physic-chemical interactions of the adsorbate-adsorbent [13]. The batch adsorption of Ni^{2+} at different pH values would enable for the determination of the optimum pH range favorable for the adsorption process.

The investigation of adsorption capacity of scrap tire derived activated carbon for Ni^{2+} at different values of pH of 1–9 at constant adsorbate concentration of 20 ppm, adsorbent dose of 0.1 g/L and contact time of 50 min is depicted in Figure 3.4. It shows that the uptake

capacity increased significantly with increase in pH up to 6 but gradually slows down up to 8 and thereafter decreases rapidly. A maximum capacity was observed at pH of 7 at 55°C and a pH range of 6-8 can be considered as favorable for Ni²⁺ adsorption.

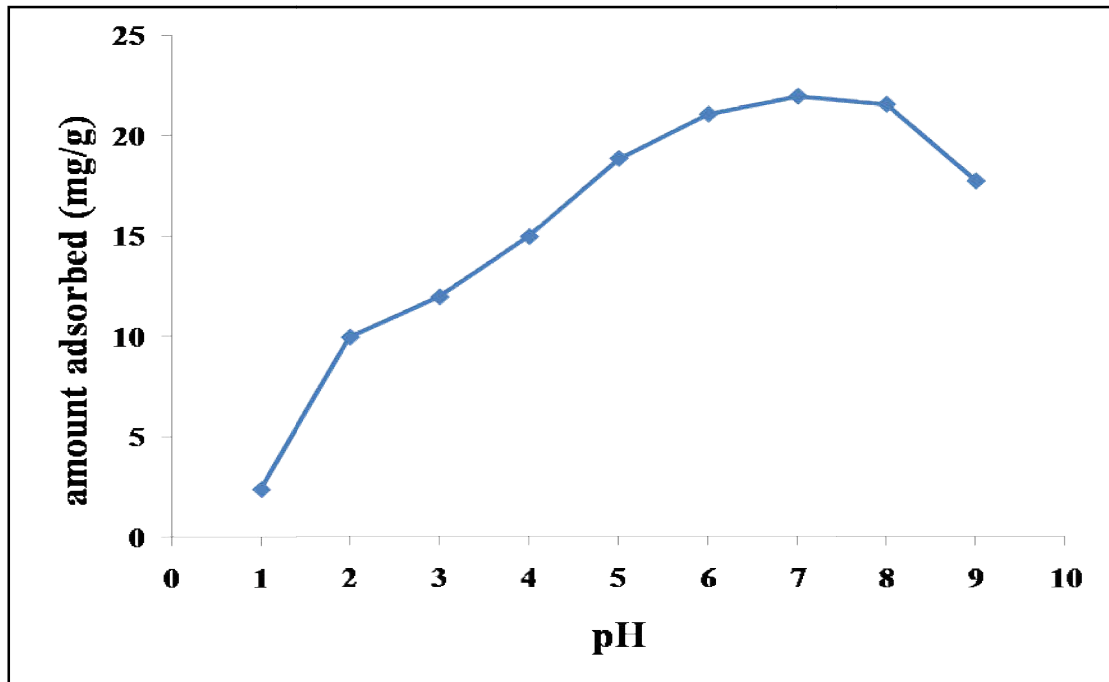
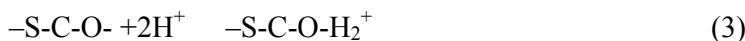
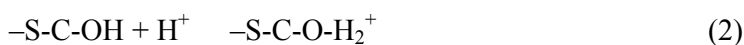


Figure 3.4 Effect of solution pH on the adsorption capacity of activated carbon for Ni²⁺ (adsorbent dose of 0.1 g/L, Ni²⁺ concentration of 20 ppm, temperature of 55°C)

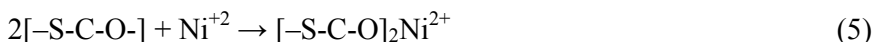
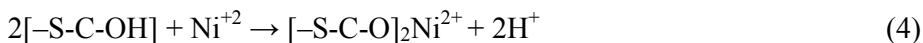
The observed trend can be attributed to the surface charge of the adsorbent and pH_{pzc} . The hydroxyl group and the carbonyl group on the activated carbon as revealed by the FTIR spectrum (Figure 3.3) may play a dominant role in the Ni²⁺ adsorption. Such groups on the surface of the adsorbent undergo protonation at lower pH values as follows:



At $pH < pH_{pzc}$ (pH_{pzc} of the activated carbon is 6.5), $-S-C-O-H_2^+$ species on the activated carbon surface having high positive charge density make the Ni²⁺ adsorption unfavorable due to electrostatic repulsion. Also, stiff competition between H⁺ and Cd²⁺ for the active sites will decrease Cd²⁺ adsorption [14, 15].

But, at $pH > pH_{pzc}$, $-S-C-OH$ and $-S-C-O^-$ are the dominant deprotonated species on the adsorbent surface. They undergo electrostatic attraction for Ni²⁺ and result in the formation of complexes [16], this complex formation leads to the enhancement of Ni²⁺ adsorption on to the activated carbon prepared from scrap tire.

From the following equation 4-5 it can be explained that ion exchange and complexation are principle mechanism in the adsorption process.



The sharp decline in uptake at higher pH values (> 8) can be ascribed due to the formation of $Ni(OH)_2$, which tends to precipitate at higher pH values.

3.2.2.2. Effect of initial concentration

Batch adsorption experiments were carried out at various initial concentrations of Ni^{2+} solutions (0.1, 1, 2, 10, 20, 40 ppm) at pH 7, adsorbent dose of 0.1 g/L and varying contact time (5-120 min); the results obtained are presented in the form of Figure 3.5. It was observed that the adsorption capacity increases with increase in initial Ni^{2+} concentration indicating that the initial adsorbate concentration provided a powerful driving force to overcome the mass transfer resistance between the aqueous and solid phases [17]. However, the steeper increase in the value of the adsorption capacity was observed on increasing the Ni^{2+} concentration to 20 ppm, which was later followed by a gradual and very slow increase at further higher concentrations i.e. 40 ppm. Hence a fixed Ni^{2+} concentration of 20 ppm is selected as optimized initial concentration for further batch adsorption studies.

3.2.2.3. Effect of contact time

In order to determine the equilibration time for maximum uptake of noxious Ni^{2+} , its adsorption at fixed concentration (20 ppm) on activated carbon derived from scrap tire was studied as a function of contact time. The results obtained from Figure 3.6, revealed that irrespective of initial metal ion concentration, the adsorption of Ni^{2+} onto the activated carbon is relatively fast in the starting phase, however it decreases later and finally reaches the equilibrium. This initial rapid adsorption can possibly be attributed to the greater availability of the active sites on the surface of the adsorbent indicating surface diffusion. Later on these active sites become saturated at the equilibrium stage and adsorption proceeds via pore diffusion [18]. Also, it was quite interesting to observe that the equilibrium was resulted within 50 min of contact time, signifying that the adsorbent owns greater adsorption performance with high adsorption kinetics. Initial concentration doesn't affect the equilibrium time and Figure 3.6 depicted the similarity among the shapes of the curves. This also indicates that Ni^{2+} ions form a monolayer on the external surface of the adsorbent and that the adsorbent surface has a fixed number of active sites.

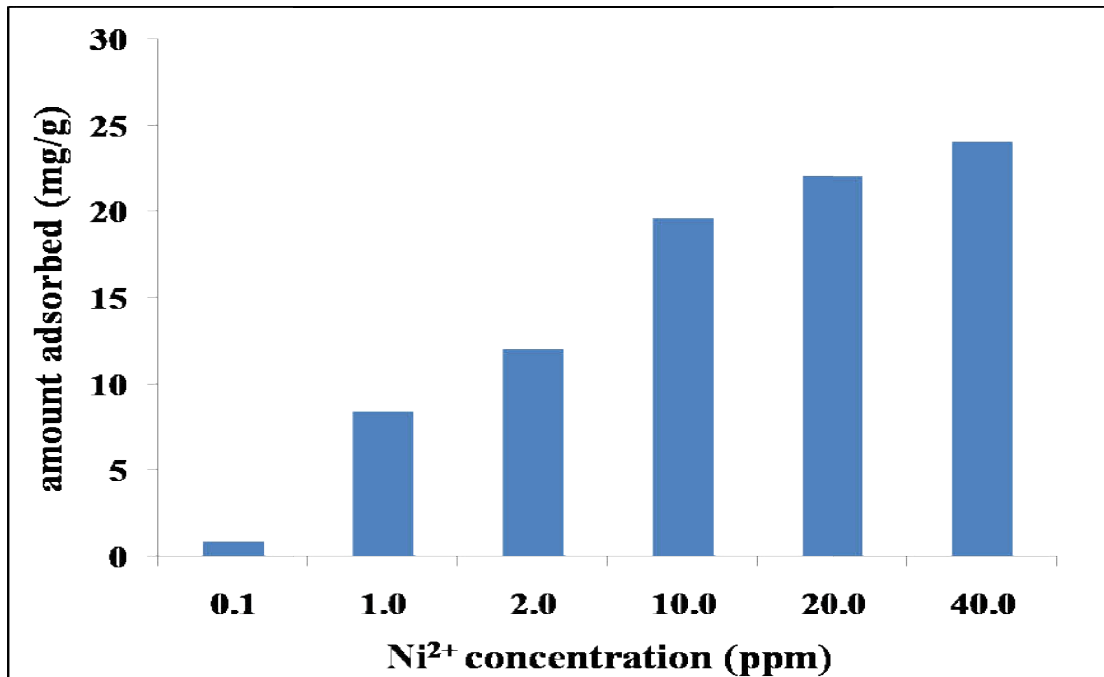


Figure 3.5 Effect of initial Ni²⁺ concentration on the adsorption capacity of activated carbon for Ni²⁺ (fixed contact time of 50 min, adsorbent dose of 0.1 g/L, pH of 7, temperature of 55°C)

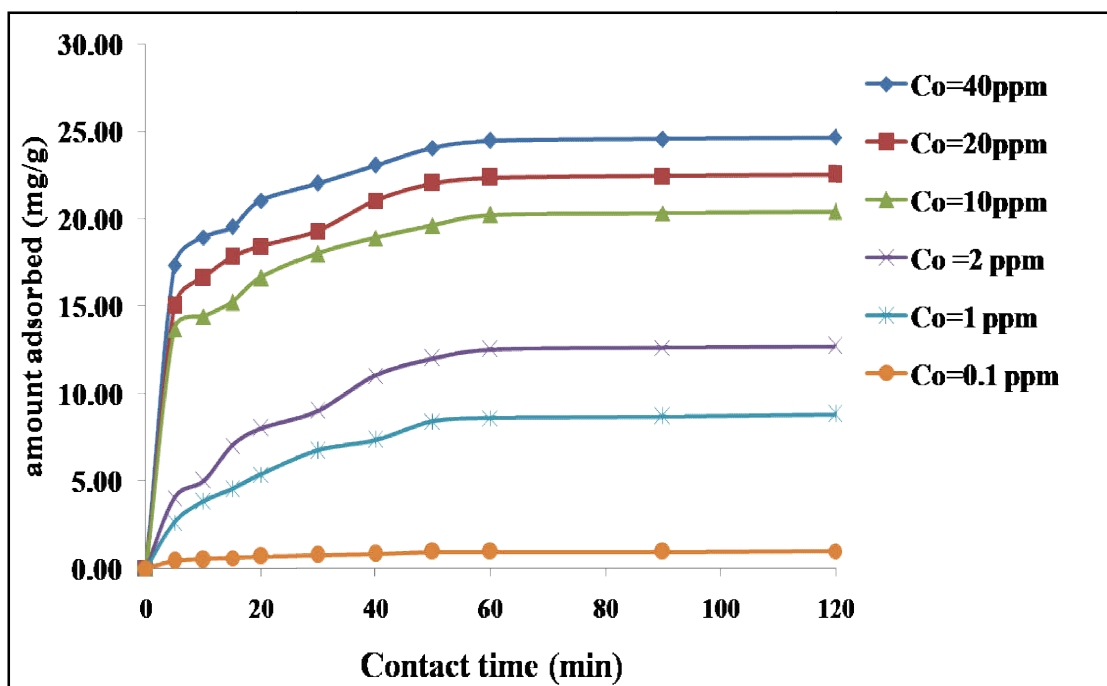


Figure 3.6 Effect of contact time and initial Ni²⁺ concentration on the adsorption capacity of activated carbon for Ni²⁺ (adsorbent dose of 0.1 g/L, pH 7, temperature 55°C)

3.2.2.4. Effect of Adsorbent Dose

The effect of adsorbent dosage was studied by varying the amounts of activated carbon (0.5-4 g/L) at fixed Ni²⁺ concentration of 20 and 0.1 ppm under optimum pH and contact time.

Novel adsorbent for noxious impurities removal

The obtained results at a fixed Ni^{2+} concentration i.e. 20 ppm is presented in Figure 3.7a, the obtained facts revealed that the adsorption capacity decreases continuously with an increase in the adsorbent dosage. The same trend is observed in Figure 3.7b at a fixed Ni^{2+} concentration i.e. 0.1 ppm and fixed contact time i.e. 50 min. Hence from the results observations it is established that lower adsorbent dose results in a higher adsorption capacity. Many researchers [19, 20] have quoted that at a lower adsorbent dose all the active sites present on the developed adsorbent surface are entirely exposed resulting in its faster saturation and a higher q_t value.

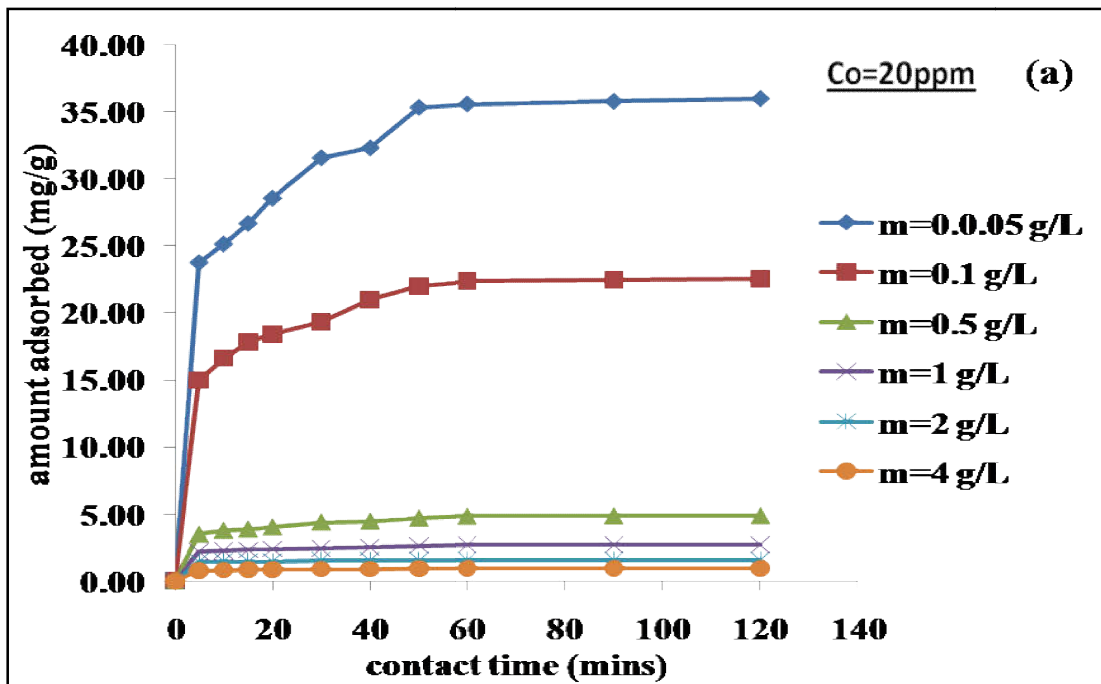


Figure 3.7 (a) Effect of adsorbent dose on the adsorption capacity of activated carbon for Ni^{2+} (Ni^{2+} concentration of 20 ppm, pH 7, temperature 55°C)

But at a higher adsorbent dose, the availability of higher energy sites decreases with a larger fraction of lower energy sites being occupied, resulting in a lower q_t value. While on the other hand it was observed that the removal of Ni^{2+} ions showed an obvious increase up to 0.5 g/L (Figure 3.7c). Further increase in adsorbent dose from 0.5 g/L to 1, 2 and 4 g/L showed a Ni^{2+} ions removal of 96, 97 and 98% respectively. Hence, for achieving $>95\%$ Ni^{2+} ions removal from aqueous solution having a Ni^{2+} ion concentration of 0.1 ppm, a 0.5 g/L adsorbent dose is considered as optimum at a pH of 7, contact time of 50 min and temperature of 55°C .

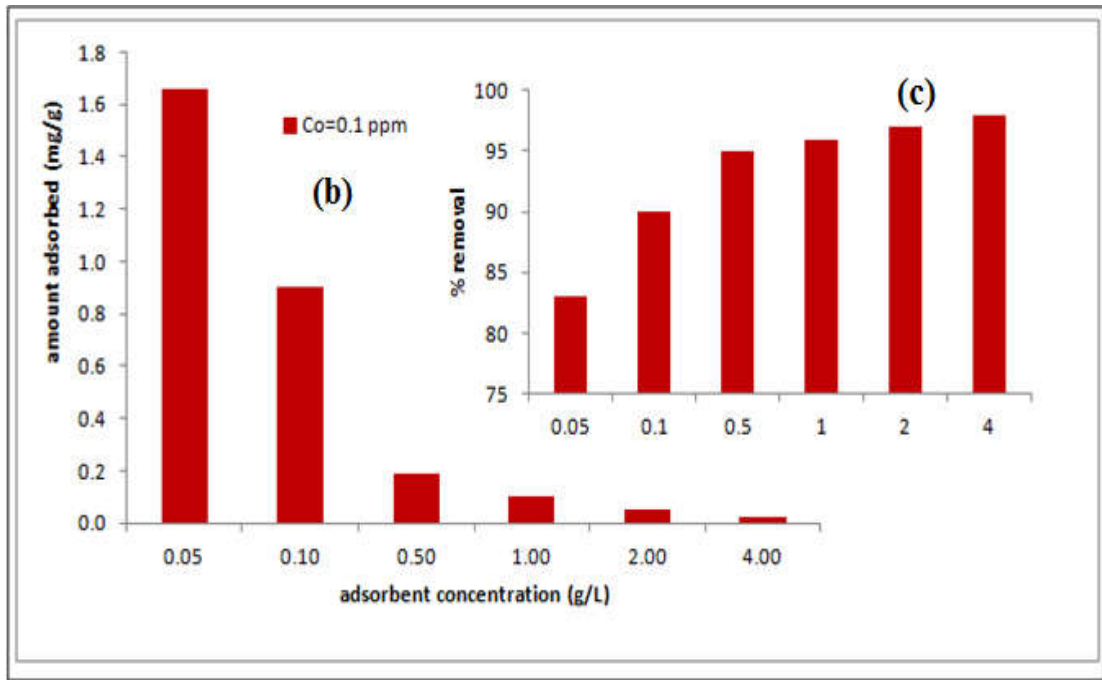


Figure 3.7 (b) Effect of adsorbent dose on the adsorption capacity of activated carbon (Ni²⁺ concentration of 0.1 ppm, pH 7, temperature 55°C); **(c)** Effect of adsorbent dose on % removal of Ni²⁺ (Ni²⁺ concentration of 0.1 ppm, pH 7, temperature 55°C)

3.2.2.5. Adsorption isotherm modelling

To find out the most suitable adsorption model, the isotherm data thus obtained were simulated, by the well known mathematical equations of Langmuir and Freundlich model. The values of regression coefficients obtained from these model's plots were also evaluated, which were used as a fitting criteria to find out suitable model. The results of their linear regression i.e. correlation coefficients and the parameters obtained from the plots of Langmuir ($1/q_e$ vs $1/C_e$), Freundlich ($\log q_e$ versus $\log C_e$) are listed Table 3.2.

Results obtained from Figure 3.8a and 3.8b and Table 3.2 clearly reveals that the correlation coefficients (R^2) at three different temperature i.e. 308, 318, and 328 K for Ni²⁺ are higher than 0.99, indicating the applicability of the Langmuir model with the metal ions getting adsorbed onto the adsorbent surface to form a monolayer. The value q_m was 19.53, 21.28, and 25.00 mg/g at 35, 45, and 55°C respectively. The b values (L/mg) indicated an ascending series of affinity of metal ions to the adsorbent with increasing temperature as follows: 35°C (3.39) > 45°C (4.05) > 55°C (4.82). Additionally the value of n (Table 3.2) of the Freundlich isotherm model was found to be 3.89 at 35°C, 4.42 at 45°C and 5.29 at 55°C reveals the physical nature of adsorption of Ni²⁺ ions onto the developed activated carbon from scrap tire.

Table 3.2 Langmuir and Freundlich isotherm parameters for adsorption of Ni²⁺ at different temperature on activated carbon prepared from scrap tire

Isotherm parameters	35°C	45°C	55°C
Langmuir isotherm			
q_m (mg/g)	19.53	21.28	25.00
b (L/mg)	3.39	4.05	4.82
R²	0.994	0.997	0.999
Freundlich isotherm			
K_f	7.55	9.77	12.88
N	3.89	4.42	5.29
R²	0.993	0.991	0.991

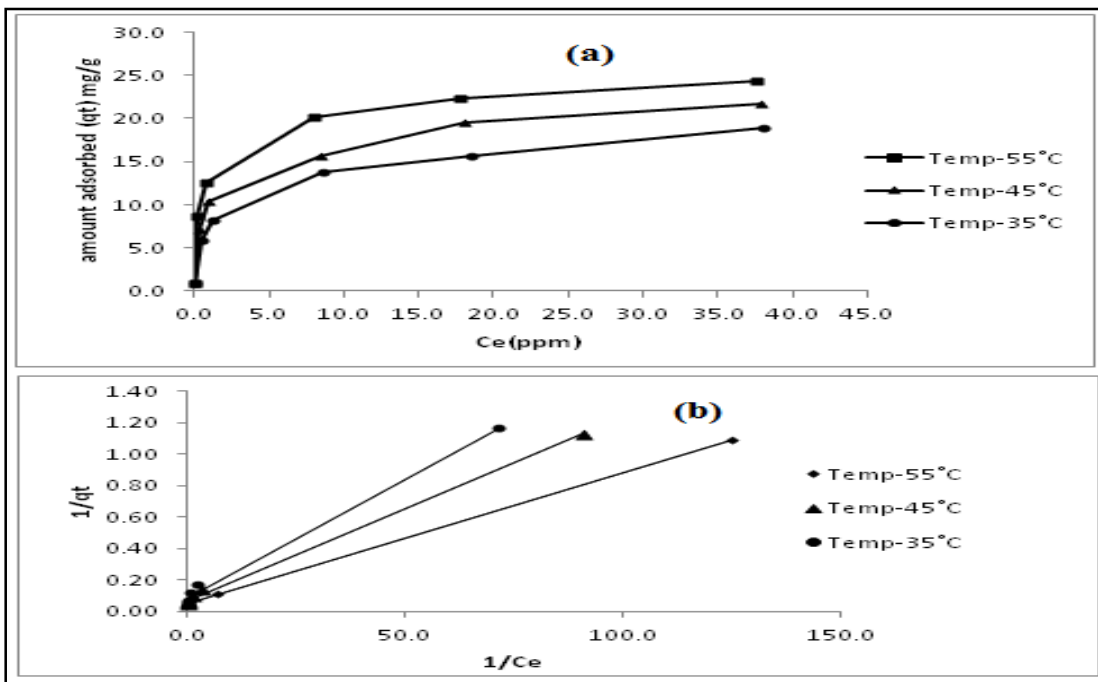


Figure 3.8 (a) Adsorption isotherms at three different temperatures (b) Langmuir model isotherms

3.2.2.6. Thermodynamic study and the effect of temperature

The values of free energy change (ΔG°), enthalpy change (ΔH°) and entropy change (ΔS°) for adsorption process were calculated and are summarized in Table 3.3. The enthalpy change ΔH° in case of activated carbon prepared from the scrap tire is positive (Endothermic) due to increase in adsorption on successive increase of temperature. A possible explanation is that the metal ions in aqueous suspension are well hydrated and will require breaking of the hydration sheath so as to proceed for adsorption. This in turn requires high energy for which a higher temperature is favoured [21]. Further negative ΔG° values dictate the spontaneous nature of the adsorption process in addition to this positive ΔS° reveals the increased randomness at the solid-solution interface during the fixation of Ni²⁺ on the active sites of the adsorbent. As the value of ΔH° (14.768 kJ/mol) indicates that the adsorption process is purely physical rather than physicochemical or chemical, as the heat of physicochemical and chemisorptions adsorption lies in the range of 40-80 kJ/mol and 80-200 kJ/mol respectively.

Table 3.3 Thermodynamic parameters for adsorption of Ni²⁺ at different temperature on activated carbon prepared from scrap tire

Isotherm parameters	308K	318K	328K
Thermodynamic Parameters			
ΔG (kJ/mol)	-3.13	-3.70	-4.29
ΔH (kJ/mol)	14.768		
ΔS (kJ/mol/K)	0.058		

3.2.2.7. Adsorption Kinetics

Two kinetic models namely pseudo-first-order and pseudo-second-order have been applied and were used to test adsorption kinetics data in order to investigate the mechanism involved during the adsorption of Ni²⁺ onto the developed activated carbon adsorbent.

Table 3.4 lists the results of the kinetic parameters of the two models as well as their regression coefficients (R^2) at different concentration ranging from 40 ppm to 0.10 ppm of Ni²⁺ ions. The value of correlation coefficient (R^2) for the pseudo-second-order kinetic model is comparatively high (>0.99), and the adsorption capacities calculated by the model are also close to those values which are obtained experimentally. Figure 3.9 and Figure 3.10 indicates

Novel adsorbent for noxious impurities removal

the linear plots of t/q_t vs. T for Ni^{2+} showing the applicability of the pseudo-second-order model and thus can be concluded to be more suitable to describe the adsorption kinetics of the Ni^{2+} onto the activated carbon prepared from scrap tire.

Table 3.4 Kinetic Parameters for the adsorption of Ni^{2+} onto activated carbon from scrap tire

Ni^{2+} conc. (ppm)	40	20	10	2	1	0.10
exp q_e (mg/g)	24.60	22.50	20.40	12.70	8.80	0.94
Pseudo First Order						
q_e (mg/g) (theoretical)	22.54	19.50	17.02	13.80	8.91	1.30
k_1 (min ⁻¹)	0.0684	0.0682	0.0670	0.0580	0.0539	0.0518
R^2	0.991	0.989	0.989	0.956	0.956	0.956
Pseudo Second Order						
q_e (mg/g) (theoretical)	25.45	23.47	21.28	13.33	10.20	1.035
k_2 (g/mg/min)	0.0024	0.0024	0.0025	0.0019	0.0036	0.092
R^2	0.999	0.999	0.999	0.993	0.994	0.997

3.2.2.8. Mechanism of the adsorption process

Prediction of the rate- limiting step is an important factor to be considered in the adsorption process. For solid-liquid adsorption process, the solute transfer process is usually characterized by either external mass transfer (boundary layer diffusion) or intraparticle diffusion or both. In the present study, intraparticle diffusion plot of q_t vs. $t^{0.5}$ (Figure 3.11) were plotted for Ni^{2+} . From Figure 3.11, the adsorption process tends to be followed by three phases the first phase was quite sharp and it is finished under 50 min therefore indicating the instantaneous mass transfer of the adsorbate molecules from aqueous phase to the activated carbon surface; also the second linear phase was the gradual adsorption stage signifying the rate limiting step being the intraparticle diffusion of the dye molecules and in the end the third phase shows the final equilibrium stage signifying the saturation of the carbon surface and also the presence of very low adsorbate concentration in aqueous solution.

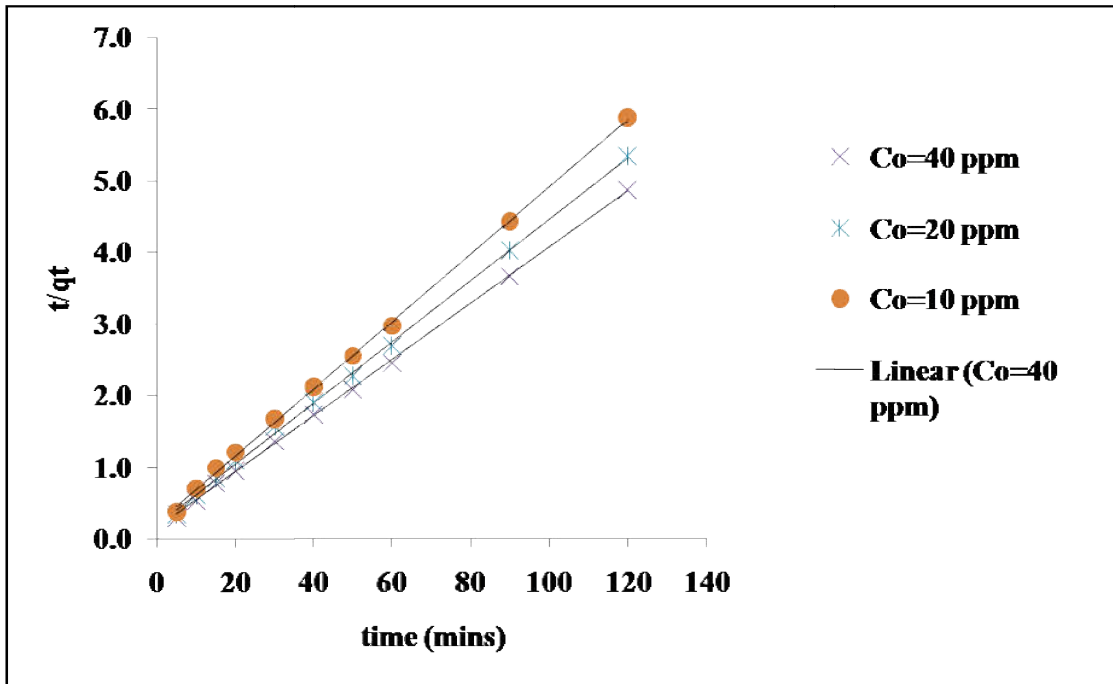


Figure 3.9 Pseudo-second order plots for the adsorption of Ni²⁺ onto the activated carbon at various concentrations ranging from 10 ppm to 40 ppm

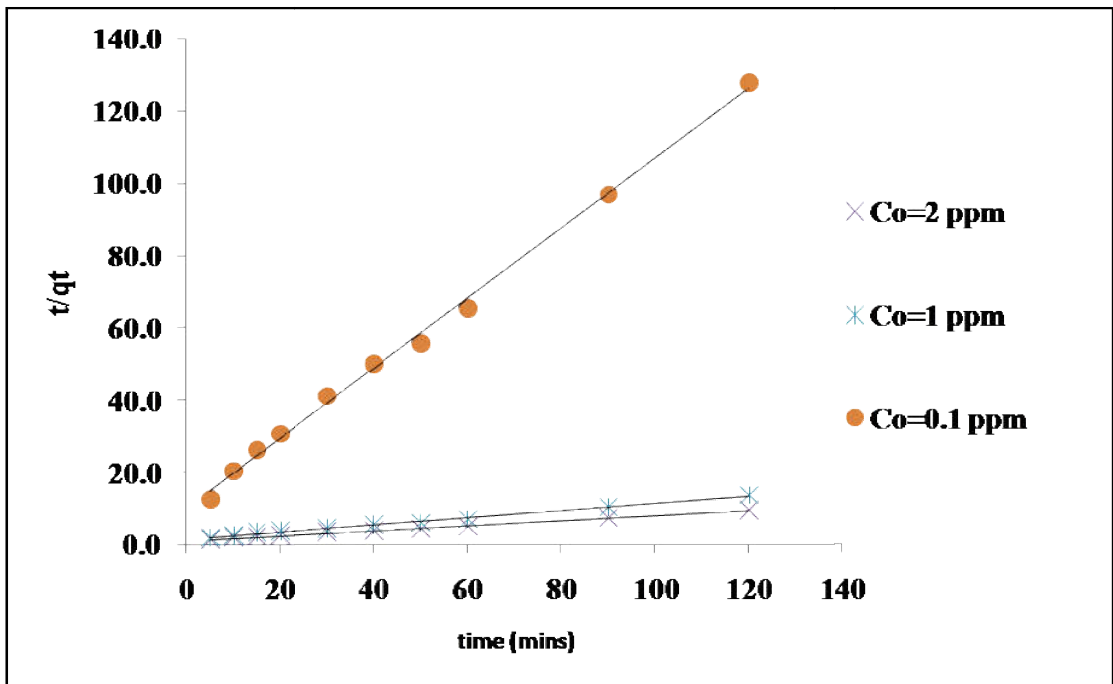


Figure 3.10 Pseudo-second order plots for the adsorption of Ni²⁺ onto the activated carbon at various concentrations ranging from 0.1 ppm to 2 ppm

Again, as evident from Figure 3.11 and Table 3.5 at low adsorbate concentration of 0.1 ppm, the intra particle diffusion rate as well as the thickness of the boundary layer was very

Novel adsorbent for noxious impurities removal

low as indicated by the slope and intercept of the second region. On increasing the adsorbate concentration to 2 ppm there is a simultaneous steep increase in the slope and intercepts thereby signifying an enhancement of the driving force for the adsorption process as well as the increase in the thickness of the boundary layer. But further increase in the Ni^{2+} concentration to 40 ppm showed a gradual increase in the slope and intercept. But none of the linear plots of the second and third region passed through the origin. The deviation from the origin however can be due to the difference in the rate of mass transfer in the initial and final stages of adsorption. This further indicates the interplay of film and particle diffusion during the transport of Ni^{2+} from aqueous phase to the solid phase and that the intraparticle diffusion is not only the rate-limiting step.

Table 3.5 Intraparticle diffusion model parameters for the adsorption of Ni^{2+} onto activated carbon from scrap tire

Ni^{2+} conc. (ppm)	40	20	10	2	1	0.10
exp q_e (mg/g)	24.60	22.50	20.40	12.70	8.80	0.94
Intraparticle diffusion						
k_i (mg/g/min ^{1/2})	1.39	1.36	1.31	1.25	1.19	0.10
C	14.44	12.08	10.52	0.184	0.155	0.126
R ²	0.99	0.99	0.985	0.988	0.990	0.996

3.2.2.9. Testing under industry effluent simulation condition

The prime objective of the adsorption technology using the activated carbon prepared from scrap tire as adsorbent is removal of Ni^{2+} from the industrial and real wastewater that often contains several metal ions simultaneously. Metal fabricated industrial wastewater was collected from Roorkee city and analyzed as per standard methods [22]. The wastewater revealed the presence of Ni^{2+} ions which were present to the tune of 4.16 ppm. Besides, other metal ions present were chromium (1.05 ppm), cadmium (0.30 ppm) and zinc (6.66 ppm). The waste effluent had an alkaline pH of 9.8. The discharge standards as recommended by WHO and EPA are very stringent and require that a limit of 0.1 ppm be met for chromium, 0.01 ppm for cadmium, 0.2 ppm for nickel and 1 ppm for zinc.

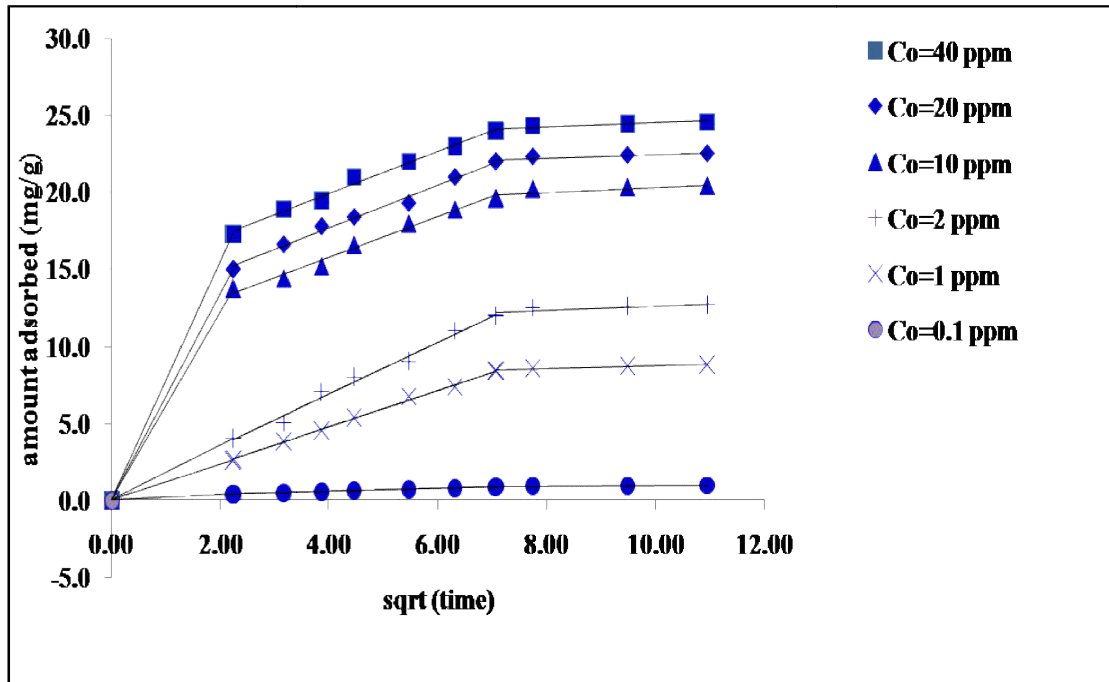


Figure 3.11 Weber Morris plots at varying initial Ni²⁺ concentration

Under such conditions, the practical application of the developed adsorbent was tested by undertaking batch adsorption experiments as stated earlier under optimum conditions of pH and contact time. Results reveal (Table 3.6) that not only 95 % of Ni²⁺ ions were removed, but also other toxic metal ions present were removed to a significant extent as a result of treatment with the developed adsorbent.

Table 3.6 Testing of activated carbon from scrap tyre under metal fabricating industrial waste effluent condition

	pH	Ni ²⁺ Ppm	Zn ²⁺ ppm	Cr ⁶⁺ Ppm	Cd ²⁺ ppm
Quality of waste water before treatment	9.8	4.16	6.66	1.05	0.30
Maximum discharge limit	6-9	0.20	1.0	0.10	0.01
Quality of waste water after treatment	7.00	0.17	0.82	0.08	0.009
% metal ions removal		95.9	87.7	92.3	97.0

3.2.2.10. Comparison with other reported adsorbents

The adsorption capacity (values of Q_{\max} derived from the Langmuir equation) of Ni^{2+} adsorption on activated carbon with other previously developed adsorbents, is summarized in **Table 3.7**. The obtained summarized data clearly revealed that the developed activated carbon from scrap tire possess higher adsorption capacity in comparison to the other previously developed adsorbent [4].

Table 3.7 Comparison of maximum adsorption capacity for the removal of noxious Ni^{2+} by different previously developed adsorbents.

Adsorbent	Metal ion	Adsorption capacity (mg g^{-1})	Ref.
Calcined phosphate	Ni^{2+}	15.53	[4]
Red mud	Ni^{2+}	13.69	[4]
Clarified sludge	Ni^{2+}	14.3	[4]
Activated carbon prepared from scrap tire	Ni^{2+}	25.00	[Present Study]

3.3. Conclusion

This study was focused on assessing the adsorptive capacity of activated carbon prepared by physico-chemical treatment of scrap tire pyrolytic carbon for removal of noxious Ni^{2+} from a real industrial waste effluent which is fabricated with metal. The following conclusions are bulletined:

1. The carbonaceous activated carbon revealed porous topological features and favorable surface chemistry for adsorption of cationic metal ions.
2. The optimum levels for maximizing the efficiency were revealed by the batch adsorption studies.
3. Results obtained revealed that a 0.5 g/L adsorbent dose was found to be optimum at a pH of 7, contact time of 50 min and temperature of 55°C for achieving $\geq 95\%$ Ni^{2+} removal from synthetic solution. Similar performance of the developed adsorbent was found for Ni^{2+} from a industrial wastewater fabricated with metal

4. The adsorption equilibrium data was well fitted and found to be in good agreement with Langmuir isotherm model; so it benefitted in the marking of the basic mechanism of adsorption process.
5. Kinetic modelling revealed the applicability of the pseudo-second-order model and intra particle diffusion to be more suitable to describe the adsorbate-adsorbent system.
6. Endothermic nature and feasibility of the developed system was depicted by thermodynamic studies.
7. Summarily, the developed adsorbent i.e. activated carbon prepared from scrap tire has the potential for removal of Ni²⁺ from wastewater to a significant extent ($\geq 95\%$).

References

- [1] Akhtar N., Iqbal J., Iqbal M., “Removal and recovery of nickel (II) from aqueous solution by loofa sponge-immobilized biomass of *Chlorella sorokiniana*: characterization studies”, *J. Hazard. Mater. B*, 108, (2004), 85–94.
- [2] Beliles R.P., The lesser metals, in: F.W. Oehme (Ed.), “Toxicity of Heavy Metals in the Environment”, Part 2, Marcel Dekker, New York, (1978), 547–616.
- [3] Farooq U., Kozinski J.A., Khan M.A., Athar M., “Biosorption of heavy metal ions using wheat based biosorbents – a review of the recent literature”, *Bioresour. Technol.*, 101, (2010), 5043–5053.
- [4] Hannachi Y., Shapovalov N.A., Hannachi A., “Adsorption of nickel from aqueous solution by the use of low-cost adsorbents”, *Korean J. Chem. Eng.*, 27, (2010), 152–158.
- [5] WHO, “Guidelines for Drinking Water Quality”, Health Criteria and Other Supporting Information, *WHO, Geneva*, (1996), 973.
- [6] Arief V.O., Trilestari K., Sunarso J., Indraswati N., Ismadji S., “Recent progress on biosorption of heavy metals from liquids using low cost biosorbents: characterization, biosorption parameters and mechanism studies”, *Clean Soil Air Water*, 36, (2008), 937–962.
- [7] Kurniawan T.A., Chan G.Y.S., Lo W.H., Babel S., “Comparisons of low-cost adsorbents for treating wastewaters laden with heavy metals”, *Sci. Total Environ.*, 366, (2006), 409–426.
- [8] Ceribasi H.I., Yetis U., “Biosorption of Ni (II) and Pb (II) by Phanerochaete Chrysosporium from a binary metal system-kinetics”, *Water SA*, 27, (2001), 15-20.
- [9] Kwon J.S., Yun S.T., Lee J.H., Kim S.O., Jo H.Y., “Removal of divalent heavy metals (Cd, Cu, Pb, and Zn) and arsenic (III) from aqueous solutions using scoria: kinetics and equilibria of sorption”, *J. Hazard. Mater.*, 174, (2010), 307–313
- [10] Nuhoglu Y., Malkoc E., “Thermodynamic and kinetic studies for environmentally friendly Ni(II) biosorption using waste pomace of olive oil factory”, *Bioresour. Technol.*, 100, (2009), 2375–2380.
- [11] Gupta V.K., Rastogi A., Nayak A., “Adsorption studies on the removal of hexavalent chromium from aqueous solution using a low cost fertilizer industry waste material”, *J. Colloid Interface Sci.*, 342, (2010), 135-141.

- [12] Wang S., Hu J., Li J., Dong Y., “Influence of pH, soil humic/fulvic acid, ionic strength, foreign ions and addition sequences on adsorption of Pb(II) onto GMZ bentonites”, *J. Hazard. Mat.*, 167, (2009), 44–51.
- [13] Gupta V.K., Rastogi A., Nayak A., "Biosorption of nickel onto treated alga (*Oedogonium hatei*): Application of isotherm and kinetic models”, *J. Colloids Inter. Sci.*, 342, (2010), 533-539.
- [14] Banerjee S.S., Chen D.H., “Fast removal of copper ions by gum arabic modified magnetic nano-adsorbent”, *J. Hazard. Mater.*, 147, (2007), 792–799.
- [15] Yong-Meia H., Mana C., Zhong-Bob H., “Effective removal of Cu(II) ions from aqueous solution by amino-functionalized magnetic nanoparticles”, *J. Hazard. Mater.*, 184, (2010), 392–399.
- [16] Badruddoza, A.Z.M., Tay A.S.H., Tan P.Y., Hidajat K., Uddin M.S., “Carboxymethyl- β -cyclodextrin conjugated magnetic nanoparticles as nano-adsorbents for removal of copper ions: Synthesis and adsorption studies”, *J. Hazard. Mater.*, 185, (2011), 1177–1186.
- [17] Wang S., Boyjoo Y., Choueib A., Zhu Z.H., ‘Removal of dyes from aqueous solution using fly ash and red mud”, *Water Res.*, 39, (2005), 129-138.
- [18] Krishnan K.A., Sreejalekshmi K.G., Baiju R.S., “Nickel(II) adsorption onto biomass based activated carbon obtained from sugarcane bagasse pith”, *Bioresource Tech.* 102, (2011), 10239–10247.
- [19] Kobya M., “Adsorption kinetic and equilibrium studies of Cr(VI) by hazelnut shell activated carbons”, *Adsorpt. Sci. Technol.*, 22, (2004), 51–64.
- [20] Park D., Yun Y.S., Park J.M., “Use of dead fungal biomass for the detoxification of hexavalent chromium: screening and kinetics”, *Process. Biochem.*, 40, (2005), 2559–2565.
- [21] Gupta V.K., Nayak A., “Cadmium removal and recovery from aqueous solutions by novel adsorbents prepared from orange peel and Fe₂O₃ nanoparticles”, *Chem. Eng. J.*, 180, (2012), 81–90.
- [22] APHA Standard Methods for the Examination of Water and Wastewater, 20th edition, APHA, AWWA and WEF, Washington, DC; 1998



CHAPTER 4

Alumina Composite Modified Rubber Tire For Removal of Arsenic



4.1. Introduction

Arsenic is well known naturally occurring steel grey metalloid. It is generally present in two forms i.e. inorganic and organic arsenic. Arsenic combined with elements such as oxygen, chlorine and sulfur is referred to as inorganic arsenic and arsenic combined with carbon and hydrogen is referred to as organic arsenic. Organic forms of arsenic are less harmful than the inorganic form. Arsenic beyond the safe limit possesses severe detrimental and hazardous effect on the human health and hence, excess level of arsenic in drinking water is now a day's great concern of environmental pollution problem [1]. Arsenic enters the ecosystem through a combination of natural processes and anthropogenic activities. Dissolved arsenic reaches the ground water primarily due to soil leaching [2]. The United States Environmental Protection Agency [3] has decreased the old standard of 50ppb to a new arsenic standard of 10ppb as the maximum permissible limit for drinking water.

Arsenic is generally found as trivalent arsenite or pentavalent arsenate form in the aqueous solution. In surface water under oxidizing conditions, arsenate predominates while arsenite becomes stable in anaerobic water under reducing conditions [4]. As(V) is less hazardous and mobile than As(III) [5]. Several traditional techniques like Ion exchange, reverse osmosis, adsorption, coagulation, precipitation, adsorption-coprecipitation with hydrolyzing metals are used as efficient methods for removal of toxic metal ions from water but among them, adsorption appears to have the best potential for overall treatment, and it can be expected to be useful for a wide range of compounds [6]. Several adsorbents [7-23] are used for the arsenic removal from the aqueous solutions but the removal and adsorption caused by these are not efficient as well as expensive. Therefore a keen attention and serious effort is required to generate the more efficient and low cost adsorbent so that the rapid removal and fast adsorption of noxious arsenic from the aqueous solution will take place.

A composite of activated carbon and alumina may be used as an effective adsorbent for the removal of different types of water pollutants. To the best of our knowledge, activated carbon obtained from waste tire rubber festooned with alumina is not reported yet, in the present study we focused on the development of low cost waste tire rubber derived activated carbon alumina composite for the rapid and active removal of As(III) and As(V) from aqueous solution.

4.2. Results and Discussion

4.2.1. Characterization of adsorbents

The BET surface area, total pore volume, pore size and average pore radius of the adsorbents ACAL11, ACAL12, ACAL21 and TRAL are summarized in Table 4.1. Among the three developed ACAL adsorbents, ACAL11 possesses the highest BET surface area, total pore volume and average pore radius. The pore size data of all four adsorbents reveals that the developed adsorbents are microporous in nature. The N₂ adsorption desorption graph of ACAL11 and TRAL are shown in Figure 4.1.

Table 4.1 The physical properties of adsorbents.

Adsorbent	BET specific surface area (m ² /g)	Total pore volume (cc/g)	Pore size (nm)	Average pore radius (nm)
ACAL11	147.35	0.0648	< 0.97	1.84
ACAL12	100.39	0.0394	< 0.91	1.55
ACAL21	139.94	0.0543	< 0.90	1.51
TRAL	175.68	0.0687	< 1.01	1.29

The XRD pattern of ACAL11 and TRAL are presented in Figure 4.2. These XRD patterns confirm that the developed adsorbents i.e. ACAL11 and TRAL have mixed crystalline and

amorphous nature. The XRD result of ACAL11 possesses some weak peaks of alumina and carbon while that of TRAL shows weak peaks of γ -alumina only.

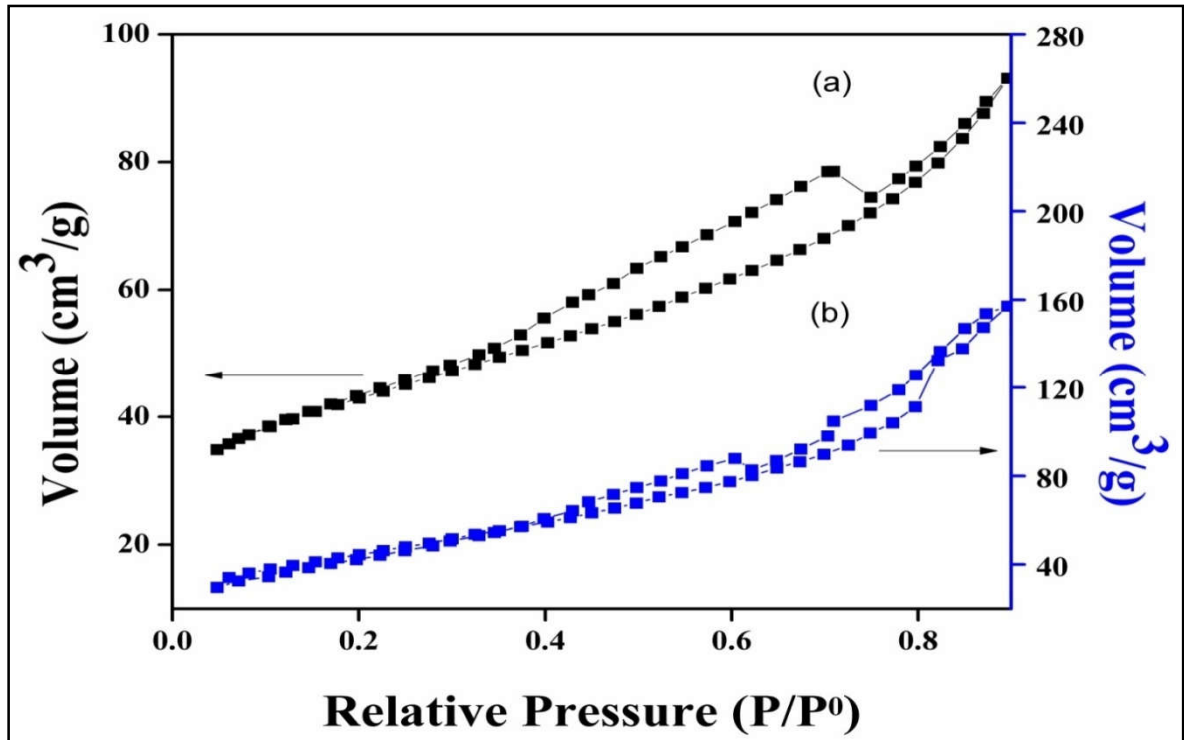


Figure 4.1 Nitrogen adsorption-desorption isotherms of (a) ACAL11 and (b) TRAL

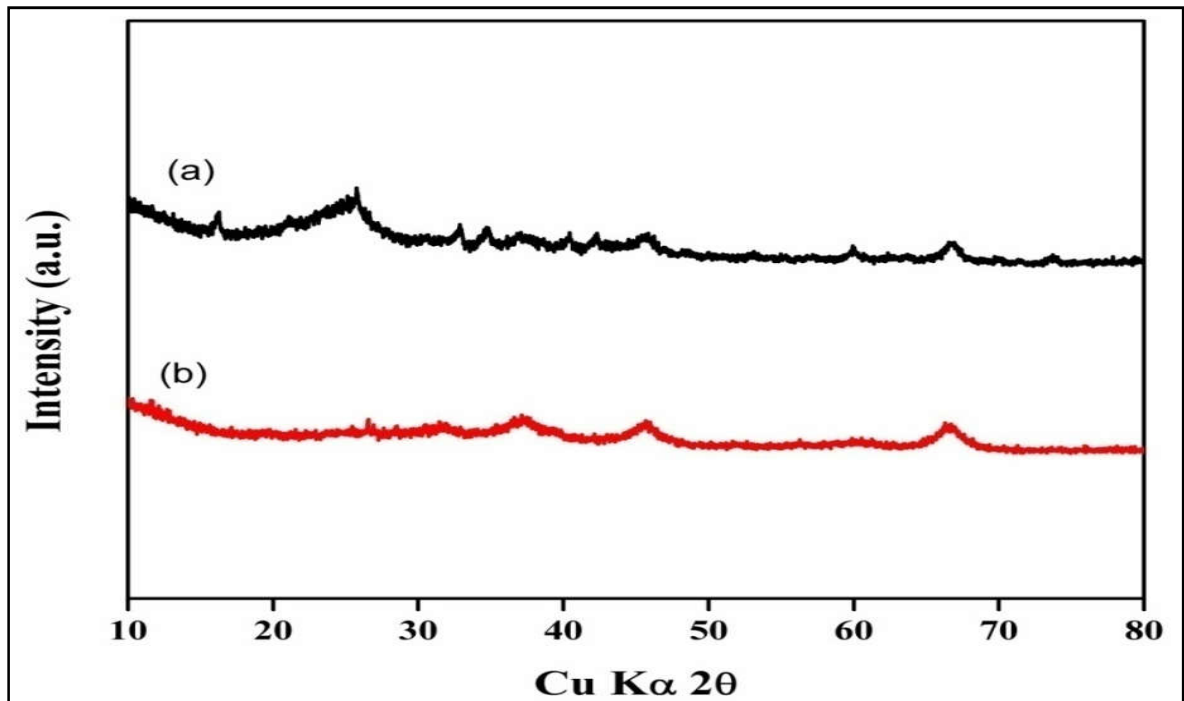


Figure 4.2 X-ray diffraction patterns of (a) ACAL11 and (b) TRAL

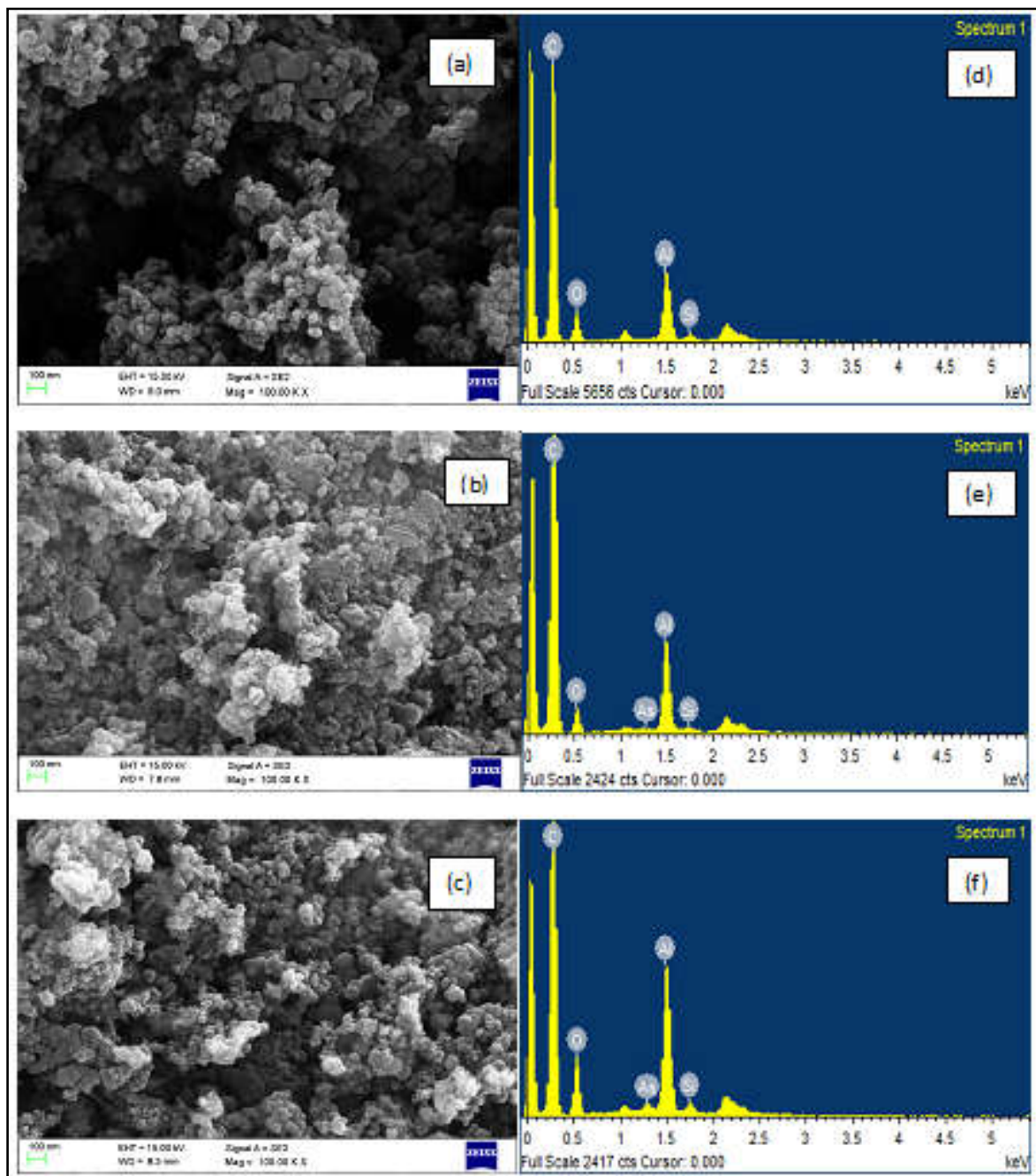


Figure 4.3 FE-SEM images of (a) ACAL11, (b) ACAL11 after As(III) adsorption, (c) ACAL11 after As(V) adsorption and (d,e,f) corresponding EDX spectra.

The FE-SEM images and corresponding EDX spectrum of the adsorbents ACAL11 and TRAL before and after adsorption of As(III) and As(V) are presented in Figure 4.3 and Figure 4.4 respectively.

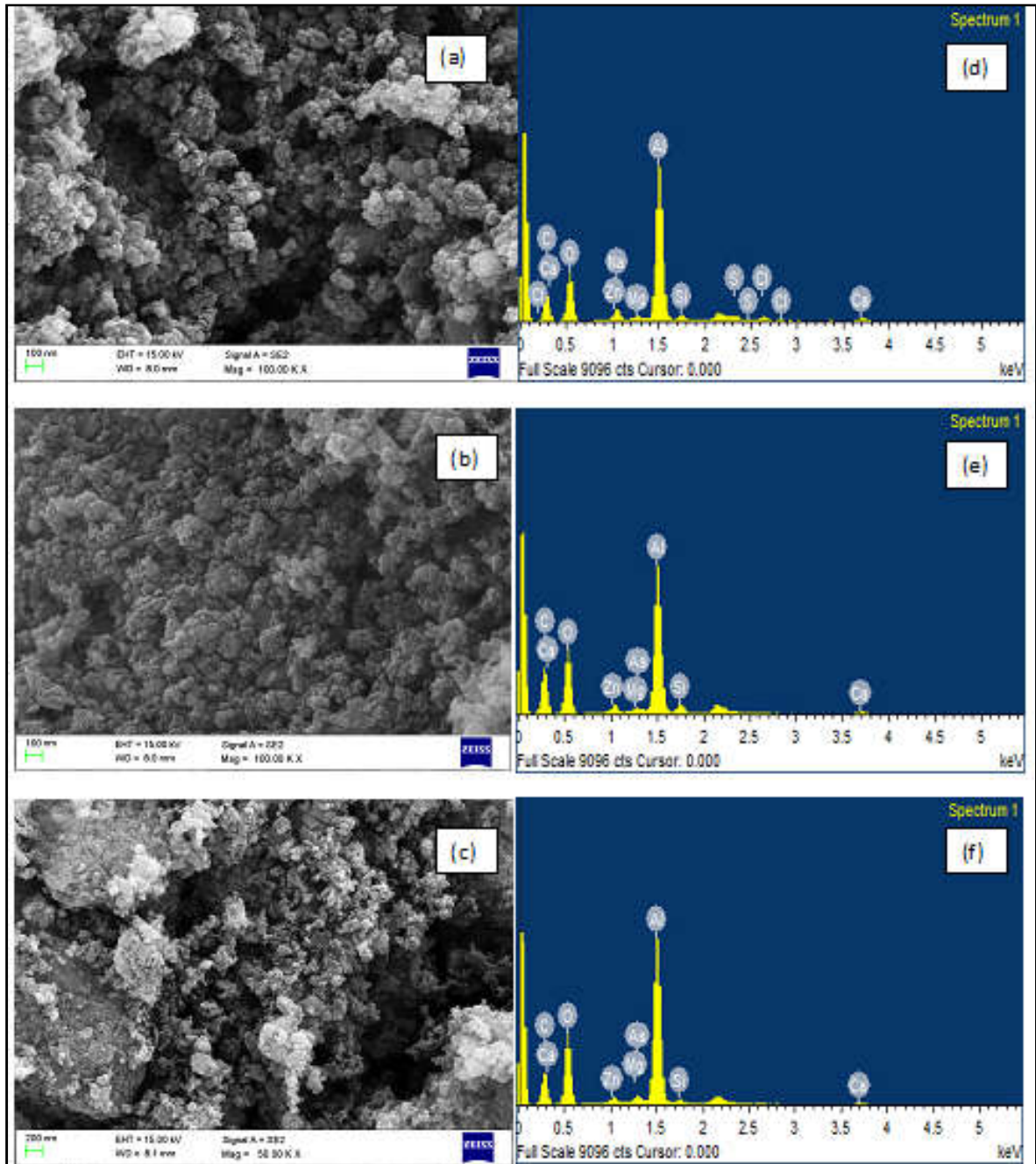


Figure 4.4 FE-SEM images of (a) TRAL, (b) TRAL after As(III) adsorption, (c) TRAL after As(V) adsorption and (d, e, f) corresponding EDX spectra.

The FE-SEM images of the developed adsorbents are presented in Figure 4.3(a) and Figure 4.4(a), the obtained results reveal the heterogeneous and porous topology of the surface. The surface morphology of the adsorbents was changed after adsorption of As(III) and As(V).

The EDX spectrum of TRAL in Figure 4.4(d) shows the presence of elements C, O, Al as the major elements along with other elements Si, Na, Zn, Mg, Ca, Cl and S while that of ACAL11 in Figure 4.3(d) shows presence of only C, O, Al and Si. The extra elements present in TRAL are derived from the raw tire rubber used in its preparation. The EDX spectra of both ACAL11 and TRAL after adsorption of As(III) and As(V) show peak of As which are shown in Figure 4.3 (e) and (f) and Figure 4.4 (e) and (f) respectively. The elements Na, Cl and S present in TRAL are disappeared after adsorption of As(III) and As(V). These elements may be leached to the adsorbate solution during adsorption process.

The FT-IR spectrum of HCl treated pyrolytic char of waste tire rubber, namely AC-HCl, in Figure 4.5(a) shows the prominent peaks of -OH group at 3388.36 cm^{-1} , C-C stretch in ring at 1560.15 cm^{-1} and 1398.16 cm^{-1} , C-O-C stretch at 1268.95 cm^{-1} , C-O stretch at 1103.10 cm^{-1} and alkyne hydrocarbon C-H bending at 642.18 cm^{-1} . There is distinct difference in peak size of the -OH group of AC-HCl with that of ACAL11 and TRAL as shown in Figure 4.5(b) and Figure 4.5(c). The broad peak of ACAL at 3428.86 cm^{-1} and that of TRAL at 3432.72 cm^{-1} can be attributed to hydrogen bonded -OH stretching vibration on the alumina surface. The appearance of small peak at 1635.36 cm^{-1} in ACAL11 and 1637.29 cm^{-1} in TRAL correspond to presence of Al-OH stretching bond. The difference in region at $600\text{-}700\text{ cm}^{-1}$ of ACAL11 and TRAL with that of AC-HCl is due to Al-O stretching vibration of alumina [24]. Remaining other peaks of AC-HCl is also slightly shifted in the alumina composites.

4.2.2. Preliminary batch experiment

Results of the preliminary batch experiment carried out for As(III) adsorption on ACAL11, ACAL21 and ACAL12 are summarized in Table 4.2. It shows ACAL21 has the lowest adsorptive capacity towards As(III) adsorption while ACAL11 and ACAL12 have nearly equal capacity. The aim of this study is to develop good adsorbent using waste tire rubber. Furthermore, BET surface area, pore volume and pore size of ACAL11 are also greater than that of ACAL21 and ACAL12. Hence, ACAL11 was chosen for further experiments.

4.2.2.1. Effect of initial pH

Arsenate species exist in aqueous phase as H_3AsO_4 at pH less than 2.2, H_2AsO_4^- at pH between 2.2 and 6.98, HAsO_4^{2-} at pH between 6.98 and 11.5 and AsO_4^{3-} at pH above 11.5 [2]

while Arsenite species exist as neutral H_3AsO_3 at pH range between 1 and 9 and AsO_2^- at pH higher than 9 [25].

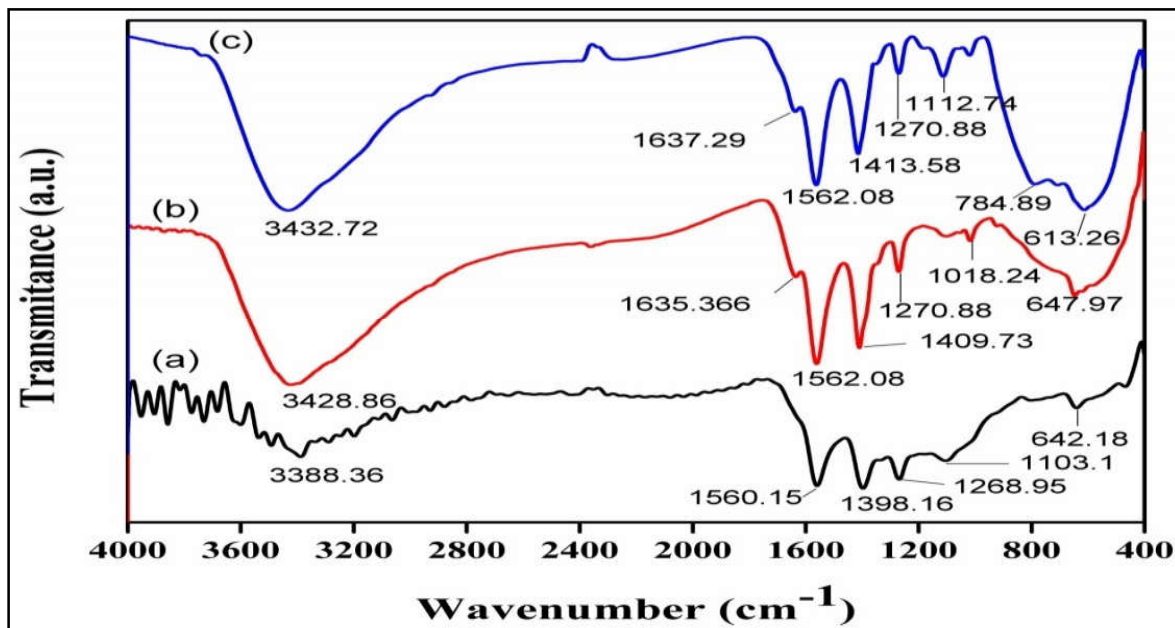


Figure 4.5 FTIR spectra of (a) AC-HCl, (b) ACAL11 and (c) TRAL

Table 4.2 Result of preliminary batch experiment

Adsorbent	Q_e for different initial As(III) concentration (mg/g)			
	20mg/L	30mg/L	40mg/L	100mg/L
ACAL11	2.52	3.60	4.21	8.95
ACAL12	1.34	2.18	2.98	6.78
ACAL21	2.49	3.54	4.29	9.10

Adsorption process is highly influenced by the surface charge density of the adsorbent. The pH_{pzc} of ACAL11 and TRAL were found to be 3.98 and 3.89 respectively which was shown in Figure 4.6. It was found that the adsorption of As(V) is more favorable at lower pH where surface of the adsorbent is positively charged. The arsenic adsorption as a function of initial pH of solution is shown in Figure 4.7. It reveals that the optimized pH for the removal of As(V) using ACAL11 as well as TRAL was 3.

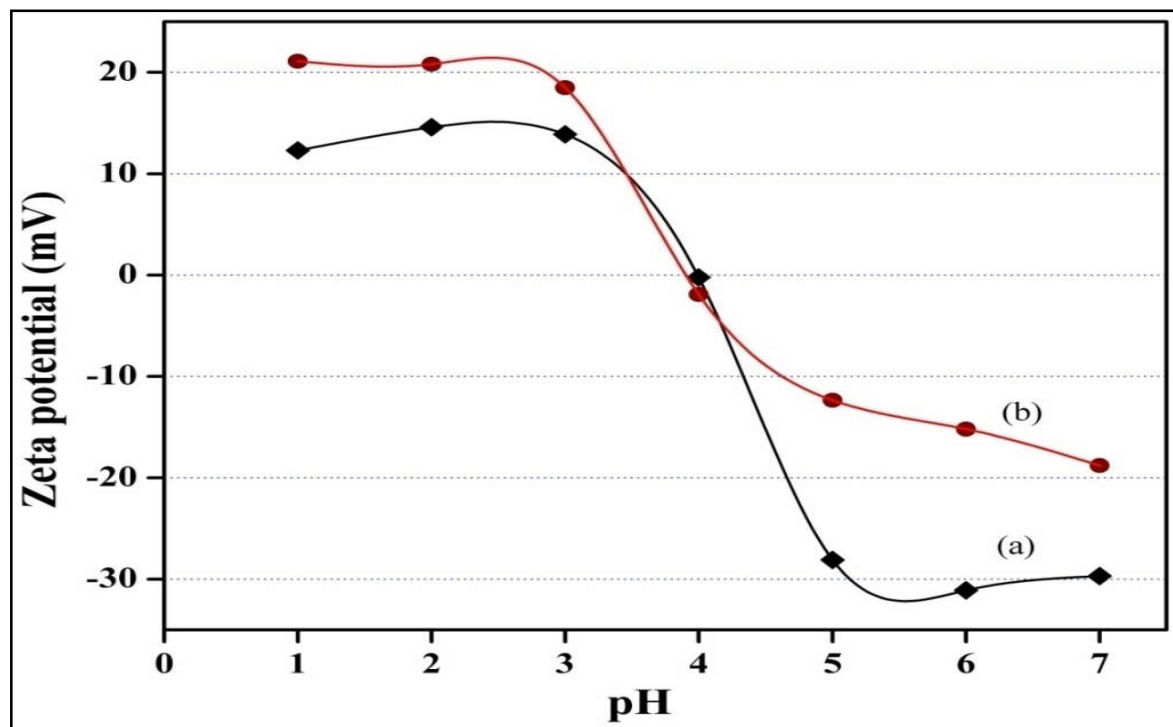


Figure 4.6 Determination of pH_{pzc} of (a) ACAL11 and (b) TRAL.

On the other hand removal of As(III) from both ACAL11 and TRAL were found to be favorable in range of pH 6 to 9. At pH greater than 9 As(III) exists in anionic form and its adsorption on the negatively charged surface is unfavorable. Hence, in all the further study, initial pH of As(V) and As(III) solutions were adjusted at pH 3 and 9 respectively.

4.2.2.2. Effect of adsorbent dose

The effect of adsorbent dose on the adsorption of As(III) and As(V) on ACAL11 and TRAL is presented in Figure 4.8, the obtained results revealed that the percentage removal of As(III) on both of the adsorbents increased rapidly with increase in adsorbent dose up to 4g/L, it was later followed by slow increase with increase in adsorbent dose up to 8g/L.

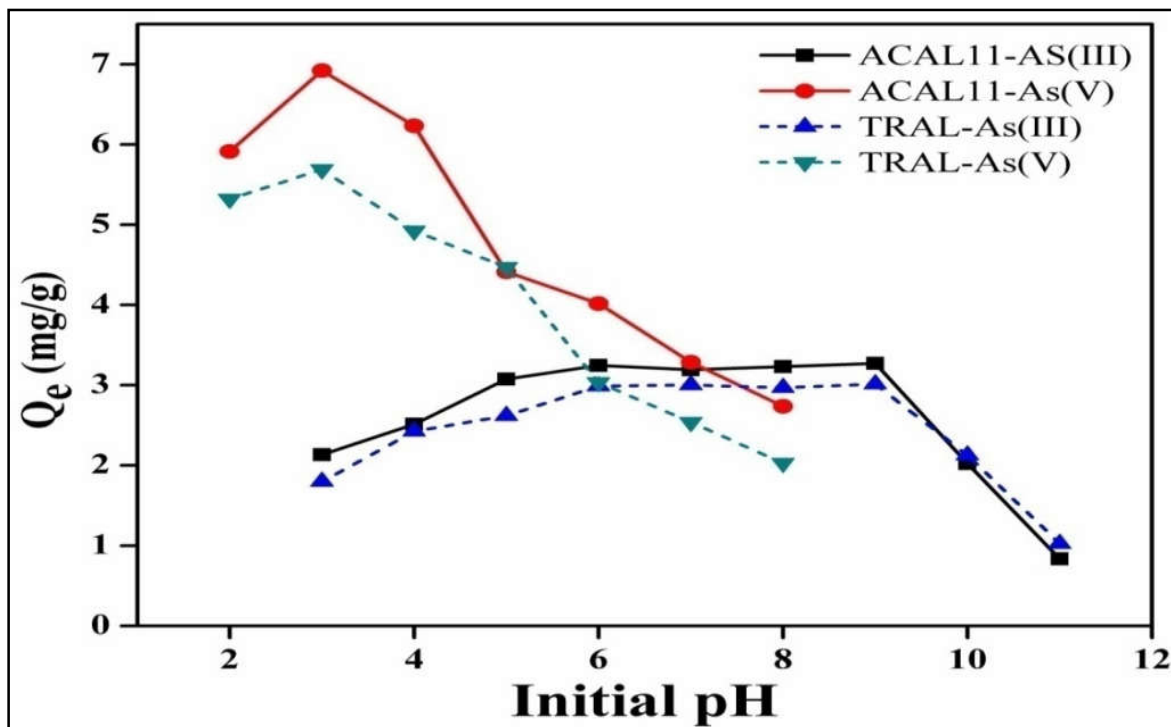


Figure 4.7 Effect of initial pH on arsenic removal at concentration 20mg/L, adsorbent dose 2.0g/L and contact time 8 h

The maximum percentage removal of As(III) by ACAL11 and TRAL were nearly 57% and 52% respectively, while on the other hand, the removal percentage of As(V) increases sharply with the increase in adsorbent dose up to 2g/L for both the adsorbents, which was later followed by slow increase in removal percentage of As(V) with the increase in adsorbent dose.

The maximum percentage removal of As(V) by ACAL11 and TRAL were found to be around 80% and 65% respectively. In addition to this a significant decrease in the adsorptive capacity (Q_e) with increase in adsorbent dose from 1g/L to 8g/L in all cases is observed. Hence, 4g/L and 2g/L were fixed as optimized adsorbent dose for As(III) and As(V) removal respectively using ACAL11 and TRAL.

4.2.2.3. Adsorption Kinetic Study

Kinetic study describes the time required for the adsorbate uptake at the solid–solution interface including the diffusion process to reach equilibrium. The process efficiency of the adsorption is controlled by kinetics and, hence, Lagergren's pseudofirst-order and pseudo

second-order models are applied to investigate kinetic data. The regression analysis of resulted plots was carried out to observe the suitability of any model.

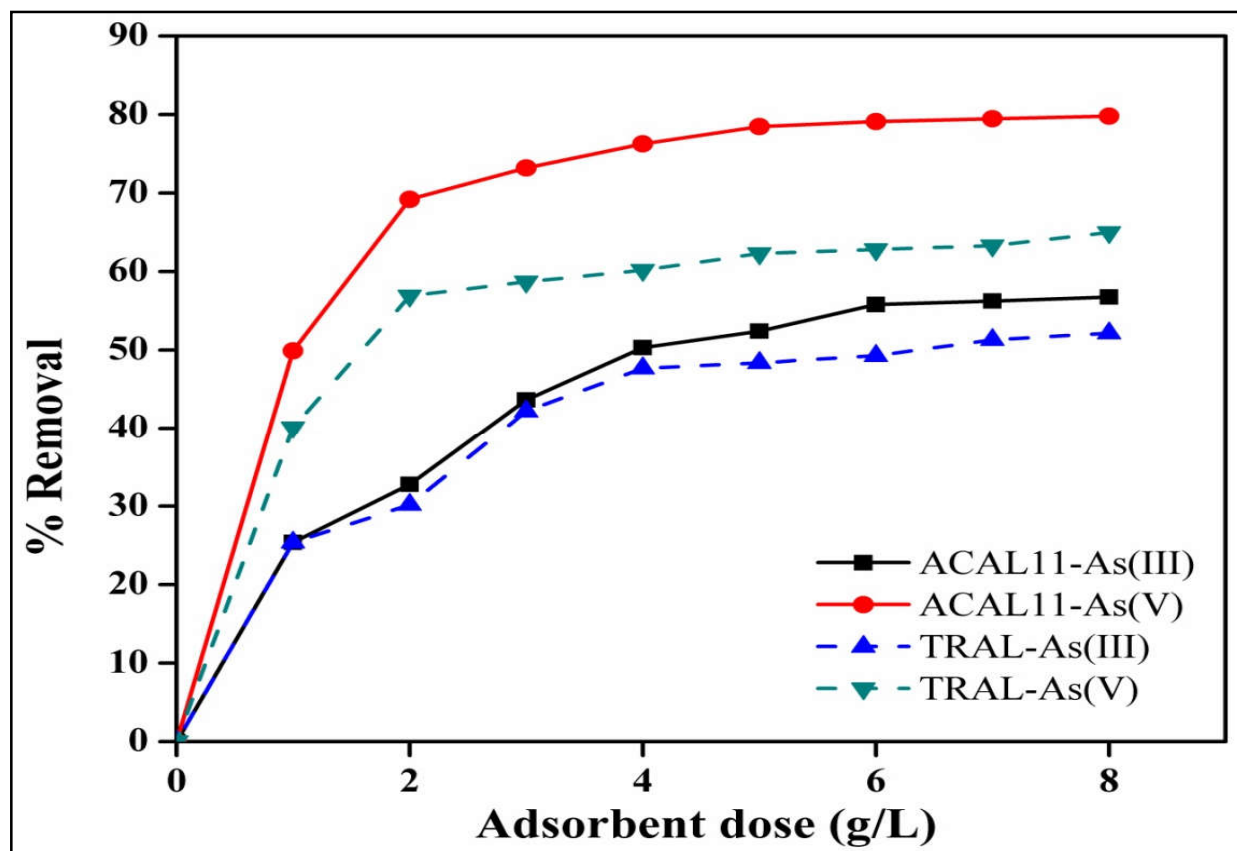


Figure 4.8 Effect of adsorbent dose at initial concentration 20mg/L, pH 9 for As(III) solution, pH 3 for As(V) and contact time 8 h.

The results obtained from Figure 4.9 and Figure 4.10 suggests the applicability of the pseudo-second-order kinetic model. The kinetic parameters obtained from graph are tabulated in Table 4.3. It lists the results of kinetic rate constant studies of pseudo-first order and pseudo second order. The value of correlation coefficient R^2 for the pseudo-second-order kinetic model for both the adsorbents is relatively high (0.999). However the values of R^2 for the pseudo-first-order are not satisfactory. Therefore the entire adsorption kinetics process of As (III) and As(V) on to the developed adsorbent i.e. ACAL11 and TRAL are found to be controlled by pseudo-second-order kinetics with greater coefficient of determination value.

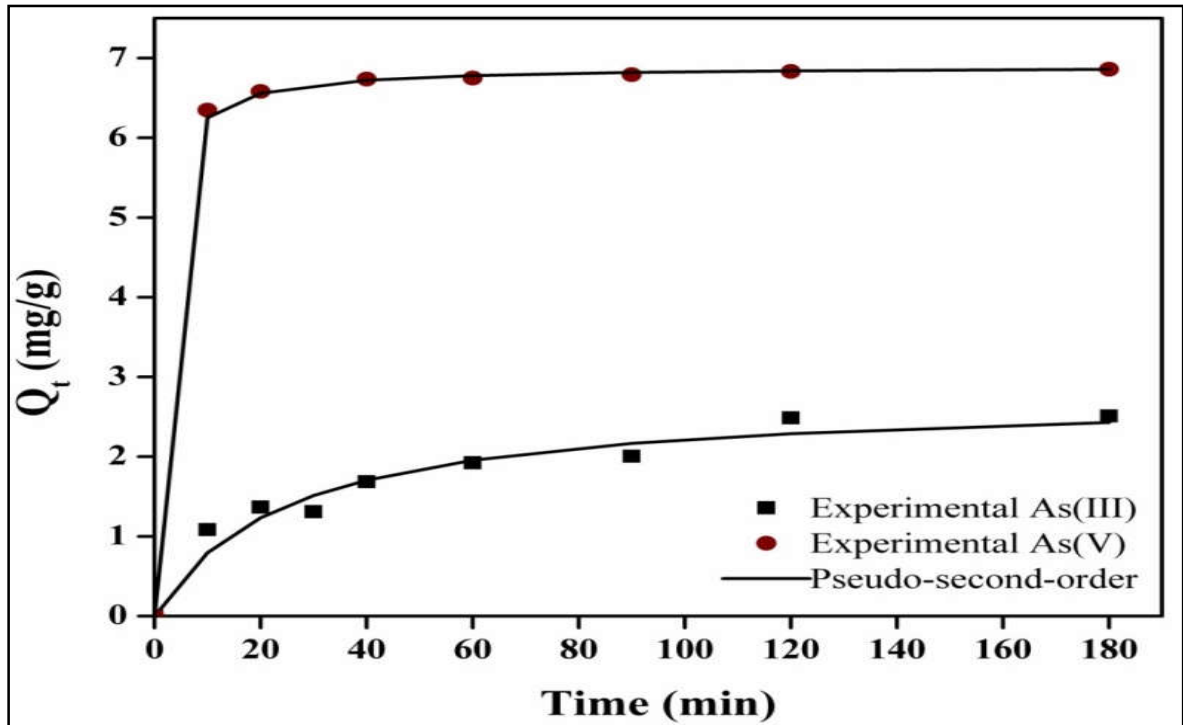


Figure 4.9 Effect of contact time on arsenic removal by ACAL11 at initial concentration 20mg/L, pH 9 for As(III) solution, pH 3 for As(V), adsorbent dose 4g/L for As(III) and 2g/L for As(V).

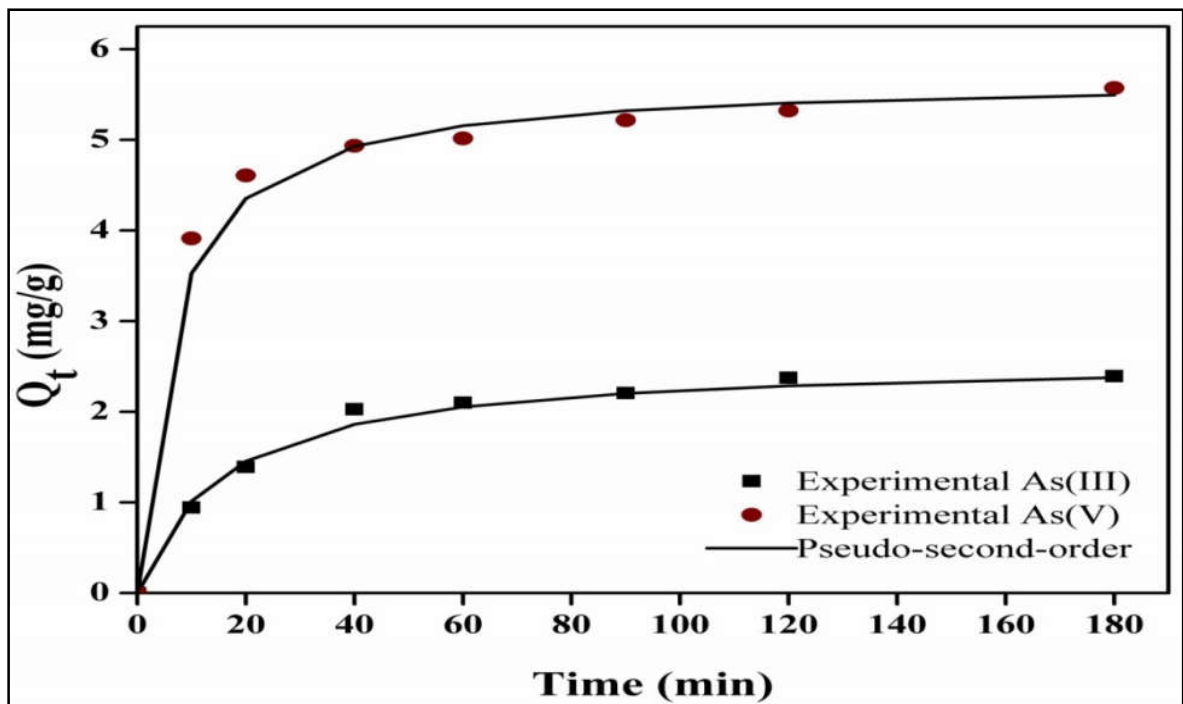


Figure 4.10 Effect of contact time on arsenic removal by TRAL at initial concentration 20mg/L, pH 9 for As(III), pH 3 for As(V), adsorbent dose 4g/L for As(III) and 2g/L for As(V).

Table 4.3 Kinetic parameters of As(III) and As(V) adsorption on ACAL11 and TRAL

Adsorbent	Adsorbate	Pseudo-first-order model			Pseudo-second-order model		
		Q _e (mg/g)	K ₁ (min ⁻¹)	R ²	Q _e (mg/g)	K ₂ (g mg ⁻¹ min ⁻¹)	R ²
ACAL11	As(III)	2.094	2.073x10 ⁻²	0.953	2.762	1.461x10 ⁻²	0.988
	As(V)	5.437	1.381x10 ⁻²	0.913	6.896	1.411x10 ⁻¹	0.999
TRAL	As(III)	2.747	3.915x10 ⁻²	0.960	2.631	2.405x10 ⁻²	0.988
	As(V)	5.820	1.612x10 ⁻²	0.964	5.681	2.884x10 ⁻²	0.999

4.2.2.4. Modelling of Adsorption isotherms

To find out the most suitable adsorption model, the isotherm data thus obtained were simulated, by the well-known mathematical equations of Langmuir and Freundlich. The values of regression coefficients obtained from these model’s plots were also evaluated, which were used as a fitting criteria to find out suitable model. Values of resulting parameters and regression coefficients (R²) are listed in Table 4.4.

The adsorption equilibrium data are generally represented by adsorption isotherms which correspond to the relationship between the amounts of the solute adsorbed per unit mass of adsorbent (Q_e) and the solute concentration in the solution at equilibrium (C_e) as shown in Figure 4.11 and Figure 4.12 (Solid line: Langmuir, Dotted line: Freundlich).

The value correlation coefficient (R²) of Langmuir isotherm model for As(III) on the developed adsorbent i.e. ACAL 11 and TRAL is 0.995 and 0.991 respectively and the value correlation coefficients (R²) of Langmuir isotherm model for As(V) on the developed adsorbent i.e. ACAL 11 and TRAL is 0.996 and 0.998 respectively.

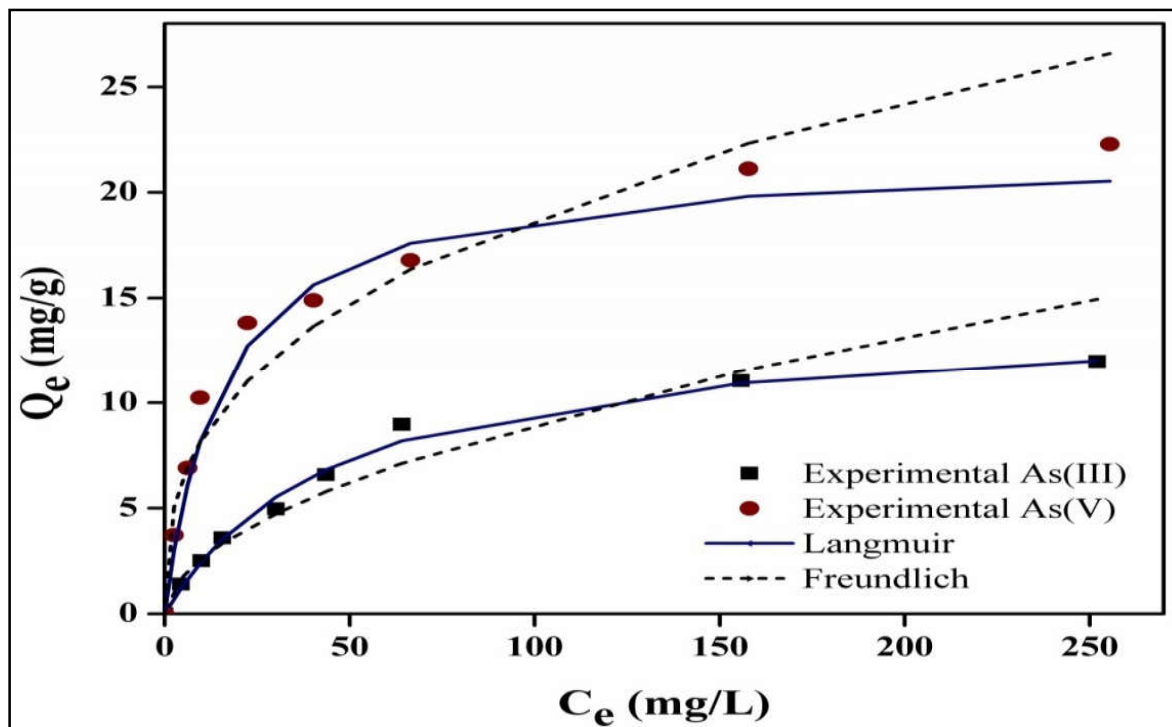


Figure 4.11 Arsenic adsorption model of ACAL11 at pH 9 and adsorbent dose 4 g/L for As(III), and pH 3 and adsorbent dose 2 g/L for As(V), contact time 1 h.

On the other hand the value correlation coefficient (R^2) of Freundlich isotherm model for As (III) on the developed adsorbent i.e. ACAL 11 and TRAL is 0.966 and 0.956 respectively and the value correlation coefficient (R^2) of Freundlich isotherm model for As (V) on the developed adsorbent i.e. ACAL 11 and TRAL is 0.907 and 0.914 respectively as shown in Table 4.4.

On comparing the results presented in Table 4.4, it can be seen that the plots of Langmuir model showed higher correlation ($R^2 > 0.99$) and the value of χ^2 for Langmuir model is smaller than that of Freundlich model which conclude that adsorption of As(III) and As(V) on ACAL11 and TRAL. These facts suggest that the adsorption of As(III) and As(V) on to the ACAL11 and TRAL involves the monolayer coverage of the heavy metal on the surface of the adsorbent. Corresponding R_L values are found to be between 0 and 1 which is in agreement with the favourable adsorption.

The values of the free energy change (ΔG°) for the adsorption process are summarized in Table 4.4. The negative ΔG° values for ACAL11 and TRAL dictates the spontaneous nature of the adsorption process.

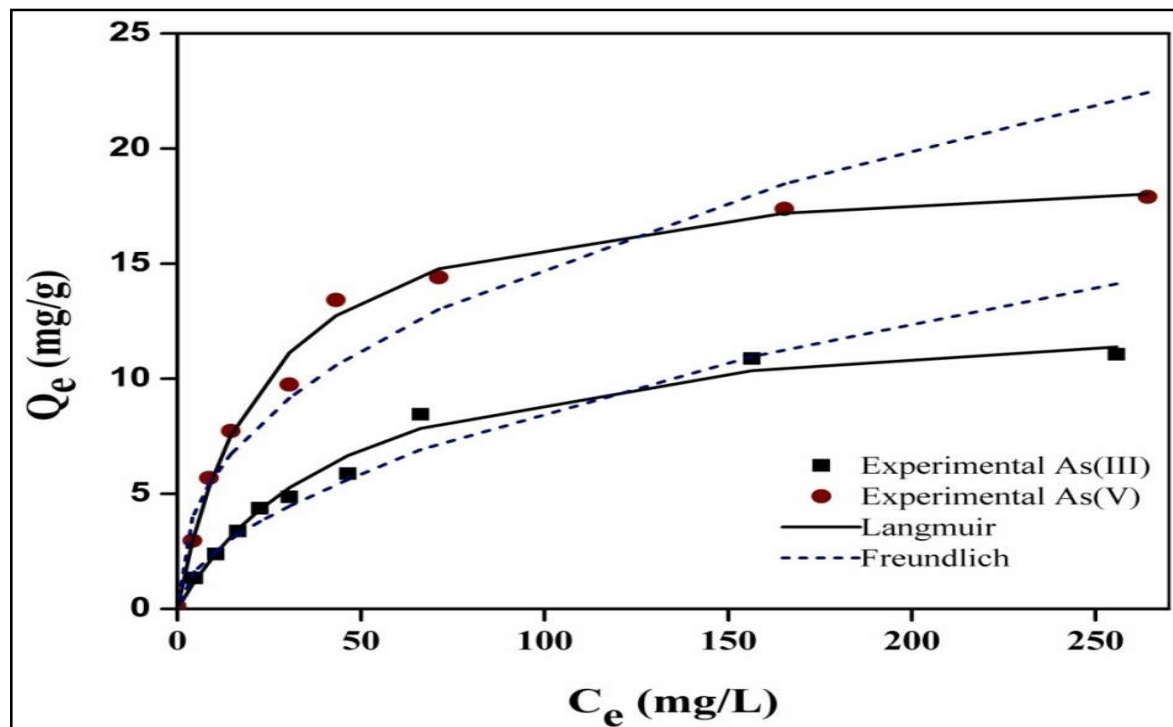


Figure 4.12 Arsenic adsorption model of TRAL at pH 9 and adsorbent dose 4 g/L for As(III), and pH 3 and adsorbent dose 2 g/L for As(V), contact time 1 h.

4.2.2.5. Effect of competitive ions

ACAL11 has shown the highest adsorptive capacity towards As(V). Hence the effect of competitive ion was studied only for adsorption of As(V) on ACAL11. Real ground water contains various metal ions and anions. To study the effect of various ions on adsorption of and As(V) in aqueous solution by ACAL11, solutions were prepared from potassium carbonate (K_2CO_3), magnesium sulphate ($MgSO_4 \cdot 7H_2O$), sodium nitrate ($NaNO_3$) and calcium chloride ($CaCl_2 \cdot 2H_2O$). Various initial concentrations of these solutions were taken in fixed 10mg/L initial concentration of arsenic solution and adsorbent dose was fixed at 4 g/L. Initial pH was fixed at 3 and batch experiments were carried out. The results obtained from the experiment are presented in Table 4.5. It shows that the competing ions have very less effect towards uptake of As(V) from aqueous solution by ACAL11.

4.2.2.6. Regeneration of adsorbent

Change in free energy in the adsorption confirmed that the adsorption of As(V) on to ACAL11 is physical adsorption. Since the adsorption of As(V) is favorable at low pH,

As(V) should be desorbed at high pH. So, 0.1M NaOH was used for the desorption of As(V) from As(V) adsorbed ACAL11.

Table 4.4 Langmuir and Freundlich parameters for adsorption of As(III) and As(V) on ACAL11 and TRAL

Adsorbent	Adsorbate	Langmuir model					Freundlich model			
		Q_{max} mg/g	b (L/mg)	R^2	ΔG (kJ/mol)	χ^2	$K_f[(\text{mg/g})$ $(\text{L/mg})^{1/n}]$	$1/n$	R^2	χ^2
ACAL11	As(III)	14.28	0.021	0.995	-18.548	0.176	0.755	0.540	0.966	1.271
	As(V)	23.80	0.057	0.996	-21.074	1.227	3.614	0.360	0.907	2.479
TRAL	As(III)	13.51	0.020	0.991	-18.532	0.227	0.711	0.540	0.956	1.196
	As(V)	19.60	0.043	0.998	-20.333	0.253	2.218	0.415	0.914	2.343

To determine the regeneration capacity of ACAL11 batch adsorption studies were run in succession with the adsorbent being regenerated between every adsorption cycle [26]. 0.5g of ACAL11 was added to 10mg/L AS(V) solution at pH 3 and it was shaken for 1 h. The percentage removal was determined which was 83%. The adsorbent was then washed, dried at 110 C and regenerated by shaking it with 0.1M NaOH solution for 1 h. Concentration of As(V) in filtrate obtained after regeneration was analyzed. There was more than 95% desorption of As(V). The regenerated adsorbent was washed, dried at 110 C again applied for second adsorption cycle. The percentage removal was 72%. On further regeneration and adsorption, percentage adsorption was only 57%. There was still more than 95% desorption in second regeneration. In every adsorption and regeneration, the adsorbent dose was fixed at 4g/L. These results show that the adsorbent ACAL11 can be used for arsenic adsorption up to two cycles effectively and arsenic can be successfully desorbed from the adsorbent by using 0.1M NaOH solution for its safe disposal.

4.2.2.7. Comparison with other adsorbents

The adsorption capacity (values of Q_{max} derived from the Langmuir equation) of ACALs and TRALs with other previously developed adsorbents, is summarized in Table 4.6.

Novel adsorbent for noxious impurities removal

Table 4.5 Effect of co-ions in removal of As(V) on ACAL11.

Concentration (mg/L)									%Removal
As(V)	Mg ²⁺	SO ₄ ²⁻	Na ⁺	NO ₃ ⁻	K ⁺	CO ₃ ²⁻	Ca ²⁺	Cl ⁻	
10	-	-	-	-	-	-	-	-	83.35
10	5	19.75	-	-	-	-	-	-	83.18
10	10	39.50	-	-	-	-	-	-	83.01
10	20	79.00	-	-	-	-	-	-	82.89
10	-	-	5	13.47	-	-	-	-	82.21
10	-	-	10	26.95	-	-	-	-	83.12
10	-	-	20	53.90	-	-	-	-	81.87
10	-	-	-	-	10	7.67	-	-	80.85
10	-	-	-	-	20	15.34	-	-	79.96
10	-	-	-	-	40	30.69	-	-	78.89
10	-	-	-	-	-	-	5	8.89	82.52
10	-	-	-	-	-	-	10	17.79	81.48
10	-	-	-	-	-	-	20	35.58	82.01

The obtained summarized data clearly revealed that the developed ACALs and TRAL possess higher adsorption capacity in comparison to the other previously developed adsorbent [61-65].

Table 4.6 Comparison of maximum adsorption capacity for the removal of noxious As(III) and As(V) by different previously developed adsorbents.

Adsorbent	Metal ion	Adsorption capacity (mg g ⁻¹)	Ref.
Magnetite maghemite nanoparticles	As(III)	3.69	[27]
	As(V)	3.71	
Iron-doped activated micro/ nano carbon particles	As(III)	15.00	[28]
	As(V)	5.00	
Fe-hydrotalcite supported magnetite nanoparticle	As(III)	0.12	[29]
	As(V)	1.28	
MnFe₂O₄ nanoadsorbents	As(III)	0.72	[30]
	As(V)	2.13	
Magnetic iron oxide/CNT composites	As(III)	8.13	[31]
	As(V)	9.74	
Activated carbon-alumina composites (ACALs)	As(III)	14.28	[Present Study]
	As(V)	23.80	
Tire rubber alumina composite (TRALs)	As(III)	13.51	[Present Study]
	As(V)	19.60	

4.3. Conclusion

The focus of the present study was to assess the feasibility of activated carbons prepared from waste rubber tire modified with alumina composite, the developed adsorbent i.e. ACAL and TRAL for the removal of hazardous As(III) and As(V) from the solvent phase. The following conclusions are bulletined:

1. Ratio metric preparation of the ACAL was carried out using activated carbon and aluminium hydroxide in 1:1 ratio by weight i.e. ACAL11, 1:2 ratio by weight i.e. ACAL12 and 2:1 ratio by weight i.e. ACAL21. It was observed that ACAL11 has greater BET surface area and arsenic adsorptive capacity as compared to other developed adsorbent.

Novel adsorbent for noxious impurities removal

2. Removal of As(V) is found to be more effective than that of As(III) by both ACAL11 and TRAL. Though TRAL has greater BET surface area, its adsorptive capacity towards arsenic in aqueous solution is lower than that of ACAL11.
3. Adsorption of As(III) as well as As(V) on ACAL11 and TRAL are best fitted to Langmuir adsorption isotherm with pseudo-second order kinetics.
4. Adsorption of As(III) as well as As(V) on ACAL11 and TRAL are best fitted to Langmuir adsorption isotherm with pseudo-second order kinetics.
5. Regeneration of the adsorbent was possible due to 0.1 M NaOH solution up to 95% of As(V) is desorbed from the developed adsorbent. Hence the adsorbent ACAL11 prepared from activated carbon obtained from waste tire rubber and aluminium hydroxide in 1:1 ratio by weight can be effectively applied for arsenic removal from arsenic contaminated ground water.
6. The proposed adsorbent “alumina composite modified waste rubber tire and activated carbon prepared from tire rubber” in other words, the adsorbent-adsorbate system is cost effective, environment friendly with no generation of secondary pollutant, efficient and fast for the removal of dyes from contaminated wastewater.

References

- [1] Zhang Q.L., Lin Y.C., Chen X., Gao N.Y., “A method for preparing ferric activated carbon composites adsorbents to remove arsenic from drinking water,”*J. Hazar. Mater.*, 148, (2007), 671–678.
- [2] Chang Q., Lin W., Ying W.C., “Preparation of iron-impregnated granular activated carbon for arsenic removal from drinking water,”*J. Hazar. Mater.*, 184, (2010), 515–522.
- [3] USEPA, National Primary Drinking-Water Regulations: Arsenic and Clarifications to Compliance and New source contaminants Monitoring; Final Rule: Federal Register, *U.S. Code of Federal Regulations*, 66, (2001), 6976-7066.
- [4] Payne K.B., Abdel-Fattah T.M., “Adsorption of Arsenate and Arsenite by Iron Treated Activated Carbon and Zeolites: Effects of pH, Temperature, and Ionic Strength,” *J. Environ. Sci. Health., Part A*, 40, (2005), 723–749.
- [5] Tuna A.O.A., Ozdemir E., Simsek E.B., Beker U., “Removal of As(V) from aqueous solution by activated carbon-based hybrid adsorbents: Impact of experimental conditions,”*Chem. Eng. J.*, 223, (2013), 116–128.
- [6] Gupta V.K., Saini V.K., Jain N., “Adsorption of As(III) from aqueous solutions by iron oxide-coated sand,”*J. Colloid Interface Sci.*, 288, (2005), 55–60.
- [7] Mondal P., Majumder C.B., Mohanty B., “Laboratory based approaches for arsenic remediation from contaminated water: Recent developments,”*J. Hazar. Mater.*, 150, (2008), 695–702.
- [8] Dong L., Zinin P.V., Cowen J.P., Ming L.C., “Iron coated pottery granules for arsenic removal from drinking water,”*J. Hazar. Mater.* 168, (2009), 626–632.
- [9] Han C., Pu H., Li H., Deng L., Huang S., He S., Luo Y., “The optimization of As(V) removal over mesoporous alumina by using response surface methodology and adsorption mechanism” *J. Hazar. Mater.* 254, (2013), 301–309.
- [10] Ghanizadeh G., Ehrampoush M.H., Ghaneian M.T., Application of iron impregnated activated carbon for removal of arsenic from water *Iran. J. Environ. Health. Sci. Eng.*, 7, (2010), 145-156.
- [11] Chen W., Parette R., Zou J., Cannon F.S., Dempsey B.A., “Arsenic removal by iron-modified activated carbon,”*Water Research* 41, (2007), 1851 – 1858.

- [12] Raut P.A., Dutta M., Sengupta S., Basu J.K., "Alumina-carbon composite as an effective adsorbent for removal of Methylene Blue and Alizarin Red-s from aqueous solution," *Indian J. Chem. Tech.*, 20, (2013), 15-20.
- [13] Yan-Qing C., Ren-Ping W., Xian-Feng Y., "Structural characterization and property study on the activated alumina-activated carbon composite material," *Chinese J. Struct. Chem.*, 31, (2012), 315–320.
- [14] Williams P.T., Besler S., Taylor D.T., "The pyrolysis of scrap automotive tyres, the influence of temperature and heating rate production composition," *Fuel*, 69, (1990), 1474-1782.
- [15] Tanthapanichakoon W., Ariyadejwanich P., Japthong P., Nakagawa K., Mukai S.R., Tamon H., "Adsorption-desorption characteristics of phenol and reactive dyes from aqueous solution on mesoporous activated carbon prepared from waste tires," *Water Res.*, 39, (2005), 1347–1353.
- [16] Miguel G.S., Fowler G.D., Sollars C.J., "A study of the characteristics of activated carbons produced by steam and carbon dioxide activation of waste tyre rubber," *Carbon*, 41, (2003), 1009–1016.
- [17] Ariyadejwanich P., Tanthapanichakoon W., Nakagawa K., Mukai S.R., Tamon H., "Preparation and characterization of mesoporous activated carbon from waste tires," *Carbon*, 41, (2003), 157–164.
- [18] Jha V.K., Subedi K., "Preparation of Activated Charcoal Adsorbent from Waste Tire," *J. Nepal Chem. Soc.*, 27, (2011), 19-25.
- [19] Gupta V.K., Jain A.K., Maheshwari G., "An iron(III) ion-selective sensor based on a bis(tridentate) ligand," *Talanta* 72(4) (2007) 1469-1473.
- [20] Gupta V.K., Ganjali M.R., Norouzi P., Khani H., Nayak A., Agarwal S., "Electrochemical Analysis of Some Toxic Metals by Ion-Selective Electrodes," *Crit. Rev. Anal. Chem.*, 41 (2011) 282–313.
- [21] Jain R., Gupta V.K., Jadon N., Radhapyari K., "Voltammetric determination of cefixime in pharmaceuticals and biological fluids," *Anal. Biochem.* 407 (2010) 79–88.
- [22] Goyal R.N., Gupta V.K., Chatterjee S., "Voltammetric biosensors for the determination of paracetamol at carbon nanotube modified pyrolytic graphite electrode," *Sens. Actuators. B*, 149, (2010), 252-258.

- [23] Gupta V.K., Ali I., "Removal of ddd and dde from wastewater using bagasse fly ash, a sugar industry waste," *Wat. Res.*, 35(2001), 33-40.
- [24] SaravananL., Subramanian S., "Surface chemical studies on the competitive adsorption of poly(ethylene glycol) and ammonium poly(methacrylate) onto alumina," *J. Colloid Interface Sci.*, 284, (2005), 363–377.
- [25] Zhu J., BaigS.A., Sheng T., Wang Z., Xu X., "Fe₃O₄ and MnO₂ assembled on honeycomb briquette cinders (HBC) for arsenic removal from aqueous solutions," *J. Hazard. Mater.*, 286, (2015), 220-228.
- [26] Bhat A., MegeriG.B., Thomas C., Bhargava H., JeevithaC., ChandrashekarS., MadhuG.M., "Adsorption and optimization studies of lead from aqueous solution using g-Alumina," *J. Environ. Chem. Eng.*, 3, (2015), 30–33
- [27] Chowdhury S.R., YanfulE.K., "Arsenic and chromium removal by mixed magnetiteemaghemite nanoparticles and the effect of phosphate on removal," *J. Environ. Manage.*, 91, (2010), 2238- 2247.
- [28] Sharma A., Verma N., Sharma A., Deva D., SankararamakrishnanN., "Iron doped phenolic resin based activated carbon micro and nanoparticles by milling: Synthesis, characterization and application in arsenic removal," *Chem. Eng. Sci.* 65, (2010), 3591-3601.
- [29] TürkT., Alp I., "Arsenic removal from aqueous solutions with Fe-hydrotalcite supported magnetite nanoparticle," *J. Ind. Eng. Chem.* 20, (2014), 732-738.
- [30] Parsons J.G., Lopez M.L., Peralta-VideaJ.R., Gardea-TorresdeyJ.L., "Determination of arsenic(III) and arsenic(V) binding to microwave assisted hydrothermal synthetically prepared Fe₃O₄, Mn₃O₄, and MnFe₂O₄ nanoadsorbents," *Microchem. J.* 91, (2009), 100-106.
- [31] Ma J., Zhu Z., Chen B., Yang M., Zhou H., Li C., Yu F., Chen J., "One-pot, large-scale synthesis of magnetic activated carbon nanotubes and their applications for arsenic removal," *J. Mater. Chem. A*, 1, (2013), 4662-4666.



CHAPTER 5

**RTACMC and RTAC for
phenols and p-Cresol
removal**



5.1. Introduction

Phenolic compounds were selected as model adsorbates because of their widespread prevalence in industrial wastewater as a result of their rampant use in many chemical and petrochemical industries, oil refinery, ceramic and steel plants, disinfectant manufacturing, or metal refining [1]. Their concentration in some of the industrial wastewaters in India has been found to be very high varying from 1000 to 2000 ppm in coal mining, 50–700 ppm in petrochemical, 1000 ppm in pharmaceutical and 2000–20,000 ppm in oil refining industries [2]. Also, such phenolic compounds are known to have high toxicity and carcinogenic nature. Because of their stability and bioaccumulation, they remain in the environment for longer periods and hence cause considerable damage and possess severe detrimental threat to the aquatic ecosystem and human health [3]. They are considered toxic for some aquatic life forms in concentrations above 50 ppb and the ingestion of one gram of phenol has shown fatal consequences in humans. Phenols have the capacity to combine with existing chlorine in drinking water, giving rise to chlorophenols, compounds that are even more toxic and difficult to eliminate. Hence phenolic compounds have been included in the list of priority pollutants by the Environmental Protection Agency (EPA) and the European Environmental Agency (EEA) [4–6].

Carbon black from waste rubber tire has been another interesting alternative as a low cost adsorbent basically because its carbonaceous nature resembles that of a commercial AC [7,8]. Also since it constitutes approximately 32% by weight of carbon, its recovery and reuse as adsorbent would solve the waste tire disposal problem thereby benefiting the environment in a dual way. But the carbon black obtained by untreated tire pyrolysis has a less developed porous structure and a lower internal surface area [9]. Appropriate activation conditions of temperature, time etc. have been found to enhance both surface area and pore volume of activated carbons developed from carbon black [10–21] and this has resulted in improved adsorption behavior. Recent progress has shown the use of microwave assisted physical and chemical methods in the preparation of activated carbon from various low cost precursors as a substitute to conventional heating [22]. The advantage associated with using microwave heating is that the treatment time and consumption of gases can be considerably reduced, which further results in the reduction in energy consumption as well. In comparison with conventional heating techniques, microwave heating has been seen to demonstrate interior heating, higher heating rates, selective heating, greater control of the heating process, no direct contact between the heating source and heated materials, and reduced equipment size and waste. Additionally, microwave furnaces are generally smaller than conventional furnaces. Also, the activated

carbons prepared by microwave heating have been seen to demonstrate lesser oxygenated functionalities from their carbon surfaces [23]. The textural and chemical properties of the carbons thus prepared have been found to be comparable to those from conventional heating but the time of preparation of the activated carbon is seen to be far shortened [24].

The objective of the present study is focused on preparing activated carbons (RTACMC and RTAC) by microwave assisted chemical treatment as well as by conventional physical activation respectively from waste rubber tire followed by the assessment of their physical and chemical characteristics for the ultimate objective of determining their adsorption capacity for organic pollutants like p-cresol and phenol. Experimental data were fitted to various adsorption isotherms and kinetic models in order to determine the adsorption capacities and rates.

5.2. Results and discussion

5.2.1. Effect of pretreatment conditions of microwave on the performance of activated carbons

Figure 5.1a reveals the effect of microwave power, impregnation ratio and microwave irradiation time on the adsorption capacity of activated carbons prepared as well as on the percentage removal of p-cresol from synthetic wastewaters. Batch adsorption experiments were performed at constant adsorbate concentration of 150 ppm and adsorbent dose of 0.6 g/L at pH of 7 and contact time of 90 min. While studying the effect of microwave power on the adsorption performance of the activated carbons at constant chemical impregnation ratio of 1.5 and irradiation time of 10 min, it is seen that the adsorption performance improves drastically (22.50 mg/g to 197.70 mg/g) on increasing the power from 200 to 600 W followed by a corresponding decrease at higher operating microwave powers (Figure 5.1a). Increasing the microwave power to 600 W has induced higher internal and volumetric heating leading to the development of new pores thereby enhancing the adsorption capacity. But higher microwave power of 800 W may have destroyed the pore structures [23].

While performing the adsorption experiments on activated carbons prepared under constant microwave power of 600 W and irradiation time of 10 min but of varying impregnation ratios, it was observed that increasing the chemical impregnation ratio from 0.50 to 1.50 improved the adsorption capacity for p-cresol removal from 82.0% to 94.0% (Figure 5.1b). Newer pores may have been developed and existing pores may have been widened due to the destruction of volatiles and from impregnated KOH as can be seen from SEM images (Figure 5.2).

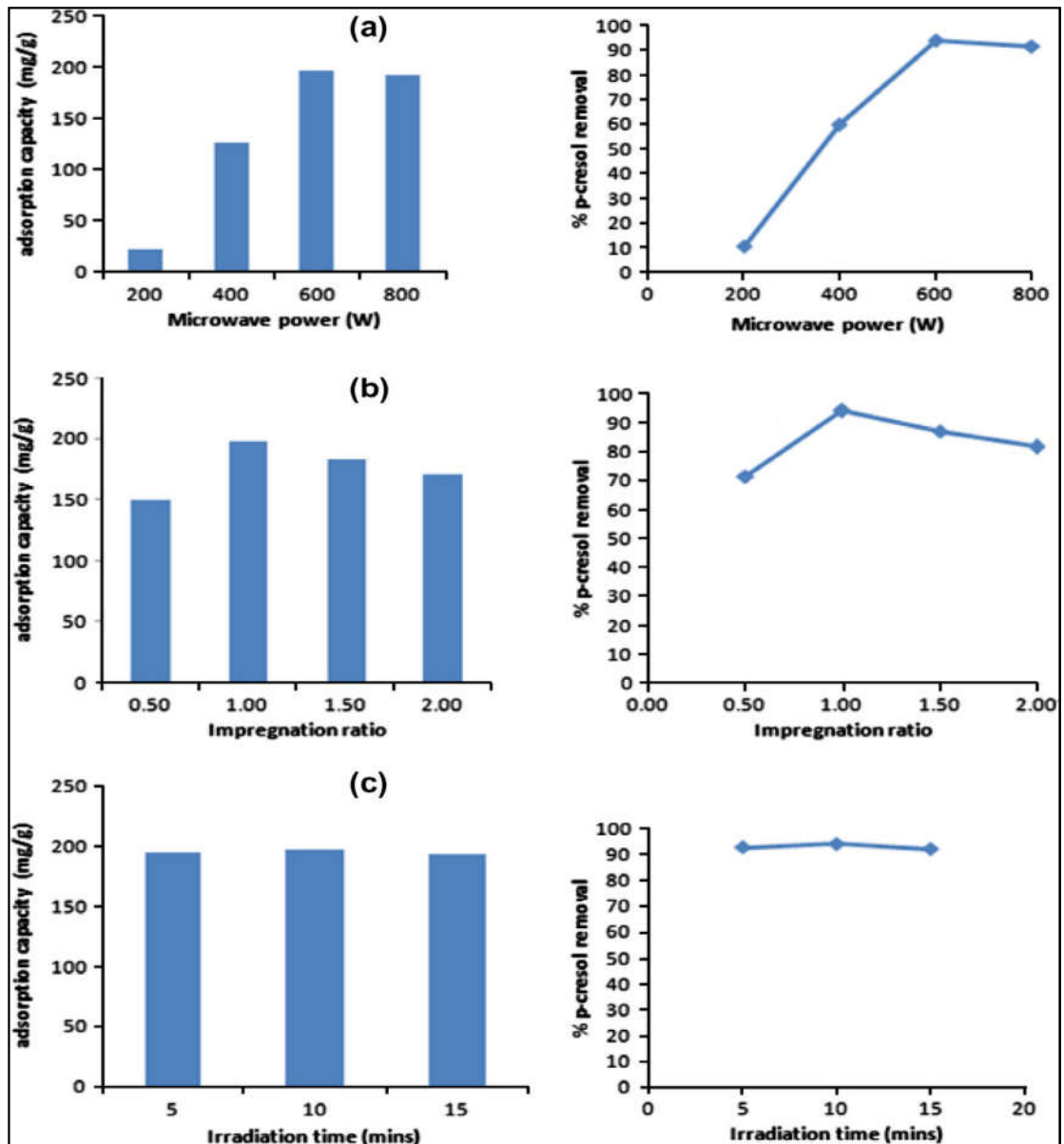


Figure 5.1 Effect of (a) microwave power (at constant impregnation ratio of 1.5 and irradiation time of 10 min) (b) impregnation ratio (at constant microwave power of 600W and irradiation time of 10 min), (c) irradiation time (at constant microwave power of 600W and impregnation ratio of 1.5) on the adsorption capacity of RTACMC and removal % of p-cresol [adsorbate conc. 150 ppm; temperature 45 °C, adsorbent dose: 0.6 g/L, pH-7; contact time-90 min].

Studying the effects of the microwave irradiation time on the adsorption capacity under constant microwave power of 600W and impregnation ratio of 1.50 showed a slight improvement in the adsorption capacity on increasing the time from 5 min to 10 min (195.00 mg/g to 197.70 mg/g) followed by a slight decrease. Prolonging the irradiation time would obviously cause an increase in temperature which in turn would increase the reaction rates and

devolatilization, thereby developed the porosity and the pore structure. However, further increasing the treatment time might produce local hotspots, leading to the shrinkage and destruction of pore structure [23].

5.2.2. Characterization of adsorbent material

From the textural characteristics of the RTACMC and RTAC, it is revealed that RTAC has a surface area of 562 m²/g with majority of its porosity retained in mesopores (0.69 cc/g). The volume of mesopores accounts for 71% of the total pore volume (0.97 cc/g) thereby signifying a mesoporous structure in RTAC. But, in case of RTACMC, both the surface area and the total pore volume (1802 m²/g, 1.52 cc/g respectively) are found to be increased in comparison with those of RTAC indicating the development and refinement of pore structure during the microwave assisted chemical activation stage. There is a probability that the microwave heating has caused the destruction of the volatiles and impregnated KOH resulting in the widening of the AC pores, giving rise to an increase in the total pore volume. The data further reveal that both the mesopore and micropore volume in RTACMC are increased to the tune of 80.00% and 19.70% of total pore volume. This reveals that the mesoporous structure is retained in RTACMC. High surface area and well developed porosity were likewise obtained in microwave assisted KOH activated cotton stalk, pineapple peel and rice husk [23,26–28]. Thus the microwave assisted chemical impregnation method of activation has resulted in enhancing the porosity and pore structure of rubber tire derived activated carbon.

The carbon was found to increase in RTACMC to the tune of 87.23% as compared to that of RTAC (78.76%) followed by a significant decrease in oxygen levels (2.12% in RTACMC as compared to 7.04% in RTAC) thereby revealing the destruction and decomposition of organic compounds and decomposition of volatiles under microwave treatment. This was further confirmed by EDAX data. The enhancement of the carbonaceous nature is responsible for the improved porosity in RTACMC which is further revealed from Scanning Electron Micrograph (SEM) images of RTACMC (Figure 5.2). The SEM image reveals the presence of highly scattered irregular cavities on the surface of the RTACMC which may have been due to the destruction of the volatile components and the impregnated KOH under microwave heating. Such cavities are found to be distinctly absent on the RTAC surface as can be seen from SEM image of RTAC.

The FTIR spectrum of the RTAC sample, indicates the presence of carboxylic groups as revealed by the characteristic peaks at 1710 cm⁻¹ (C=O stretch of acid), 1266 cm⁻¹ (C-O stretch of acid) and 2921 cm⁻¹ (O-H stretch of acid) (Figure 5.3). The presence of phenolic group is

corroborated by the presence of additional peaks at 3365 cm^{-1} (H bonded OH group) and at 1108 cm^{-1} (C-O stretch) on the RTAC surface.

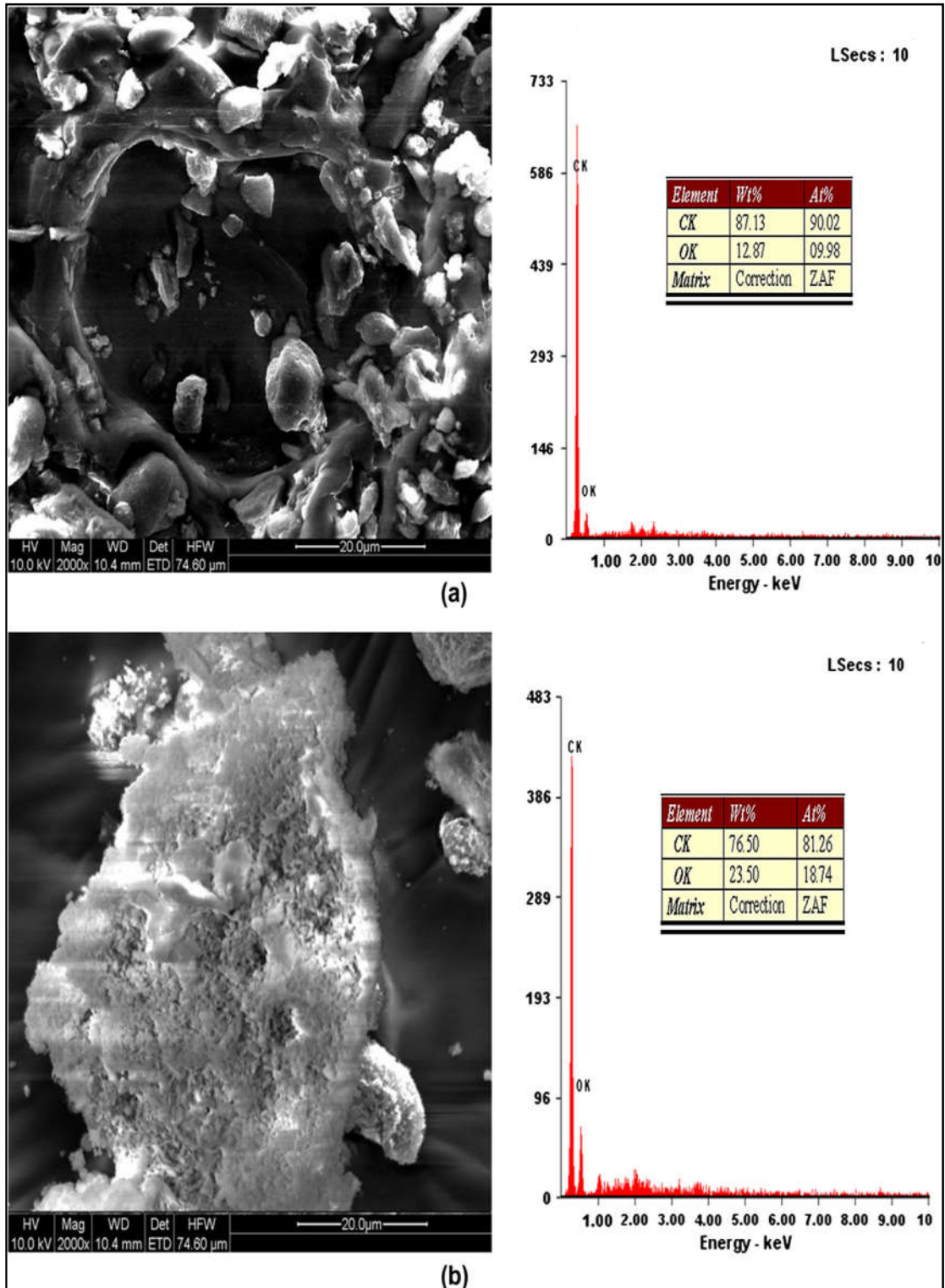


Figure 5.2 SEM micrograph and EDAX of (a) RTACMC (b) RTAC before adsorption

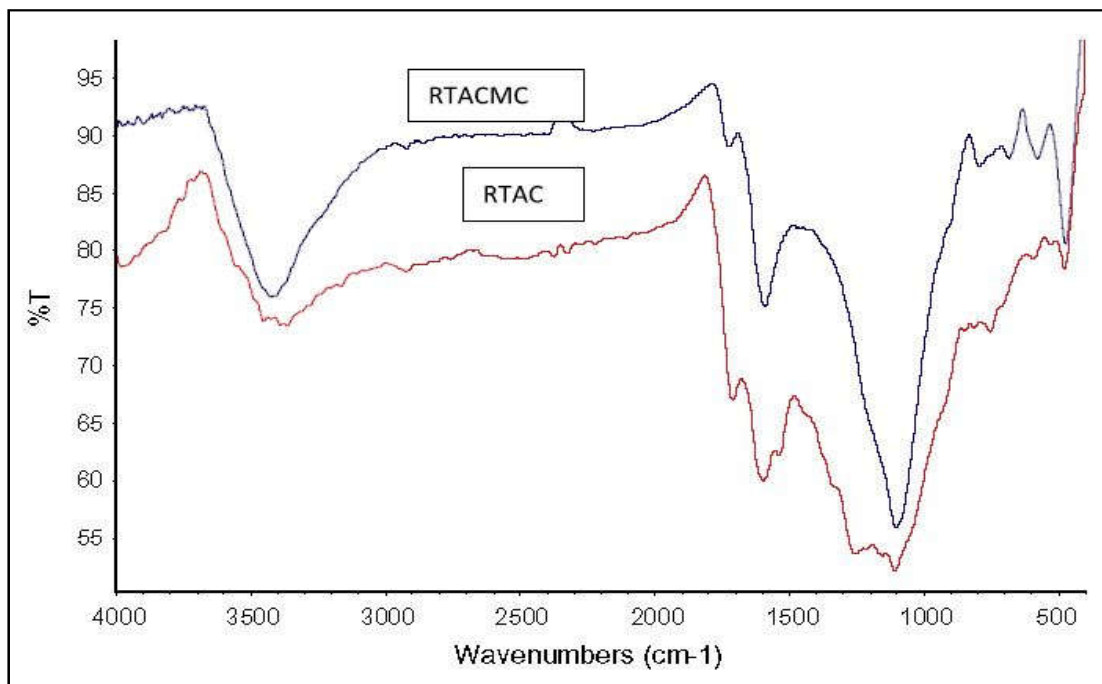


Figure 5.3 FTIR spectra of the RTACMC and RTAC.

The C=O, C-O and the OH stretch peaks of acids were found to be significantly absent on the RTACMC sample, thereby revealing that microwave heating resulted in the decomposition of carbon-oxygen functionalities. The basic nature of RTACMC is further evident from the pH_{pzc} studies (8.50 in RTACMC and 7.00 in RTAC).

5.2.3. Effect of pH

The effect of pH on the adsorption of p-cresol onto RTACMC was well studied and elucidated by varying the pH of the medium from 1 to 12 at a fixed adsorbent dose of 0.06 g/L with a fixed p-cresol concentration of 150 ppm and the results are depicted in Figure 5.4. The amount adsorbed was found to be almost constant between pH of 4.00 and 8.50 for RTACMC and it showed a gradual decrease as the solution became more basic. These results can be explained on the basis of the pH_{pzc} value of RTACMC (8.50) and pK_a of p-cresol (10.26). At this pH range, p-cresol exists in the molecular form and is basic in nature due to the electron-releasing groups of methyl and hydroxyl. Also, RTACMC which has a net positive charge (pH_{pzc} = 8.50) has more affinity for the molecular form of p-cresol and this results in its high adsorption uptake. But at higher pH values of greater than 10, there is electrostatic repulsion between the negative RTACMC surface and the anionic form of p-cresol resulting in decreased adsorption uptake. There is also a significant decrease in p-cresol uptake at lower pH values as evident from Figure 5.4. Under highly acidic conditions, the lone pair of electron on

the hydroxyl groups which is available for hydrogen bonding is protonated [33] thereby causing strong electrostatic repulsion for the positively charged RTACMC surface. RTAC is more acidic and hydrophilic ($pH_{pzc} = 7.00$) as compared to RTACMC ($pH_{pzc} = 8.50$). But the trend of its adsorption capacity for p-cresol removal with change in pH is more or less similar as compared to that of RTACMC. The decreased uptake of RTAC may be due to the difference in its surface properties as compared to RTACMC.

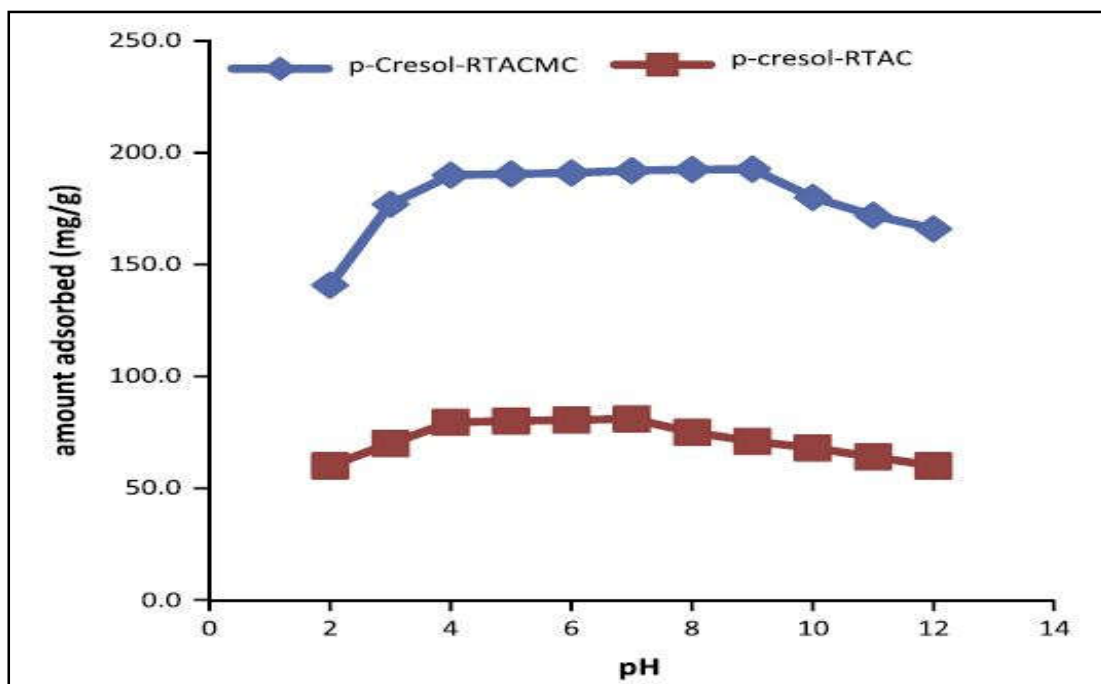


Figure 5.4 Effect of pH on the adsorption of p-cresol on the two adsorbents RTACMC and RTAC [adsorbate conc. 150 ppm; temperature 45 °C, adsorbent dose: 0.6 g/L, pH-7; contact time-90 min for RTACMC and 150 min for RTAC].

5.2.4. Effect of contact time

The uptake of p-cresol and phenol onto RTACMC and RTAC depicts that the adsorption is quite rapid initially, gradually slows down and then reaches the equilibrium (Figure 5.5). The decrease in amount of the adsorbates adsorbed with time may be due to the aggregation of such molecules around the adsorbent particles. This aggregation may hinder the migration of the adsorbate, as the adsorption sites become saturated; thereby resistance to diffusion also increases [25].

Irrespective of the adsorbates, a distinct difference in the equilibrium time for RTACMC and RTAC was observed (90 min for RTACMC and 120 min for RTAC (Figure 5.5) and this difference might be due to differences in the surface properties of the adsorbents caused by

Novel adsorbent for noxious impurities removal

microwave heating. Again irrespective of the adsorbents, there is a higher uptake of p-cresol as compared to phenol and such high affinity of p-cresol for the adsorbents is somewhat expected because of its lower solubility and higher logK_{ow} values in water (Table 5.1). But phenol being smaller in size the time for attaining equilibrium should have been shorter as compared to that of p-cresol [29]; but this is not visible from the results obtained. But overall, the high uptake of the selected adsorbates and the fact that equilibrium is attained within 2 h reveals the effectiveness of the developed adsorbents for wastewater treatment.

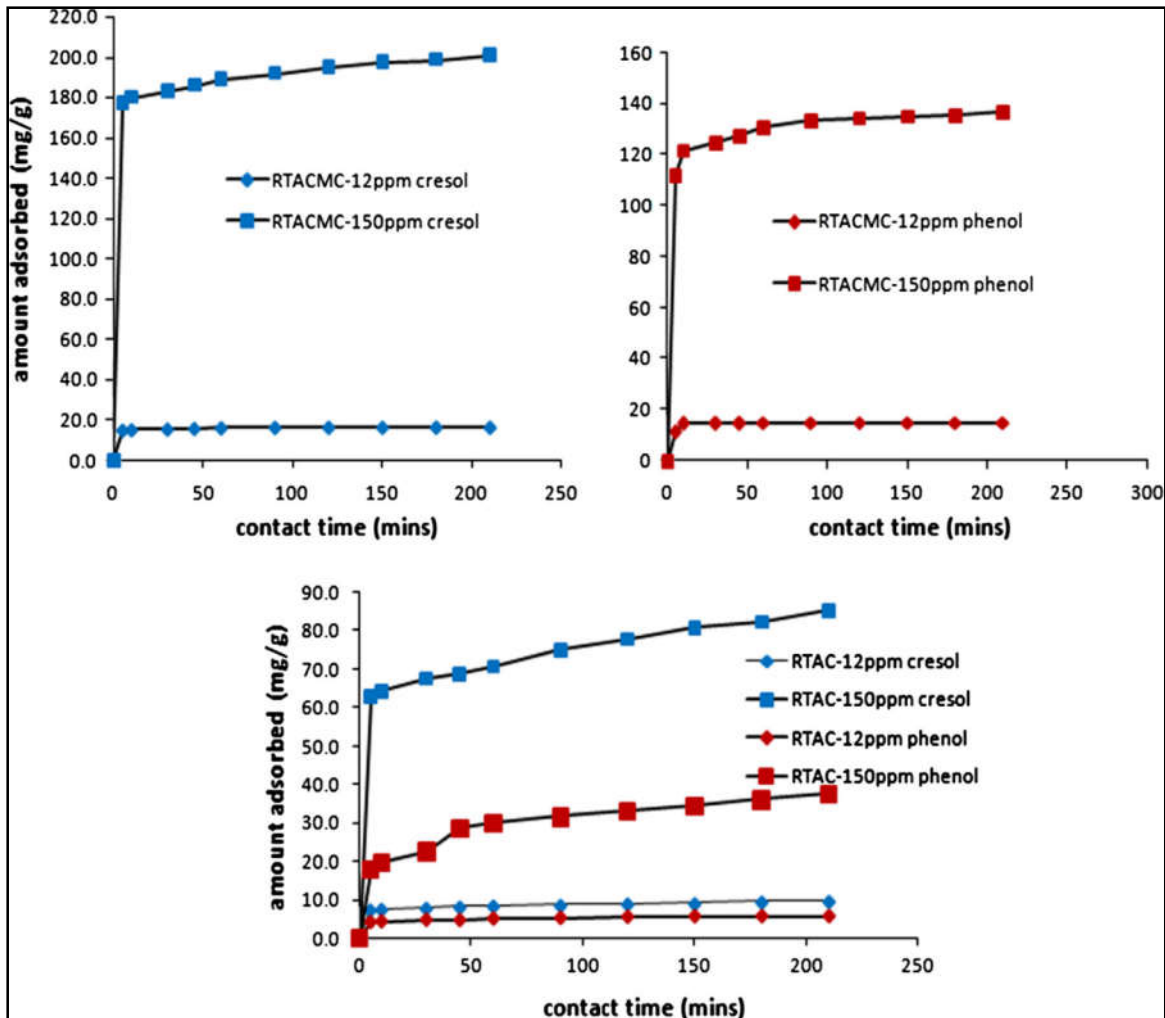


Figure 5.5 Effect of contact time on the adsorption of p-cresol and phenol onto RTACMC and RTAC [adsorbate conc. 12 ppm and 150 ppm; temperature 45 °C; adsorbent dose 0.6 g/L, pH 7]

Figure 5.5 further reveals that for RTACMC, the adsorption equilibrium, q_e increased from 16.52 to 201.0 mg/g and from 15.0 to 136.50 mg/g for p-cresol and phenol respectively (Table 5.1) when their initial concentration was increased from 12 to 150 ppm. Similar trend was

observed for other developed adsorbent RTAC for the under observation adsorbates. The above facts are due to the higher concentration gradient which acts as a driving force for the adsorption process [25].

Table 5.1 Octanol-water partition coefficient values ($\log K_{ow}$) and experimental adsorption equilibrium (q_e) at different concentration for both RTACMC and RTAC

Adsorbent	RTACMC				RTAC			
Adsorbate	p-Cresol		Phenol		p-Cresol		Phenol	
Log Kow	1.95		1.46		1.95		1.46	
Molecular Weight	108.13		94.11		108.13		94.11	
Concentration (in ppm)	12	150	12	150	12	150	12	150
Exp q_e (mg/g)	16.52	201.00	15.00	136.50	9.60	85.50	5.66	37.50

5.2.5. Adsorption isotherm modelling

To find out the most suitable adsorption model, the isotherm data thus obtained were simulated, by the well-known mathematical equations of D-R, Langmuir and Freundlich isotherm models. The values of regression coefficients obtained from these model's plots were also evaluated, which were used as a fitting criteria to find out suitable model. The results of their linear regression i.e. correlation coefficients and the parameters obtained from the plots of D-R ($\log q_e$ vs ϵ^2), Langmuir ($1/q_e$ vs $1/C_e$), and Freundlich ($\log q_e$ versus $\log C_e$) are listed Table 5.2.

The results presented in Table 5.2 clearly reveal the value of correlation coefficients (R^2) at three different temperatures i.e. 25, 35 and 45C for the p-Cresol and phenol. The correlation coefficients at different temperatures were considerably high ($R^2 > 0.99$) for the Langmuir model followed by the D-R and the Freundlich isotherm model; the linearity of plots as evident from Figure 5.6 and from high correlation coefficient values in Table 5.2 suggests the applicability of the Langmuir model with the p-cresol getting adsorbed onto the adsorbent surface to form a monolayer.

Novel adsorbent for noxious impurities removal

The values of b are seen to be higher for RTACMC indicating higher affinity of adsorbates than for RTAC. This can be attributed to the fact that the adsorption of the adsorbates takes place onto sites having stronger binding energy. Because of the higher values of Q_0 and b , RTACMC having favorable pore size distribution is a better option for use in wastewater treatment.

The values of n are significantly higher than unity at all the temperatures studied illustrating the favorable adsorption [31] and the mean free energy of adsorption (E_D) as computed from was found to be $<8 \text{ kJ mol}^{-1}$ at all temperatures (Table 5.2) implying the involvement of a physisorption nature of the adsorption process.

Table 5.2 Adsorption isotherm parameters for adsorption of p-Cresol and phenols at different temperature on to different adsorbents i.e. RTACMC and RTAC

Adsorbent & Adsorbate	Temp (°C)	D-R model			Freundlich model			Langmuir Isotherm		
		q_d	E_D	R^2	K_F	n	R^2	Q_0 (mg/g)	b (L/mg)	R^2
RTACMC										
p-Cresol	25°C	257.0	1.68	0.92	15.96	1.43	0.99	250	0.091	0.99
	35°C	165.9	1.60	0.95	11.97	1.36	0.99	142.7	0.085	0.99
	45°C	102.3	1.55	0.90	9.53	1.26	0.99	111.1	0.077	0.99
Phenol	25°C	95.50	1.51	0.86	7.62	1.25	0.99	100.0	0.074	0.99
	35°C	87.09	1.48	0.85	5.87	1.22	0.99	90.91	0.069	0.99
	45°C	79.43	1.44	0.84	4.59	1.18	0.99	83.33	0.063	0.99
RTAC										
p-Cresol	25°C	77.63	1.38	0.87	4.07	1.12	0.99	71.43	0.050	0.99
	35°C	66.07	1.36	0.85	3.55	1.11	0.97	62.50	0.048	0.99
	45°C	52.48	1.35	0.90	3.24	1.10	0.98	55.56	0.044	0.99
Phenol	25°C	42.65	1.32	0.90	3.08	1.08	0.95	47.62	0.040	0.99
	35°C	38.02	1.30	0.96	2.89	1.06	0.99	41.67	0.038	0.99
	45°C	31.62	1.29	0.99	2.81	1.02	0.99	38.46	0.035	0.99

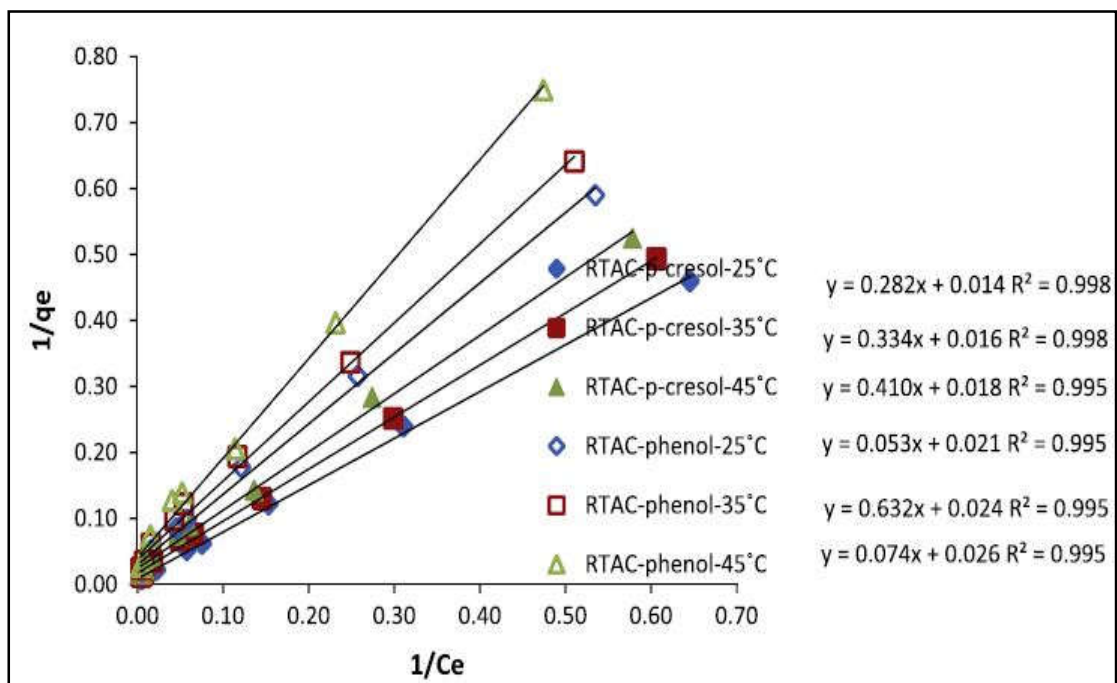
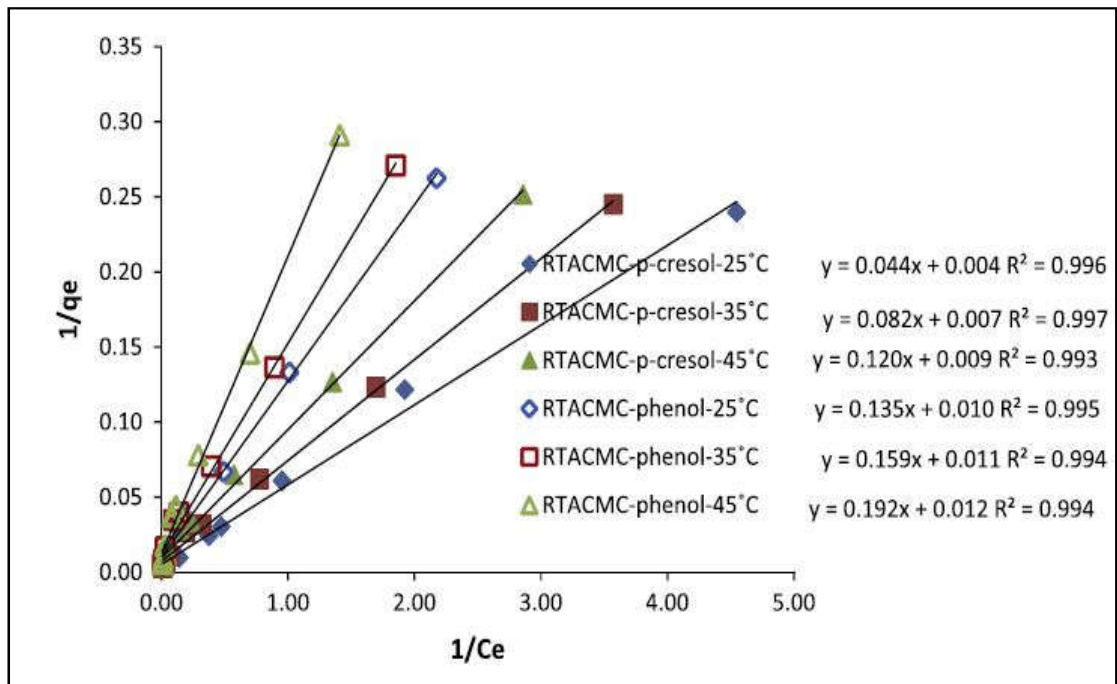


Figure 5.6 Langmuir adsorption isotherms of adsorption of p-cresol and phenol onto RTACMC and RTAC at three different temperatures

5.2.6. Thermodynamic study and effect of temperature

The values of free energy change (ΔG°), enthalpy change (ΔH°) and entropy change (ΔS°) for adsorption process were calculated and are summarized in Table 5.3. The enthalpy change ΔH° in case of developed adsorbent i.e. RTACMC and RTAC prepared from the rubber

Novel adsorbent for noxious impurities removal

ture is negative (Exothermic) i.e. adsorption capacity decreases on successive increase of temperature. Further, negative ΔG values for RTACMC and for RTAC dictate the spontaneous nature of the adsorption process [30, 32] and in addition to this the positive value of ΔS for RTACMC and RTAC reveals the increased randomness at the solid–solution interface during the fixation of the aromatic compounds on the active sites of the adsorbent.

Table 5.3 Thermodynamic parameters for adsorption of p-Cresol and phenol at different temperature on to developed adsorbents i.e. RTACMC and RTAC

Adsorbent & Adsorbate	Temp (C)	Thermodynamic Parameters		
		ΔG (kJ/mol)	ΔH (kJ/mol)	ΔS (kJ/Kmol)
RTACMC				
p-Cresol	25°C	-5.94	-7.61	0.045
	35°C	-6.30		
	45°C	-6.78		
Phenol	25°C	-6.45	-6.71	0.044
	35°C	-6.71		
	45°C	-7.26		
RTAC				
p-Cresol	25°C	-7.44	-4.87	0.041
	35°C	-7.78		
	45°C	-8.26		
Phenol	25°C	-8.00	-4.75	0.040
	35°C	-8.38		
	45°C	-8.85		

5.2.7. Adsorption kinetics

Two kinetic models namely pseudo-first-order and pseudo-second-order have been applied and were used to test adsorption kinetics data in order to investigate the mechanism

involved during the adsorption of p-Cresol and phenol onto the developed adsorbent i.e. RTACMC and RTAC.

Table 5.4 lists the results of the kinetic parameters of the two models as well as their regression coefficients (R^2) at different concentration initial concentration 12 ppm and 50 ppm of p-Cresol and phenol concentration. The value of correlation coefficient (R^2) for the pseudo-second-order kinetic model is comparatively high (>0.99), and the adsorption capacities calculated by the model are also close to those values which are obtained experimentally.

Table 5.4 Kinetic parameters for the adsorption of p-Cresol and phenol onto RTACMC and RTAC

Adsorbent	RTACMC				RTAC			
	p-Cresol		Phenol		p-Cresol		Phenol	
Concentration (in ppm)	12	150	12	150	12	150	12	150
Exp q_e (mg/g)	16.52	201.00	15.00	136.50	9.60	85.50	5.66	37.50
Pseudo-first-order								
Theoretical q_e (mg/g)	3.846	26.303	2.582	22.39	2.05	21.38	1.76	19.95
K_1 (min^{-1})	0.032	0.012	0.0368	0.0138	0.021	0.007	0.028	0.009
R^2	0.976	0.992	0.965	0.993	0.917	0.948	0.944	0.976
Pseudo-second-order								
Theoretical q_e (mg/g)	16.95	200.00	15.15	133.33	9.71	90.91	5.00	37.04
K_2 (g/mg/min)	0.021	0.002	0.089	0.004	0.015	0.001	0.084	0.003
R^2	0.996	0.999	0.999	0.999	0.997	0.993	0.998	0.993

Figure 5.7 indicates the linear plots of t/q_t vs. T at two different adsorbate concentrations for RTACMC and RTAC showing the applicability of the pseudo-second-order model and thus can be concluded to be more suitable to describe the adsorption kinetics of the p-Cresol and phenol onto the developed adsorbent i.e. RTACMC and RTAC.

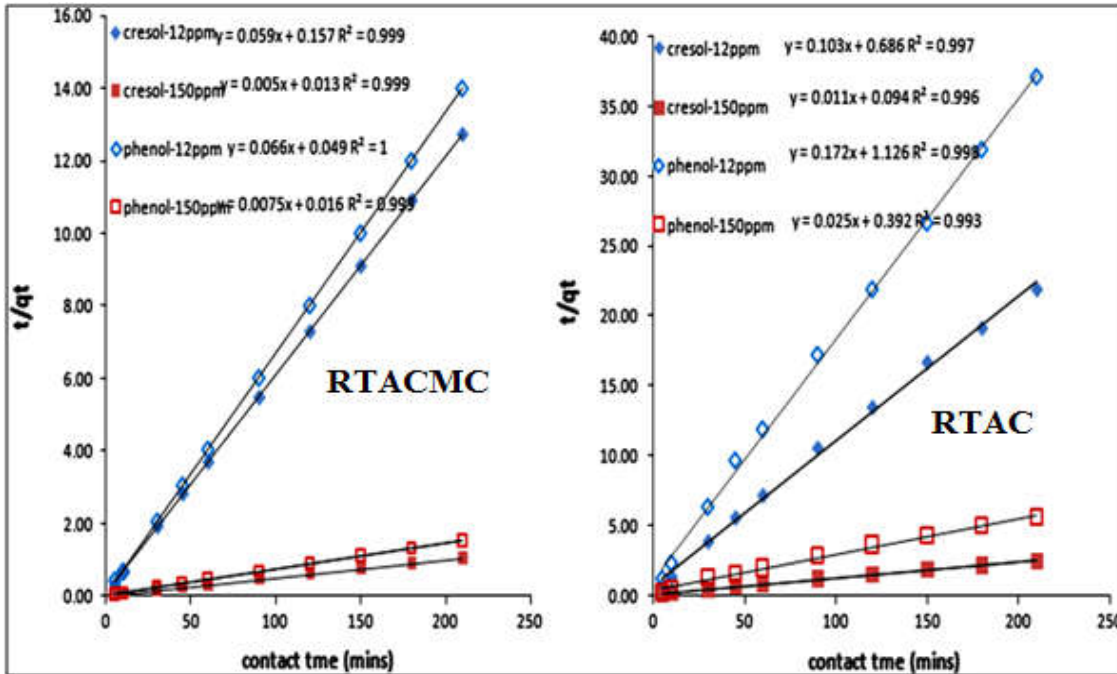


Figure 5.7 Lagergren pseudo-second order plots at two different adsorbate concentrations for adsorbents RTACMC and RTAC.

5.2.8. Adsorption mechanism

Prediction of the rate-limiting step is an important factor to be considered in the adsorption process [29]. For solid-liquid adsorption process, the solute transfer process is usually characterized by either external mass transfer (boundary layer diffusion) or intraparticle diffusion or both. In the present study, intraparticle diffusion plot of q_t vs. $t^{0.5}$ (Figure 5.8) were plotted for RTACMC for phenol and p-Cresol at two different concentrations i.e. 12 ppm and 50 ppm. From Figure 5.8, the adsorption process tends to be followed by three phases the first phase was very sharp and was completed within 90 minutes thereby signifying the instantaneous mass transfer of the adsorbate molecules from aqueous phase to the RTACMC surface; the second linear phase was the gradual adsorption stage signifying the rate limiting step being the intraparticle diffusion of the dye molecules and in the end the third phase shows the final equilibrium stage signifying the saturation of the carbon surface and also the presence of very low adsorbate concentration in aqueous solution.

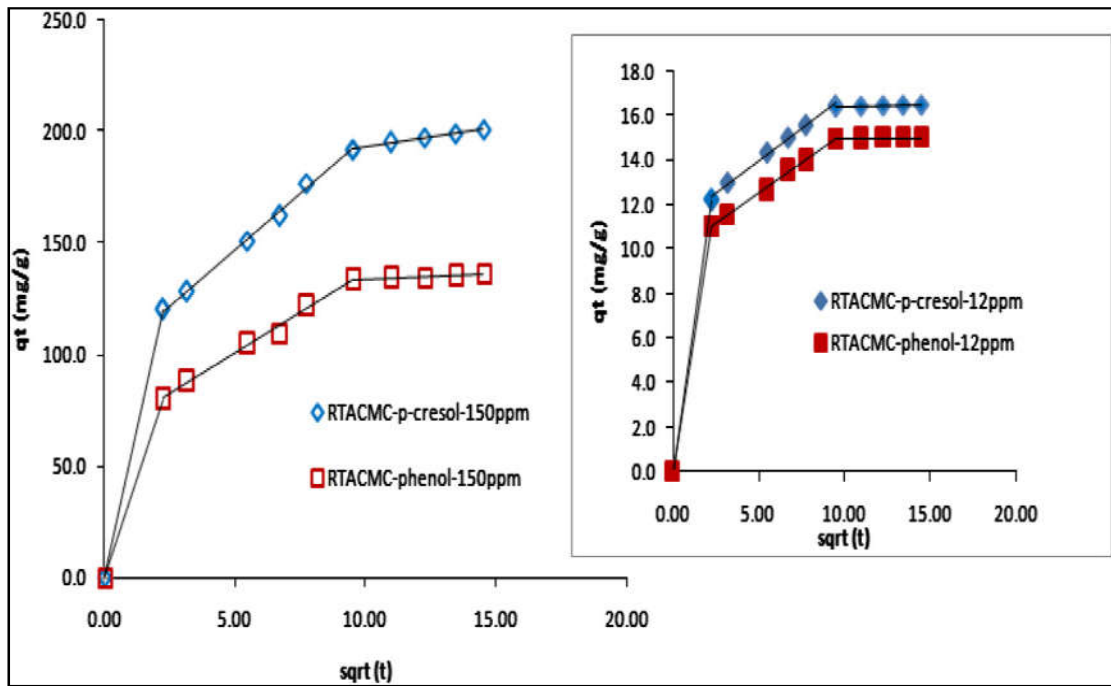


Figure 5.8 Weber Morris plot of adsorption of p-cresol and phenol onto RTACMC at two different concentrations of 12 ppm and 150 ppm.

Table 5.5 Intraparticle diffusion model parameters for the adsorption of p-Cresol and phenol onto developed adsorbent RTACMC and RTAC

Adsorbent	RTACMC				RTAC			
	p-Cresol		Phenol		p-Cresol		Phenol	
Concentration (in ppm)	12	150	12	150	12	150	12	150
Exp _{q_e} (mg/g)	16.52	201.00	15.00	136.50	9.60	85.50	5.66	37.50
Intra-particle diffusion								
K _{id} (mg/g/min ^{1/2}) ^{2nd} region	0.124	1.944	0.095	1.46	0.182	0.184	0.132	1.592
C	14.97	173.1	13.84	117.01	6.893	57.90	3.91	15.41
R ²	0.884	0.995	0.794	0.941	0.990	0.989	0.963	0.957

Novel adsorbent for noxious impurities removal

For both phenol and p-cresol, (Figure 5.8 and Table 5.5) at low adsorbate concentration of 12 ppm, the pore diffusion rate as well as the thickness of the boundary layer was very low as indicated by the slope and intercept of the second region. Increasing the adsorbate concentration to 150 ppm resulted in a simultaneous increase in the slope and intercept thereby signifying an enhancement of the driving force for the adsorption process as well as the increase in the thickness of the boundary layer. But none of the linear plots of the second and third region passed through the origin thus implying that although intraparticle diffusion is involved in the adsorption process, it is not the sole rate-controlling step and that some other mechanisms may play an important role.

5.2.9. Comparison with other reported adsorbents

The adsorption capacity (values of Q_{\max} derived from the Langmuir equation) of Ni^{2+} adsorption on activated carbon with other previously developed adsorbents, is summarized in Table 5.6. The obtained summarized data clearly revealed that the developed activated carbon i.e. RTACMC and RTAC possess higher adsorption capacity in comparison to the other previously developed adsorbent [30,34-36].

Table 5.6 Comparison of maximum adsorption capacity for the removal of noxious p-Cresol and phenol by different previously developed adsorbents.

Adsorbent	Adsorbate	Adsorption capacity (mg g^{-1})	Ref.
Fly ash	Phenol	13.16	[34]
Bagasse fly ash	Phenol	0.060	[30]
Coal fly ash	p-Cresol	85.40	[35]
Wood fly ash	p-Cresol	52.50	[36]
RTAC	p-Cresol	71.43	[Present Study]
RTAC	Phenol	47.62	[Present Study]
RTACMC	p-Cresol	250.00	[Present Study]
RTACMC	Phenol	100.00	[Present Study]

5.3 Conclusion

The focus of the present study was to assess the feasibility of activated carbons prepared from waste rubber tire by a microwave induced chemical impregnation technique, the developed adsorbent i.e. RTACMC and RTAC for the removal of model phenolic compounds from the solvent phase. The following conclusions are bulletined:

1. The developed adsorbent (RTACMC) upon characterization revealed the improved porosity and total pore volume as compared to a fairly acidic RTAC which was prepared by the conventional physical activation of rubber tire. Such favorable characteristics helped in improving the adsorption capacity and kinetics of RTACMC for both p-cresol and phenol removal as compared to RTAC.
2. Irrespective of the adsorbents, p-cresol showed higher affinity due to its low solubility whereas phenol showed higher kinetic rate constant due to its smaller size.
3. Results obtained revealed that a 0.6 g/L adsorbent dose was found to be optimum at a pH of 7, contact time of 90 min and 120 min for RTACMC and RTAC, in addition to this the temperature of 45°C is fixed as optimized time for achieving maximum removal from the solvent phase.
4. The kinetic study revealed a pore diffusion mechanism to be operative in all cases. The microwave technique thus helped in the development of an enhanced porous morphology in a shorter time resulting in the improvement of the cost effectiveness of the process.
5. Finally, a comparative study with other reported adsorbents reveals the potential of the developed activated carbon for wastewater treatment.
6. Summarily, the developed adsorbent i.e. RTACMC and RTAC has the potential for removal of p-Cresol and phenol from wastewater to a significant extent.

References

- [1] Agency for Toxic Substances and Disease Registry (ATSDR), Toxicological profile for cresols (Draft). US Public Health Service, US Department of Health & Human Services, Atlanta, GA, 1990.
- [2] Wanga K.H., Hsieh Y. H. , Chou M.Y. , Chang C. Y., “Photocatalytic degradation of 2-chloro and 2-nitrophenol by titanium dioxide suspensions in aqueous solution,” *Appl. Catal. B Environ.*, 21, (1999), 1–8.
- [3] Garcia,J.,Diez,F., Coca,J., “Métodos alternativos para el tratamiento de efluentes fenólicos industriales”, *Ing. Quim.*, 238, (1989), 151–158.
- [4] US-EPA, Environmental Protection Agency. Integrated Risk Information System (IRIS) on 4-Methylphenol, National Center for Environmental Assessment, Office of Research and Development, Washington, DC, 1999.
- [5] Directive 2000/60/EC of the European Parliament and of the Council establishing a framework for the Community action in the field of water policy, Official Journal L 327 on 22 December 2000 (2000).
- [6] World Health Organization (WHO), International standards for Drinking water, Geneva, 1963, p. 40.
- [7] Williams P.T., Besler S., Taylor D.T., “The pyrolysis of scrap automotive tyres, the influence of temperature and heating rate production composition,” *Fuel*, 69, (1990), 1474–1482.
- [8] Murillo R., Aylón E., Navarro M.V., Callén M.S., Aranda A., Mastral A.M., “The application of thermal processes to valorise waste tyre,” *Fuel. Process. Technol.* 87, (2006), 143–147.
- [9] Knocke W.R., Hemphill L.H., “Mercury(ii) sorption by waste rubber,” *Water Res.*, 15, (1981), 275–282.
- [10] Mechant, A.A., Petrich, M.A., “Pyrolysis of scrap tires and conversion of chars to activated carbon,” *AIChE J.*, 39, (1993), 1370–1376.
- [11] Teng H., Serio M.A., Wojtowicz M.A., Bassilakis B., Solomon P.R., “Reprocessing of used tires into activated carbon and other products,” *Ind. Eng. Chem. Res.*, 34, (1995), 3102–3111.
- [12] Cunliffe A., Williams P.T., “Influence of Process Conditions on the Rate of Activation of Chars Derived from Pyrolysis of Used Tires,” *Energy Fuel*, 13, (1999), 166–175.
- [13] Lin Y.R., Teng H., “Mesoporous carbons from waste tire char and their application in wastewater discoloration,” *Micropor. Mesopor. Mater.*, 54, (2002), 167–174.

- [14] Miguel G.S., Fowler G.D., Sollars C.J., “A study of the characteristics of activated carbons produced by steam and carbon dioxide activation of waste tyre rubber,” *Carbon*, 41, (2003), 1009–1016.
- [15] Helleur R., Popovic N., Ikura M., Stanciulescu M., Liu D., “Characterization and potential applications of pyrolytic char from ablative pyrolysis of used tires,” *J. Anal. Appl. Pyrol.*, 58–59, (2001), 813–824.
- [16] Ariyadejwanich P., Tanthapanichakoon W., Nakagawa K., Mukai S.R., Tamon H., “Preparation and characterization of mesoporous activated carbon from waste tires,” *Carbon*, 41, (2003), 157–164.
- [17] González J.F., Encinar J.M., González-García C.M., Sabio E., Ramiro A., Canito J.L., Gañán J., “Preparation of activated carbons from used tyres by gasification with steam and carbon dioxide,” *Appl. Surf. Sci.* 252 (2006) 5999–6004.
- [18] Suuberg E.M., Aarna I., “Porosity development in carbons derived from scrap automobile tires,” *Carbon*, 4, (2007), 1719–1726.
- [19] Betancur M., Martínez J.D., Murillo R., “Production of activated carbon by waste tire thermochemical degradation with CO₂,” *J. Hazard. Mater.*, 168, (2009), 882–887.
- [20] Suuberg E.M., Aarna I., “Kinetics of tire derived fuel (TDF) char oxidation and accompanying changes in surface area,” *Fuel*, 88, (2009), 179–186.
- [21] López G., Olazar M., Artetxe M., Amutio M., Elordi G., Bilbao J., “Catalytic pyrolysis of HDPE in continuous mode over zeolite catalysts in a conical spouted bed reactor,” *J. Anal. Appl. Pyrol.*, 85, (2009), 539–543.
- [22] Hesas, R.H., Daud, W.M.A.W., Sahu, J.N., Niya, A.A., “The effects of a microwave heating method on the production of activated carbon from agricultural waste: A review,” *J. Anal. Appl. Pyrol.*, 100, (2013), 1–11.
- [23] Foo K.Y., Hameed B.H., “Preparation, characterization and evaluation of adsorptive properties of orange peel based activated carbon via microwave induced K₂CO₃ activation,” *Bioresour. Technol.*, 103, (2012), 398–404.
- [24] Maldhure A.V., Ekhe J.D., “Preparation and characterizations of microwave assisted activated carbons from industrial waste lignin for Cu(II) sorption,” *Chem. Eng. J.*, 168, (2011), 1103–1111.
- [25] Gupta V.K., Gupta B., Rastogi A., Agarwal S., Nayak A., “A comparative investigation on adsorption performances of mesoporous activated carbon prepared from waste rubber tire and activated carbon for a hazardous azo dye—Acid Blue 113,” *J. Hazard. Mater.*, 186, (2011), 891–901.

- [26] Deng H., Li G., Yang H., Tang J., Tang J., "Preparation of activated carbons from cotton stalk by microwave assisted KOH and K₂CO₃ activation," *Chem. Eng. J.*, 163, (2010), 373–381.
- [27] Foo K.Y., Hameed B.H., Utilization of rice husks as a feedstock for preparation of activated carbon by microwave induced KOH and K₂CO₃ activation," *Bioresour. Technol.*, 102, (2011), 9814–9817.
- [28] Foo K.Y., Hameed B.H., "Porous structure and adsorptive properties of pineapple peel based activated carbons prepared via microwave assisted KOH and K₂CO₃ activation," *Micropor. Mesopor. Mater.*, 148, (2012), 191–195.
- [29] Huang J., "Treatment of phenol and p-cresol in aqueous solution by adsorption using a carbonylated hypercrosslinked polymeric adsorbent," *J. Hazard. Mater.*, 168, (2009), 1028–1033.
- [30] Dubinin M.M., Zaverina E.D., Radushkevich L.V., "Sorption and structure of activated carbons, I. Adsorption of organic vapours," *Zh. Fiz. Khim.*, 21, (1947), 1351–1362.
- [31] Gupta V.K., Gupta B., Rastogi A., Agarwal S., Nayak A., "Pesticides removal from waste water by activated carbon prepared from waste rubber tire," *Water Res.*, 45, (2011), 4047–4055.
- [32] Mahvi A.H., Maleki A., Eslami A., "Potential of Rice Husk and Rice Husk Ash for Phenol Removal in Aqueous Systems," *Am. J. Appl. Sci.*, 1, (2004), 321–326.
- [33] Nouri S., Haghseresht F., Lu G.Q.M., "Comparison of Adsorption Capacity of p-Cresol & p-Nitrophenol by Activated Carbon in Single and Double Solute," *Adsorption*, 8, (2002), 215–223.
- [34] Sarkar, M., Acharya, K.P., "Use of fly ash for the removal of phenol and its analogues from contaminated water," *Waste Manage.*, 26, (2006), 559–570.
- [35] Ahmaruzzaman M., Sharma D.K., "Adsorption of phenols from wastewater," *J. Colloid Interface Sci.*, 287, (2005), 14–24.
- [36] Otero M., Rozada F., Calvo L.F., García A.I., Morán A., Elimination of organic water pollutants using adsorbents obtained from sewage sludge," *Dyes Pigments*, 57, (2003), 55–60.



CHAPTER 6

CuO-NP-AC For Removal of Noxious Acid Blue 129



6.1. Introduction

Nowadays, in such an industrial world one of the most important concerns is securing the health of human race and environment. Presence of dyes and pigments in wastewaters of manufacture and textile industry contain auxiliary chemicals [1] lead to generation of hazardous injuries to the animal and human health [2]. Colored dyes are not only aesthetic, carcinogenic but also hinder light penetration and disturb life processes of living organisms in water.

Acid Blue 129 (AB129), an acidic dye, it possess severe detrimental effect on human health, itcauses eyes irritation, respiratory system, pulmonary disorder and several dermatitis problems. Therefore, the removal of such colored agents from aqueous effluents is necessary. Recently, adsorption has become one of the most popular techniques because of some advantages such as high efficiency and ability to use generable non-toxic and cheap adsorbents [3-17]. For this, nanoparticles as sorbents for separation, removal and or pre-concentration are applicable for enrichment of trace elements are its effective protocol [18].

The objective of the presented work is to investigate the preparation of a new and effective sorbent for the adsorption of AB 129 dye. The effects of adsorbent dosage, initial dye concentration, pH, contact time and temperature on AB 129adsorption onto CuO-NP-AC were studied. Adsorption kinetics, isotherms and thermodynamic parameters were also evaluated and reported.

6.2. Results and discussion

6.2.1. Characterization of CuO nanoparticles

XRD analysis as powerful tools was used to study the crystal structures of the CuO nanoparticles. Figure 6.1(a) displays the XRD spectrum of CuO nanoparticles, it reveals the sample indexes to tenorite, syn CuO (JCPDS number 00-045-0937) although have different intensities of crystallinity. The two reflection at $2\theta = 35.54$ [002] and $2\theta = 38.52$ [111] were observed in the diffraction patterns, and are ascribed to the formation of the CuO monoclinic crystal phase. The average size of nanocrystallites (D) was estimated by the Scherer's formula [19].The average crystallite thickness of CuO is estimated about 26.57nm by Scherer's formula.

The FE-SEM is the primary tool used for characterization of the surface morphology and fundamental physical properties of photo-catalyst surface. It is useful for determination of the particle size, shape, porosity. Morphology and microstructure of the CuO nanoparticles

according to FE-SEM studies (Figure 6.1 (b)) reveals that the CuO nanoparticles possess considerable number of pores, with irregular pore distribution which helps in the trapping and adsorption of dyes into these pores.

The volume average hydrodynamic diameter for the CuO nanoparticles, which is determined by the laser light scattering, was found less than 25 nm with narrow size distribution of 0.15 polydispersity (Figure 6.1 (c)).

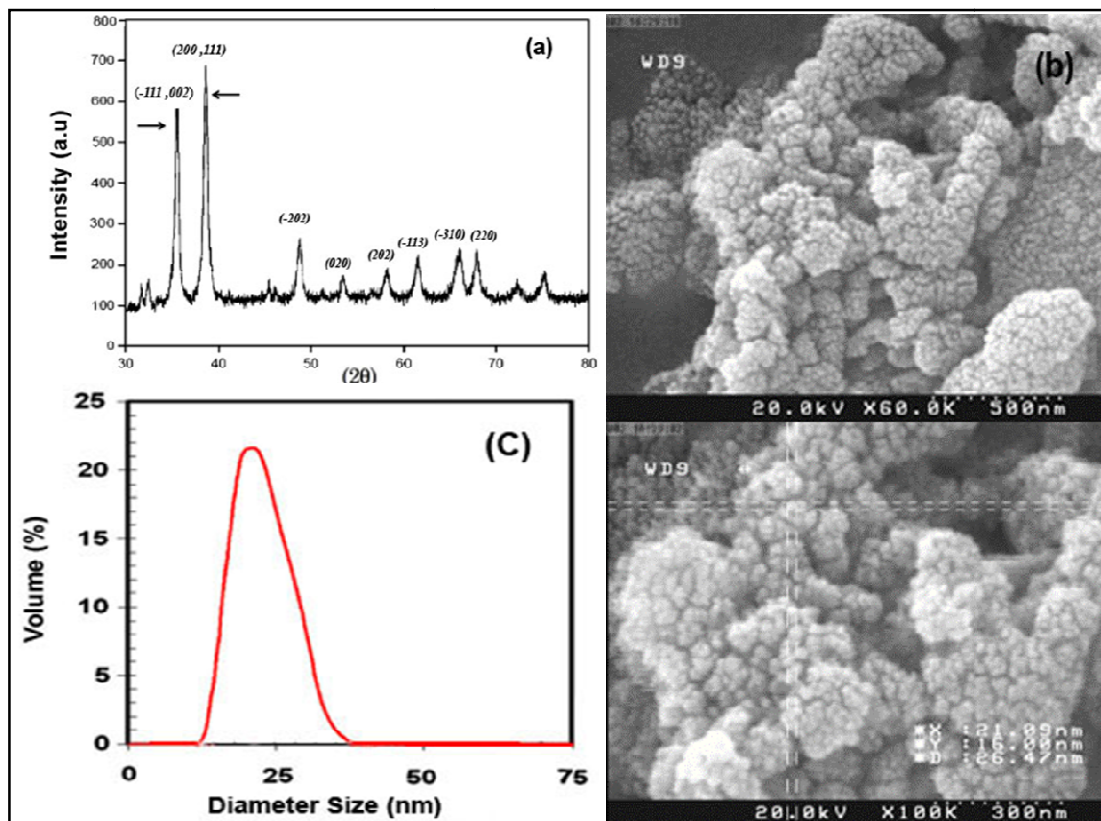


Figure 6.1 (a) X-ray diffraction (XRD) pattern (b) FE-SEM images and (c) Histogram of size distribution of the CuO nanoparticles.

6.2.2 Effect of initial solution pH

The pH of the solution is considered to be the most important controlling parameter in the adsorption process [20]. Figure 6.2 shows the effect of solution pH on the removal of AB 129 on the CuO-NP-AC. It was observed that the AB 129 removal was highly dependent on the pH of the solution which affected the surface charge of the sorbent. The maximum removal efficiency (around 99.9%) occurred at pH 2.0, then the removal percentage decreased dramatically as the initial solution pH increased from 4.0 to 8.0. At lower pH, both activated carbon functional groups and oxygen atoms were protonated and adsorbent acquired positive charge and finally AB 129 dye (anionic dye molecule) adsorbed onto CuO-NP-AC through

attraction forces. Dye adsorption via physical or chemical forces is another alternative possible adsorption mechanism. At lower pH, probably surface of adsorbent has positive charge due to (protonation of functional group of CuO-AC in highly acidic solution) which favors the adsorption of the dye over CuO-AC. While on increasing pH, the number of negatively charged sites of adsorbent increase hence as a result of electrostatic repulsion between dye anions and adsorbent the removal efficiency was decreased. It seems that in alkaline pH, number of OH⁻ ions, on the adsorbent surface significantly increased that led to decrease in removal efficiency [21, 22].

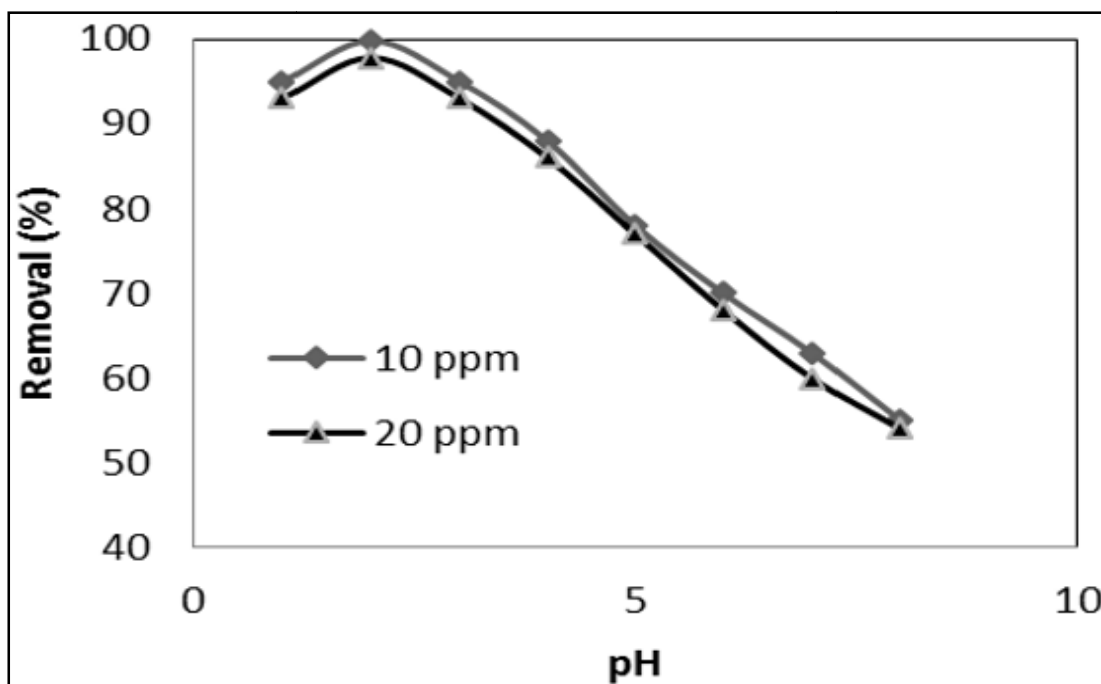


Figure 6.2 Effect of pH on the removal of AB 129 by CuO-NP-AC at room temperature, adsorbent dosage of 0.045g in 50 mL, contact time of 20 and 25 min for dye concentrations of 10 and 20 mg L⁻¹, respectively.

6.2.3 Effect of contact time

Equilibrium time is one of the important parameters to design a low cost wastewater treatment system [21]. The effect of the contact time on the adsorption was investigated in the range of 1.0 to 30 min at room temperature. The results obtained are presented in the form of Figure 6.3, it shows the removal percentage of AB 129 dye at initial concentrations of 10 and 20 mg L⁻¹ at pH 2.0. The adsorption efficiency increases with increasing contact time and reaches constant and maximum value after 20 and 25 min. Hence, the optimum time of 20 and 25 min at 400 rpm stirring rate was selected for quantitative adsorption of AB 129 dye at initial concentrations of 10 and 20 mg L⁻¹ for subsequent works. At higher concentration due to a

decrease in the ratio of AB 129 to CuO-NP-AC surface area the rate of diffusion and migration decreased.

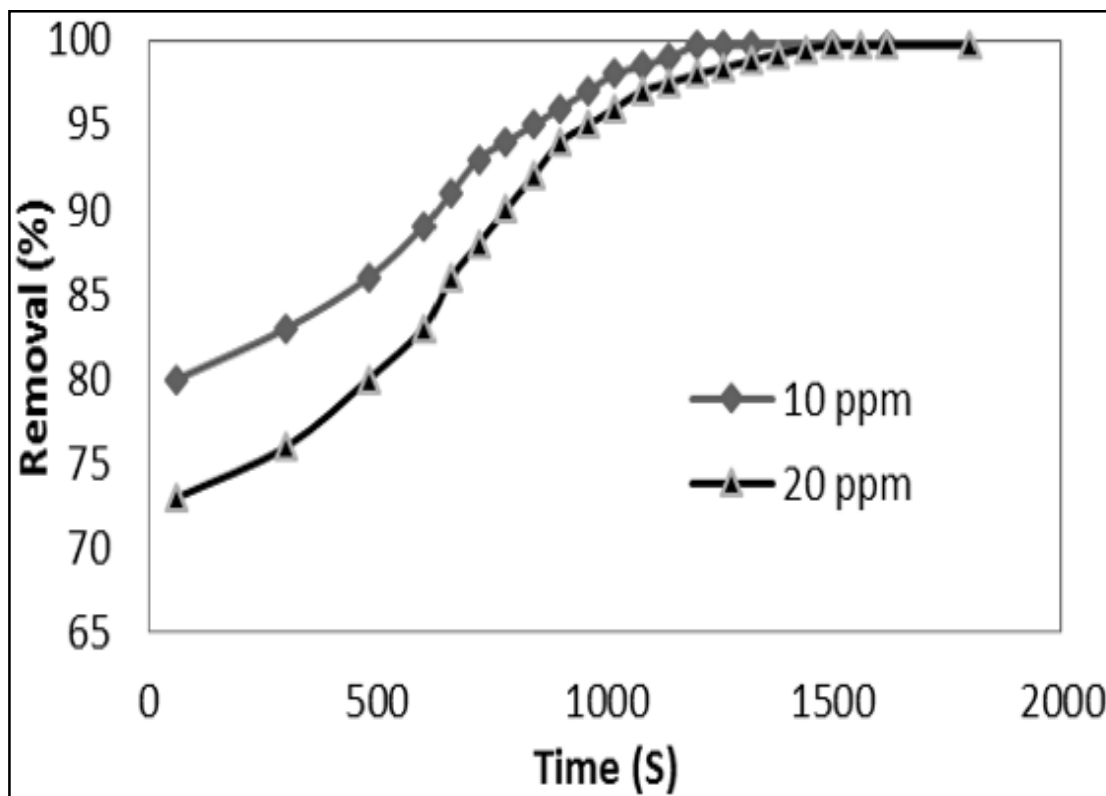


Figure 6.3 Effect of contact time on the removal of AB 129 at 0.045 g of CuO-NP-AC in 50 mL at pH 2, at room temperature and AB 129 concentration of 10 and 20 mg L⁻¹.

6.2.4 Effect of the amount of adsorbent

Amount of adsorbent is another important parameter which also controls the adsorption capacity of adsorbent. The effect of CuO-NP-AC dose on the adsorption of AB 129 from aqueous solutions was investigated using various adsorbent doses (0.01–0.06 g) at a constant AB 129 concentration of 10 and 20.0 mgL⁻¹. As shown in Figure 6.4, the removal efficiency of AB 129 by CuO-NP-AC increased sharply as the sorbent dose increased from 0.01 to 0.045g, then reached an almost constant value. However, as expected, the adsorption capacities decreased with increasing adsorbent mass, due to the reduction in both effective surface area and adsorbate/adsorbent ratio [20]. The removal efficiency was maximum when the CuO-NP-AC dose was 0.9 g/L, hence 0.9 g/L was chosen as the optimum adsorbent dose for further experiments.

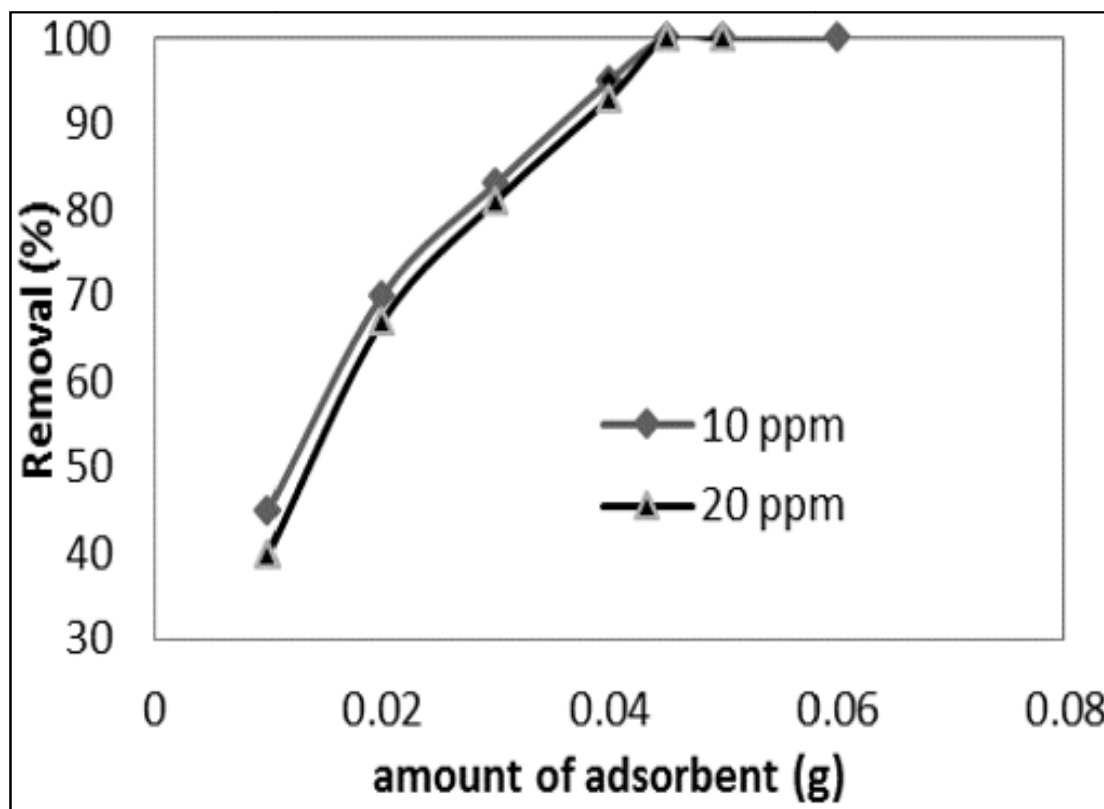


Figure 6.4 Effect of adsorbent dosage on the removal of AB 129 at pH 2, at room temperature and AB 129 concentration of 10 and 20 mg L⁻¹.

6.2.5 Effect of initial dye concentration on adsorption of AB 129

In order to investigate the effect of initial concentration of AB 129 on adsorption of AB 129, the effect of AB 129 concentration in the range of 10–80 mg L⁻¹ on its adsorption using the CuO-NP-AC was well investigated and elucidated and the amount and percentage of AB 129 removal at different initial concentrations were presented in Figure 6.5. From Figure 6.5, it is observable that increase in initial dye concentration has positive correlation with removal percentage and the percentage of dyes removal was greater at lower initial concentrations and smaller at higher initial concentrations. This synergic correlation is assigned to the enhancement in the bulk and film diffusion of target compounds to the external surface of adsorbent and their subsequent pore diffusion [23]. Initial dyes concentration at fixed value of adsorbent has reverse correlation with equilibrium time. The limiting factor for dye adsorption is the available sites on the adsorbent. It is obvious in Figure 6.5, at 0.045 g of adsorbent by increasing concentration from 10 to 60 mg L⁻¹ of AB 129, the removal percentage decrease from 99.8% to 85.4%.

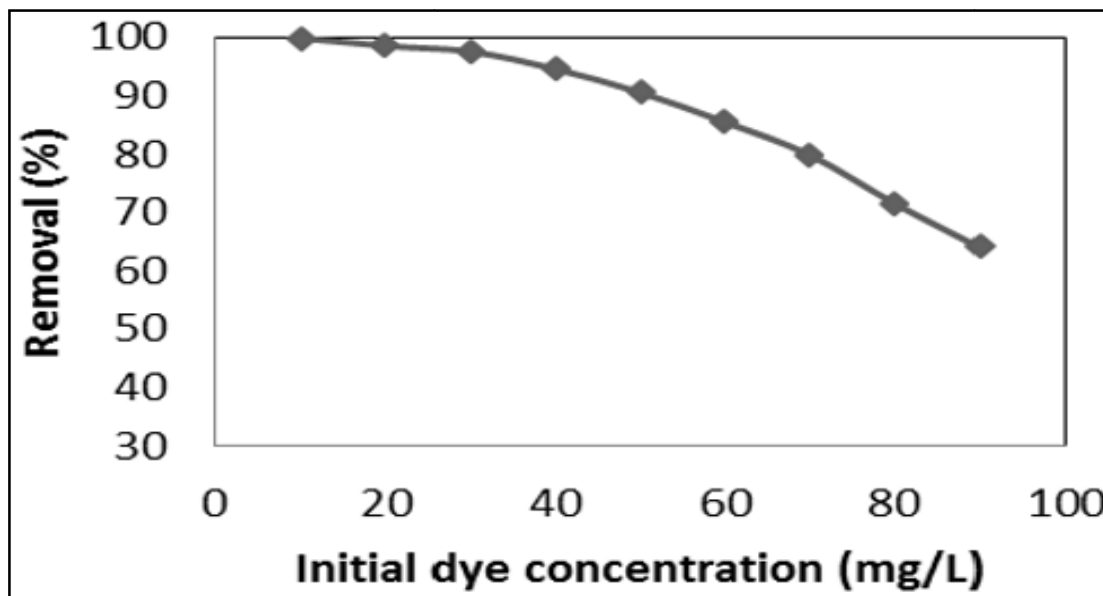


Figure 6.5 Effect of initial dye concentration on the removal of AB 129 at 0.045 g of CuO-NP-AC in 50 mL at pH 2.0 at room temperature.

6.2.6 Effect of temperature

Temperature plays an important factor in order to determine whether the ongoing adsorption process is endothermic or exothermic naturally. Figure 6.6 shows that the removal percentage of AB 129 increases with increasing temperature and the maximum adsorption occurs at temperature of 333.15 K, this shows the endothermic nature of adsorption. It is observable from Figure 6.6 that the temperature has main effect on the adsorption process.

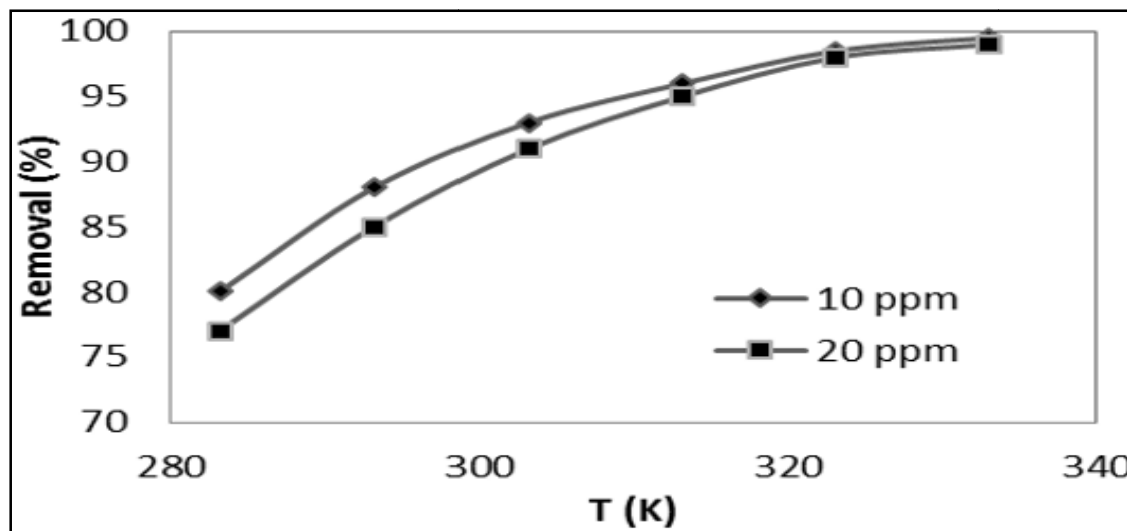


Figure 6.6 Effect of temperature on the removal of AB 129 at 0.045 g of CuO-NP-AC in 50 mL at pH 2, and AB 129 concentration of 10 and 20 mg L⁻¹.

6.2.7. Adsorption isotherm modelling

To find out the most suitable adsorption model, the isotherm data thus obtained were simulated, by the well-known mathematical equations of Langmuir, Freundlich, Temkin and D-R, isotherm models. The values of regression coefficients obtained from these model's plots were also evaluated, which were used as a fitting criteria to find out suitable model. The results of their linear regression i.e. correlation coefficients and the parameters obtained from the plots of Langmuir ($1/q_e$ vs $1/C_e$), Freundlich ($\log q_e$ versus $\log C_e$), Temkin q_e vs $\ln C_e$ and D-R ($\log q_e$ vs ε^2), are listed Table 6.1.

The results presented in Table 6.1 clearly reveal the value of correlation coefficients (R^2) for Acid Blue 129. The correlation coefficient was considerably high ($R^2 > 0.99$) for the Langmuir model followed by the Freundlich, Temkin and D-R, isotherm models; the linearity of plots as evident from Figure 6.7 and from high correlation coefficient values in Table 6.1 suggests the applicability of the Langmuir model with the Acid Blue 129 getting adsorbed onto the adsorbent surface to form a monolayer.

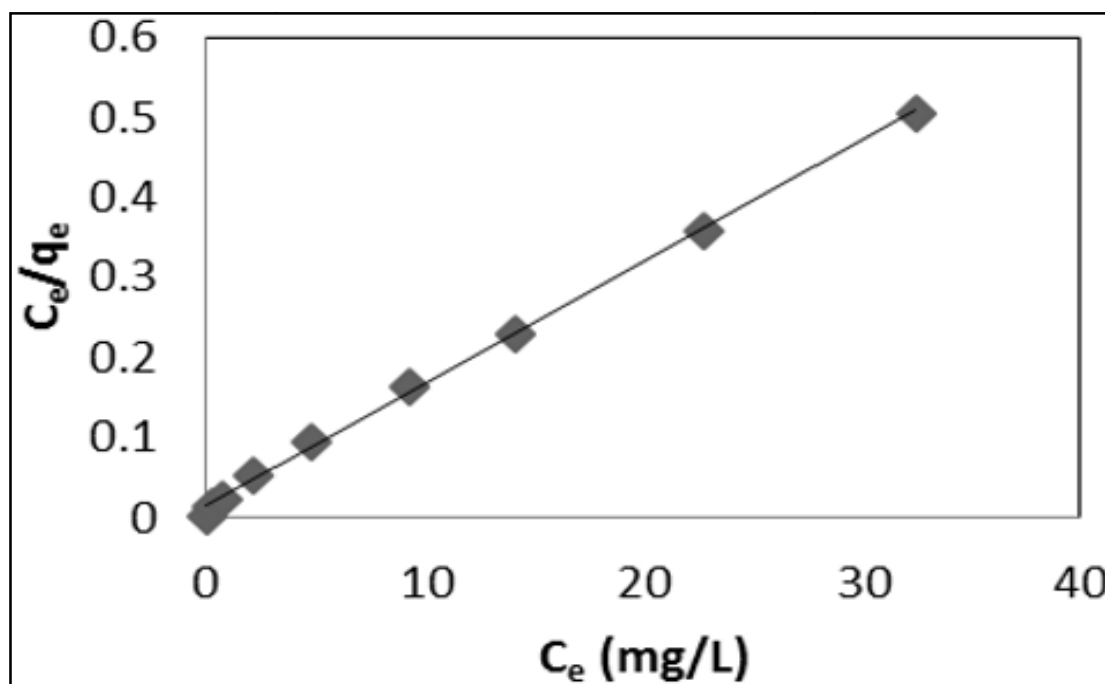


Figure 6.7 Langmuir isotherm for adsorption of AB 129 onto 0.045 g of CuO-NP-AC in 50 mL of different initial dye concentration, room temperature, pH 2.

The value of R_L indicates the shape of Langmuir isotherm and nature of the adsorption process. The R_L value in the range of 0-1 reveals the favourable nature of the isotherm model.

Novel adsorbent for noxious impurities removal

As per results revealed in the Table 6.1 the calculated values of R_L were found to be in the range of 0–1, indicating that the adsorption process was favorable for CuO-NP-AC.

From the calculated values of D–R presented in Table 6.1, as the value of E is 5.0 kJ mol⁻¹ it reveals that the physio-sorption process plays an important role in the adsorption of AB 129 onto CuO-NP-AC.

Table 6.1 Isotherm parameters correlation coefficients calculated by various adsorption models onto 0.045 g of CuO-NC-AC in 50 mL, pH 2, and room temperature.

Isotherm	Values of parameters
Langmuir	
Q _m (mg/g)	65.36
K _L (L/mg)	1.142
R _L	0.0096-0.081
R ²	0.9985
Freundlich	
1/n	0.2461
K _F (L/mg)	31.35
R ²	0.9777
Temkin	
B ₁	7.970
K _T (L/mg)	108.92
R ²	0.9721
D-R Model	
Q _s (mg/g)	48.740
E (KJ/mol)	5
R ²	0.755

6.2.8. Thermodynamic study

Thermodynamic parameters including change in the Gibbs free energy (ΔG^0 , kJ/mol), enthalpy (ΔH^0 , kJ/mol), and entropy (ΔS^0 , kJ/(mol K)) during the adsorption process was well evaluated and investigated. The negative value of ΔG^0 and the decrease in its value with raising temperature confirms the spontaneous nature and feasibility of the adsorption via physical force (Table 6.2). The data (Figure 6.8 and Table 6.2) show positive values of ΔH^0 that indicate the endothermic nature of the adsorption.

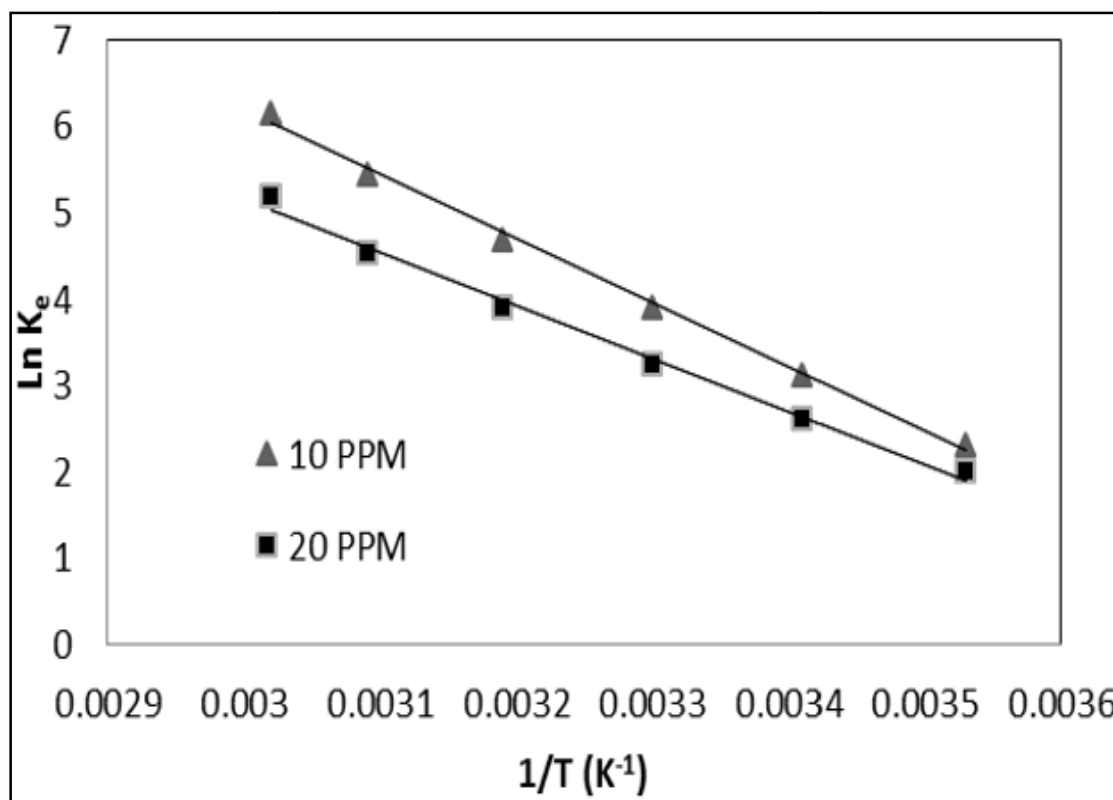


Figure 6.8 Van't Hoff plots of AB 129 dye onto CuO-NP-AC for evaluating thermodynamics parameters.

Furthermore, the positive values of ΔS^0 show the affinity of CuO-NP-AC for AB 129 and the increasing randomness at the solid–solution interface with some structural changes in the adsorbates and adsorbents during the adsorption process. To further support the assertion that physical adsorption is the predominant mechanism, the values of activation energy (E_a) and sticking probability (S^*) were estimated. The values of S^* presented in Table 6.2 was found to be 3.59×10^{-12} and 1.68×10^{-10} that lie in the range $0 < S^* < 1$ and is dependent on the temperature of the system.

Table 6.2. Thermodynamic parameters for adsorption of AB 129 onto 0.045 g of CuO-NP-AC at pH 2.0 at initial dye Concentration of 10 and 20 mg/L

Co mg/L	Temp (K)	Thermodynamic Parameters					S*
		Ke	ΔG KJ/mol	ΔH KJ/mol	ΔS KJ/Kmol	Ea KJ/ mol	
10	283.15	10.17	-5.46	61.60	236.18	48.77	3.59×10^{-12}
	293.15	22.55	-7.33				
	303.15	50.16	-9.87				
	313.15	110.30	-12.24				
	323.15	230.89	-14.62				
	333.15	471.25	-17.05				
20	283.15	7.50	-4.74	50.94	195.67	44.44	1.68×10^{-10}
	293.15	13.61	-6.36				
	303.15	25.55	-8.17				
	313.15	49.17	-10.14				
	323.15	93.78	-12.2				
	333.15	178.87	-14.37				

6.2.9. Adsorption Kinetics

Two kinetic models namely pseudo-first-order and pseudo-second-order have been applied and were used to test adsorption kinetics data in order to investigate the mechanism involved during the adsorption of Acid Blue 129 onto the developed adsorbent i.e. CuO—NP-AC.

Table 6.3 lists the results of the kinetic parameters of the two models as well as their regression coefficients (R^2) at different concentration initial concentration 10 and 20mg/L of Acid Blue 129 concentration. The value of correlation coefficient (R^2) for the pseudo-second-order kinetic model is comparatively high (>0.99), and the adsorption capacities calculated by the model are also close to those values which are obtained experimentally.

Table 6.3 Adsorption kinetic parameters at different initial AB 129 onto 0.045 g of CuO-NC-AC in 50 mL at pH 2.0 at room temperature and AB 129 concentration of 10 and 20 mg/L.

Adsorbent	CuO-NP-AC	
	10	20
Concentration (in mg/L)	10	20
Exp q_e (mg/g)	11.08	22.16
Pseudo-first-order		
Calculated q_e (mg/g)	5.14	18.20
K_1 (min^{-1})	0.181	0.192
R^2	0.8668	0.9035
Pseudo-second-order		
Calculated q_e (mg/g)	11.52	23.87
K_2 (g/mg/min)	0.0170	0.085
R^2	0.9957	0.9937

Figure 6.9 indicates the linear plots of t/q_t vs. t at two different adsorbate concentrations for RTACMC and RTAC showing the applicability of the pseudo-second-order model and thus can be concluded to be more suitable to describe the adsorption kinetics of the Acid Blue 129 onto the developed adsorbent i.e. CuO-NP-AC.

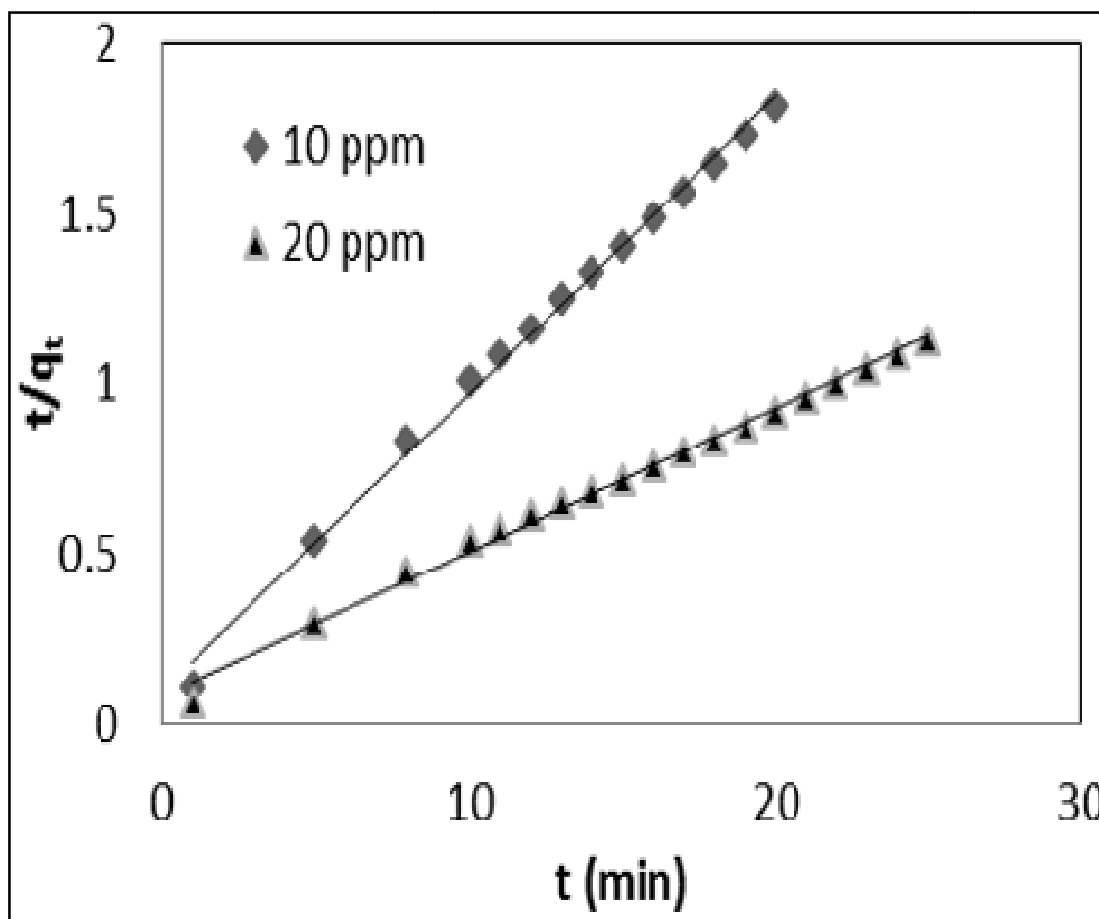


Figure 6.9 Pseudo-second-order plots at two different adsorbate concentrations i.e. 10 and 20 mg/L for adsorbent CuO-NP-AC

6.2.10. Adsorption mechanism

Prediction of the rate-limiting step is an important factor to be considered in the adsorption process [29]. For solid-liquid adsorption process, the solute transfer process is usually characterized by either external mass transfer (boundary layer diffusion) or intraparticle diffusion or both. In the present study, intraparticle diffusion plot of q_t vs. $t^{0.5}$ (Figure 6.10) were plotted for CuO-NP-AC for Acid Blue 129 at two different concentrations i.e. 10 mg/L and 20 mg/L.

A larger C value indicates a greater effect of the boundary layer [50]. The deviation of correlation coefficient values (R^2) values (Table 6.4 and Figure 6.10) from unity indicates suggests the inapplicability of this model and hence the rate-limiting step is not the intraparticle diffusion process.

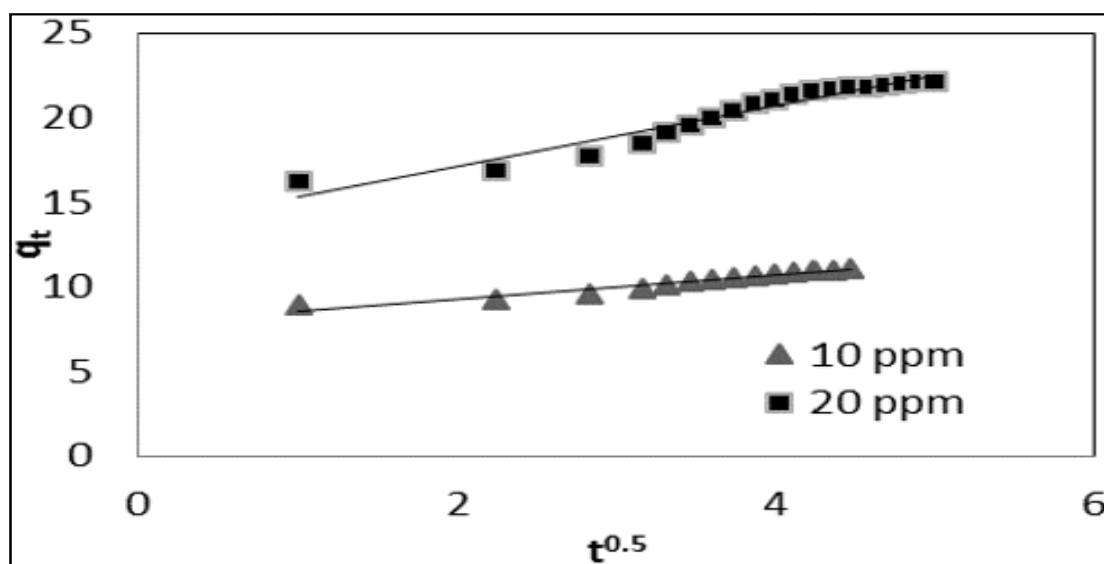


Figure 6.10 Plots of Intraparticle diffusion model for dye concentration of 10 and 20 mg/L.

6.2.11. Comparison with other previously developed adsorbents

The adsorption capacity (values of Q_{\max} derived from the Langmuir equation) and contact time of Acid Blue 129 adsorption on activated carbon with other previously developed adsorbents is summarized in Table 6.4. The obtained summarized data clearly revealed that the developed adsorbent i.e. CuO-NP-AC possess higher adsorption capacity and short contact time in comparison to the other previously developed adsorbent [24-26].

Table 6.4 Comparison of performance of proposed method with some previously reported acid blue dyes adsorption systems.

Adsorbent	Q_{\max} (mg g^{-1})	Contact time (min)	Ref.
Activated carbon cloth	61.43	498	[25]
Almond shell	11.95	14	[24]
Bentonite-CTAB	1.54	>100	[26]
Raw bentonite	1.05	>1000	[26]
CuO-NP-AC	65.36	1-25	[Present Study]

6.3 Conclusions

The focus of the present study was to assess the feasibility of nanoparticle as efficient adsorbent for the removal of noxious Acid Blue 129 from the solvent phase. The following conclusions are bulletined:

1. The developed adsorbent i.e. CuO-NP-AC upon characterization revealed the reveals that the CuO nanoparticles possess considerable number of pores, with irregular pore distribution which helps in the trapping and adsorption of dyes into these pores. Such favorable characteristics helped in improving the adsorption capacity and kinetics of CuO-NP-AC
2. Results obtained revealed that a 0.9 g/L adsorbent dose was found to be optimum at a pH of 2, contact time of 20 min and 25 min for dye concentration 10 and 20 mgL⁻¹, in addition to this the room temperature is fixed as optimized temperature for achieving maximum removal from the solvent phase.
3. The maximum removal efficiency (around 99.9%) occurred at pH 2.0, then the removal percentage decreased dramatically as the initial solution pH increased from 4.0 to 8.0. At lower pH, both activated carbon functional groups and oxygen atoms were protonated and adsorbent acquired positive charge and finally AB 129 dye (anionic dye molecule) adsorbed onto CuO-NP-AC through attraction forces.
4. Increase in initial dye concentration has positive correlation with removal percentage and the percentage of dyes removal was greater at lower initial concentrations and smaller at higher initial concentrations.
5. Change in activation enthalpy (ΔH°), free energy of adsorption (ΔG°) and entropy (ΔS°) show the spontaneous and the endothermic feature of adsorption process.
6. Finally, a comparative study with other reported adsorbents reveals the potential of the synthesized nanoparticle i.e. CuO-NP-AC for wastewater treatment.
7. Summarily, the developed adsorbent i.e. CuO-NP-AC has the potential for removal of Acid Blue 129 from wastewater to a significant extent.

References

- [1] Noroozi B., Sorial G.A., Bahrami H., Arami M., “Adsorption of binary mixtures of cationic dyes,” *Dyes Pigm.* 76, (2008), 784–791.
- [2] Sturm K., Williams E., Macek K.J., “Fluorescent whitening agents. Acute fish toxicity sand accumulation studies,” *Water Resour.*, 9, (1973), 211–219.
- [3] Mittal A., Mittal J., Kurup L., Singh A.K., “Process development for the removal and recovery of hazardous dye erythrosine from wastewater by waste materials—bottom ash and deoiled soya as adsorbents,” *J. Hazard. Mater.*, 138, (2006), 95–105.
- [4] Mittal A., Mittal J., Kurup L., “Utilization of hen feathers for the adsorption of indigo carmine from simulated effluents,” *J. Environ. Prot. Sci.*, 1, (2007), 92–100.
- [5] Mittal A., Mittal J., Malviya A., Gupta V.K., “Removal and recovery of Chrysoidine Y from aqueous solutions by waste materials,” *J. Colloid. Interface. Sci.*, 344, (2010), 497–507.
- [6] Mittal A., Gajbe V., Mittal J., “Removal and recovery of hazardous triphenyl methane dye, Methyl Violet through adsorption over granulated waste materials,” *J. Hazard. Mater.*, 150, (2008), 364–375.
- [7] Mittal A., Kaur D., Mittal J., “Batch and bulk removal of a triarylmethane dye, fast green FCF, from wastewater by adsorption over waste materials,” *J. Hazard. Mater.*, 163, (2009), 568–577.
- [8] Mittal A., Kaur D., Mittal J., “Applicability of waste materials-bottom ash and deoiled soya-as adsorbents for the removal and recovery of a hazardous dye, brilliant green,” *J. Colloid. Interface. Sci.*, 326, (2008), 8–17.
- [9] Mittal A., Kaur D., Malviya A., Mittal J., Gupta V.K., “Adsorption studies on the removal of coloring agent phenol red from wastewater using waste materials as adsorbents,” *J. Colloid. Interface. Sci.*, 337, (2009), 345–354.
- [10] Mittal A., Mittal J., Malviya A., Kaur, D., Gupta V.K., “Decoloration treatment of a hazardous triarylmethane dye, Light Green SF (Yellowish) by waste material adsorbents,” *J. Colloid. Interface. Sci.*, 342, (2010), 518–527.
- [11] Mittal A., Gupta V.K., “Adsorptive removal and recovery of the azo dye Eriochrome Black T,” *Toxicol. Environ. Chem.*, 92, (2010), 1813–1823.
- [12] Mittal A., “Removal of the dye, amaranth from waste water using hen feathers as potential adsorbent,” *Electron. J. Environ. Agri. Food Chem.*, 5, (2006), 1296–1305.

- [13] Mittal A., Jain R., Mittal J., Shrivastava M., "Adsorptive removal of hazardous dye quinoline yellow from wastewater using coconut-husk as potential adsorbent," *Fresenius Environ. Bull.* 19 (2010) 1–9.
- [14] Mittal A., Thakur V., Gajbe V., "Evaluation of adsorption characteristics of an anionic azo dye brilliant yellow onto hen feathers in aqueous solutions," *Environ. Sci. Pollut. Res.*, 19, (2012), 2438–2447.
- [15] Mittal A., Jain R., Mittal J., Varshney S., Sikarwar S., "Removal of yellow ME 7 GL from industrial effluent using electrochemical and adsorption techniques," *Int. J. Environ. Pollut.*, 43, (2010), 308–323.
- [16] Mittal A., Thakur V., Gajbe V., "Adsorptive removal of toxic azo dye amido black 10B by hen feather," *Environ. Sci. Pollut. Res.*, 20, (2013), 260–269.
- [17] Gupta V.K., Mittal A., Jhare D., Mittal J., "Batch and bulk removal of hazardous colouring agent Rose Bengal by adsorption techniques using bottom ash as adsorbent," *RSC Advances*, 2, (2012), 8381–8389.
- [18] Zhang L., Zhu Y., Li H.M., Liun N., Liu X.Y., Guo X.J., "Kinetic and thermodynamic studies of adsorption of gallium(III) on nano-TiO₂," *Rare Met.* 29, (2010), 16-20.
- [19] Goudarzi A., MotedayenAval G., Sahraei R., Ahmadpoor H., "Ammonia-free chemical bath deposition of nanocrystalline ZnS thin film buffer layer for solar cells," *Thin Solid Films.*, 516, (2008), 4953–4957.
- [20] Liu W., Zhang J., Zhang Ch., Wang Y., Li Y., "Adsorptive removal of Cr (VI) by Fe-modified activated carbon prepared from Trapanatans husk," *Chem. Eng. J.*, 162, (2010), 677–684.
- [21] Taghizadeh F., Ghaedi M., Kamali K., Sharifpour E., Sahraie R., Purkait M.K., "Comparison of nickel and/or zinc selenide nanoparticle loaded on activated carbon as efficient adsorbents for kinetic and equilibrium study of removal of Arsenazo (III) dye," *Powder Technol.* 245, (2013), 217–226.
- [22] Amin N.K., "Removal of reactive dye from aqueous solutions by adsorption onto activated carbons prepared from sugarcane bagasse pith," *Desalination*, 223, (2008), 152-161.
- [23] Ghaedi M., Ansari A., Sahraei R., ZnS:Cu nanoparticles loaded on activated carbon as novel adsorbent for kinetic, thermodynamic and isotherm studies of Reactive Orange 12 and Direct yellow 12 adsorption, *Spectrochim. Acta A*: 114, (2013), 687–694.

- [24] Fathi M.R., Asfaram A., Hadipour A., Roosta M., Kinetics and thermodynamic studies for removal of acid blue 129 from aqueous solution by almond shell, *J. Environ. Health. Sci. Eng.* 12, (2014), 1-7.
- [25] Hoda N., Bayram E., Ayranci E., “Kinetic and equilibrium studies on the removal of acid dyes from aqueous solutions by adsorption onto activated carbon cloth,” *J. Hazard. Mater. B*, 137, (2006), 344–351.
- [26] Yesi, Sisnandy F.P., Ju Y-H, Soetaredjo F.E., Ismadji S., “Adsorption of Acid Blue 129 from Aqueous Solutions onto Raw and Surfactant-modified Bentonite: Application of Temperature dependent Forms of Adsorption Isotherms,” *Adsorpt. Sci. Technol.*, 28, (2010), 847-868.



CHAPTER 7

Surfaces of Hydrogel Polymers as Adsorbent For Removal of Dyes



7.1 Introduction

The presence of several types of hazardous azo dyes in the effluents of industries, such as textile, rubber, paper, leather, plastics, cosmetic, printing industries, etc. [1]. The removal of azo dyes is of great concern, because they themselves and their degradation products cause severe health problems and negative impact on the sustaining ecosystem.

Congo red (CR), is an anionic, and Malachite green (MG), is an cationic dye, are the popular hazardous azo dyes used in many industries, and hence the wastewater containing it have to be treated adequately and efficiently with great concern before discharge into the environment, because it can be metabolized to the toxic intermediate i.e. benzidine, which is a human carcinogen [2, 3]. Among the chemical and physical methods available for dye removal from wastewater, adsorption has been recognized as a most attractive separation technique for the rapid removal of dyes from wastewater, because of its highly efficient removal rate, relatively low-cost technique and simple design [4].

Recently, polymeric hydrogels adsorbents with high potential include large surface area and pore structure [5] are proved to be the most promising adsorbent for the adsorption phenomenon [6, 7] for removal of some ions such as phosphate [8], nitrate [9] and noxious heavy metals from aquatic sources [10-12]. Polymers which can selectively adsorb these hazardous dyes must consist of monomer groups such as 2-Hydroxy ethyl methacrylate (HEMA), 2-Hydroxyethyl methacrylate-ethoxy ethyl methacrylate-methacrylic acid (HEMA-EEMA-MA), and Polyvinyl alcohol (PVA), each having a different prominent role in this relevant process [13].

In this study, we investigated the removal rate and extent of adsorption of CR and MG onto developed adsorbent i.e. HEMA, HEMA-EEMA-MA and PVA as adsorbents in aqueous solutions. The influence of several parameters such as kinetics, contact time, dye concentration, solution pH and agitation speed on the removal capacity was very well evaluated and elucidated.

7.2 Results and discussion

7.2.1 Spectral analysis

The characteristic of the HEMA, HEMA-EEMA-MA and PVA were analyzed by attenuated total reflection-Fourier transform infrared spectrometer (ATR-FTIR, Nicolet Impact NEXUS-670), ATR-FTIR spectrum method to examine the surface groups of HEMA before and after dye adsorption (Figure 7.1a). The broad band around 3400 cm^{-1} and the narrow band around $1642\text{-}1704\text{ cm}^{-1}$ may be assigned to the -OH stretching vibration and bending

vibrations of adsorbed water involved in the formation of hydrogen bonding [14, 15]. The band at 1421 cm^{-1} was assigned to the C=O stretching vibration of the CO_3^{2-} groups [16]. After adsorption of MG and CR, some new absorption bands were occurred on dye-loaded HEMA. The band at 1589 cm^{-1} was assigned to aromatic ring [17, 18]. The bands at 1389 cm^{-1} and 1377 cm^{-1} were due to $-\text{CH}_3$ bending vibration. The peak at 1322 cm^{-1} represented C-N bond in aromatic compound. These groups of MG and CR indicated the dyes were adsorbed onto the HEMA. Additionally, the intensity of -OH group at 3422 cm^{-1} was weakening in dye-loaded HEMA, which implied possibly interactions between the dye ions and -OH group to form hydrogen bond.

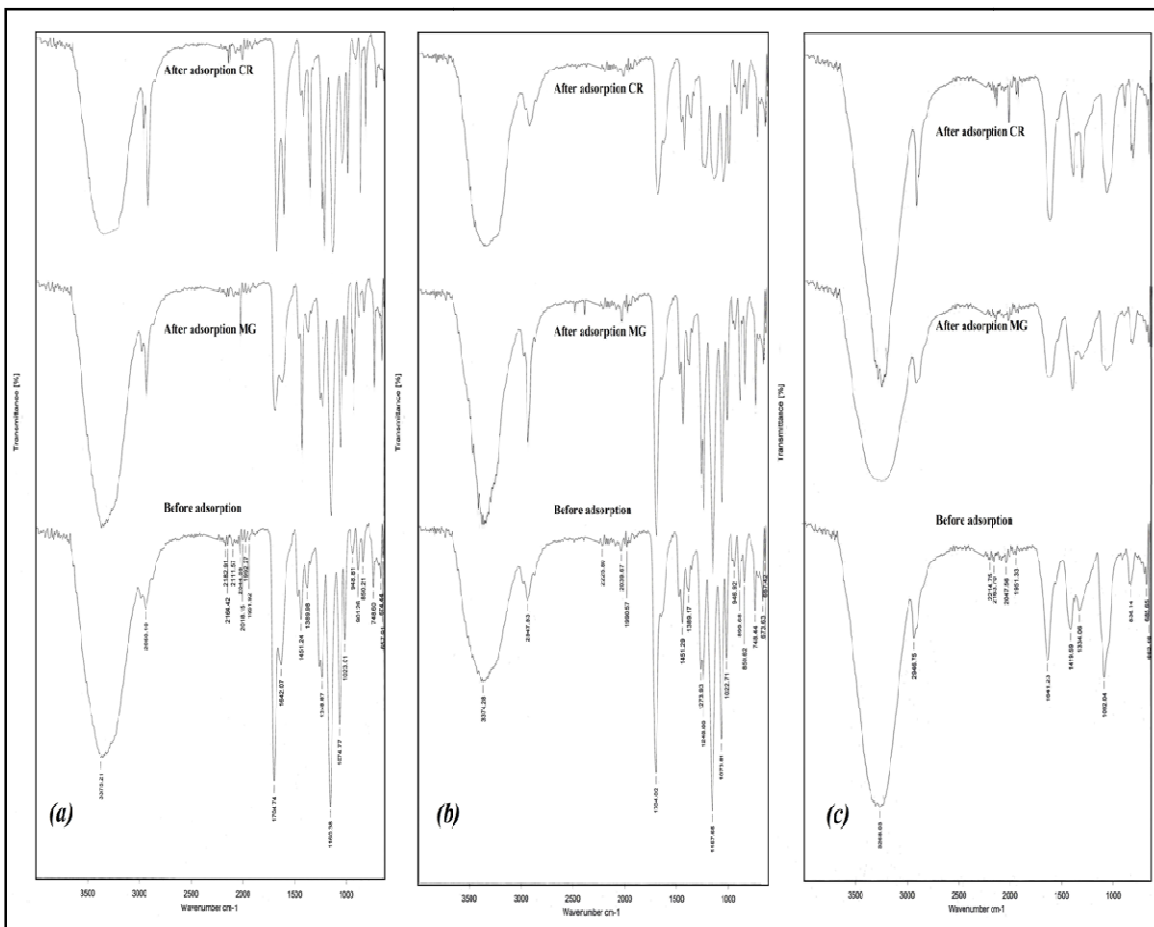


Fig. 7.1 ATR-FTIR of (a) HEMA, (b) HEMA-EEMA-MA and (c) PVA before and after adsorption

The ATR-FTIR spectrum of HEMA-EEMA-MA (Figure 7.1b) shows the absorption peaks of the HEMA-EEMA-MA, before and after adsorption of MG and CR. It can be seen both the HEMA-EEMA-MA--CR and HEMA-EEMA-MA--MG had the characteristic stretching vibration band of hydrogen-bonded alcohol (O–H) around 3450 cm^{-1} , the C=O stretching vibration of the ester group also appeared at 1730 cm^{-1} , and an absorption band with

a weak shoulder around 2950cm^{-1} , which correspond to the stretching of aliphatic $-\text{CH}_2-$, C–H and $-\text{CH}_3$ groups, respectively (Figure 7.1b). On the other hand, several bands appeared in the fingerprint region for alkylene glycol units between 1600 and 1000cm^{-1} on the HEMA-EEMA-MA--MG structure. These peaks were assigned to the $-\text{CH}_2$ scissoring band of alkylene glycol units at 1480cm^{-1} and the anti-symmetric and symmetric stretching bands ($-\text{O}-\text{R}$) of alkylene glycol units at 1160 and 1080cm^{-1} , respectively. Other characteristic bands represent C–C and C–H vibrations of $-\text{CH}_3$ and $-\text{CH}_2$ groups.

The ATR-FTIR spectrum of PVA (Figure 7.1c) showed adsorption peaks around 2500 – 3500 , which is indicative of the existence of bonded hydroxyl groups, and the peak observed at 2946cm^{-1} can be assigned to the C–H group. The peak observed at 1620cm^{-1} is due to C=N. The peak around 1334cm^{-1} is due to the C–C. The peak around 1092cm^{-1} can be assigned to the C–O. The adsorption band at 410cm^{-1} is also ascribed to the symmetric bending of C–O and C–C.

According to the experimental results, combining with the structure and properties of the adsorbates and adsorbent, the possible adsorption mechanisms of MG and CR onto the HEMA, HEMA-EEMA-MA and PVA following: (i) Electrostatic interaction between the presence of positive charge on cationic dye and the negative charge on HEMA and HEMA-EEMA-MA presented by ion exchange. (ii) Electrostatic interaction between the presence of negative charge on anionic dye and the positive charge on PVA presented by ion exchange. (iii) Hydrogen bonding between the nitrogen atoms on dyes and -OH on HEMA, HEMA-EEMA-MA and PVA surfaces.

A morphological analysis was carried out using a scanning electron microscopy. Figure 7.2 represents the scanning electron microscopy (SEM) micrographs of the HEMA, HEMA-EEMA-MA and PVA before and after adsorption of MG and CR. All of the polymers displayed discontinuous porous inner structure. The pore sizes were between 10 and $40\text{ }\mu\text{m}$. It is known that the reaction junctions increased with the increasing EEMA and MA group's content from HEMA to HEMA-EEMA-MA. Thus, the cross linking levels of the polymers improved correspondingly, leading to the decreasing average pore sizes of hydrogels from HEMA to PVA as shown in **Figure 7.2**. It is clearly observed that HEMA, HEMA-EEMA-MA and PVA show an entangled three-dimensional structured network with many interconnected pores. Inside these pores, some lines as the stripes on a leaf are visible. One can anticipate that this coarse, porous surface is beneficial for an adsorption process.

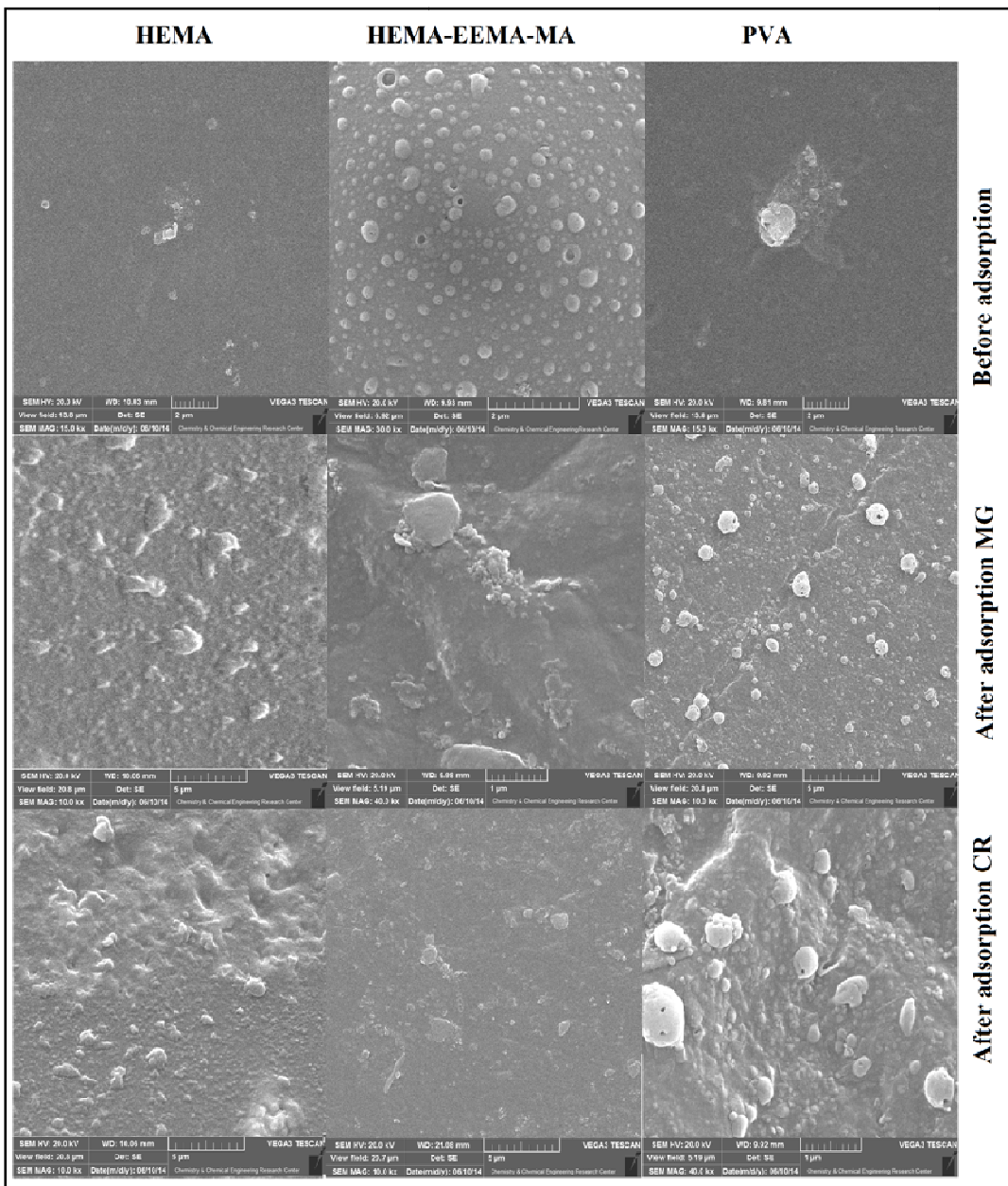


Figure 7.2 SEM images of HEMA, HEMA-EEMA and PVA before and after adsorption

Also, before adsorption, irregular surface structure and many pores in the surface were observed, which may exist as adsorption site. It is also considered helpful for mass transfer of MG or CR to HEMA, HEMA-EEMA-MA and PVA. After adsorption of hazardous dyes, the adsorbent surface became abnormal and a great deal of crystal adhered to the surface. From the results obtained it was found that dyes was adsorbed by all adsorbent into its pores and developed a layer dye substance on the surface.

7.2.2 Effect of contact time

To establish equilibration time for maximum uptake and to know the kinetics of the adsorption process, the adsorption of MG and CR onto HEMA, HEMA-EEMA-MA and PVA as adsorbent was studied as a function of contact time; results are shown in Figure 7.3. The rate of uptake of the MG and CR is rapid in the beginning, and 50% adsorption is completed within 90 min onto HEMA, HEMA-EEMA-MA and PVA surfaces, respectively. Less than 5% adsorption CR by HEMA and 10% adsorption MG by PVA and CR onto HEMA-EEMA-MA was observed. Figure 7.3 also indicates that the time required for equilibrium adsorption of MG onto HEMA, HEMA-EEMA-MA and PVA is 80, 90, and 100 min, respectively, and that of CR onto HEMA, HEMA-EEMA-MA and PVA is 70, 80, and 100 min respectively. Thus, for all equilibrium adsorption studies, the equilibration period was 100 min. In this section, concentration each of MG and CR was 50 ppm, pH 7, temperature 298 K, and weight of each adsorbent (HEMA, HEMA-EEMA-MA and PVA) is 50 mg/L.

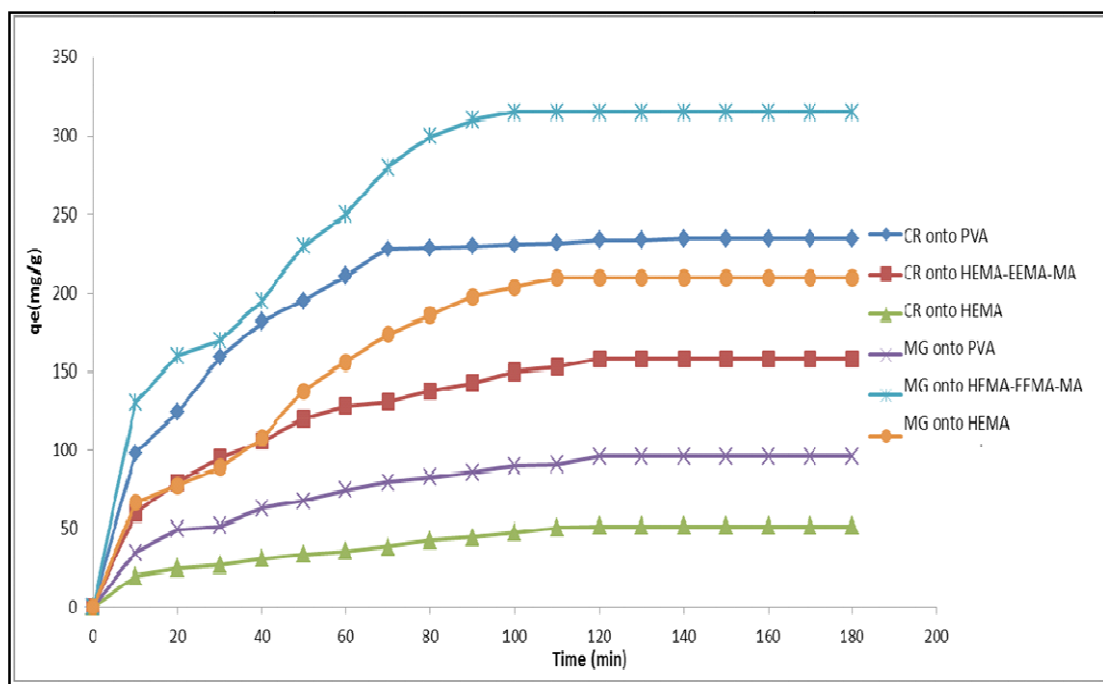


Figure 7.3 The effect of contact time on the amount of dyes adsorbed on different adsorbents

The adsorption affinity order of MG and CR onto HEMA, HEMA-EEMA-MA and PVA surfaces is MG- HEMA-EEMA-MA > CR- PVA > MG- HEMA > CR-HEMA-EEMA-MA > MG- PVA > CR- HEMA under experimental conditions. It is because the MG is positively charged and CR negatively charged at pH experiment. Another reason for higher adsorption of MG onto HEMA-EEMA-MA and CR onto PVA is the existence of negatively charged on HEMA-EEMA-MA and positively charged on PVA [19]. Here, MG has a positive charge and

HEMA-EEMA-MA a negative surface charge; therefore, attraction interaction is main reason for high adsorption. For adsorption CR onto PVA, MG onto HEMA, CR onto HEMA-EEMA-MA, MG onto PVA and CR onto HEMA, positive and negative are the main reasons for adsorption. According to the literature reports HEMA for removal of CR, PVA for removal of MG and HEMA-EEMA-MA for removal of CR are expected to have a poor adsorption capacity for removal comparing with HEMA for removal of MG, PVA for removal of CR and HEMA-EEMA-MA for removal of MG.

7.2.3 Effect of pH

Solution pH is an important parameter that affects adsorption of dye molecules. The effect of the initial pH of the solution on the MG and CR adsorption by HEMA, HEMA-EEMA-MA and PVA surfaces were assessed at different values, ranging from 1 to 11, with a contact time of 100 minutes. The initial concentrations of each dyes and amount of adsorbent were set at 50 ppm and 0.5 g, respectively, for all batch tests in this experiment. As shown in Figure 7.4, adsorption of MG onto HEMA-EEMA-MA was increased from 245 to 330 mg/g > CR onto PVA 169-236 mg/g > MG onto HEMA 130-205 mg/g > CR onto HEMA-EEMA-MA 90-155 mg/g > MG onto PVA 35-140 mg/g > CR onto HEMA 17-57 mg/g, respectively. Since the adsorption of MG and CR increased to its maximum value at a pH of 9, the electrostatic attraction between the MG molecules (positively charged) and HEMA-EEMA-MA surface (negatively charged) and CR molecules (negatively charged) and PVA surface (positively charged) might be the predominant adsorption mechanism. If this were true, increasing solution pH would result in increasing adsorption capacity.

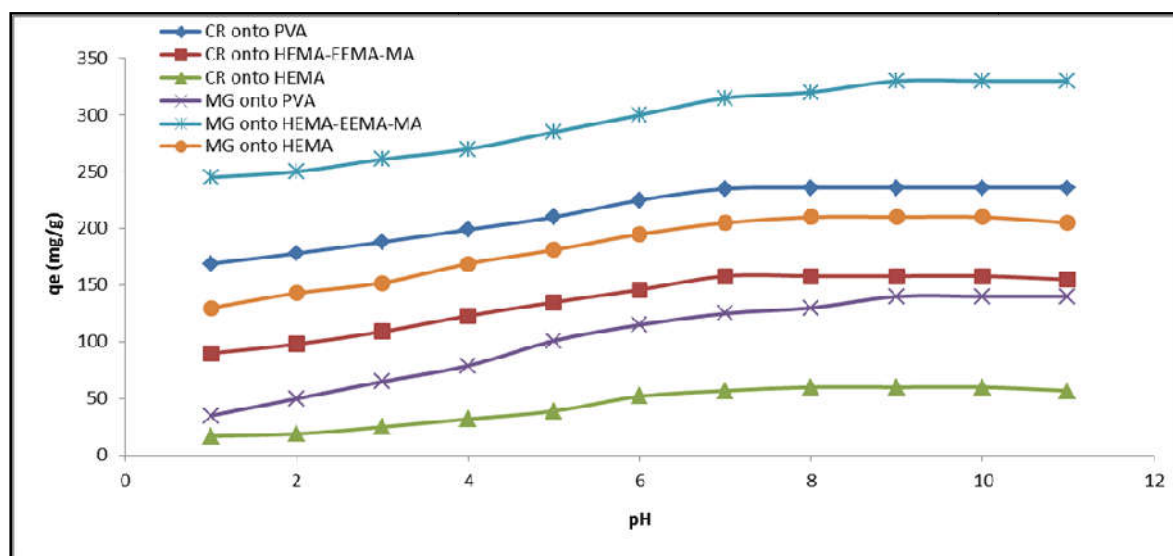


Figure 7.4 The effect of pH on the amount of dye adsorbed on the adsorbent

The increasing of adsorption of MG from aqueous solutions at alkaline pH might be explained by the formation and increasing concentration of $-OH$ in aqueous solution and subsequent competition with the CR molecules for adsorption sites [20] on the surface of adsorbents with surface charged positively, on the other hand the acidic pH range lead to the vice versa results and increasing H^+ concentration in aqueous solution creates a competition with the MG molecules for adsorption site. Differences in the adsorption mechanisms of dyes by the all adsorbent surfaces can be related to their physicochemical properties and structure [21]. The independent behaviour of adsorption of the toxic dyes from the liquid pH suggests that in addition to the electrostatic attraction, other adsorption mechanisms such as hydrogen bonding may also be at play [22]. According to the above results, a pH of 9 was chosen as the optimum pH for adsorption of dyes by the all adsorbents in the next experiments. Because the amount of MG and CR adsorbed by HEMA, HEMA-EEMA-MA and PVA surfaces for pH of 9, 10 and 11 are almost fixed.

7.2.4 Effect of initial concentration

In batch adsorption systems, available adsorbate initial concentration in solution plays a crucial role as a driving force which overcomes mass transfer resistance of adsorbate between aqueous and solid phase [23]. The effect of initial concentration on the equilibration time was investigated as a function of initial MG and CR concentration. In the present study, the adsorption experiments are performed to study the effect of dye initial concentration by varying it from 50 to 200 ppm, while maintaining the amount of adsorbent fixed i.e. 0.5 g and obtained results are presented in **Figure 7.5**.

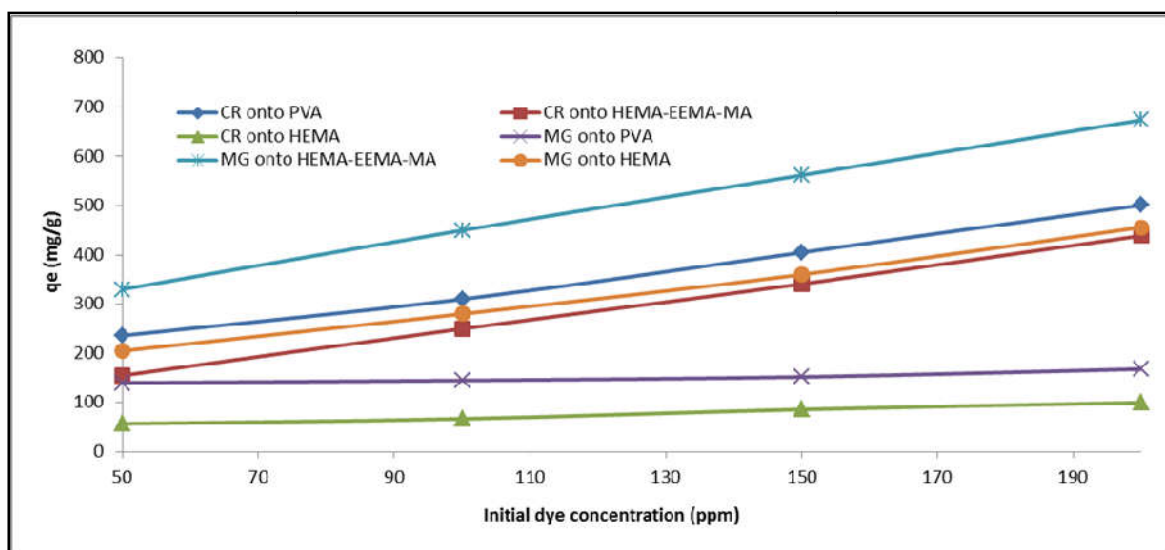


Figure 7.5 The effect of initial concentration on the amount of dye adsorbed on the adsorbent

The increase in adsorption capacity with increase in dye concentration may be due to the higher adsorption rate and utilization of all activated site available to the adsorption at higher concentration.

7.2.5 Effect of agitation speed

The effect of agitation speeds was investigated within a range from 0 rpm to 150 rpm, Figure 7.6 clearly depicts that the adsorption of MG and CR are low without or at low agitation speed and increases with the increase in the agitation speed to 150 rpm. This effect can be attributed to the decrease in boundary layer thickness around the adsorbent particles being a result of increasing the degree of mixing.

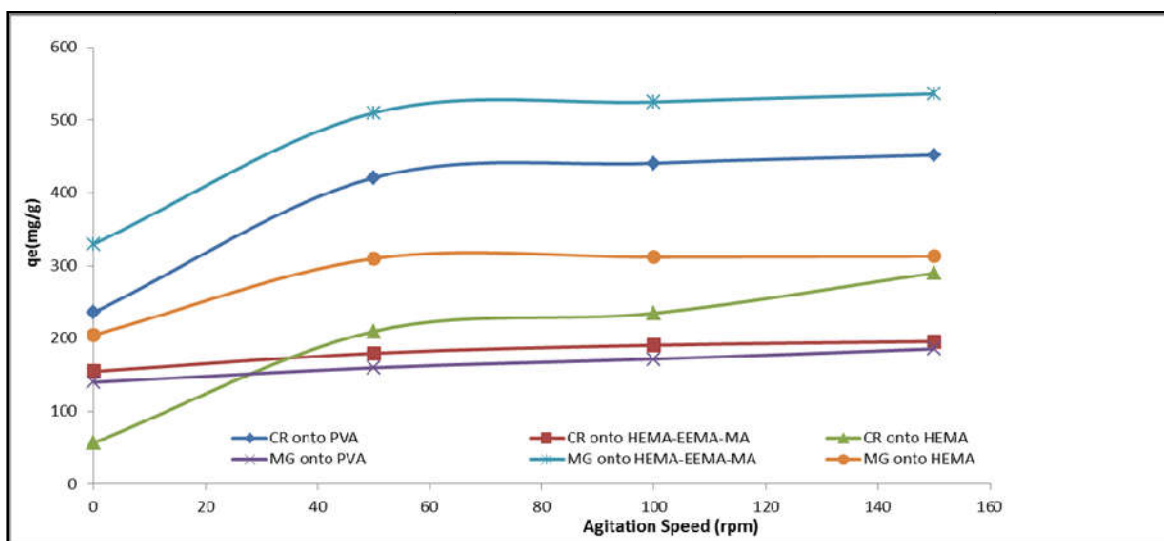


Figure 7.6 The effect of agitation speed on the amount of dye adsorbed on the adsorbent

7.2.6 Adsorption kinetics

Two kinetic models namely pseudo-first-order and pseudo-second-order have been applied and were used to test adsorption kinetics data in order to investigate the mechanism involved during the adsorption of azo dyes onto the developed adsorbent i.e. HEMA, HEMA-EEMA-MA, and PVA.

Table 7.1 lists the results of the kinetic parameters of two models as well as their regression coefficients (R^2) for both the azo dyes i.e. Congo red (CR) and Malachite green (MG). The value of correlation coefficients (R^2) for the pseudo-second-order kinetic model is comparatively high (>0.99). Figure 7.7 indicates the linear plots of t/q_t vs. T for azo dyes i.e. CR and MG showing the applicability of the pseudo-second-order model and thus can be concluded to be more suitable to describe the adsorption kinetics of the CR and MG onto the HEMA, HEMA-EEMA-MA, and PVA.

Table 7.1 Kinetic Parameters for the adsorption of CR and MG onto surface hydrogel polymer i.e. HEMA, HEMA-EEMA-MA, and PVA.

System	Model	Pseudo-first order		Pseudo-second order	
		K	R ²	k	R ²
CR onto PVA		2.5	0.971	2.5518	0.999
CR onto HEMA-EEMA-MA		2.6	0.977	3.6584	0.996
CR onto HEMA		1.9	0.966	1.8680	0.999
MG onto PVA		3.2	0.992	1.9856	0.997
MG onto HEMA-EEMA-MA		2.6	0.980	38.2517	0.999
MG onto HEMA		18.3	0.9794	2.765	0.998

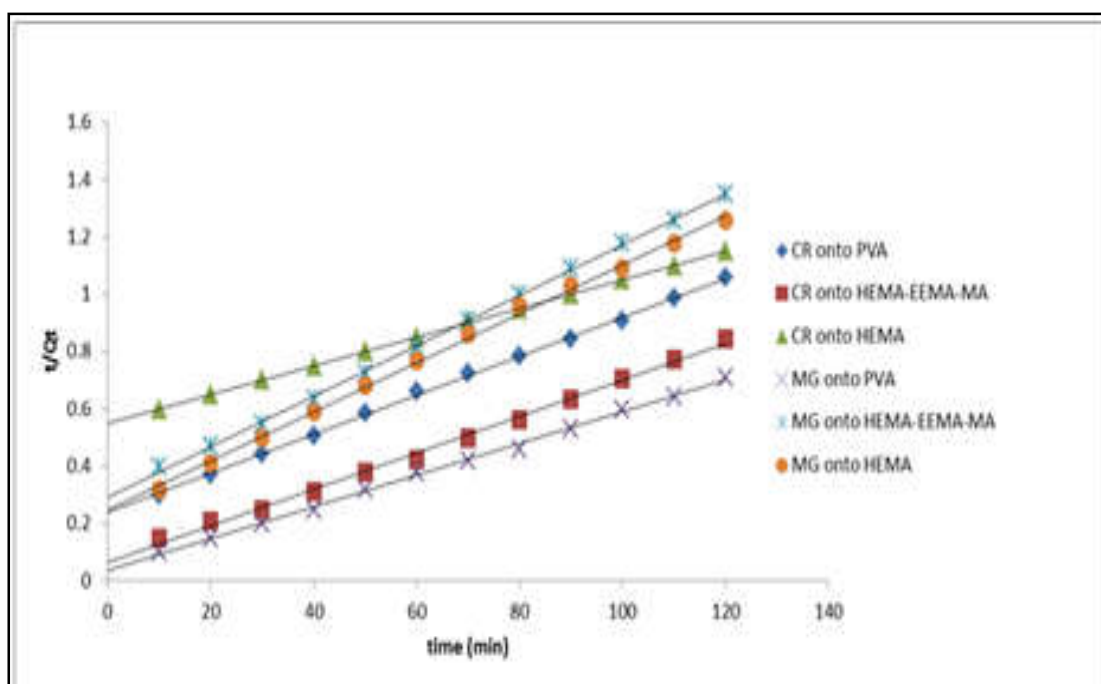


Figure 7.7 Pseudo-second order adsorption kinetics of MG and CR onto HEMA, HEMA-EEMA-MA and PVA surfaces.

7.2.7 Mechanism of the adsorption process

Prediction of the rate- limiting step is an important factor to be considered in the adsorption process. For solid-liquid adsorption process, the solute transfer process is usually characterized by either external mass transfer (boundary layer diffusion) or intraparticle diffusion or both. In the present study, intraparticle diffusion plot of q_t vs. $t^{0.5}$ (Figure 7.8) were plotted for CR and MG. From Figure 7.8, the adsorption process tends to be followed by two phases the first linear phase was the gradual adsorption stage signifying the rate limiting step being the intraparticle diffusion of the dye molecules and in the end the second phase shows the final equilibrium stage signifying the saturation of the carbon surface and also the presence of very low adsorbate concentration in aqueous solution. But none of the linear plots passed through the origin. This deviation from the origin may perhaps be due to the difference in the rate of mass transfer in the initial and final stages of adsorption. This further indicates the interplay of film and particle diffusion during the transport of CR and MG from aqueous phase to the solid phase and that the intraparticle diffusion is not only the rate-limiting step. Values presented in Table 7.2 give an idea about the thickness of the boundary layer, i.e., the larger intercept the greater is the boundary layer effect.

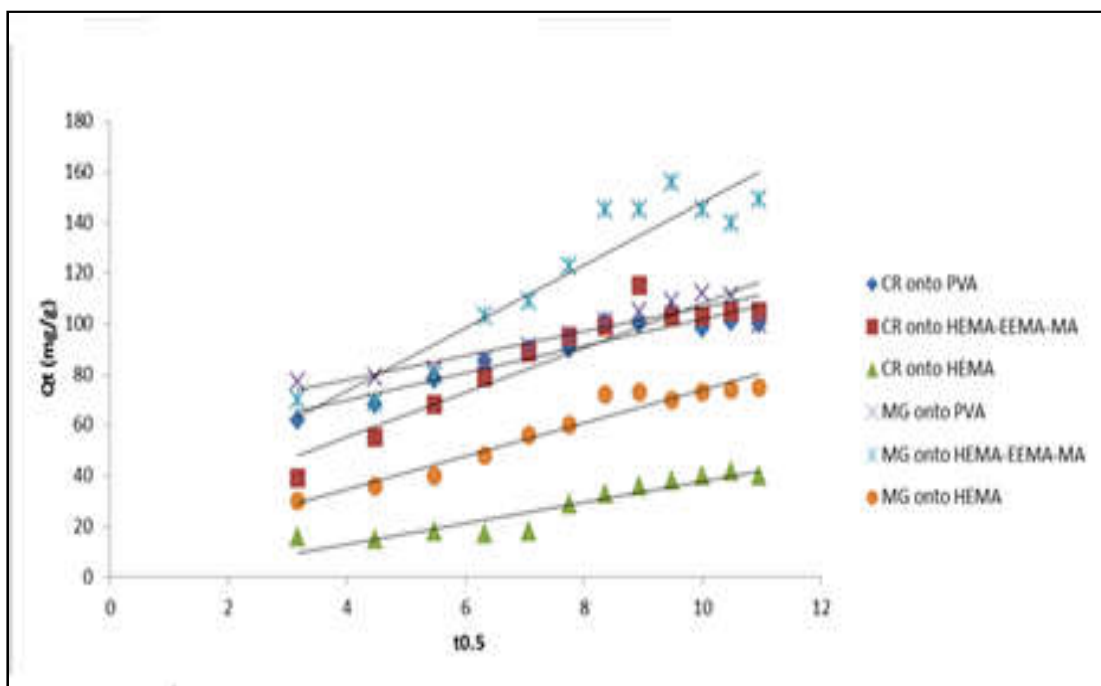


Figure 7.8 Intraparticle diffusion model of MG and CR onto HEMA, HEMA-EEMA-MA and PVA surfaces.

Table 7.2 Intraparticle diffusion model parameters for the adsorption of CR and MG onto surface hydrogel polymer i.e. HEMA, HEMA-EEMA-MA, and PVA.

System	Model	Intraparticle diffusion	
		k_p	R^2
CR onto PVA		12.547	0.8906
CR onto HEMA-EEMA-MA		13.6203	0.881
CR onto HEMA		14.586	0.8758
MG onto PVA		1.2560	0.8652
MG onto HEMA-EEMA-MA		0.3373	0.8924
MG onto HEMA		5.286	0.9411

7.3 Conclusion

This study was focused on assessing the adsorptive capacity of surface hydrogel HEMA, HEMA-EEMA-MA and PVA for removal of noxious Congo Red (CR) and Malachite Green (MG) from industrial waste effluent which is fabricated with metal. The following conclusions are bulletined:

1. The HEMA, HEMA-EEMA-MA and PVA were synthesized and upon characterization reveal the entangled three-dimensional structured network with many interconnected pores.
2. Adsorption of MG onto HEMA-EEMA-MA was increased from 245 to 330 mg/g > CR onto PVA 169-236 mg/g > MG onto HEMA 130-205 mg/g > CR onto HEMA-EEMA-MA 90-155 mg/g > MG onto PVA 35-140 mg/g > CR onto HEMA 17-57 mg/g, respectively. Since the adsorption of MG and CR increased to its maximum value at a pH of 9.
3. The adsorption capacity increase with increase in dye concentration may be due to the higher adsorption rate and utilization of all activated site available to the adsorption at higher concentration.
4. The adsorption of MG and CR are low without or at low agitation speed and increases with the increase in the agitation speed to 150 rpm.

Novel adsorbent for noxious impurities removal

5. The linear plots of t/q_t vs. T for azo dyes i.e. CR and MG showing the applicability of the pseudo-second-order model and thus can be concluded to be more suitable to describe the adsorption kinetics of the CR and MG onto the HEMA, HEMA-EEMA-MA, and PVA.
6. Summarily, the developed adsorbent i.e. HEMA, HEMA-EEMA-MA, and PVA has the potential for removal of CR and MG from wastewater to a significant extent.

References

- [1]. Tan I. A. W., Ahmad A. L., Hameed B. H., “Adsorption of basic dye on high-surface-area activated carbon prepared from coconut husk: Equilibrium, kinetic and thermodynamic studies,” *J. Hazard. Mater.*, 154, (2008), 337–346.
- [2]. Liu S., Ding Y., Li P., Diao K., Tan X., Lei F., Huang Z., “Adsorption of the anionic dye Congo red from aqueous solution onto natural zeolites modified with N,N-dimethyl dehydroabietylamine oxide,” *Chem. Eng. J.*, 248, (2014), 135-144.
- [3]. Zhang L., Zhang H., Guo W., and Tian Y., “Removal of malachite green and crystal violet cationic dyes from aqueous solution using activated sintering process red mud,” *Appl. Clay Sci.*, 93, (2014), 85-93.
- [4]. Wu C. H., “Adsorption of reactive dye onto carbon nanotubes: Equilibrium, kinetics and thermodynamics,” *J. Hazard. Mater.*, 144, (2007), 93-100.
- [5]. El-Hag Ali A., Shawky H. A., Abd El Rehim H. A., Hegazy E. A., “Synthesis and characterization of PVP/AAC copolymer hydrogel and its applications in the removal of heavy metals from aqueous solution,” *Eur. Polym. J.*, 39, (2003), 2337-2344.
- [6]. Joo D. J., Shin W. S., Choi J. H., Choi S. J., Kim M. C., Han M. H., Kim Y. H. , “Decolorization of reactive dyes using inorganic coagulants and synthetic polymer,” *Dye. Pigment.*, 73, (2007), 59-64.
- [7]. Janaki V., Oh B. T., Shanthi K., Lee K. J., Ramasamy A. K., Kamala-Kannan S., “Polyaniline/chitosan composite: An eco-friendly polymer for enhanced removal of dyes from aqueous solution,” *Synth. Met.*, 162, (2012), 974-980.
- [8]. Zhao D., Sengupta A.K., “Ultimate removal of phosphate from wastewater using a new class of polymeric ion exchangers,” *Water Res.*, 32, (1998), 1613-1625.
- [9]. Cheng H., Scott K., Christensen P. A., “Application of a solid polymer electrolyte reactor to remove nitrate ions from wastewater,” *J. appl. Electrochem.*, 35, (2005), 551-560.
- [10]. Fu F., Wang Q., Removal of heavy metal ions from wastewaters: a review. *J. Environ. Manag.*, 92, (2011), 407-418.
- [11]. Kaşgöz H., Özgümüş S., Orbay M., “Modified polyacrylamide hydrogels and their application in removal of heavy metal ions,” *Polym.*, 44, (2003), 1785-1793.
- [12]. Denizli A., Salih B., Pişkin E., “Alkali Blue GB-attached poly(EGDMA-HEMA) microbeads for removal of heavy-metal ions,” *React. Funct. Polym.*, 29, (1996), 11-19.

- [13]. Bezbradica D., Obradovic B., Leskosek-Cukalovic I., Bugarski B., Nedovic V., "Immobilization of yeast cells in PVA particles for beer fermentation," *Process Biochem.*, 42, (2007), 1348-1351.
- [14]. Rahmat A.R., Rahman W.A., Sin L.T., Yussuf A.A., "Approaches to improve compatibility of starch filled polymer system: A review," *Mater. Sci. Eng.: C*, 29, (2009), 2370-2377.
- [15]. Sanchez-Vazquez S.A., Hailes H.C., Evans J.R.G., "Hydrophobic Polymers from Food Waste: Resources and Synthesis," *Polym. Rev.*, 53, (2013), 627-694.
- [16]. Klotz E., Doyle R., Gross E., Mattson B., "The Equilibrium Constant for Bromothymol Blue: A General Chemistry Laboratory Experiment Using Spectroscopy," *J. Chem. Educ.*, 88, (2011), 637-639.
- [17]. Guo J. Z., Li B., Liu L., Lv K., "Removal of methylene blue from aqueous solutions by chemically modified bamboo," *Chemosp.*, 111, (2014), 225-231.
- [18]. Janković B., Smičiklas I., Stajić-Trošić J., Antonović D., "Thermal characterization and kinetic analysis of non-isothermal decomposition process of Bauxite red mud. Estimation of density distribution function of the apparent activation energy," *Int. J. Miner. Process.*, 123, (2013), 46-59.
- [19]. Sahu M. K., Mandal S., Dash S. S., Badhai P., Patel R. K., "Removal of Pb(II) from aqueous solution by acid activated red mud," *J. Environ. Chem. Eng.*, 1, (2013), 1315-1324.
- [20]. Santona L., Castaldi P., Melis P., "Evaluation of the interaction mechanisms between red muds and heavy metals," *J. Hazard. Mater.*, 136, (2006), 324-329.
- [21]. Song W. Ma, X., Pan Y., Cheng Z., Xin G., Wang B., Wang X., "Adsorption behavior of crystal violet onto opal and reuse feasibility of opal-dye sludge for binding heavy metals from aqueous solutions," *Chem. Eng. J.*, 193, (2012), 381-390.
- [22]. Jalil A. A., Triwahyono S., Yaakob M. R., Azmi Z. Z. A., Sapawe N., Kamarudin N. H., Hameed B. H. , "Utilization of bivalve shell-treated *Zea mays* L. (maize) husk leaf as a low-cost biosorbent for enhanced adsorption of malachite green," *Bioresour. Technol.*, 120, (2012), 218-224.
- [23]. Nekouei F., Nekouei S., Tyagi I., Gupta V. K., "Kinetic, thermodynamic and isotherm studies for acid blue 129 removal from liquids using copper oxide nanoparticle-modified activated carbon as a novel adsorbent," *J. Mol. Liq.*, 201, (2015), 124-133.